Investigation of Compression Ignition Engine Characteristics with Gaseous and Liquid Biofuels

A Thesis

Submitted in Partial Fulfillment of the requirements for

The Award of the Degree of

DOCTOR OF PHILOSOPHY

BY

SAMAR DAS

(Registration number: 166151102)

School of Energy Science and Engineering

Indian Institute of Technology Guwahati

Guwahati-781039, Assam, India

September, 2023

Dedicated to my parents...

Mrs. Renu Das

&

Mr. Pradip Kumar Das

DECLARATION

I hereby certify that the work presented in this thesis entitled '***Investigation of Compression Ignition Engine Characteristics with Gaseous and Liquid Biofuels***' is entirely my own account of research performed under the guidance of Dr. Pankaj Kalita and Prof. Vinayak Kulkarni. Any part of this work has not been submitted earlier for the award of any degree, diploma, fellowship or its equivalent to any University or Institution.

Date:

Samar Das

Registration number: 166151102

School of Energy Science and Engineering

Indian Institute of Technology Guwahati

School of Energy Science and Engineering

INDIAN INSTITUTE OF TECHNOLOGY GUWAHATI

भारतीय प्रौद्योगिकी संस्थान गुवाहाटी, गुवाहाटी- 781039

CERTIFICATE

This is to certify that the work contained in the thesis entitled '***Investigation of Compression Ignition Engine Characteristics with Gaseous and Liquid Biofuels***' submitted by **Samar Das,** a student in the School of Energy Science and Engineering**,** Indian Institute of Technology Guwahati, India for the award of the degree of Doctor of Philosophy has been carried out under our supervision. He has fulfilled all the requirements according to the rules of the institute and the investigations embodied in his thesis have not been submitted elsewhere for the award of any other degree or diploma.

Dr. Pankaj Kalita
Associate Professor
School of Energy Science and Engineering
Indian Institute of Technology Guwahati
Guwahati – 781039

Prof. Vinayak Kulkarni
Professor
Department of Mechanical Engineering
Indian Institute of Technology Guwahati
Guwahati – 781039

Abstract

Due to global population growth, energy demand has surged, especially in developing countries with dispersed rural communities. Consequently, the centralized grid system is unable to keep up with the escalating energy demand, leading to electricity shortage. Moreover, providing affordable electricity to remote areas is a challenge. Hence, decentralized power in these regions has been becoming an increasingly important issue. Power generation using fossil diesel in compression ignition engines (CI) is an old practice in remote locations of developing nations. However, the use of diesel engines leads to over exploitation of conventional fuels causing concern over environmental degradation. Hence, there is a huge demand for generating remote electricity by utilizing available renewable resources with the help of existing diesel engines. Dual fuelling of a conventional diesel engine is a mode of combustion which involves a small pilot injection of high cetane liquid fuel that ignites a pre-mixed combination of high octane gaseous fuel and air. The liquid fuel is called the pilot fuel and the gaseous fuel is called the primary fuel. The use of biofuels (liquid and gaseous form) can provide a clean alternative substitute for conventional diesel in dual fuel (DF) engines. Biogas (BG) and producer gas (PG) have emerged as a low cost renewable fuels. Both BG and PG have their own advantages and limitations to be used as a primary fuel for DF operations. Operations in DF mode individually with BG and PG exhibits inferior combustion characteristics compared to conventional diesel. However, these gases possess high anti-knocking properties and they have the potential to control the exhaust emissions. Moreover, combining these two gases might subdue each other's limitations when introduced to the DF engines. Therefore, it is important to study the performance and emission characteristics of a DF engine run on BG-PG mixtures under varying operating conditions, namely, load, compression ratio (CR) and injection timing (IT). The present contribution is focused to perform a systematic experimental analysis for a diesel engine powered by BG and PG using biodiesel-diesel blend as pilot fuel. The motivation of this present investigation is to provide a perfect competitive promotion of biodiesel-biogas-producer gas as the alternative fuel for clean energy generation for rural electrification.

First of all, a comparative experimental investigation is carried out with ten different tri-biodiesel-diesel blends to evaluate the best blend to be used as pilot fuel for DF operation. Three non-edible biodiesels namely Jatropha (JB), Karanja (KB) and Mahua (MB) are mixed with the conventional diesel fuel at 30:70 ratio to prepare tri-biodiesel-diesel blends. The tri-biodiesel-diesel blends resulted in lower brake thermal efficiency (BTE) than that of diesel

fuel, while emission of carbon monoxide (CO) and hydrocarbon (HC) was found to be lower. The blended fuels with higher cetane number resulted in shorter ignition delay compared to diesel. Tri-biodiesel-diesel blend with combination of 15%JB+10%KB+5%MB, namely Blend-2 is found to be the best blend with comparable BTE of 24.65% and minimum CO and HC emission of 46.24 ppm and 22.17 ppm, respectively.

For DF experimentation, a 3.5 kW single cylinder, four-stroke, variable compression ratio diesel engine is modified to operate under DF mode connecting a novel venturi gas mixer. The primary gaseous fuels utilized for the study are simulated biogas (SBG), simulated producer gas (SPG), and SPG-SBG mixture. For the preparation of SBG, methane (CH_4) and carbon dioxide (CO_2) are mixed at four different ratios (55:45, 60:40, 65:35 and 70:30). Similarly, hydrogen (H_2) and carbon monoxide (CO) are also mixed at four different ratios (40:60, 50:50, 60:40 and 70:30) for the preparation of SPG. Again, H_2 and CO at a 50:50 ratio are mixed with a four different ratio of CH_4 and CO_2 to simulate the SPG-SBG mixture. Compared to fossil diesel with a BTE of 27.57% at standard operating condition, SBG-4 (70% CH_4 and 30% CO_2), SPG-4 (70% H_2 and 30% CO) resulted with maximum BTE of 25.1 and 25.58% at full engine load, CR of 18 and IT of 29° BTDC. At similar operating conditions, maximum PFR of 90.59 and 87.77% was achieved for SBG-4 and SPG-4, respectively. In case of SPG-SBG mixture, SG-4 (SPG-2/SPG-4) showed the maximum BTE and PFR of 24.44% and 86.41%, respectively. Moreover, NO_X emission for SPG-SBG mixture was found to be 64.2% lower than that of SPG-DF operation.

This is followed by on-field investigation of DF diesel engine run on BG and PG mixture generated from anaerobic digester and biomass gasifier, respectively. The experiments were carried out with raw BG, PG and four different BG-PG mixtures. The BG-PG mixture combinations were inducted to the engine based on controlled regulation of valve opening of BG and PG. DFM-3 i.e. 60° opening of BG valve and 30° opening of PG valve showed highest BTE and PFR i.e. 23.28% and 90.22%, respectively at full load, CR of 18 and IT of 29° BTDC. At similar condition, the BG and PG flow rate was monitored to be 2.21 and 2.51 kg/hr, respectively. The minimum emission of CO and HC was 267.21 and 175.31 ppm, respectively. Higher CR and advancement of IT provides supplementary benefits in terms of augmenting the engine performance and minimizing the exhaust emission. Hence, this novel technology package could be prescribed for remote decentralized power generation.

Keywords: Tri-biodiesel-diesel blend; Simulated gaseous fuels; Biogas; Producer gas; Dual fuel diesel engine; Compression ratio; Injection timing

Acknowledgment

A person cannot navigate through life without support and guidance from others. It is inevitable to owe debts to others, whether they be of physical, mental, psychological, or intellectual nature, whether known or unknown. It would be challenging to enumerate all of them. Even expressing gratitude in words surpasses my ability. The present work is a culmination of the efforts of many individuals who have significantly contributed to its materialization. I take great pleasure in expressing my gratitude to the many individuals who have made this thesis possible.

Firstly, I take this opportunity to express my sincere appreciation to the Indian Institute of Technology Guwahati for providing me with an excellent research environment. I am especially grateful to my supervisors, Dr. Pankaj Kalita and Prof. Vinayak Kulkarni, for their constant support, encouragement, and active guidance throughout the entire research process. Thanks to their exceptional abilities in organization, planning, and management, I was able to pursue my research goal with utmost determination.

My sincere acknowledgement goes to Prof. Niranjan Sahoo, chairperson of Doctoral committee, for his unwavering encouragement, guidance, and support throughout all stages of my PhD research. I am also indebted to the members of Doctoral Committee, Prof. Vaibhav V. Goud and Dr. Siddhratha Singha for their invaluable suggestions about critical issues related to my work.

I express my profound gratitude to the Science and Engineering Research Board (SERB), Government of India, for their invaluable financial support provided through Project Grant number: ECR/2016/001830.

I would like to thank Head, faculty members and all the staffs of School of Energy Science and Engineering for their wholehearted support and cooperation throughout my work. I extend my thanks to Dr. Lepakshi Barbora, Mr. Debarshi Baruah and Mr. Dhiren Huzuri for their resolute technical advice and constant support. I am also thankful to Mr. Pranjal Bhuyan, Mr. Paragjyoti sharma, Mr. Nabajit Rajbongshi, Mr. Nayan Jyoti Das for their help in looking into all official documents during the course of my research work.

My gratitude extends to the Head, Department of Chemical Engineering for granting me access to the Petroleum Laboratory facilities to conduct vital experimental work related to my thesis. I am grateful to the senior technician and technical support staff of Central Workshop Mr. Nandan K. Das, Mr. Chandan Banikya, Mr. Dilip Chetry, Mr. Mrinal Sarma, and Mr. Dhaneshwar Khaklary for their assistance at different stages of the experimental setup fabrication. Without their time and support, this work could not have been accomplished.

I am thankful to my seniors Dr. Bhaskor J. Bora, Dr. Achinta Sarkar and Mr. Santosh K. Hotta for their enthusiastic cooperation and support during the various stages of the experimental work for my thesis. I am also thankful to my colleagues Dr. Anil Kumar Rout, Dr. Mrinal Bhowmik, Dr. Sunita Dev, Dr. Muniraja Tippa, Dr. Ojing Siram and Mrs. Ankita Pandey for their encouragement and support.

I would like to thank Mr. Dipankar Kalita, Mr. Kamal Das and Pankesh Das for their invaluable assistance in configuring the experimental setup. Their support and expertise were crucial to the success of this project.

I would like to extend my profound appreciation to Mr. Shayaram Basumatary and Mr. Debangsu Kashyap, Dr. Dudul Das and Dr. Harrison Hihu Muigai whose resolute support and valuable insights were instrumental in the success of my research. I would also like to express my gratitude to Mr. Rabindra Kangsha Banik, Mr. Biraj Das, Miss Puja Hazarika, Miss Urbashi Bordoloi and Mr. Akash Dilip Kamble for their support and encouragement throughout the doctoral research tenure. I am thankful to Dr. Firdausa Ahmed, Dr. Devarshi Kashyap, Dr. Kamal Basumatary, Dr. Rajnish Kumar and Mr. Hirak Basumatary for their help at various stages of my thesis work. I am grateful to Mr. Mukunda Madhab Khanikar for his encouragement and constant help. I also thank Miss Sudipta Bijoy Sarmah, Miss Vijaya, Mrs. Tapashi Kalita and Mr. Dushyanta Madhav Sharma for their support in all ways possible.

All my love and gratitude go to my parents, Mrs. Renu Das and Mr. Pradip Kumar Das for all their unyielding patience and unrelenting support. I would not be who I am today without their constant presence and guidance in my life. My heartfelt thanks go to my sister Mrs. Karabi Das and my brother-in-law Mr. Uday Sankar Saloi for their unceasing love and support. I would also like to take this opportunity to thank my close friends, Miss. Kabyashree Dutta and Mr. Pranjal Protim Sarmah for their continual support and motivation.

Finally, I express my deep sense of gratitude to God, the almighty who gave me patience and strength to complete this work.

Samar

Contents

Nomenclature

Abbreviations			
AFR	Air flow rate	H_2S	Hydrogen sulphide
ATDC	After top dead centre	HC	Hydrocarbon
BP	Brake power (kW)	HDI	Human development index
BTDC	Before top dead centre	IC	Internal combustion
BTE	Brake thermal efficiency (%)	ID	Ignition delay
BSEC	Brake specific energy consumption (kg/kWh)	IT	Injection timing
BSFC	Brake specific fuel consumption (kJ/s of fuel/kW output)	JB	Jatropha biodiesel
BG	Biogas	KB	Karanja biodiesel
BGFR	Biogas flow rate (kg/hr)	LCV	Lower heating value (MJ/kg)
BMEP	Brake mean effective pressure	LFCM	Liquid fuel control mechanism
CA	Crank angle (Degree)	LPG	Liquefied Petroleum Gas
CD	Combustion duration	MB	Mahua biodiesel
CFD	Computational Fluid Dynamics	MFB	Mass fraction burned
CH_4	Methane	N_2	Nitrogen
CI	Compression ignition	NA	Naturally aspirated
CNG	Compressed Natural Gas	NHRR	Net heat release rate
CO	Carbon monoxide	NOx	Oxides of nitrogen
CO_2	Carbon dioxide	PCP	Peak cylinder pressure
CR	Compression ratio	PFR	Pilot fuel replacement
CP	Cylinder pressure	PG	Producer gas
DAS	Data acquisition system	PGFR	Producer gas flow rate, kg/hr
DDG	Decentralized distribution generation	PM	Particulate Matter
DF	Dual fuel	PPM	Parts per million
DFCI	Dual fuel compression ignition	SBG	Simulated biogas
DI	Direct injection	SI	Spark Ignition
EGT	Exhaust gas temperature	SO_2	Sulphur dioxide
ER	Equivalence ratio	SPG	Simulate producer gas
ESFC	Energy specific fuel consumption	TDC	Top dead centre
FD	Fossil diesel	TKE	Turbulent Kinetic Energy
H_2	Hydrogen	UI	Uniformity Index

Notations			
A_{den}	Density of ambient air (kg/m^3)	$\dot{m}_{pf}$	Mass flow rate of pilot fuel (kg/s)
b	Body force	$\dot{m}_{pg}$	Mass flow rate of producer gas or simulated producer gas (kg/s)
C_μ	Turbulence velocity factor	M_i	Molecular weight of air constituents
D	engine cylinder diameter (m)	M_j	Molecular weight of fuel constituents
d	Diameter of the orifice of air flow (m)	n	number of revolution per cycle
C_d	Coefficient of discharge	N	Speed of the engine (rpm)

E_{ij}	Component of rate of deformation	P	Pressure
f_μ	turbulence velocity factor	P_n	instantaneous pressure (N/m²)
h	Manometer reading across orifice (m)	ΔP	Total pressure drop
k	Turbulence kinetic energy	$\left(\frac{dP_n}{d\theta}\right)$	pressure gradient
K	number of cylinders	$\frac{dQ_n}{d\theta}$	Net heat release rate (J/°CA)
L	engine stroke length (m)	r	Dynamometer arm radius (m)
LHV_{bg}	Lower heating value of biogas or simulated biogas (kJ/kg)	t	Time
LHV_f	Lower heating value of fuel (kJ/kg)	u_i	Velocity component
LHV_{FD}	Lower heating value of diesel (kJ/kg)	V_n	instantaneous volume (m³)
LHV_{pf}	Lower heating value of pilot fuel (kJ/kg)	W_{den}	Density of water (kg/m³)
LHV_{pg}	Lower heating value of producer gas or simulated producer gas (kJ/kg)	W	Engine load (kg-m/s²)
$\dot{m}_{bg}$	Mass flow rate of biogas or simulated biogas (kg/s)	x_i	Mass fraction of air constituents
$\dot{m}_f$	fuel flow rate (kg/s)	x_j	Mass fraction of fuel constituents
$\dot{m}_{FD}$	Mass flow rate of diesel (kg/s)	Z	Pilot fuel replacement (%)

Greek symbols

η_{vol}	Volumetric efficiency	θ_{IN}	standard injection timing
β	Ratio of the throat diameter to the inlet diameter	θ_{CS}	crank angle at which combustion begins
γ	ratio of specific heats	μ_t	Turbulent eddy viscosity coefficient
ε	Eddy turbulent dissipation	λ	Second order coefficient of viscosity
ρ	Density	τ_{ij}^R	Reynolds stress tensor
μ	Dynamic viscosity		

List of Figures

List of Tables

1

Introduction

Chapter Outline:

1.1. Motivation
1.2. Role of decentralized power in rural development
1.3. Use of biofuel for remote power generation
1.4. Biofuel in IC engine
1.5. Emission standard
1.6. Objective of the study
1.7. Organization of the thesis

CHAPTER 1: INTRODUCTION

1.1 Motivation

Energy is the most sought concern in the 21st century. Rapid population growth and industrialization have dramatically increased the global energy demand which is leading towards the faster depletion of fossil fuels [1]. It is predicted that the total global energy consumption will grow from 19% in 2018 to 24% in 2040 [1]. As of 2019, fossil fuels remained the dominant source of energy, comprising over 80% of all types of available energy sources [2]. Coal has traditionally been a primary source of energy for electricity generation, accounting approximately 38.1% globally [3]. As far as petroleum consumption is concerned, it is expected to rise to 112.2 million barrels per day in 2035 [4]. Such ever-increasing demand and large quantities of fossil fuel consumption could significantly affect the current energy structure and also potentially harm the world environmental condition due to the emission of carbon monoxide (CO), carbon dioxide (CO_2), sulphur dioxide (SO_2), nitrogen oxide (NO_X) gases and global warming [5]. As per the IEA report, global CO_2 emission is recorded to be increased by 0.9% or 321 Megatonnes (Mt) in 2022, reaching a record high of more than 36.8 Gigatonnes (Gt) crossing the safe limit (350 ppm of CO_2) in the atmosphere [6,7]. **Fig. 1.1** shows the trends of world energy and electricity demand along with the global CO_2 emission over the different periods.

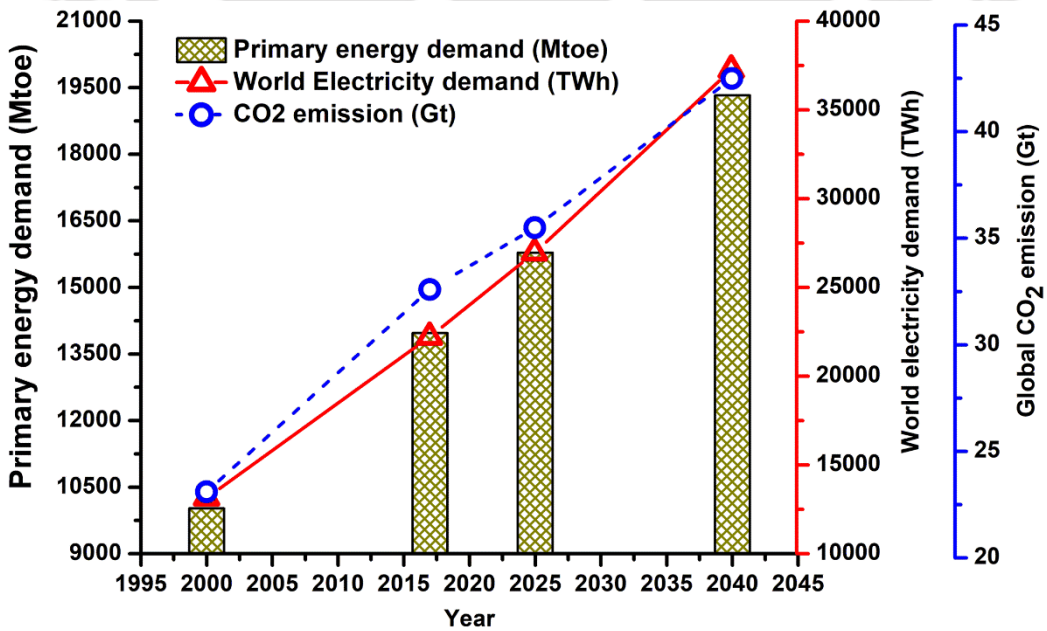

Fig. 1.1 Trends of energy demand, electricity demand and CO_2 emission with years [8]

The rapid rise in CO_2 emissions, primarily caused by the excessive usage of coal and petroleum products to fulfill the growing energy requirements, has prompted the global

community to shift towards renewable energy sources to fulfill various energy needs [9]. In addition, the ratification of the 2016 Paris agreement has expanded GHG emission mitigation responsibilities to all the nations. This obligation to fulfill such responsibilities, coupled with increasing concerns about energy security, has revitalized global interest in exploring renewable and domestic energy sources as viable alternatives or supplements. These sources have the potential to significantly reduce emissions and aid in fulfilling the commitments made in the Paris agreement [10]. According to International Energy Agency (IEA), renewable electricity generation has experienced a substantial increase of nearly 7% in 2021, marking a record-breaking rise of 522 TWh of electricity. **Fig. 1.2** illustrates the growth in global renewable power generation from year 2010-2021. Wind and solar PV technologies contributed significantly to this growth, accounting for nearly 90% of it. As a result, the share of renewables in global electricity generation reached 28.7% in 2021. Bioenergy power generation contributed to the remaining 15% surge, whereas hydropower generation experienced its first decline in 20 years, dropping by approximately 0.4%. The limited progress in the growth of renewables' share can be attributed to two factors: the worldwide surge in electricity demand, propelled by the rebound of economic activity following the Covid-19-related slowdown, and hydropower generation decline due to droughts in multiple regions. However, adoption of renewables is a crucial aspect of facilitating clean energy transitions and preventing the global average temperature from exceeding 1.5°C, underscoring the significance of renewable power deployment [11].

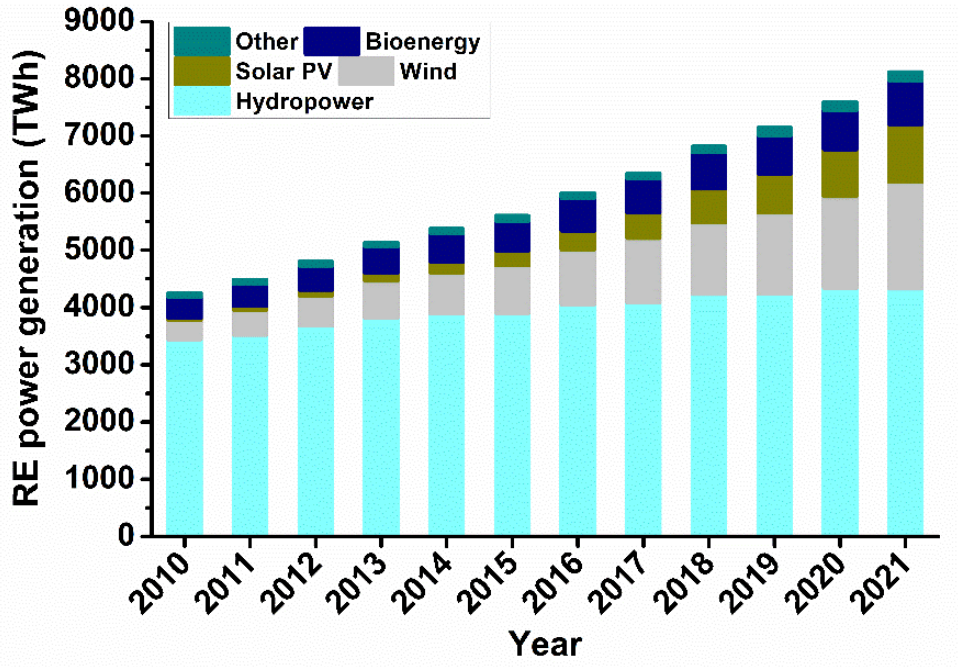

Fig. 1.2 Renewable power generation by technology [11]

1.2 Role of decentralized power in rural development

Electricity is the key behind multifaceted progress and prosperity of human kind and plays a predominant role in uplifting living standards by eliminating poverty across the globe. Countries having insufficient access to electricity ranks radically low at human development index (HDI), clearly implying the firm relation between human development and their access to electricity [12]. With the launch of the SDGs (Sustainable Development Goals) in 2015, access to energy (SDG 7.1) has received a universal attention, however the progress towards the goal has remained sluggish compared to the population growth which also hampers the achievement of overall SDGs by 2030 [12,13]. About 759 million people are deprived with access to electricity and millions more, who have centralized electric grid connections with inferior quality service [14]. Such lacking in electricity distribution are mostly seen in the village and suburb region of Africa, Latin America and South Asia where the concerned authority has been ineffective in providing uninterrupted electricity from the centralized grid due to economic reasons. According to reports, 400 million individuals in India had no access to electricity back then in 2011 [15]. Through collaborative efforts of the central and state governments, India achieved electrification of all villages in April 2018 and nearly universal household electrification in March 2019. However, a recent study revealed that the rate of electricity access in India is considerably lower at 87%, with household, agricultural, and institutional customer access rates being 96%, 52%, and 78%, respectively [14]. Another research also observed that the widespread electrification in India has not resulted in 24*7 electricity supply for rural households or enterprises [16]. Providing energy access to billions of people within a limited timeframe and while facing resource limitations presents a significant challenge. Therefore, as a remedial measure for rural electrification, small-scale off-grid power generation and distribution through mini/micro-grid has gained serious attention on global scale [17]. Improving energy access hold the potential to a reduction in rural poverty, an improvement in rural living conditions, and a reduction in the strain on urban areas [13]. There are several literatures available on regional and global platform considering different dimensions of decentralized remote electricity generation [18–22].

1.3 Use of biofuels for remote power generation

In India, mini-grids powered by solar, micro-hydro, or biomass have been implemented by both government and private sector entities. Decentralized power generation from solar and wind has the potential to transform rural India's energy landscape by bringing reliable electricity to remote areas [23]. However, one of the most significant challenges with solar and wind power generation in decentralized mode is the initial cost of installing these

technologies. Although the cost of solar panels and wind turbines has decreased significantly in recent years, the upfront investment can still be a significant barrier, especially for rural communities with limited financial resources. Another challenge is the variability of these sources as solar and wind power generation are dependent on weather conditions, which can be unpredictable and vary significantly from day to day. This means that additional backup power sources may be necessary to ensure a reliable supply of electricity, which can add to the overall cost of decentralized power generation. On the other hand, biomass energy has become an increasingly popular alternative to traditional fossil fuels for power generation in remote areas. There has been significant research and development focused on various pathways for converting biomass into bioenergy, commonly referred to as 1st, 2nd, and 3rd generation biofuels [24]. Modern bioenergy pathways contribute approximately 637 TWh of electricity globally, which accounts for approximately 2% of the world's total electricity generation [25]. India's abundance of agricultural biomass has led to several initiatives aimed at harnessing its significant biomass energy potential [25]. Decentralized power generation using biomass energy resources has emerged as a sustainable solution for the energy needs of rural and remote areas. The most significant advantage is the availability of these resources, especially in rural areas where there is an abundance of agricultural waste and forestry residues. India produces a considerable amount of surplus dry biomass, with 145.02 million tons originating from agriculture and 59.68 million tons from forests annually. Thus, decentralized power generation can be done close to the point of consumption, thereby reducing transmission losses and improving energy efficiency. Despite this vast potential, much of the biomass power remains untapped, leading to ecological harm. Therefore, it is crucial to prioritize the utilization of this resource, particularly with regard to the country's energy security and ecological considerations [26].

1.4 Biofuels in internal combustion (IC) engines

Internal combustion engine provides immediate and straightforward control of power generation while consuming a variety of commonly available fuels [27]. Its, high combustion efficiency, robust nature, reliability, adaptability, cost effectiveness and quick response to varying electricity demand makes it more receptive among rural communities for small-scale electricity generation [28]. Compression ignition (CI) or diesel engine captive power generation is a long-standing practice in rural or dispersed areas of developing countries like India, primarily for domestic utilities and agricultural applications. Therefore, diesel engine usage can be a solution to India’s acute problem of power shortage in rural areas [29,30]. Meanwhile, release of hazardous substances from diesel engines are not only contributing to

the environmental pollutions but also posing a serious threat to human health [31–33]. Additionally, concern over the relentless dwindling of fossil fuel reserve caused by the excessive use of conventional diesel and stringent government regulations on engine emissions have compelled the scientific community to shift towards alternate strategies that can control the severe growth in emission levels. Hence, concentrating on technical developments for utilization of renewable alternative fuels in existing engines may be an appropriate solution. The concept of dual fuel (DF) technology is gaining serious attention and have been studied expansively by researchers in the field of diesel engines due to lower emission and fuel flexibility [34]. Application of gaseous fuels have the potential to substitute an extensive quantity of conventional fuel use along with minimum emissions [35]. Wide ignition limits, higher hydrogen to carbon (H_2/C) ratio and capability of forming homogeneous mixtures with air makes these gases more favourable for DF operations. Renewable fuels like Biogas (BG) and producer gas (PG) can be utilized in DF diesel engine for power production. Because of high auto-ignition temperature, these gases cannot be used directly in diesel engines but they are appropriate for DF operation owing to their high anti-knocking characteristics [36–38]. In addition to that, DF engine uses small amount of liquid fuel, i.e. petro-diesel as pilot fuel for ignition of primary fuel. It also provides a possible way to eliminate the use of conventional fuel with the use of biodiesel blends. Hence, clean gaseous fuel induction in CI engine has emerged as a potential energy carrier due to its low environmental impact and also offer advantages in terms of performance and emission characteristics [28,36]. Hence, biogas plant and gasifier unit coupled with a diesel engine-generator can be an appropriate method for decentralized power generation in remote locations. But, along with this, there are certain factors such as quantity and type of biomass feedstock, end use requirement, economic conditions, environmental standards which determines the successful operation of this technology in the long run [39]. Suitability in the selection of power plant location plays a significant role in biomass feedstock collection, as this would reduce the costs related to the transaction of feedstock. Also, the costs of manpower and facilities are essential in cost economic analysis of biomass-based power plants [40]. Presently, the utilization of biomass power in IC Engine setups has led to higher reliability and provides a higher internal rate of return for investigated range of electrical power production [41].

1.4.1. Biofuels

The research and development of alternative fuels for diesel engines have gained significant momentum in recent years. Governments, industries, and academia are investing heavily in

this area to find solutions to the growing concerns over climate change and environmental pollution. Some countries have already started implementing policies that promote the use of alternative fuels in diesel engines, such as biofuels mandates and incentives for hydrogen-powered vehicles. While the adoption of alternative fuels may present technical, economic, and logistical challenges, the potential benefits of reducing harmful emissions from diesel engines are enormous.

1.4.1.1. Biodiesel

Among the various alternate fuels, biodiesel is considered as one of the most suitable fuels for diesel engine. Biodiesel is produced by a trans-esterification process with renewable agricultural resources like vegetable oils, animal fats and waste oils etc. There is a wide range of vegetable oils that can be utilized as a potential source of raw materials for the production of biodiesel. These oils can be broadly classified into two categories, edible and non-edible oils. In addition to vegetable oils, there are other sources of biofuels, such as microalgae, waste frying oil, animal fat, fish oil, pyrolysis oil, which constitute the third generation of biofuels. These sources of biofuel present promising alternatives that address the challenges encountered by previous generations of feedstocks. They overcome the obstacles related to availability, economic feasibility, impact on the food chain, and adaptability to climatic conditions, etc. [42]. One strength of biodiesel is its superior ignition quality, caused by its higher cetane number when compared to traditional diesel fuel. Another advantage is that biodiesel can be utilized in diesel engines with little or no engine modifications [43]. However, the use of biodiesel also presents certain weaknesses, such as its tendency to degrade more quickly than fossil diesel fuel, particularly in cold temperatures. Despite these weaknesses, biodiesel presents various opportunities for sustainable energy production, such as the utilization of non-edible feedstocks and the potential for carbon sequestration.

India has the potential to become a major global producer of biodiesel due to its ability to source non-edible oils, which can be easily harvested. Biodiesel production relies heavily on non-edible oils derived from trees such as the Jatropha tree (Jatropha cursas), Karanja (Pongamia pinnata), and Mahua (M. indica). These trees are a significant source of fuel and are widely utilized in India and Southeast Asia [44]. Jatropha curcas and Pongamia pinnata are two trees that possess exceptional properties for biodiesel production. They are adaptable to a wide range of soil types and require minimal input and management. Additionally, these trees have low moisture demands, and start producing seeds after three to five years of plantation. With a 25-30% oil content, they offer a rich source of oil for biodiesel production.

Furthermore, the productive life of these trees extends beyond 40 years [45]. Biodiesel production using feedstocks such as rapeseed oil, palm oil, castor oil, and sunflower oil has been previously considered. However, due to their negative impact on food crops, their use as biodiesel feedstocks has been limited. **Fig. 1.3** shows some of the non-edible biodiesel feedstock available in India.

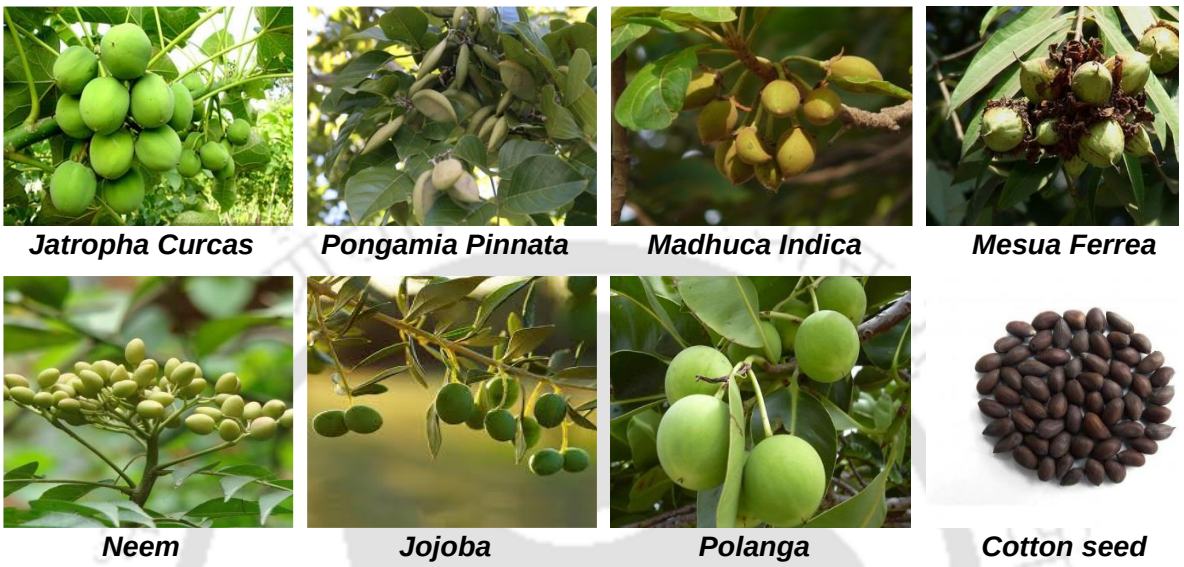

Fig. 1.3 Non-edible biodiesel feedstock

1.4.1.2. Biogas

Biogas is emerging as a viable alternative energy source for internal combustion engines, and can replace a significant portion of fossil fuels in times of oil crisis. Other advantages of biogas include its potential to mitigate greenhouse gas emissions and its ability to be produced from a variety of organic waste sources. The adoption of biogas as a fuel source presents opportunities for sustainable energy production, as well as reduced dependence on finite fossil fuels. Biogas is produced from anaerobic digestion of organic matters such as cattle dung, food waste, agricultural waste etc. The biogas composition varies according to parameters such as humidity, gas pockets, and variations of the waste location [46–48].

Biogas primarily contains 50 -75% of methane (CH_4), 25 - 45% of carbon dioxide (CO_2), 0 -10% of nitrogen (N_2), 1 - 2% of hydrogen (H_2), 0 - 0.5% of hydrogen sulphide (H_2S) and 0 - 2% of oxygen (O_2) [49]. The amount of CH_4 present in the biogas mainly defines the quality and energy content of the gas. Higher values of CH_4 signifies high heating value and generates blue flame while burning in air [36]. Makareviciene *et al.* [49] reported the variation in the calorific value of biogas concerning to CH_4 concentration, i.e. 60% and 96% of CH_4 has a calorific value of 21.5 MJ/m^3 and 35 MJ/m^3, respectively. National standards are maintained

in some of the countries where the CH_4 concentration is restricted not to be less than 96%, and CO_2 should not be more than 4%. Moreover, the presence of excessive sulphur, hydrogen and water vapour in biogas is restricted due to its corrosive nature inside the engine. The standard of biogas can also be tested with the Wobbe index, which indicates the fuel quality based on its higher heating value. Some national standards for biogas are shown in **Table 1.1** [49]. Bureau of Indian Standards (BIS) has prepared an Indian Standard on biogas (bio-methane)-specification (IS 16087:2013) with a motive to provide safe engine operation, fuel system protection and less greenhouse gas emission. This standard provides a general guideline for the composition and quality of biogas considering its application in different areas such as stationary engines, automotive, thermal and piped supply network. **Table 1.2** shows the requirements of biogas for the mentioned application with standard test method [50].

Table 1.1 National standards for biogas used in transport [49]

Specification	Countries					
	France	Sweden	Netherland	Germany	Austria	Switzerland
Methane (%vol)	96	>97	-	-	96	>96
Carbon dioxide (%vol)	<2.5	<4	<6	<6	<3	<6
Hydrogen sulphide (mg S/N m^3)	<5	<15	<5	<5	<5	<5
Hydrogen (%vol)	<6		<12	<5	<4	<4
Total sulphur (mg S/N m^3)	<30	<23	<45	<30	<10	<30
Oxygen (%vol)	<1	<1	<0.5	<0.5	<0.5	<0.5
Calorific value (MJ/N m^3)	38.52-46.08	-	31.6-38.7	30.2-47.2	38.5-46.0	38.5-47.2

Table 1.2 Requirements for Biogas (Bio-methane) [50]

Characteristics	Requirements	Test methods
Methane (%vol), *Min*	90	IS 15130 (Part 3)
Moisture, mg/m^3, *Max*	16	IS 15641 (Part 2)
H_2S, mg/m^3, *Max*	30.3	ISO 6326-3
CO_2+N_2+O_2 (%vol), *Max*	10	IS 15130 (Part 3)
CO_2 (%vol), *Max*	4	IS 15130 (Part 3)
O_2, (%vol), *Max*	0.5	IS 15130 (Part 3)

1.4.1.3. Producer Gas

Producer gas obtained from biomass gasification contains about 40% combustible gases, i.e., H_2 and CO containing 18–20% each along with 2% of CH_4. The remaining non-combustible part is mainly consisting of N_2 and CO_2 [51,52]. Selection of biomass feedstock, upstream and downstream condition of gasification process primarily defines the composition of PG, calorific value, gas outlet temperature etc., which ensures its suitability to run internal

combustion engine [40,53]. Biomass particle size, density and moisture content are important parameters to be considered to achieve better quality gas composition.

Producer gas is a low energy density fuel having low product-reactant mole fraction (0.87) contributes to the de-rating of the engine [51,54,55]. Some fundamental data of producer gas compared with other combustible gases are presented in **Table 1.3**. Yet, H_2 in PG with low energy density enhances the laminar flame speed which minimizes the knocking intensity caused by preignition problems. Moreover, presence of inert gases like CO_2 and nitrogen (N_2) suppresses the pre-flame reaction and also controls engine knock [56–59]. PG with higher concentration of H_2 delivers high thermal efficiency and also lowers the emission of unburned CO and HC by substituting carbon particles in the fuel mixture. But, high combustion flame temperature due to H_2 raises the heat release rate and cylinder pressure which are responsible for higher NO_X emission. In reverse, presence of carbon monoxide (CO) in PG lowers the adiabatic flame temperature and controls the release of NO_X pollutant. Moreover, higher fraction of CO_2 in PG increases the specific heat capacity of the fuel mixture, which diminishes the in-cylinder combustion temperature leading to lower NO_x emission [60–63].

Table 1.3 Producer gas properties compared with other combustible gases [51]

Fuel+ Air	LCV (MJ/kg)	A/F ratio at Ø=1 (mass)	Mixture density (MJ/kg)	Ø (limit)		S_L (limit) (cm/s)		S_L (cm/s) at Ø=1	Peak flame temperature (K)
				Lean	Rich	Lean	Rich		
Hydrogen (H_2)	121	34.4	3.41	0.01	7.17	65	75	270	2400
Carbon monoxide (CO)	10.2	2.46	2.92	0.34	6.80	12	23	45	2400
Methane (CH_4)	50.2	17.2	2.76	0.54	1.69	2.5	14	35	2210
Producer gas (PG*)	5.0	1.35	2.12	0.47	1.60	10.3	12	50	1800

PG*= 20% H_2; 20% CO and 2% CH_4

1.5 Emission standards

Stringent laws are necessary to limit exhaust emissions from vehicles that rely on fossil fuels, as they contribute to air pollution. The vehicular air pollution first attempted to measure in the USA in 1965. Then in 1970, the first European vehicle emissions limits were implemented, and by 1982, controlled emissions levels had decreased by approximately 50% compared to 1970 levels [23]. The first European emissions standard for new vehicles was Euro 1, which came into effect in 1992. Over time, more rigorous emissions standards were introduced, including Euro 2, Euro 3, Euro 4, Euro 5, and Euro 6. **Table 1.4** presents the European emission standards for diesel and gasoline vehicles. The Ministry of Environment and Forests initiated

the first regulations to control vehicle emissions in India in 1989 under the Environment (Protection) Act [64]. **Table 1.5** shows the Indian emissions standards for heavy diesel vehicles, while **Table 1.6** shows the Indian emissions standards for dual fuel diesel engines.

Table 1.4 European emissions norms for diesel and gasoline vehicles, g/km [65]

Norms	Vehicle type	CO	HC + NOx	PM	NO_x	HC
1992-Euro 1	Diesel	2.72	0.97	0.14	-	-
	Gasoline	2.72	0.97	-	-	-
1996-Euro 2	Diesel	1.0	0.7	0.08	-	-
	Gasoline	2.2	0.5	-	-	-
2000-Euro 3	Diesel	0.64	0.56	0.05	0.5	
	Gasoline	2.3	-	-	0.15	0.2
2005-Euro 4	Diesel	0.5	0.3	0.025	0.25	-
	Gasoline	1.0	-	-	0.08	0.1
2009-Euro 5	Diesel	0.5	0.23	0.005	0.18	-
	Gasoline	1.0	-	0.005	0.06	0.1
2014-Euro 6	Diesel	0.5	0.17	0.005	0.08	-
	Gasoline	1.0	-	0.005	0.06	0.1

Table 1.5 Indian emissions norms for heavy diesel vehicles [65]

Norms	CO (g/km-hr)	HC (g/km-hr)	NOx (g/km-hr)	PM (g/kW-hr)
1991 Norms	14	3.5	18	-
1996 Norms	11.2	2.4	14.4	-
India stage 2000 norms	4.5	1.1	8.0	0.36
Bharat stage-II	4.0	1.1	7.0	0.15
Bharat Stage-III	2.1	1.6	5.0	0.10
Bharat Stage-IV	1.5	0.96	3.5	0.02

Table 1.6 Dual Fuel Diesel (Genset) Engine Emission Norms [65]

Power Limit	Emission Limits (g/kWh)			Smoke Limit (light absorption coefficient, m^{-1})
	NO_x + HC	CO	PM	
Up to 19 kW	≤ 7.5	≤ 3.5	≤ 0.3	≤ 0.7
19 ≤ kW ≤ 75	≤ 4.7	≤ 3.5	≤ 0.3	≤ 0.7
75 ≤ kW≤ 800	≤ 4.0	≤ 3.5	≤ 0.2	≤ 0.7

1.6 Objective of the study

Emission reduction, and enhanced thermodynamic efficiency in internal combustion engine along with sustainability is the matter of concern while meeting the targets of COP27 and COP28. To achieve these targets, researchers are focusing on exploring the potential of biofuels in IC engine based on the availability of fuels and technological maturity. The existing research findings highlights the use of biodiesel extracted from various plant source as pilot fuel for IC engine operation. Additionally, BG and PG are gaining traction as promising alternatives for standalone power generation. In the published literature, use of biodiesel and gaseous biofuels have been reported. However, there is no literature on use of biodiesel blends as pilot fuel and two gaseous biofuels together for reduction of emission and maximization of thermodynamic efficiency by varying the engine parameters. The production of biogas and producer gas from locally available raw materials can provide a continuous supply of gaseous fuel for long-term applications. However, significant research and development efforts are required to select appropriate raw materials for fuel production, characterize the fuel, test its energy conversion efficiency and performance, optimize the system, and evaluate the economic feasibility of these alternative fuels. Addressing these key areas of research can significantly promote the use of biodiesel-biogas/producer gas as a competitive alternative fuel for clean energy production and rural applications.

Based on the current challenges and research gaps, the present contribution is focused to perform a systematic experimental analysis for a diesel engine powered by BG and PG using biodiesel-diesel blend as pilot fuel. The operating parameters considered for this investigation are compression ratio (CR) and injection timing (IT). The motivation of this present investigation is to provide a perfect combination of biodiesel-biogas-producer gas as the alternative fuel for clean energy generation for rural electrification.

The following objectives have been addressed in the present investigation:

- To analyse the performance, combustion and emission characteristics of a diesel engine using different tri-biodiesel-diesel blends to be applied as pilot fuel for dual fuel operations
- To investigate the performance, combustion and emission characteristics of a dual fuel diesel engine run by simulated biogas (SBG) and producer gas (SPG) using tri-biodiesel-diesel blends as pilot fuel.
- On-field investigation on improvement of diesel engine characteristics powered by biogas-producer gas mixture with biodiesel blends as pilot fuel.

1.7 Organization of the thesis

This thesis comprises of seven chapters. **Chapter 1** introduces the motivation, background and objectives of the present work. **Chapter 2** presents the detailed literature review on diesel engine run on biodiesel-diesel blends, application of biogas and producer gas on diesel engine under dual fuel mode followed by the research gap and scopes of work. **Chapter 3** explains the experimental setup description and procedure. **Chapter 4** discusses the results of diesel engine experiments carried out with tri biodiesel-diesel blends for selection of pilot fuel. **Chapter 5** discusses the experimental findings observed with simulated biogas, simulated producer gas and mixture at different operating condition. **Chapter 6** discusses the results of the experiment performed with raw biogas-producer gas (on-field generation) mixer based on DF engine performance, combustion and emission characteristics. **Chapter 7** summarizes the key findings of the experimental investigation and scopes for future work.

2

Literature Review

Chapter Outline:

2.1. Introduction
2.2. Dual fuel engine combustion mechanism
2.3. Application of biogas in dual fuel diesel engine
2.4. Application of producer gas in dual fuel diesel engine
2.5. Government's initiatives in decentralization
2.6. Summary of the literature
2.7. Scope of the present work
2.8. Summary of the chapter

CHAPTER 2: LITERATURE REVIEW

2.1 Introduction

The internal combustion engine has undergone significant evolution over the years. J. J. E. Lenoir (1822-1900) developed the first commercial two-stroke engine using a coal gas-air mixture, but it had only 5% thermal efficiency [66]. Around the same time in 1867, N. A. Otto (1832-1891) and E. Langen (1833-1895) developed a more efficient engine running on gas with a free piston and rack mechanism, achieving an efficiency of 11% [67]. In 1876, Otto proposed the first prototype four-stroke engine, known as the spark-ignition (SI) engine, which laid the foundation for modern automotive engines [68]. In 1892, Sir Rudolf Diesel developed the compression ignition (CI) engine, which had even higher efficiency than the SI engine [69]. This engine was based on the reversible cycles proposed by French Engineer Sadi Carnot in 1824 [70]. In 1898, a patent application was filed by Sir Rudolf Diesel, proposing a method for igniting and regulating combustion in internal combustion engines using a less reactive gaseous fuel and a more reactive secondary fuel. This patent was accepted in 1901 and marked an early attempt to ignite a less reactive fuel in a 4-stroke internal combustion engine. Today, the ability to ignite a premixed charge of a low reactivity fuel like natural gas and air using a high reactivity fuel like Diesel, or operating solely on the high reactivity fuel, is a key feature of a dual-fuel combustion strategy [71].

The dual-fuel engine faced commercial obstacles for several years due to its mechanical complexity and rough running caused by auto-ignition and knocking. It was not until 1939 when the National Gas and Oil Engine Co. in Great Britain produced the first commercial dual-fuel engine. This engine, fueled by town gas or other gaseous fuels, was relatively easy to operate and mainly used in areas where low-cost stationary power production was necessary [72]. The production of dual fuel engines ramped up during World War II in Great Britain, Italy, and Germany because of a shortage of fossil oil. As concerns about the negative environmental impacts of fossil oil use and the faster depletion and rising prices of fossil fuels grew after the war, the development and evolution of dual fuel engines were accelerated [73]. During that time, various types of gaseous fuels such as coal gas, sewage gas, and methane were used in traditional diesel engines [27]. However, after World War II, due to economic and environmental considerations, the dual-fuel engine was further developed and applied to a wide range of uses, including stationary power production, road transportation, and marine transport, including long and short haul trucks and buses [72]. Researchers worldwide are currently exploring different gaseous fuels as a viable alternative to traditional fossil fuels.

A variety of alternative fuels, including biogas [49,74,75], producer gas [76–78], hydrogen [79–81], methane [82–85], natural gas [86–88], compressed natural gas (CNG) [89,90], and liquefied petroleum gas (LPG) [91–93] have been successfully used for diesel engines under dual fuel mode. Apart from that, the use of renewable liquid fuel, such as biodiesel, either in pure form or blended with diesel [56,94–99] has become a popular practice due to its effectiveness in initiating combustion in dual fuel operation.

Considering the high potential uses of BG and PG in existing diesel engine, numerous studies have been performed to understand the effect of engine different operating parameters such as load, speed, compression ratio, ignition advance, injection pressure, pilot fuel mass, gaseous fuel composition etc. on the performance, combustion and emission characteristics of the dual fuel compression ignition (DFCI) engine. This chapter provides a comprehensive review on the BG and PG application in the DFCI engine.

2.2 Dual fuel engine and combustion mechanism

Diesel engines can be converted to run on gaseous fuels efficiently. These engines are called 'dual fuel engines' or 'gas diesel engines', where the gaseous fuel is mixed with the air to form the charge and a liquid fuel (pilot fuel) is used to ignite the charge. There are two different ways dual-fuel engine can be operated; in the first type a lean mixture of fuel gas and air is compressed in the combustion chamber and in the second type, the gaseous fuel injected at very high supply pressures directly into the engine cylinder so that the fuel burns into the wake of the earlier injected and already ignited liquid fuel jet. **Fig 2.1** show the two different mode of operation for dual-fuel engine.

A DF engine is a conventional compression ignition (CI) engine where the gaseous fuel is mixed with the air to form the charge, and a small quantity of liquid fuel is injected to ignite the charge [27,100]. However, the combustion of the DF engine starts similarly as CI engine, but the propagation of a flame front occurs in a fashion similar to the SI engine [100]. The DF combustion mechanism comprises of five stages as shown in **Fig. 2.2**. The first stage (AB) is the pilot fuel ignition delay which stays for a more extended period compared to conventional diesel operation and occurs because of the presence of reduced oxygen concentration in the charge resulting from air substitution by gaseous fuel. Next stage (BC) is the premixed combustion of pilot fuel, where an abstemious rise of pressure can be seen due to the ignition of a small amount of pilot fuel. The high self-ignition temperature of the gaseous fuel results in ignition delay of the gas-air mixture, known as primary fuel ignition delay (CD). This ignition delay is shorter than the initial ignition delay. There is a reduction of pressure until

the actual combustion of fumigated gas starts. Unstable rapid combustion of primary fuel (DE) is noticed after the delay where flame propagation is initiated by the spontaneous ignition of pilot fuel resulted in a pressure rise. After this rapid pressure rise, the slower burning rate of gaseous fuel and diluent present in the pilot fuel ends up with Diffusion combustion stage (EF), and it continues well into the expansion stroke. Heat release phenomenon of DF engine illustrates the continuation of combustion to expansion stroke [72]. Diesel fuel operation indicates contrary heat release before the main start of combustion due to the cooling effect of the injected liquid fuel which cannot be seen in DF operation due to the occurrence of primary fuel pre-oxidation process before pilot fuel injection.

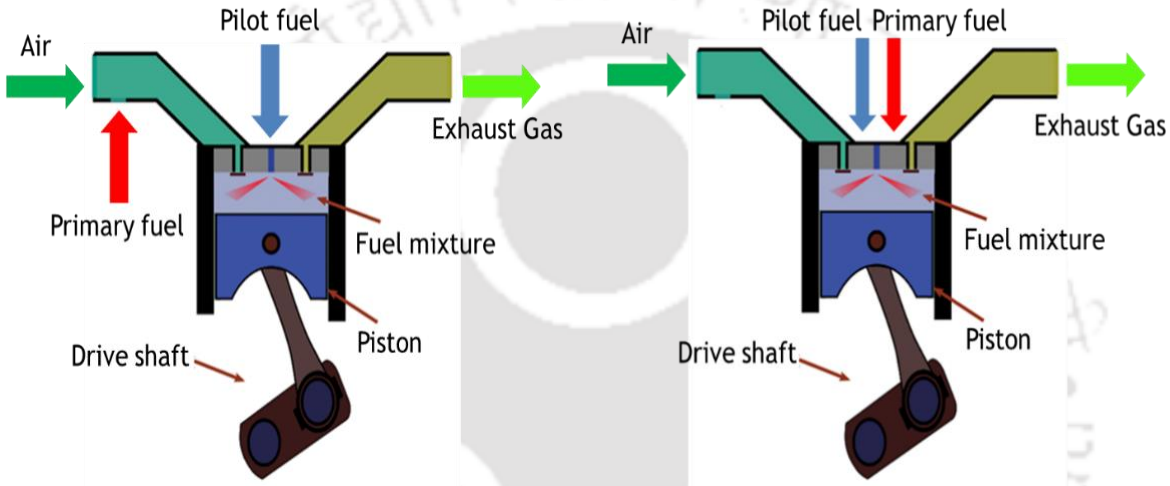

Fig. 2.1 DF engine mechanism (a) premixed injection (b) direct gas injection

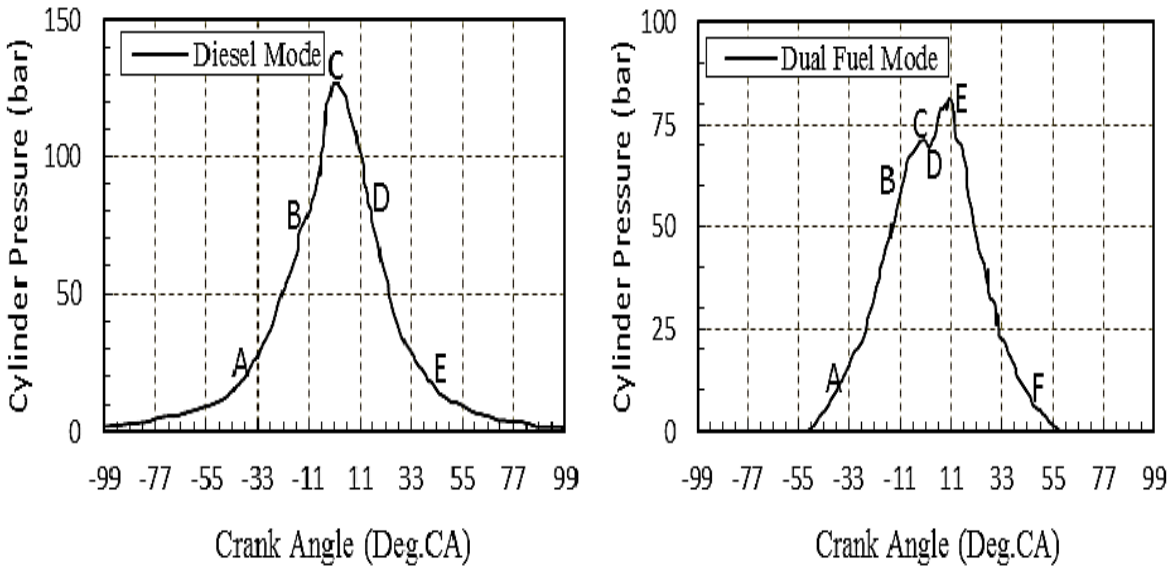

Fig. 2.2 Comparison of P-θ diagram for diesel and dual fuel mode [72]

2.3 Application of Biogas in dual fuel diesel engine

2.3.1 Biogas properties

Dual fuel combustion mechanism is a more complex phenomenon compared to single fuel mode. The sharing of combustible and non-combustible components in biogas makes the combustion mechanism even more complicated. Qian *et al.* [101] reported that the combustion of CO, CH_4 and H_2 present in biogas primarily describes the combustion phenomenon considering the effect of dilution due to the presence of CO_2. The selection of raw materials and preparation technologies changes the composition of biogas, which directly influences the combustion mechanism. The presence of CH_4 resulted in higher octane rating and auto-ignition temperature of biogas enhances the anti-knocking property compared to conventional diesel and makes it suitable for use at higher CRs [102–104]. Barik *et al.* [105–107] stated that biogas application with high CRs increases the thermal efficiency and reduces smoke and NOx emissions. Moreover, the low carbon content of CH_4 compared to conventional diesel positively reduces the pollutant level in the exhaust. On the other hand, Pattanaik *et al.* [94] reported that higher auto-ignition temperature of biogas acts as a heat sink during the combustion process which results in decrease of combustion temperature during biogas induction. A summary of biogas properties investigated by selected researchers is presented in **Table 2.1**.

Table 2.1 Summary of biogas fuel properties

Author	Type of Biogas	Chemical composition	Octane no	Density (kg/m^3)	Stoichiometric A/F ratio	LHV (MJ/kg)	Max flame speed (m/s)	Auto ignition temperature	Boiling point (^{0}C)
Tippayawong *et al.* [47]	Raw biogas	65.6% CH_4, 26.4% CO_2, 2% O_2, 6% N_2, (V/V)	-	1.1	-	24.5	-	-	-
Duc and Wattanavichien [48]	Raw biogas	73% CH_4, 19.7% CO_2, 1.2% O_2, 6.5% N_2	-	0.9145	17.23	26.17	-	-	-
Bedoya *et al.* [108]	Raw biogas	60% CH_4, 40% CO_2 (V/V)	-	-	6.05	23.73	-	-	-
Yoon and Lee [75]	Raw biogas	30-73% CH_4, 20-40% CO_2, 0-5% O_2, 1-3% H_2, 5-40% N_2	130	0.65-0.91	17.2	26.17		632-813	(-) 126-162
Cacau *et al.* [109]	Raw biogas	60% CH_4	-	-	-	23.73	-	-	-
Barik *et al.* [105–107,110]	Pongamia pinnata (25%) + cow dung (75%)	73% CH_4, 17.37% CO_2, 1.5% O_2, 1.45% H_2, 6.5% N_2, 0.23% H_2S (V/V)	130	1.2	17.23	27.53	25	600-650	-120 to -150
	Cow dung biogas	50-70% CH_4, 25-30% CO_2, 0-3% O_2, 0-1% H_2, 0-10%, N_2, 0-3% H_2S (V/V)	110	1.31	15.3	17.2	21	640-670	-130 to -162

	Jatropha curcus biogas	60-68% CH_4, 20-30% CO_2, 1-2% O_2, 0-1% H_2, 1-15%, N_2, 0-2% H_2S (V/V)	-	-	-	-	-	-	-
	Municipal solid waste biogas	40-60% CH_4, 20-40% CO_2, <1% O_2, 2-20%, N_2 (V/V), 40-100 ppm H_2S	-	-	-	-	-	-	-
	Upgraded biogas	90.6% CH_4, 4.26% CO_2, 0.4% O_2, 4.7% N_2, 0.04% H_2S (V/V)	132	0.91	15.75	41.32	32	540	-
Ramesha *et al.* [111]	Raw biogas	70-75% CH_4, 25-30% CO_2, 0-5% O_2, 5-20% N_2	130	0.65-0.91	-	26.17	-	632-813	(-) 126-162
Bora and Saha [112]	Raw biogas	60% CH_4, 40% CO_2 (V/V)	-	0.91	10	20.67	-	1086	-
Verma *et al.* [113]	Raw biogas	75.2% CH_4, 19.7% CO_2, 1.2% O_2, 3.9% other gases	-	0.928	8.93	27.22	-	-	-
F.Z. Aklouche *et al.* [46]	Raw biogas	60% CH_4, 40% CO_2 (V/V)	110	1.33	6.04	17.65	-	-	-
P. Rosha *et al.* [36]	Raw Biogas	60-70% CH_4, 30-40% CO_2, 0.18% CO, 0.18% H_2 (V/V)	120	1.2	6	20-25	0.25	700	-

2.3.2 Performance characteristics of biogas run DF engine

The performance of the engine is primarily investigated by analyzing Brake Thermal efficiency (BTE), Brake specific fuel consumption (BSFC), Exhaust gas temperature (EGT), Liquid fuel replacement (LFR) etc. The study related to this is presented below.

Tippayawong *et al.* [47] modified a single cylinder, direct-injection, CI engine to run in DF mode with biogas and observed to have higher thermal efficiency compared to regular diesel operation. A maximum thermal efficiency of 23% at 1500 rpm was obtained. An experimental investigation was conducted by Duc and Wattanavichien [48] in indirect injection biogas premixed charged DFCI engine and estimated an energy conversion efficiency of 29.1% at a speed of 1800 rpm which is higher than diesel with 28.7%. Yoon and Lee [75] varied the load from 20% to 100% and observed its effect on BTE with different pilot fuel. The authors found that BTE increases with increasing load for both single and DF modes. However, BTE is slightly lower in the case of DF operation. Authors mentioned that biogas residuals, combusted residual gas, a higher rate of fuel flow, lower combustion temperatures are the factors responsible for lower BTE. Moreover, the induction of a large amount of biogas-air mixture and higher heat transfer through the wall decreases the flame propagation speed and increases the negative compression work that resulted in lower BTE. Again, Luijten and Kerkhof [95] stated that BTE is hardly affected at higher loads, but largely depends on the CH_4/CO_2 ratios in biogas composition. Cacua *et al.* [109] examined the effect of O_2 enriched air on the and improvement in the thermal efficiency of 28% was estimated at 40% load with 27% O_2 in the air. This better thermal efficiency with enriched O_2 is mainly because of higher propagation of diesel flame fronts and increased overall mixture temperature resulted from an increased pre-oxidation reaction. Bedoya *et al.* [108] investigated the effects of mixing system on engine performance with simulated biogas (60% CH_4, 40% CO_2). CR plays a significant role in DF engine performance. Bora *et al.* [114] investigated the effect of CR on BTE and observed an increment with an increase in CR. The authors calculated the variation of BTE at CR of 16, 17, 17.5 and 18. The fact behind the increase of BTE is the rise of pressure and temperature at high CR which in turn allows more quantity of biogas to undergo complete combustion. Moreover, at high CR, fast micro-explosion occurs which initiates early pilot fuel ignition and provide adequate time for combustion [35,112,114]. Barik *et al.* [110] also analyzed the effect of CR and obtained an increase in BTE at high CR. Effect of ignition advance on the performance of a DF engine has been evaluated by different researchers [35,105,115]. Bora and Saha [35] obtained a maximum BTE of 23.62% at injection timing (IT) of 29° BTDC using Emulsified Rice bran biodiesel as pilot fuel. Barik *et al.* [105] varied the IT from 21.5° to 27.5°

using Karanja biodiesel as pilot fuel and observed an optimum result with IT of 24.5° BTDC. Authors mentioned that advancement of IT allows early injection of pilot fuel into the chamber which provides sufficient time to form a homogeneous mixture with the charge resulting in an efficient burning. Moreover, greater vaporization of pilot fuel due to advanced IT also improves the BTE [35,115]. Aklouche *et al.* [46] demonstrated the effect of equivalence ratio (ER) and obtained an increment of 13% when the ER increased from 0.3 to 0.7 (**Fig. 2.3**). The author justified that at a higher value of ER, a homogeneous mixture of biogas-air is achieved which allows complete combustion. On the other hand, Sarkar *et al.* [116] reported a drastic reduction in BTE with the increase in ER. Authors described that with the increase in ER consumption of biogas increases, which results in a reduction of pre-ignition reaction rate and flame propagation.

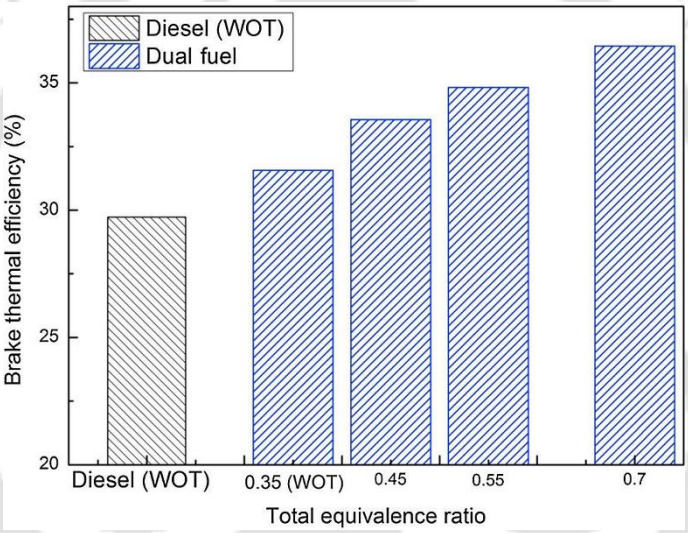

Fig. 2.3 Evolution of the BTE with equivalence ratio [46]

In DF operation BSFC is the sum of primary and pilot fuel flows. Variation in engine load majorly influences the BSFC in both single and DF operations. According to Yoon and Lee [75], at high load condition, the rate of combustion increases due to higher air-fuel ratio and combustion temperature, and resulted in the improvement of BSFC. Pattanayak *et al.* [94] also reported improvements in BSFC at higher load over 60%. Similar results have been presented by Ramesh *et al.* [111]. Moreover, as discussed by Barik and Murugan [117], at a low energy density of biogas, the low temperature inside the cylinder and slow burning of biogas also cause high BSFC in DF operation. In a different experiment, a gradual decrease in the BSFC was noted by Barik and Murugan [115] when the IT was increased from 23° BTDC to 27.5° BTDC. The authors explained that ignition advance allows higher injection of fuel into the cylinder during controlled premix combustion which increases the heat release rate which

positively affects the biogas combustion rate during diffused combustion. Effect of exhaust gas recirculation (EGR) on specific fuel consumption was analyzed by Makareviciene *et al.* [49] and assessed a significant reduction in fuel consumption at low loading condition with EGR (**Fig. 2.4**). Upgraded biogas (90% CH_4) along with Diethyl ether (DEE) was used by Barik *et al*. [110], and obtained a significant reduction in BSFC at high CR. Moreover, energy specific fuel consumption (ESFC) has been evaluated by Aklouche *et al.* [46] and reported a lower for DF mode compared to conventional mode. The authors also added that an increase in the ER resulted in reduction in ESFC.

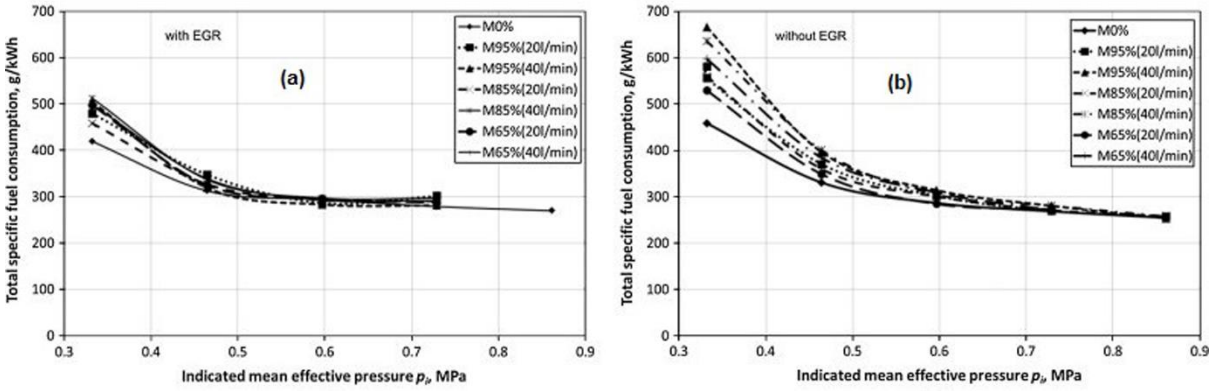

Fig. 2.4. Variation in the total fuel consumption; (a) with EGR, (b) without EGR [49]

The relationship of EGT with different engine operating parameters considered to be an essential factor for performance evaluation. Yoon and Lee [75] obtained a lower EGT for DF operation in comparison with single fuel mode and explained that the extended ignition delay of biogas shifted the combustion process to occur in the power stroke. This behaviour caused a rapid decrease of cylinder pressure, and temperature resulted in lower EGT. Additionally Barik and Sivalingam [74] described that the biogas-air mixture absorbs heat energy to reach its self-ignition temperature which reduces the adiabatic flame temperature during the combustion process resulting in the reduction of EGT. On the other hand, Bora and Saha [118] obtained higher EGT in case of DF operation compared to diesel mode at all load condition. According to the authors, slow combustion of biogas is the reason, which lowers the extraction period of power from fuel and allows the combustion products to come out at a higher temperature. The increase of CR during DF operation showed significant improvement in lowering the EGT as reported by Bora and Saha [112]. The authors mentioned that higher CR leads to early combustion of biogas which simultaneously increases the burning velocity of biogas-air mixture. This behaviour lowered the time required for complete combustion and resulted in the reduction of EGT. However, Barik *et al.* [110] explained that at high CR, biogas-air mixture attains a higher temperature during combustion that resulted in higher EGT.

Experimental studies conducted by Barik and Murugan [115,119] addressed the effect of advanced IT on EGT. According to the authors, increased cylinder temperature at advanced IT resulted in higher EGT. This is because advanced IT allows more extended spray of pilot fuel which enhances the rate of combustion.

The energy share of diesel and biogas during DF operation can be analyzed using two different parameters, i.e. liquid fuel replacement (LFR) and biogas flow rate (BFR). An experiment conducted by Tippayawong *et al.* [47] on DF operation reported a diesel replacement of 90% at an engine speed of 1800 rpm. Duc and Wattanavichien [48] found higher diesel replacement of about 93-94% at low load compared to about 43-49% at high or full load. Biogas energy share was calculated by Barik and Sivalingam [74] with increasing brake power and biogas flow rate (BFR). With an increase in brake power, higher thermal load is imposed on the engine which increases the diesel consumption and biogas energy share reduces. On the other hand, at full load condition, increase in the BFR contributed to a high diesel replacement percentage (**Table 2.2**). Bora *et al.* [114] conducted DF experiments at different CRs and observed that with the increase of CR, there was an increase in LFR but decrease in BFR. Raw biogas (59% CH_4) and scrubbed biogas (89% CH_4) were considered for DF operation by Verma *et al.* [120]. The authors observed that at 100% load, scrubbed biogas resulted in higher LFR and lower BFR compared to raw biogas. An outstanding deal of work was published by Sarkar and Saha [121] on preheated biogas run DF engine using ternary blends of diesel, biodiesel and ethanol (D-B-E). It was revealed that blended fuel composition of TB-3 (D72-B20-E8) attained the maximum replacement for all load. Moreover, for TB-3 blend, a higher BFR was obtained for engine load of 20%. The author concluded that TB-3 blend with optimum cumulative properties shows low blended fuel energy share and also improve the performance of the engine.

Table 2.2 Energy share by diesel and biogas at full load [74]

Biogas flow rate (kg/h)	Energy share by diesel (%)	Energy share by biogas (%)
0.15	92.74	7.26
0.30	85.17	14.83
0.45	77.47	22.53
0.60	69.95	30.05

2.3.3 Combustion characteristics of biogas run DF engine

Combustion of fuel is a vital process because it addresses essential matters like diverged and effective utilization of fuel resources while curbing environmental pollution and enhancing safety. Parameters that mostly affect the combustion characteristics in DF operation are

Ignition delay (ID), Net heat release rate (NHRR), Peak cylinder pressure (PCP) and in-cylinder Pressure.

The introduction of the gas-air mixture produces substantial variation in the physical and transport properties as well as the heat transfer parameters to a lesser extent. Changes in the partial pressure of oxygen and residual present in the chamber directly influences the preignition reaction activity and the energy release associated with it. These are several reasons due to which the trend of ignition delay (ID) in DF engines differs to that of diesel engine operation [27]. Effect of engine load, CRs, advanced IT, diesel/biodiesel blend etc. on ID has been investigated by various researchers [35,114,116,118]. Experiments conducted by Bora and Saha [118] revealed a continuous decrease in ID and linear increment of PCP with increase in load for both single and DF operation. For the complete load spectrum, ID for diesel operation was estimated to be lower than DF operation where PCP unveiled the opposite trend. Bora *et al.* [114] evaluated the combined effect of load and CR on ID and PCP and reported similar findings on the variations as discussed above. The author illustrated that at a low load, low temperature of the chamber resulted in high ID which reduces gradually with the load. Further, it was explained that biogas having high overall heat capacity reduces the charge temperature which significantly delays the pilot fuel ignition. Higher CR in DF operation increases the temperature and pressure that improves the preignition reaction of the mixture and partial combustion products and affects the pilot fuel ignition. On the other hand, Bora and Saha [35] revealed longer ID with advanced IT and explained the reason as, injection of pilot fuel at low gas temperature environment. According to the authors, increase in the mass of injected fuel might be the reason behind higher PCP at higher loading condition. Moreover, for a particular load, the advancement of IT and the use of high CR in DF mode resulted in a rise of PCP. This advancement of IT in the DF engine enables the development of fuel rich mixture zone inside the combustion chamber which resulted in higher PCP [72,122]. Sarkar and Saha [116] investigated the cyclic variation of PCP at two different engine load with different operating condition (**Fig. 2.5**). The author stated that cyclic variation of PCP is essential regarding the use of high octane number fuel like biogas. The authors predicted the cyclic variation of PCP by considering 80 cycles and observed higher values at higher load and higher global ER. The authors also informed that lower cyclic variation indicates stable engine operation.

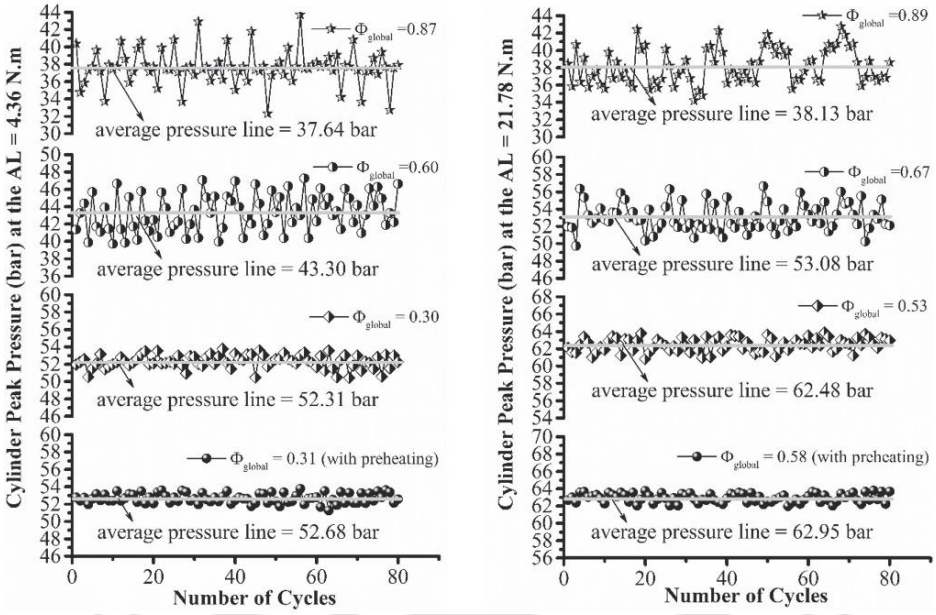

Fig. 2.5 Characteristics of cyclic variation of PCP at different engine loads [116]

In-cylinder pressure is one of the most important to be evaluated to conceptualize the combustion characteristics as it directly impacts the performance and exhaust emission of the engine [105]. An experiment was conducted by Bedoya *et al.* [108] considering two different air-gas mixing mechanism named SM1 and SM2 and analyzed the cylinder pressure variation. SM2 system showed a better result where higher PCP of about 10% occurred closer to top dead centre (TDC). Cacua *et al.* [109] found higher cylinder pressure with enriched O_2% in compared to atmospheric air condition for all loads. The authors described that O_2 enrichment lowers the ID at premixed combustion period due to high reactivity of both fuels, which resulted in high cylinder pressure. Aklouche *et al.* [46] analyzed the pressure curve in the range of 10 to 20° crank angle (CA) before top dead centre (TDC) and reported that the compression stroke in DF operation starts at low pressure compared to diesel operation. The reason is that the lower volumetric efficiency resulted from reduced air flow rate. The history of cylinder pressure variation with the CA at full load for diesel, biodiesel and biodiesel DF mode was investigated by Barik *et al.* [105] varying the IT. The PCP for biodiesel DF operation, was higher than biodiesel single fuel operation at IT of 23° BTDC. Again a maximum cylinder pressure was obtained to be 87.6 bar at 3.17° CA ATDC with advanced IT of 27.5° BTDC. This happens because of delay in the ignition process leading towards higher rate of pressure rise during premixed combustion stage [48,115,123]. It was also noticed that with the advancement of IT, the point of PCP shifted towards TDC. It is because of earlier combustion process which burns maximum amount of fuel before TDC and shifted the PCP closer to TDC [72,115,122]. A rate of pressure rise indicates impact of pressure on cylinder head and block [124].

Moreover, it also defines the smooth or noisy behaviour of the engine. The acceptable range of rate of pressure rise is 8 bar/°CA to maximize engine durability and minimize knocking [125]. An experiment was conducted by Barik *et al.* [126] to analyze the rate of pressure rise with different biogas flow rate (**Fig. 2.6**). The maximum rate of pressure rise was obtained to be 6.4 bar/°CA for DF mode with BFR of 1.2 kg/h. It was explained that delay of the combustion process and the addition of more fuel during this delay period is the reason behind the higher rate of pressure rise for DF mode [127][128,129].

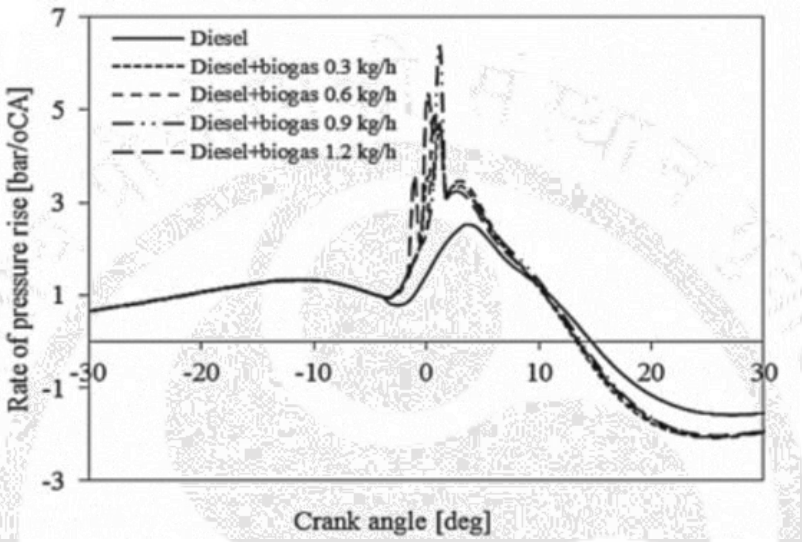

Fig. 2.6 Rate of pressure rise with crank angle at full load [126]

Simultaneous burning of two fuels inside the cylinder having different properties and characteristics make the heat release rate (HRR) in DF process enormously complex. In DF mode, there are three different processes of combustion, i.e. pilot fuel combustion, gaseous fuel combustion in the immediate locality of the ignition kernel and the pre-ignition activity with following flame propagation which resulted in HRR [130]. It fundamentally depends on the fuel-air mixture (pilot+gas+air), mass flow rate and lower heating value (LHV) of both the liquid as well as gaseous fuel [126]. In case of idling condition, combustion rate in the early combustion period, ID and mixture formation broadly define the HRR during the premixed combustion stage [48]. Bora and Saha [118] reported a higher HRR for single fuel mode compared to DF mode and explained it to be because of lower calorific value of biogas. In an investigation, Bora and Saha [112] observed an increment in the NHRR when the CR was increased from 17 to 18 and is depicted in the **Fig. 2.7**. On the other hand, Barik and Murugan [115] noticed a higher value of maximum HRR for DF compared to single diesel operation. It was clarified that due to prolonged ID, biogas accumulation increases and resulted in the extension of the flammability zone around the pilot fuel [107,131,132]. The authors also

noticed an early occurrence of HRR for DF operation with advanced injection and stated that it allows the early start of combustion with a maximum amount of fuel burning and releasing more amount of energy during the premixed phase.

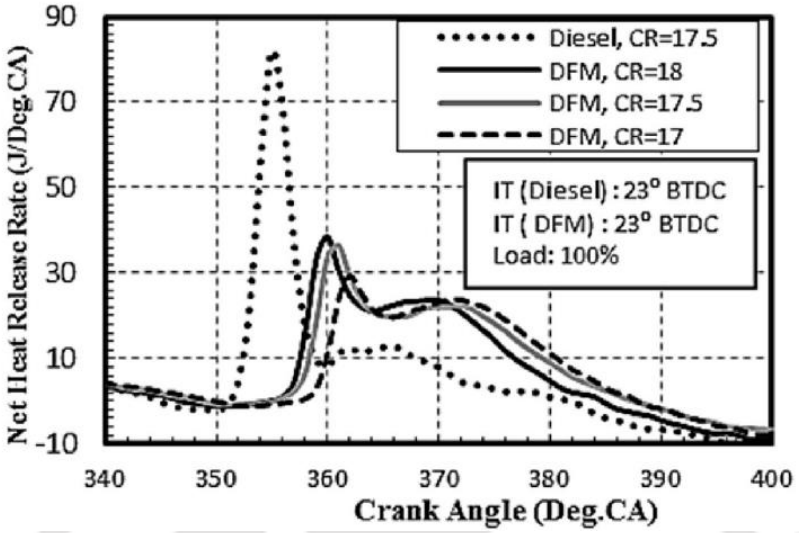

Fig. 2.7 Effect of CRs on NHRR for biogas run DF engine using rice bran biodiesel as pilot fuel [112]

The crank angle interval between 10% and 90% mass burned of the accumulated heat release is defined as the combustion duration (CD). It was estimated by Barik and Murugan [119] that CD increases with increase in load which is mainly because of higher consumption of fuel at higher loads. Moreover, authors observed longer CD for biogas DF operation and claimed the reason behind this is slower burning rate of biogas. Again, Yoon and Lee [75] suggested that the addition of biogas in DF mode deteriorates the combustion process and lengthen the CD. The effect of global ER and preheating on CD was investigated by Sarkar and Saha [116]. With an increase in global ER, CD increases for all loading condition compared to single fuel diesel mode. Moreover, in DF operation, increase in the gaseous fuel flow rate resulted in a decrease in CD due to faster premixed combustion in the presence of clean gaseous fuel [132].

2.3.4 Emission characteristics of biogas run DF engine

IC engine generates a considerable amount of unwanted emission during the combustion process. Impurities present in fuel and air, non-stoichiometric combustion, dissociation of nitrogen etc. are the primary causes responsible for engine emission. The major constituents of the DF emission are generally made up of NO_X, hydrocarbon (HC), oxides of carbon (CO and CO_2) and PM.

Controlling and reducing the emission of NO_X in a diesel engine is a significant concern as it is considered to be one of the most harmful emissions composed of nitrogen monoxide (NO)

and nitrogen dioxide (NO_2). Out of these two, major contribution comes from NO which accounts for more than 90% of NOx emission inside the cylinder [31]. The favourable temperature for NO formation is above 1800 K, and it grows exponentially with the increase of cylinder temperature [133,134]. It has been stated that the Zeldovich mechanism predominantly contributes to the total formation of NO_X in diesel engine combustion conditions [135–137]. Whereas, the formation of NO through prompt mechanism is most predominant in rich flames [138]. An experiment was conducted by Aklouche *et al.* [46] with varying ER and estimated the NOx emission for DF operation with synthetic biogas. ER =0.7 reported with a maximum reduction of 42% compared to conventional diesel mode. It was described in the study that induction of biogas reduces the concentration of O_2 in air which simultaneously affects the NOx formation. Kalsi and Subramanian [139] studied the effect of CO_2 percentage and simulated biogas energy share on NOx emission and found to be decrease with increase in CO_2 content and energy share. However, the effect of energy share was predominant over CO_2 content. Moreover, a significant reduction in the smoke emission was also observed by the authors in case of both part and high loads when the CO_2 content (50%) increased in the biogas (**Fig. 2.8**). The authors explained that induction of biogas enhances degree of charge homogeneity and substitutes high carbon content liquid fuel that resulted in reduction of soot formation rate. Similar observation has also been reported by Ramesha *et al.* [96] by conducting DF experiments with biodiesel blend as pilot fuel. It was stated that low flame temperature and high oxidation of soot particle during DF operation with biodiesel resulted in reduced smoke opacity [132].

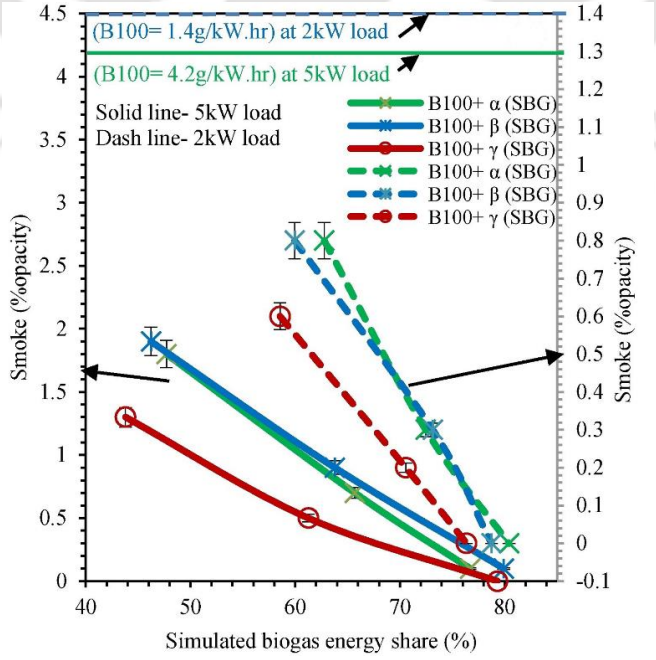

Fig. 2.8 Variation of smoke emission with simulated biogas energy share [139]

CH_4 and CO are the two primary pollutants of the exhaust gas in biogas run DFCI engine. Bedoya *et al.* [108] used two different gas mixture and observed highest CH_4 emission at 40% load for both the mixer which gradually decreases with the increase of load. It was reported that at higher load, ER approaches the stoichiometric value and combustion is dominantly influenced by the charge temperature. During low load condition, the flame front propagation does not spread out in all direction of the cylinder from the ignition point and resulted with the presence of unburned methane in the exhaust stage [140]. However, as reported by Cacua *et al.* [109], increase of oxygen enrichment level in air significantly improves the flame front propagation instigated from pilot fuel and possibly reduces the CH_4 emission even in lower load. Contrarily, the authors observed that CO emission to be increased with O_2 enrichment level. With 25% enrichment, there was a reduction of 19.5% at 40% load was obtained by the authors. Authors mentioned it to be because of decrease in fuel-air equivalence ratio and increase in biogas preignition reaction. Makareviciene *et al.* [49] in their study observed the variation of CO at different gas flow rate and IT. The authors reported a noticeable rise in CO emission with increased gas supply and advanced IT (**Fig. 2.9**), because it permits to reach higher combustion temperature and better carbon oxidation due to early ignition of fuels. Moreover, the effect of EGR was also studied by the authors and reported three times higher emission of CO with EGR compared to without EGR operation of biogas DF mode. It was explained in such a way that with EGR, higher amount of oxygen is replace by the CO_2 present in the biogas as well as in exhaust gas which in turn lowers the air-fuel ratio.

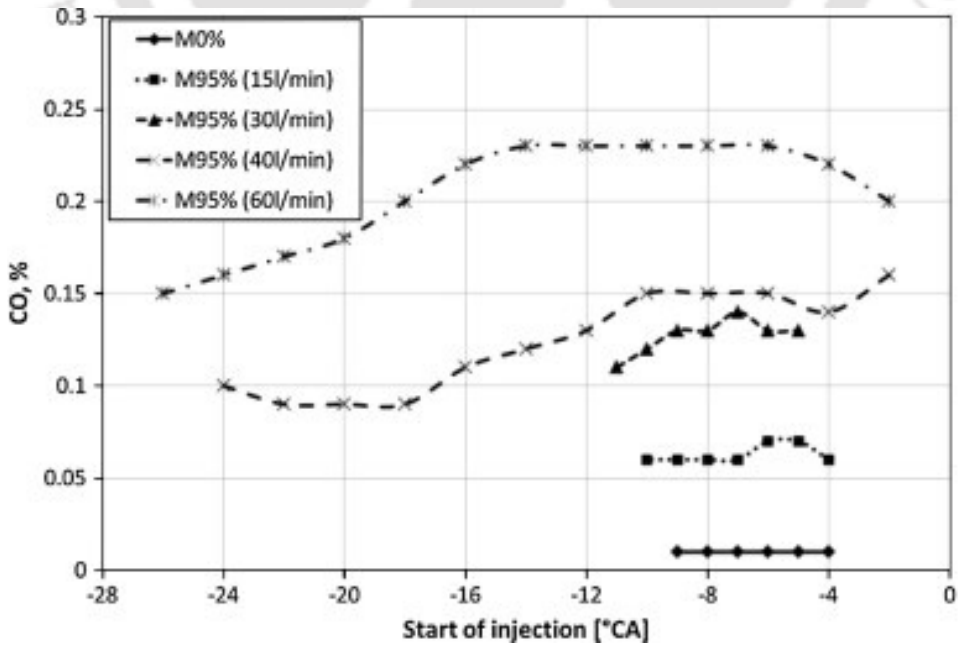

Fig. 2.9 Variation in CO emissions with the start of IT and the quantity of biogas supplied [49]

In the same context, it also important to enlighten the matter of unburned hydrocarbon (HC) emission resulted from incomplete combustion of fuel. In case of DF engine, biogas with low flame velocity augments the formation of HC in comparison with single fuel mode [120]. Moreover, it has been reported that excessive amount of induced biogas through the inlet manifold leads towards formation of rich gas-air mixture which resulted in partial burning of fuel [141,142]. Barik and Murugan [123] presented the emission of HC at different biogas flow rate as a function of biogas energy share. From the **Fig. 2.10**, it is evident that HC level goes with the increase in biogas energy share. The important fact to be mentioned here is the use of biodiesel as pilot fuel has immensely benefitted the DF operation in terms HC and CO emission reduction. Biodiesel containing more oxygen (about 11% by weight) has a lower stoichiometric need of air that enables the biogas-air mixture to undergo complete combustion [75]. Again, advanced IT and high cetane number of biodiesel jointly improves the combustion process by decreasing the fuel-rich zone inside the chamber [143]. It has also been stated in a study that DF operation with high CRs rises the temperature inside the chamber which improves the combustion process of the fuels [112]. On the other hand, better combustion deals with the formation of CO_2 inside the combustion chamber. With adequate amount of oxygen present during the combustion process, 1450 K is the threshold temperature at which the oxidation of CO to CO_2 is initiated [144,145]. Again, the temperature of 1500 K is considered to be the equilibrium reaction temperature for CO_2 formation [146]. In addition to this, biogas comprises of higher amount of CO_2 (around 40% by volume) which is again responsible for higher CO_2 emission during biogas DF operation as reported by Bora and Saha [118]. An interesting findings were reported by Kovacs and Torok [147] (**Fig. 2.11**). The author observed increase in the inert content (CO_2 content of biogas [V/V%]) of biogas, increases the maximum CO_2 proportion of the exhaust gas (CO_{2max}% [m^3 of CO_2/m^3 of fuel]) but decreases the exhaust gas amount (V_{fg}), while the CO_2 emission (CO_2 [m^3/m^3fuel]) is observed to be constant. Sarkar and Saha [116] stated that preheating of biogas-air intake charge stimulates the combustion process of biogas DF engine and improves the emission of CO_2 from part to higher loads. It was also reported during the study that with increase in the global ER, CO_2 emission increases which significantly indicates about better combustion efficiency at this situation.

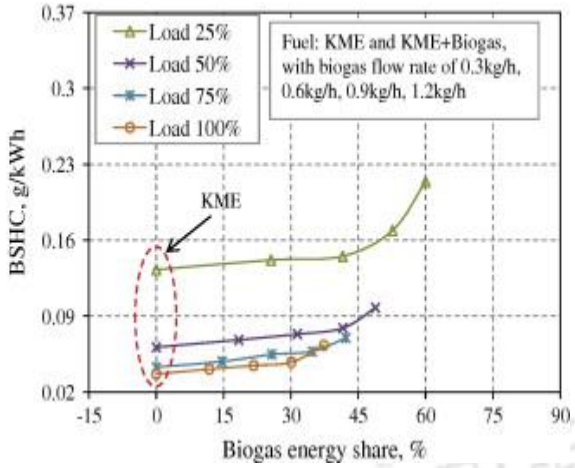

Fig. 2.10 Variation of HC emissions with biogas energy share [123]

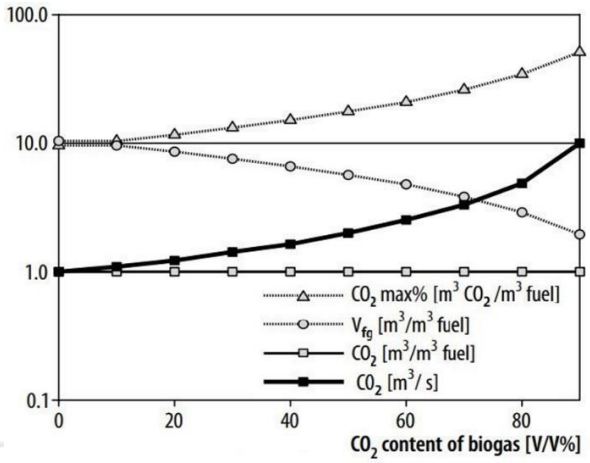

Fig. 2.11 The values of CO_{2max}, V_{fg} and CO_2 emission of different biogases against CO_2 (inert) content [147]

A summary comprising various research work performed by different researchers on biogas DF operation has been presented in **Table 2.3**.

Table 2.3 Summary of engine characteristics of CI engine operated with biogas

Investigator	Test Engine	Pilot fuel	Experimental condition	Research findings
Bora *et al.* [112]	Single cylinder, 3.5 kW, DI, natural aspirated (NA), water cooled, VCR diesel engine	Biodiesel	➢ Effect of different CR	➢ Higher BTE and LFR while lower BSEC and EGT with respect to CR ➢ Drop in ID and PCP while increase in NHRR with respect to CR ➢ Lower CO and HC emission while higher CO_2 and NOx emission
Bora *et al.* [148]	Single cylinder, 3.5 kW, DI, natural aspirated (NA), water cooled, VCR diesel engine	Diesel	➢ Effect of different CR and IT	➢ Maximum BTE at 29° BTDC ➢ Higher LFR and ID while lower rise in EGT with increase in injection timing ➢ Reduction in CO and HC emission while increase in CO_2 and NOx emission ➢ Optimum condition of DFM obtained at 29°BTDC and CR 18
Boral *et al.* [118]	Single cylinder, 3.5 kW, DI, natural aspirated (NA), water cooled, VCR diesel engine	Rice bran methyl ester, pongamia oil methyl ester, palm oil methyl ester	➢ Effect of different pilot fuels	➢ Maximum BTE of 19.97% for RBME Higher BSEC, EGT and ID using POME and lower using RBME pilot fuel ➢ Lower CO and HC but higher NOx and CO_2 emission using RBME pilot fuel
Bora *et al.* [149]	Single cylinder, 3.5 kW, DI, natural aspirated (NA), water cooled, VCR diesel engine	Diesel	➢ Effect of different CR	➢ Higher BTE while lower BSEC and EGT with increase in CR ➢ Lower ID while higher NHRR at high CR ➢ CO and HC emission decreases while CO2 and NOx emission increases with CR
Barik *et al.* [106]	Single cylinder, 4.4 kW four stroke, CI, air cooled, naturally aspirated, DI, constant	Karanja oil methyl ester	➢ Effect of varying IT	➢ 26 ^{0}CA BTDC gave an overall better result ➢ Higher BSFC, BTE, HRR and peak cylinder pressure ➢ Lower HC and CO also smoke emissions but higher NOx

Barik *et al.*[107]	Single cylinder, 4.4 kW four stroke, CI, air cooled, naturally aspirated, DI, constant	Diesel	➢ Effect of flow rate of gas	➢ Better performance and lower emission at 0.9 kg/h ➢ Longer ID ➢ Higher peak cylinder pressure maximum HRR ➢ Higher BSFC and lower BTE ➢ Higher HC and CO but lower NOx and smoke emissions
Barik *et al.* [150]	Single cylinder, 4.4 kW four stroke, CI, air cooled, naturally aspirated, DI, constant	Karanja oil methyl ester	➢ Effect of different IT	➢ IT of 24.5 ^{0}CA BTDC gave better performance and lower emissions ➢ Lower PCP but longer II ➢ Higher BTE with increasing IT ➢ Lower HC, CO and smoke but higher NOx emissions
Barik *et al.* [74]	Single cylinder, 4.4 kW four stroke, CI, air cooled, naturally aspirated, DI, constant	Diesel	➢ Effect of different biogas flow rates	➢ Optimum results obtained with 0.6 kg/hr BFR ➢ Higher BSEC and maximum diesel replacement of 30% obtained ➢ CO and HC emission were higher by 16% and 21%, respectively while NO emission reduces by 35% at optimum flow rate
Barik *et al.* [119]	Single cylinder, 4.4 kW four stroke, CI, air cooled, naturally aspirated, DI, constant	Karanja methyl ester biodiesel	➢ Effect of diethyl ether(DEE) injection	➢ Optimum results obtained at IT of 24.5° and 4% DEE injection ➢ Increase in BTE of 2.3% and decrease in BSFC of 5.8% ➢ Lower ID and higher NHRR at 4% DEE injection. ➢ CO and HC emission reduced while NO emission increased with DEE injection

Barik *et al.* [110]		Karanja methyl ester biodiesel	➢ Effect of different CR	➢ Optimum results obtained at CR 18.5 with 6% DEE injection at 24.5° BTDC ➢ Higher BTE and lower BSFC with increase in CR ➢ Decrease in CO and HC emission while an increase in NO emission obtained with increase in CR
Barik *et al.*[123]		Diesel	➢ Effect of different biogas flow rates	➢ Optimum results obtained with 0.9kg/hr BFR ➢ ID and PCP decreases with decrease in BFR ➢ CD longer by about 1.6-4.7° CA in DF mode ➢ Higher maximum HRR obtained with increase in BFR
Barik *et al.* [126]		Karanja methyl ester biodiesel	➢ Effect of different biogas flow rates.	➢ Optimum results obtained at BFR of 0.9kg/hr with biogas energy share of 30.1-58.4% ➢ Higher BSEC and lower EGT with increase BFR ➢ CO and HC emission increases while CO_2 and NO emission decreases with increase in flow rate
Yoon and Lee[75]	Four-cylinder, turbocharged, pre chamber CI engine with a single overhead cam (SOHC) diesel engine	Biodiesel Diesel	➢ Use of biodiesel as pilot fuel	➢ Lower BTE and higher BFSC at low loads ➢ Lower peak combustion pressure and HRR due to prolonged ID ➢ Lower NOx and soot emissions but higher emission of HC and CO
Himsar Ambarita [151]	Single-cylinder/4 strokes and Horizontal, Water cooled diesel engine.	Diesel	➢ Effect of biogas flow rate	➢ Optimum BTE obtained for BG70M at 2 l/min BFR and 1200 W load ➢ Higher BSFC and LFR obtained at lower load and speed ➢ CO and HC emission with BFR

Verma *et al.* [113]	A direct-injection, single cylinder, four stroke diesel engine	Diesel	➢ Effect of biogas, CNG and hydrogen at different IT and load	➢ Higher Exergy efficiency for biogas at advanced IT ➢ Highest PCP and ID were obtained for H_2 and Biogas ➢ EGT highest for Diesel-H_2 and lowest for Diesel-Biogas ➢ CO and HC emission lowers while NOx emission increases with advance IT
Mustafi *et al.* [152]	Single cylinder, DI, water cooled	Diesel	➢ Effect of natural gas and different proportions of biogas	➢ Lower BSFC obtained using natural gas ➢ NHRR increases with decrease in CH_4 concentration in biogas ➢ Lower CO and HC emission while higher NOx emission for natural gas compared to biogas
Ramachandra[153]	Single cylinder, direct injection diesel engine	Biodiesel	➢ Effect of Karanja methyl ester oil biodiesel ➢ Effect of biogas flow rate	➢ BTE and BSFC decreases while EGT increases with increase in BFR ➢ Reduction of BTE and BSFC obtained using biodiesel compared to diesel ➢ CO, HC and CO_2 emission decreases and NOx emission increases with increase in BFR
Gund *et al* [154]	Constant speed, Four Stroke ,Water cooled CI engine	Diesel Biodiesel	➢ Effect of biogas flow rate	➢ Maximum BTE is obtained at 90% of full load and 1.0m^3/hr ➢ Volumetric efficiency is minimum at 0.5 m^3/hr BFR ➢ Higher HC emission and lower CO_2 emission obtained at higher BFR
Ramesha *et al.*[111]	Single cylinder, water cooled CI engine	Biodiesel	➢ Effect of B20 fish biodiesel as pilot fuel	➢ Lower levels of BTE, CO and HC emission under DF mode compared to single fuel mode ➢ Higher BTE while lower BSFC at high load. ➢ CO, HC and NOx emission increases with load

Mahla *et al.* [155]	Single-cylinder, four-stroke, naturally aspirated, direct-injection diesel engine	Diesel	➢ Effect of different biogas flow rate ➢ Effect of load	➢ Optimum biogas flow rate observed to be 2.2 kg/h ➢ Lower BTE and higher BSEC for DF mode for all load ➢ Higher CO and HC emission while lower NOx emission under DF mode ➢ BTE increases while NOx emission increases with load
Pattanaik *et al.*[94]	4- stroke, single cylinder, constant speed,direct injection, water cooled, and CI engine	Biodiesel	➢ Use of Karanja biodiesel as pilot fuel	➢ Lower BTE and EGT while higher BSFC obtained for DF mode ➢ Higher HC and CO emission but lower NOx emissions
Duc and Wattanavichien[48]	Kubota – RT120, Single cylinder, IDI, diesel engine	Diesel	➢ Long term application of engine with biogas– diesel DF mode	➢ Higher efficiency while lower EGT obtained for DF mode ➢ Soot emission was lower while higher HC emissions ➢ High consumption of lube oil
Nathan et al[156]	Modified single cylinder, water cooled, DI, HCCI engine	Diesel	➢ Effective use of biogas in HCCI engine ➢ Effect of CO_2 percentage in biogas	➢ Brake thermal efficiency decreases in DF mode of operation ➢ Lower cylinder pressure ➢ Higher HC and CO emission and lower NOx emission
Mahla *et al.* [157]	Four-stroke, single cylinder ,direct injection, air cooled diesel engine	Diesel Biodiesel	➢ Effect of additive n-propanol	➢ Lower BTE with additive compared to diesel mode ➢ HC and NOx emission increases while smoke opacity decrease with n-propanol
Bedoya *et al.* [108]	Lister petter TR2, DI, two cylinders, NI, air cooled diesel engine	Diesel	➢ Effect of super charged mixing system ➢ Pilot fuel quality	➢ Higher BTE ➢ Higher pilot fuel substitution ➢ Lower CO emissions

Makareviciene *et al.*[108]	Four cylinder, 1Z type turbocharged DI, diesel engine	Diesel	➢ Effect of CO_2 concentration in biogas	➢ Increase in fuel consumption and decrease in thermal efficiency with increasing CO_2 ➢ Lower HC and CO but Higher NOx emission at low CO_2 content
Cacua *et al.*[109]	Four stroke, two cylinders, naturally aspirated, air cooled diesel engine	Diesel	➢ Effect of O_2 enriched air	➢ Higher BTE with 27% enriched O_2 ➢ Lower ID and Lower CH_4 emission
Cacua *et al.*[158]	Four stroke, three cylinders, naturally aspirated, water cooled, C.I. engine	Diesel	➢ Micro-trigeneration system based DF operation	➢ Higher thermal efficiency with Micro-trigeneration ➢ Maximum diesel substitution of 50% ➢ CO_2 emission decreased by 24.9%
Ray *et al* .[159]	Single cylinder 3.7 KW, water cooled diesel engine	Diesel	➢ Effect of engine speed	➢ BTE decreases while BSFC increases with Engine speed ➢ Higher CO_2 and NOx emission with speed but comparatively lower in DF mode ➢ CO and HC emission are lower with the use of biogas
Sarkar and Saha[121]	Four-stroke, mono cylinder, water-cooled, DI, NA, 3.5-kW, 1500 rpm constant speed diesel engine	Diesel, Jatropha biodiesel, Ethanol (D-B-E)	➢ Effect of different blends of pilot fuel	➢ Optimum results obtained for blending ratio D72-B20-E8 ➢ Maximum BTE of 26.73% and diesel fuel replacement of 57.75% obtained ➢ Higher drop in CO and HC emission while lower drop in NOx emission for optimum blend

Sarkar and Saha[116]	Four-stroke, mono cylinder, water-cooled, DI, NA, 3.5-kW, 1500 rpm constant speed diesel engine	Diesel	➢ Effect of various global ER ➢ Effect of preheating of biogas	➢ BTE improves with pre heating ➢ Diesel replacement and biogas energy share increases with ER ➢ Higher ID with increase in E.R while with preheating ID decreases and NHRR increases ➢ Higher CO, HC and CO_2 emissions and lower NOx emission at high ER ➢ Preheating results in higher CO_2 and NOx emission while lower CO and HC emission
Sarkar and Saha [160]	Four-stroke, mono cylinder, water-cooled, DI, NA, 3.5-kW, 1500 rpm constant speed diesel engine	Diesel	➢ Effect of ethanol blended diesel and biogas with preheating ➢ Effect of ER	➢ Increase in BTE with 5% methanol addition while preheating and methanol blend decreases BSEC5% methanol blend and preheating results in lower CO and HC emission and higher NOx emission ➢ With ER, BTE decreases while HC and CO emission increases
Verma *et al.* [120]	Single cylinder, 4 stroke, VCR, water cooled diesel engine	Diesel	➢ Effect of scrubbed biogas in engine performance	➢ BTE is higher while BSEC and EGT is lower in scrubbed biogas DF operation ➢ Lower percentage of diesel replacement, ID and NHRR ➢ Higher NOx emission while lower CO, HC and CO_2 emission
Kalsi *et al.* [139].	7.4 kW, single cylinder, naturally aspirated Kirloskar (EA10) diesel engine	Pongamia pinnata biodiesel	➢ Effect of simulated biogas (blending of natural gas with CO_2)	➢ BTE decreased with increase in biogas energy share (higher CO_2 content) ➢ Higher ID and lower heat release rate with higher biogas energy share ➢ CO and HC emission increased while NOx emission decreased with higher biogas energy share.

Aklouche *et al.* [46]	Single cylinder engine LISTER-PETTER, speed range 0-2500	Diesel	➢ Effect of ER	➢ Higher BTE and lower BSEC with increase in ER ID and NHRR increases with increase in ER ➢ Reduction of HC, CO, CO_2 and NOx emission by about 77%, 58%, 14%, and 24%, respectively with increase in ER from 0.35 to 0.7
Luijten and Kerkhof [161]	Single cylinder, naturally aspirated, direct injection, four stroke diesel engine	Diesel	➢ Effect of biogas quality	➢ Thermal efficiency decreases with increase in biogas quality ➢ Higher thermal efficiency obtained with increase in load ➢ Very small decrease in volumetric efficiency with biogas quality ➢ Lower volumetric efficiency with load
Tippayawong *et al.* [47]	Four-stroke, naturally aspirated, water-cooled, compression ignition engineMitsubishi DI-800, diesel engine	Diesel	➢ Long-term engine operation ➢ Effect of engine speed at fixed load	➢ Higher power output about 7% on average ➢ Neglected wear on 2000 h run ➢ Little carbon deposition inside combustion chamber
Henham and Makkar [162]	Two-cylinder, four-stroke, water-cooled, indirect injection Lister Petter LPWS2 diesel engine	Diesel	➢ Effects of simulated biogas (mixture of natural gas and CO_2)	➢ Overall efficiency drops and EGT increases with higher percentage of CO_2 in natural gas ➢ Diesel replacement of 60% possible without knock ➢ CO is not much effected by CO_2 in simulated biogas
Debnath *et al.* [163]	Direct injection, water cooled, VCR diesel engine.	Palm biodiesel	➢ Effect of emulsified palm biodiesel (WIP) in DF mode	➢ BTE improves by 41% and BSEC reduces by 38% ➢ Higher pilot fuel replacement and lower EGT ➢ Higher ID and PCP using WIP ➢ CO and HC emission are considerably lower while NOx emission is higher compared to raw palm biodiesel

Verma et al. [164]	Four stroke, single cylinder , direct injection, VCR diesel engine	Diesel	➢ Effect of different CR ➢ Effect of EGR	➢ Optimal performance enhancement and emission reduction were obtained with higher CR and EGR ➢ Increase in CR results is higher pilot fuel substitution and exergy efficiencies ➢ Emission of CO and HC decreased with CR while NOx emission is increased ➢ Use of EGR in DF engine results in reduction of NOx emission Maximum exergy efficiency of 22.79% at 5% EGR under full load condition.
Chandrashekar and Gumtapure [165]	Single cylinder, 4-stroke, 5.2 kW, constant speed, direct-injection (DI), natural aspirated (NA), water-cooled diesel engine	Diesel	➢ Effect of methane content in biogas	➢ At full load, BG40 (i.e. 40% CH_4) showed maximum BTE of 15.62%. ➢ While, BG20 showed minimum ignition delay of 13.2° CA. ➢ DF mode resulted in higher PCP than diesel mode for all BG mixtures. ➢ NOx emission for BG40 is 22.71% lower than diesel at 100% load.
Chandrashekar and Gumtapure [166]	Single cylinder, 4-stroke, 5.2 kW, constant speed, direct-injection (DI), natural aspirated (NA), water-cooled diesel engine	Diesel	➢ Effect of pilot fuel injection timing	➢ At full load and advanced IT of 29° BTDC, B20 showed maximum BTE of 30.1%. ➢ At same condition, B60 showed maximum PCP of 64.15 bar, 11.9% higher than diesel mode. ➢ At full load and retarded IT of 25° BTDC, B60 emits 45% lower NOx than diesel.
Sarkar and Saha [167]	4-stroke, single cylinder, water-cooled, DI, NA, 3.5 kW, constant speed diesel engine	Diesel	➢ Effect of compression ratio ➢ Hydrogen enriched biogas	➢ At full load, DF operation showed 32, 34.4 and 36.1% BTE. ➢ Increase in CR resulted in reduction of exhaust gas temperature (EGT). ➢ HEB-diesel DF mode resulted in higher cylinder pressure (CP) than diesel mode. ➢ CO and HC emission drops, whereas NOx increases with increase in CR.

2.4 Application of producer gas in dual fuel engine

2.4.1 Producer gas properties

The quality of producer gas (PG) produced through gasification process and its suitability to run an IC engine largely depend on the selection of biomass feedstock, as well as the upstream and downstream conditions of the process. These factors determine the composition of PG, its calorific value, gas outlet temperature, and other relevant parameters. To optimize the quality of PG, it is important to consider key factors such as the particle size, density, and moisture content of the biomass feedstock. By carefully controlling these parameters, it is possible to achieve a better quality gas composition that is well-suited for use in an IC engine. As reported by Banapurmath *et al*. [168], biomass size of 20-50 mm range having density more than 300 kg/m^3 with a moisture content of about 20% is appropriate for the gasification process. Use of low-density biomass in gasification produces poor quality gas which further resulted in higher fuel consumption. Whereas, high-density biomass generates PG with low tar, char and moisture. The effect of moisture content present in the biomass feedstock greatly affect the gasifier performance and the gas quality as reported by Dasappa *et al.* [169]. Authors stated that with high moisture content feedstock, energy content of the gas decreases as maximum heat is utilized in water evaporation, which also results in tar generation. Sheth and Babu [170] mentioned that gasification temperature is a function of ER, which plays a significant role in PG composition. Authors have also discussed that concentration of combustible gases highly depends on the kinetics of chemical reaction that occurs during the gasification process. Das *et al.* [171] discussed the importance of gasifying medium in the gasification process. The authors have reported that N_2 concentration increases in the PG when air is used as a gasifying medium which resulted in lower heating value between 4 to 6 MJ/m^3. Whereas, the use of oxygen and steam as produces a higher amount of H_2 and CO which subjected to higher heating value between 10-20 MJ/m^3. Mckendry [172] also reported similar findings of the selection of oxidizing medium in the gasification process. It was stated that oxygen or water steam gasification increases combustible components in PG, which allows the rise of calorific value up to 18 MJ/Nm^3 compared to air gasification, which limits the calorific value to 6 MJ/Nm^3. Air as an oxidizing agent, Martinez *et al.* [55] also reported PG with a lower calorific value around 5000 kJ/Nm^3 with 20% H_2, 20% CO and 1% CH_4. Yaliwal *et al.* [40] reported that cleaning of PG is an essential aspect of the gasifier-engine system. Impurities present in the gas may cause different problems like carbon deposition and excess wear in engine components, degradation of lubricating oil, sticky valves and rings etc. These problems resulted in slow starting and heat generation in the engine which directly

affects the engine performance. They have also reported an acceptable limit of impurities present in the PG for IC engine application, i.e. dust<50 mg/m^3, tar<50 mg/m^3 and acids<50 mg/m^3. Again, presence of significantly higher fraction of inactive gases such as CO_2 (12–15%) and N_2 (48–50%) in PG tends to suppress pre-flame reaction which is considered to be one of the reasons of knocking [51,54,173]. It is argued that producer gas is a low energy density fuel and resulted in de-rating of power [40,51,54,55,76,174] compared to higher density fuel like natural gas. Moreover, the lower calorific value of PG also contributes to de-rating of power. However, the energy density of the gas can be improved by passing through a proper cooling system which would allow supply of higher charge into the cylinder consuming less time to stabilize the engine running [40]. Again, as reported by Sridhar *et al.* [51], fuel mixture energy density must be accounted for comparison rather than fuel energy density as it contributes to de-rating of the engine. It is reported that mixture energy density of producer gas is 23% lower compared to CH_4. Moreover, product-reactant mole fraction of producer gas (0.87) is less compared to CH_4 (1.0) which can also contribute to de-rating of the engine. Martinez *et al.* [55] observed the energy density of the producer gas/air mixture to be about 2400 kJ/Nm^3 which is lower than the energy density of 3400 kJ/Nm^3 for natural gas/air mixture. Application of producer gas in high CR engine might be a solution to the de-rating problem. **Table 2.4** presents some of the essential properties of producer gas observed by different researchers.

Table 2.4 Summary of producer gas fuel properties

Author	Feedstock	Producer gas composition									
		CO %	H_2 %	CO_2 %	CH_4 %	N_2 %	HC %	Water vapour (%)	Tar and PM (mg/Nm^3)	Calorific value	Density (kg/m^3)
Singh *et al.* [97,175]	Prosopis Juliflora (gandabaval)	17.6	12.2	14.6	1.06	54.7	-	-	40-52	1042 kcal/Nm^3	-
Banapurmath *et al.* [168]	woody biomass	19	18	10	3	50	-	-	-	5000 kJ/kg	-
Ramadhas *et al.* [176]	coir-pith	18-22	15-19	-	1-5	45-55	0.2-0.4	4	-	-	-
Deshmukh *et al.* [177]	hingan shell	16.192	12.742	15.154	1.411	55.428	-	-	-	4.38 MJ/m^3	-
Roy et al. [53]	Type 1	23.9	30.4	36.6	3.1	6	-	-	-	7.4 MJ/Nm^3	-
	Type 2	27.6	22.3	23.2	2.7	24.2	-	-	-	6.8 MJ/Nm^3	-
	Type 3	22.3	13.7	16.8	1.9	45.3	-	-	-	5 MJ/Nm^3	-
	Type 4	19.4	14.6	16	28.9	21.1	-	-	-	14.4 MJ/Nm^3	-
Deva kumar and Reddy [77]	-	18-22	15-19	-	1-5	45-55	0.2-0.4	4	-	-	-
Banapurmath *et al.* [174,178]	wood	27	14	-	3	-	-	-	-	-	-
	babul wood	18-22	15-19	-	1-5	4.5-5.5	0.2-0.4	4	-	-	-

	honge wood	16-20	12-16	-	1-3	3-6	0.2-0.3	5	-	-	-
Hasan *et al.* [179]	wood	20 ± 4	14 ± 2	12 ± 3	2.5	45	-	-	-	4.2-4.5 MJ/m^3	-
Sombatwong *et al.* [78]	charcoal	27-32.3	3.2-4.2	-	-	57-62	-	-	-	4.2-4.6 MJ/Nm^3	-
Yaliwal *et al.* [34,180,181]	neem	19	14	8-14	3					4.8 MJ/Nm^3	345
	babul	18-20	15-19	8-10	1-5	4.5-5.5	0.2-0.4	4		5.6	360
	honge	20-22	12	12-14	1-3	3-6	0.2-0.3	5		3.9	305
Lal and Mohapatra [182]	sawdust and cotton stalks	18.1	8.2	14	3.1	56.6	-	-	-	4.5 MJ/Nm^3	-

2.4.2 Performance characteristics of producer gas run dual fuel engine

Bhattacharya *et al.* [183] conducted experiments on a gasifier-engine coupled system to estimate the maximum electrical power output and engine-generator efficiency. The author stated that the engine was able to run at a speed of 1500 rpm which was much lower than its maximum speed (2500 rpm). It was also reported that at a maximum possible electrical load of 11.44 kWe during DF operation, the system showed an efficiency of 14.71% which was also much lower than the efficiency of 22.41% showed by diesel operation. The introduction of producer gas allows the engine to operate at a reduced air-fuel ratiowhich hampered the combustion process and resulted in lower efficiency. Producer gas generated from two different types of feedstocks (coir-pith and wood) have been considered by Ramadhas *et al.* [76]and estimated the maximum BTE of at 70% load for both the types. Wood PG had higher calorific value (18.50 MJ/kg) compared to coir-pith PG (16.75 MJ/kg) and showed higher BTE. BTE increases with load to a certain limit of load, it starts reducing because of insufficient oxygen in air-gas mixture for proper combustion. Singh *et al.* [97] conducted DF experiments at different load of 42%, 63%, 84% and 98% with diesel and biodiesel and observed increment in BTE at higher load. It was also observed that DF operation for biodiesel-PG, BTE was higher compared to diesel-PG operation at all loading condition. Specific energy consumption (SEC) is another measure of engine performance which is more reliable than BSFC in terms comparing different fuels having different density, viscosity and calorific values. SEC shows an opposite trend with BTE. Higher BTE indicates lower SEC in DF mode and vice-versa. Uma *et al.* [184] came up with lower SEC at higher load for diesel-PG operation. The authors explained it to be because of lower heating value of PG-air mixture, gas pressure drop at air inlet and lower flame velocity. Similarly, Pathak *et al.* [185] in their report stated that slow combustion process could also cause low BTE to some extent. Again, Singh *et al.* [175] explained that producer gas enters the cylinder at a higher temperature than ambient during the starting of compression stroke which increases the temperature inside the cylinder and simultaneously resulted in higher energy input in case of PG DF operation. Experiments were conducted at higher CR of 18.4 and obtained a significant improvement in case of BTE and SEC. Yaiwal *et al.* [181] conducted DF experiments at three different CR of 15, 16 and 17.5 and observed an increased BTE at high CR. BTE and SEC were determined at different Brake mean effective pressure (BMEP) by Hassan *et al.* [179] and observed increasing and decreasing trend of BTE and SEC with BMEP, respectively. Experimented were performed with different IT (14°, 17°, 20° and 23° BTDC) and obtained a maximum BTE of 22.15% at IT of 23° BTDC for supercharged DF operation. This is may be due to the increase of air charge density, sufficient

mixing of air and PG. Effect of injection timing on BTE was also investigated by Banapurmath *et al.* [168] where they have considered three IT, i.e. 19°, 23° and 27° BTDC. In their experiments, the effect of IT was mostly noticed at higher loading condition, and for a particular load, BTE showed an increasing trend with increasing in IT (**Fig. 2.12**). In a different experiment, Banapurmath *et al.* [56] have fixed the IT at 27° BTDC and investigated the effect of PG carburettor on the performance of DF operation with three different pilot fuel (diesel, Honge oil and Honge oil methyl ester). Introduction of a carburettor resulted in improvement of BTE for all the three conditions. Shrivastava *et al.* [52] carried out DF operation with varying PG flow rate and observed that BTE decreases and SEC increases with an increase in PG flow rate. This may be due to the higher substitution of air at high PG flow rate affected the combustion process. Again, Kashipura *et al.* [186] conducted experiments with four different combustion chamber with varying shapes, i.e. hemispherical, cylindrical, toroidal and trapezoidal and observed maximum BTE with toroidal combustion chamber (TCC). TCC restricts the flame to spreads over the squish zone that improves the mixing of liquid and gaseous fuel. Which in turn resulted in better air motion and less exhaust soot formation.

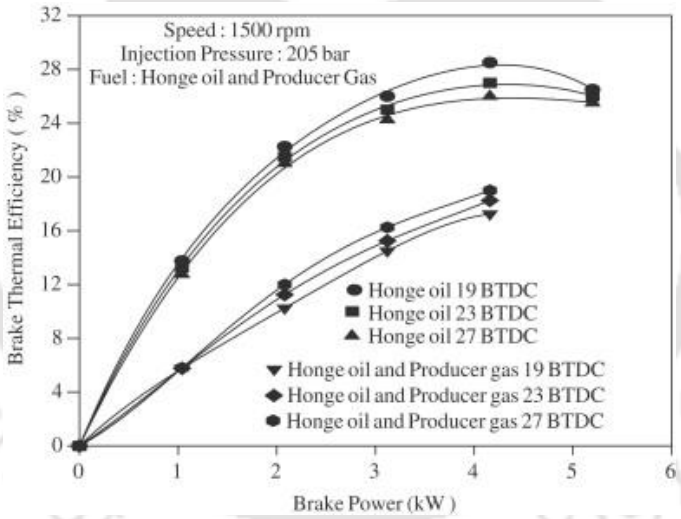

Fig. 2.12 Effect of injection timing and brake power on BTE [168]

Introduction of producer gas contributes some amount of additional energy to the engine due to which the engine speed raises and for maintaining constant engine speed, the governor regulates the liquid fuel supply. Therefore, it can be said that producer gas addition reduces the consumption of liquid fuel to some extent. Ramadhas *et al.* [176] reported that at higher load pilot fuel replacement is lower which is mainly because of incomplete combustion and low calorific value of PG. Dasappa *et al.* [169] conducted experiments and pilot fuel replacement was observed to be higher at lower load. An estimation was made on diesel saving of 14.4 litres per hour which is about 79% replacement at peak load of 57 kWe. A similar

observation is reported by Balakrishnan *et al.* [187] where they observed higher liquid fuel replacement at lower load, and it decreases with increasing load (**Fig. 2.13**). Diesel replacement percentage at advanced IT was compared with standard IT by Lekpradit *et al.* [188] and observed higher replacement with advanced IT. Maximum diesel replacement was obtained at 40% of full load condition. Banapurmath *et al.* [168] reported similar results with higher replacement at advanced IT. Maximum replacement of 67% was obtained for Honge biodiesel at 27° BTDC. Another experiment was conducted by Lal and Mohapatro [182] at varying CR of 12, 14, 16 and 18 and observed that with the increase in CR, the percentage of diesel fuel saving increases. But at higher CR, maximum diesel replacement is observed to be at lower load and vice versa. These results can be explained in a way that at higher CR, high temperature and pressure enhances the combustion of gaseous fuel resulting in high replacement of diesel but at higher load due to the requirement of rich mixture, diesel replacement increases. The authors also estimated the BSFC for the same experiments, which are presented in **Fig. 2.14** and minimum of 0.54 kg/kWh were observed at 3.2 kW with a CR of 18.

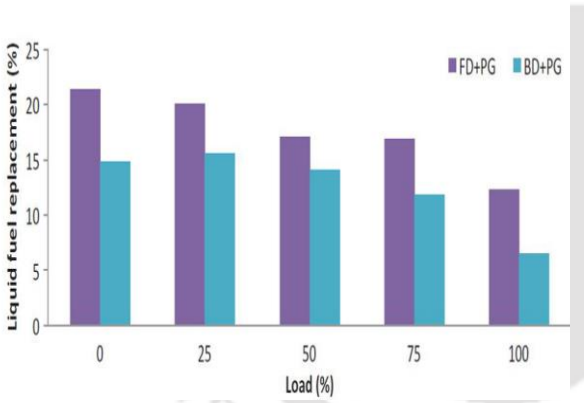

Fig. 2.13 Effect of load on liquid fuel replacement [187]

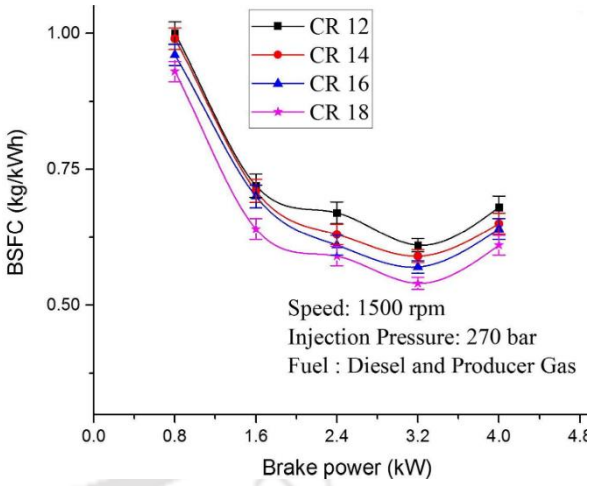

Fig. 2.14 Brake specific fuel consumption at different CR [182]

EGT for DF operation is always found to be higher compared to single fuel operation because of additional energy provided by the gaseous fuel. Ramadhas *et al.* [76] conducted experiments using two different quality producer gas and observed higher EGT in both cases compared to single diesel mode. They reported maximum EGT at higher load and also observed that with an increase in producer gas flow rate, EGT increases. The variation of EGT concerning brake power and the use of different gas carburetor (parallel, basic and Y shaped) was reported by Banapurmath *et al.* [178]. As per results, DF operation with biodiesel showed higher EGT than diesel. On the other hand, for a particular load of 60%, parallel carburettor

resulted in lower compared to basic and Y shaped carburettor. It was also mentioned that low calorific value and high moisture content present in the biomass increases the EGT during PG DF operation. Hasan *et al.* [179] reported that for supercharged DF operation EGT is higher because of entering higher density fuel mixture into the engine. The authors also reported that due to the burning of maximum portion of fuel mixture and achievement of high PCP before TDC, ignition advance resulted in lower EGT. According to Sombatwong *et al.* [78], occurrence of higher combustion rate during later stages in diesel producer gas DF operation resulted in higher EGT. In another experiment, Balakrishnan *et al.* [187] analysed the EGT for DF operation with both diesel and biodiesel and found that at full load, EGT was lower in case of biodiesel DF operation compared to diesel DF operation. Shrivastava *et al.* [52] inducted the producer gas at three different flow rates and observed higher value of EGT at higher flow rates. Again Lal and Mohapatro [182] observed the EGT for different CR and found that with an increase in CR, EGT decreases. From **Fig. 2.15** presented by Yaiwal *et al.* [34], it is clear that decrease in CR increases EGT. Low CR allows combustion of remaining unburnt gases to take place in the diffusion phase instead of premixed phase resulted in high EGT. A similar statement was made by Singh *et al.* [175] that increase in CR resulted in decrease of EGT.

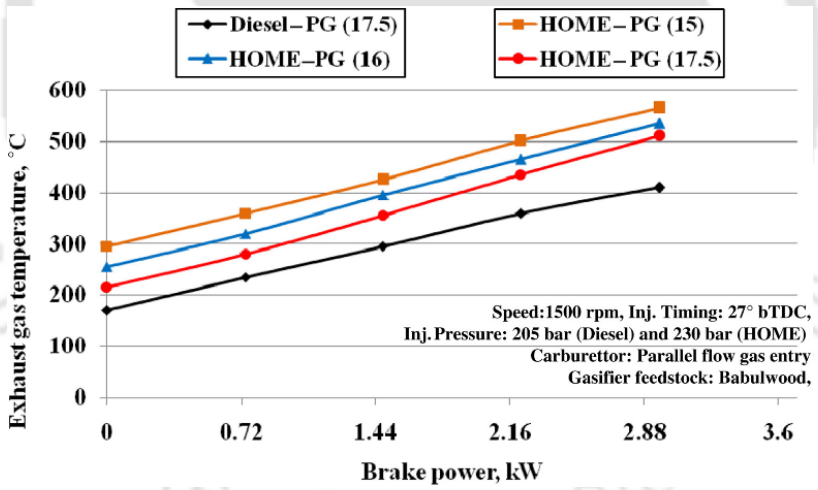

Fig. 2.15 Variation of EGT at different CR [34]

2.4.3 Combustion characteristics of producer gas run dual fuel engine

The pattern of energy release during the combustion process of DF operation is the reflection of complex physical and chemical interaction between the two fuels throughout the combustion process [27]. As discussed in the previous section about the combustion analysis of biogas, a similar comparison of parameters such as ID, PCP and NHRR are conferred in this section. Hernandez *et al.* [189] reported that premixed combustion increases with IT, load, fuel replacement and EGR linearly due to the consequences of the simultaneous burning of

most of the gas with the injected fuel. With the induction of biodiesel, premixed combustion decrease because biodiesel increases the oxygen content in the oxidizing gas and also lowers the intake temperature which resulting in lower injection timing. However, for a particular load, premixed combustion for biodiesel increases with EGR. Roy *et al.* [53] compared the combustion delay of PG with high and low H_2 content for normal and two-stage combustion process (compresses the unburnt gas in the cylinder). . As mass fraction burned (MFB) for producer gas DF engine is in the range of 80-85%, the duration of main combustion is considered to be 10-80% MFB. The author found the normal combustion to be in the range of 24.5-27.5°CA and 38.5-32°CA for high and low H_2 content, respectively. However, for two-stage combustion, a reduced CD of 8-12.5°CA and 12.5-16.5°CA was obtained for high and low H_2 content, respectively. The reason is higher cylinder pressure resulting in higher flame speed under the given conditions. The authors also observed longer ID for DF mode for entire load range due to low burning nature of producer gas [190]. Yaliwal *et al.* [34] analyzed the variation of ID with different CR and observed that when CR increases from 15 to 17.5, the ID reduces by 27.8%. This may be due to the increase in combustion temperature. Raheman and Padhee [98] used Jatropha methyl ester biodiesel in different blends with producer gas and found that the ID decreases with an increase in biodiesel percentage with diesel as shown in **Fig. 2.16**. This variation is due to the presence of oxygen in the fuel which increases the air-fuel mixing rate and also higher cetane number cause an earlier start of ignition. Under turbocharging condition, ID reduces at rated load because turbocharging resulted in more amount of air flow into the combustion chamber and increases the combustion process and reduces ID [191].

Banapurmath *et al.* [168] reported a rise in PCP with load, and while comparing the two different pilot fuel effects in DF mode, higher viscosity and lower volatility pilot fuel showed low PCP due to poor atomization. Lal and Mohapatra [182] calculated the PCP of a DF engine based on different CR and a maximum PCP of 54.49 bar is obtained for CR 18. Hydrogen is highly flammable gas which enhances the combustion process, and addition of hydrogen with PG as in a DF operation resulted with increased PCP as analyzed by Dhole *et al.* [63]. The combustion analysis as investigated by Raheman and Padhee [98] showed a decrease in PCP with Jatropha biodiesel and its blends as pilot fuel because of low volatility and higher viscosity nature. Yaliwal *et al.* [181] used producer gas derived from different origins such as babul, neem and honge woods with HOME biodiesel in DF engine. Higher quality of PG derived from babul wood shown higher PCP (**Fig. 2.17**). An addition of Bioethanol with HOME in different proportions (5%, 10% and 20%) resulted in better combustion and

improved spray characteristics which in turn raised the PCP [180]. Roy *et al.* [53] used two different mixtures of producer gas, one with low H_2 content (13.7%) and another with higher H_2 content (20%) and PCP was measured at different ER. The PCP was found to be higher with increased IT for all the ERs for both low and high H_2 content PG. The range of normal and secondary combustion of both varies for different values of ER. The authors estimated that normal and secondary combustion for low H_2 content gas occurred at IT of 14°BTDC and 15-17° BTDC, respectively, whereas for high H_2 content it is 20°BTDC and 21-23°BTDC, respectively.

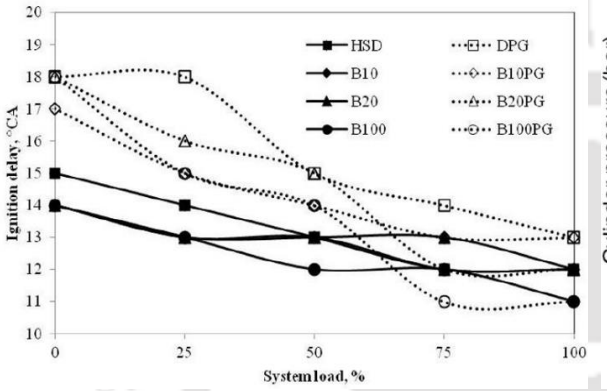

Fig. 2.16 Variation of ID with engine load [98]

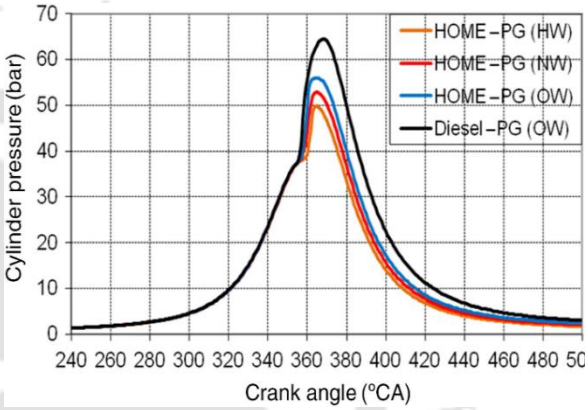

Fig. 2.17 Variation of cylinder pressure for different types of producer gas [181]

Raheman and Padhee [98] found a higher NHRR in DF mode compared to diesel mode however, use of biodiesel as pilot fuel, NHRR observed to be lowered. They explained the reason to be shorter ignition delay and less intense premix combustion phase of biodiesel and its blends. CR plays a crucial role in NHRR characteristics of a DF engine. With the increase in CR the rate of combustion increases resulting in higher NHRR. Similar results were also obtained by Lal and Mohapatra [182] as shown in **Fig. 2.18**. Nataraja *et al.* [192] investigated the combustion characteristics using two different injection timing of 23° and 27° and found a higher NHRR at an optimized setting of 27° IT. The effects of turbocharged engine was also studied which showed higher NHRR. This is due to better air-gas mixing increasing the volumetric efficiency which facilitates faster combustion. The effect of bioethanol blending with HOME biodiesel as pilot fuel is analyzed by Yaliwal *et al.* [180] and observed lower NHRR compared to diesel-PG DF mode. Based on the premixed combustion phase, Banapurmath *et al.* [168] found that with HOME and Honge oil, the duration of premixed combustion phase decreases and diffusion combustion phase increases due to the effect of viscosity and air-fuel mixing rates with producer gas. Besides, HOME-PG shows higher NHRR compared to Honge oil-PG DF mode.

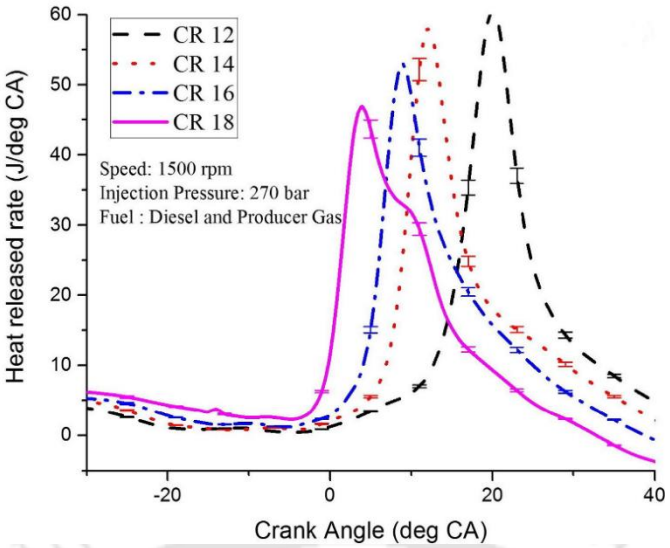

Fig. 2.18 Variation of heat release rate with CR [182]

2.4.4 Emission characteristics of producer gas run dual fuel engine

Emission from an engine is the reflection of the quality of combustion taking place inside the combustion chamber. As discussed in the above section about biogas run DF engine, similar impurities also need to be taken care in case of PG. However, emission of NOx is considered to be the most harmful pollutant, and through DF application, substantial reduction in NOx can be achieved. Uma *et al.* [184] achieved lower emission of NO_x per unit of electricity generation with DF application for all tested load condition. The authors also estimated that with the increase of load, emission of NOx showed an increasing trend. Similar results were obtained by Lal and Mohapatro [182] where the brake power was varied from 0.8 kW to 4 kW and obtained a variation of NOx. Furthermore, they variation of CR on NOx emission was observed and found that with the increase of CR, NOx increases but favours DF operation compared to single mode. . This is because high replacement of oxygen by PG during DF mode lowers the cylinder temperature as well as the intensity of premixed combustion. It can be summed up from the experimental results that concentration of NOx in the engine exhaust highly depends on both oxygen content of intake charge and temperature of combustion chamber. The effect of IT advance on emission characteristics investigated by Banapurmath *et al.* [168] indicated a rise in NO emission DF mode. The authors mentioned this variation to be due to the higher adiabatic flame temperature of DF mode caused by induction of PG. Deshmukh *et al.* [177] conducted the experiments using different mixtures of producer gas with biodiesel and biodiesel-diesel blend (B20) as pilot fuel. NOx found to be increased for DF mode with load due to lesser availability of oxygen for proper combustion. Similar results were also obtained by Nayak *et al.* [193] using quinine nut biodiesel and diesel blend as pilot

fuel. The experiments performed by Nayak and Mishra [194] with different producer gas flow rates give a comparative analysis of NOx emission for different blends of biodiesel. NOx emission decreases drastically with increase in producer gas flow rates because of low adiabatic flame temperature and absence of nitrogen in PG. The preheated blend of jojoba oil and diesel (20:80) shows a lower NOx emission compared to the blend of jojoba oil methyl ester and diesel. Nataraja *et al.* [191] studied the emission characteristics of a turbocharged engine using rice bran oil methyl ester (RBOME) as pilot fuel. With the use of turbocharger higher amount of oxygen in inducted leading to better combustion of fuel, which in turn results in higher NOx emission levels.

Carbon monoxide (CO) and unburnt hydrocarbon (HC) are another two primary pollutants resulting from the incomplete combustion in a DF producer gas engine. With the change in injection timing, a significant change in CO and HC emission were reported by Banapurmath *et al.* [168]. CO and HC emission were found to be decreased with increase in IT from 19° to 27° at a higher load condition. Based on different position of carburettor setting such as 30°,60° and parallel, Hadkar and Amaranth [195] found that with parallel position setting of carburettor shows minimum CO and HC emissions. The variation of CO and HC emission with CR in a DF operation was examined by Yaliwal *et al.* [34]. In the range of CR 15- 17.5, the CO and HC emissions drops with the increase in CR. A similar study was conducted by Lal and Mohapatra [182] where the CR was varied from 12-18, the CO and HC emission was found to be higher by 81-84% and 63.41-70.04%, respectively compared to diesel mode. Variation of CO emission was found to decrease with the increase in load as investigated by Balakrishnan *et al.* [187] and observed lower CO for biodiesel as pilot fuel compared to diesel. CO emission under part-load condition was found to be higher compared to diesel mode because of lower adiabatic flame temperature reported by Uma *et al.* [184] as shown in **Fig. 2.19**. The authors also estimated the HC emission and found to be slightly higher in part load condition. Banapurmath *et al.* [174] used diesel, Honge oil, neem oil and Rice bran oil as pilot fuel with PG in the experimental analysis. For diesel-PG, the CO and HC emission is lower than the other three modes. HC emission is shown in **Fig. 2.20**. The authors explained diffusion burning of diesel is the reason behind lower HC compared to premixed burning of other pilot fuel. In another study, Banapurmath *et al.* [180] used blends of bioethanol with Honge biodiesel in a producer gas run DF engine and a slight reduction in HC and CO emission is observed. This is because addition of bioethanol creates an oxygen-rich region compared to Honge biodiesel which results in better combustion. The mass flow rate of producer gas was varied, and the effects were analysed by Shrivastava *et al.* [52].

According to the authors, at a higher mass flow rate, producer gas replaces higher amount of air, due to which the CO and HC emission shows a higher value. Dhole *et al.* [63] investigated the effect of hydrogen-PG mixture and observed an optimum ratio of 60:40 (PG: H_2) which resulted in lower CO and HC emission compared to the use of PG as secondary fuel. The authors explained that additional H_2 in the mixture lowers the carbon particle and increases mean gas temperature, which leads to less CO and HC emission, respectively.

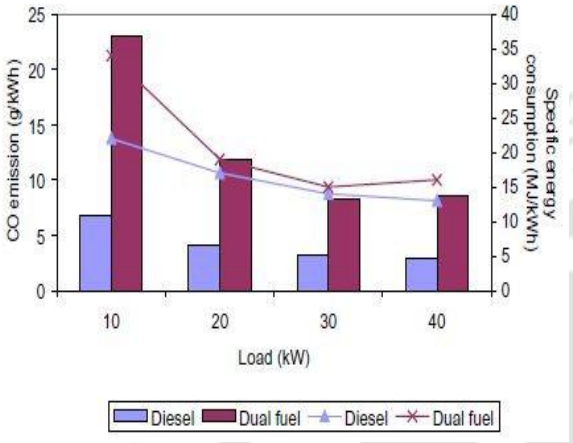

Fig. 2.19 Comparison of CO emission of diesel and Dual fuel mode [184]

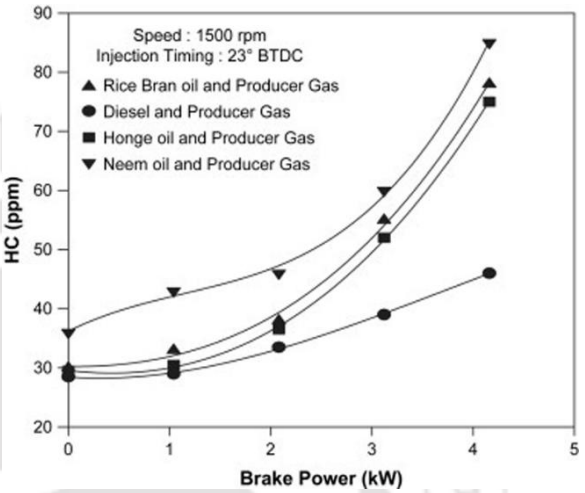

Fig. 2.20 Variation of HC emission with brake power [174]

CO_2 emission indicates the quality of combustion occurring inside the engine cylinder. The increase in CO_2 emission is an indication of better combustion of the fuel. With the increase in CR, rise in temperature and pressure enhances the combustion of fuel which results in higher CO_2 emission (**Fig. 2.21**) [182]. Singh *et al.* [97] reported an increase in CO_2 emission with load with the use biodiesel as pilot fuel. A similar variation of CO_2 emission with load was observed by Nayak *et al.* [196] when different blends of waste cooking oil were used as pilot fuel. The use of carburetor setting at 60° by Hadkar and Amaranth [195] resulted in a stoichiometric mixture of air and PG which in turn reduced CO_2 emission levels. CO_2 emission levels in diesel and DF engine are quite comparable. However, in case of biomass application, CO_2 is considered as a part of the global carbon cycle, and its contribution to global warming is negligible [97].

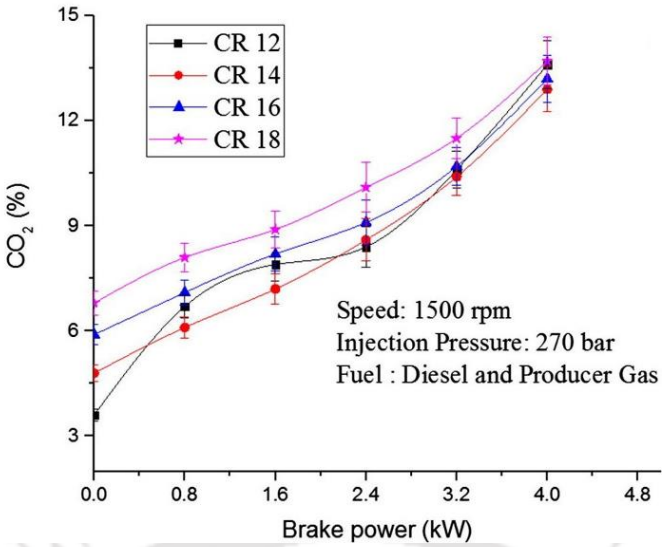

Fig. 2.21 Variation of CR with CO_2 emission [182]

A summary comprising various research work performed by different researchers on producer gas DF operation has been presented in **Table 2.5**.

Table 2.5 Summary of engine characteristics of CI engine operated with Producer gas

Investigator	Test Engine	Pilot fuel	Experimental condition	Research findings
Singh *et al*. [175]	A multi cylinder naturally aspirated diesel gen-set (DG) with matching alternator	Refined rice bran oil (RRBO) and fossil diesel (FD)	➢ Effect of pilot fuel blend	➢ Max BTE obtained for blend 50% RBRO + 50% FD at CR 17 and 84% load ➢ 75% RBRO + 25% FD blend gives maximum BSEC at CR of 17, 26°BTDC and 21% load ➢ Maximum EGT was obtained at 98% load for 50% RRBO- 50% FD under DF mode ➢ HC, NO and NO_2 reduced in mixed fuel mode at 84% load and 18.4:1 CR
Singh *et al*. [197]	Constant speed, three cylinder, naturally aspirated, four stroke, direct injection	Methyl ester of rice bran oil (MERBO) biodiesel, FD	➢ Effect of different blends of FD and biodiesel	➢ Higher BTE with PG-MERBO than PG-FD ➢ Maximum pilot fuel replacement at 63% load and CR 18.4:1 ➢ 5 % reduction in NOx with PG-MERBO but increase in emission of other pollutant ➢ CO emission increases while HC emission decreases with load
Banapurmath *et al*. [168]	Single cylinder four-stroke CI engine operated on single and DF modes	Diesel, Honge Oil and Honge Oil methyl ester(HOME)	➢ Effect of IT ➢ Effect of IP ➢ Effect of pilot fuel	➢ IT at 27^0 BTDC showed improved results for BTE and lower EGT ➢ With HOME as pilot fuel, 23% BTE was obtained ➢ Higher CO, HC and NO emission obtained with Honge- producer gas combination ➢ Advanced IT reduced HC and NO emission while increased CO emission
Hadkar and Amarnath [198]	DI, CI engine with a displacement volume of 662 cc, CR of 17:1, developing 5.2 kW@1500 rpm TV1	Honne Biodiesel	➢ Effect of gas carburettor	➢ Parallel flow carburetor showed optimum result ➢ BTE is maximum for parallel flow carburetor for all load; EGT showed negligible change ➢ Lower values of CO and HC and higher value of NOx emission for parallel carburetor

Uma *et al.* [184]	Turbo charged, four stroke I.C engine coupled with an alternator diesel engine	Diesel	➢ Effect of engine load	➢ Specific energy consumption decreases with increase in load ➢ Higher CO, HC, CO_2 and NOx emission obtained with increase in load ➢ Higher CO, HC and CO_2 emission while lower NOx emission compared to single diesel mode
Lal and Mohapatra [182]	Single cylinder water cooled constant speed 4 stroke variable compression ratio (VCR) diesel engine	Diesel	➢ Effect of CR	➢ BSFC in DFM was higher than diesel mode and maximum at CR 18; EGT reduces with CR ➢ NHRR decreases with CR and NHRR is higher for DF mode ➢ PCP increases with CR and higher for DF mode ➢ HC and CO decreases with CR; but NOx increases with CR
Yaliwal *et al.* [34]	Single-cylinder, four-stroke, direct injection diesel engine operated on a DF mode	Honge oil methyl ester (HOME)	➢ Effect of CR	➢ BTE was increased and EGT reduced with the increase of CR ➢ PCP increased by 9.65%; Maximum LFR 65.18% was achieved ➢ HC and CO reduced; whereas smoke and NOx increased
Ramadhas *et al.* [176]	Four stroke direct injection naturally aspirated, single cylinder, C.I. engine	Diesel, Rubber seed oil	➢ Effect of pilot fuel	➢ Lower BTE while higher BSEC and EGT for Rubber seed oil as pilot fuel ➢ CO and CO_2 emission are higher for Rubber seed oil under DF mode
Balakrishnan *et al.* [190]	Naturally aspirated, four-stroke, single cylinder, water-cooled, direct injection, VCR CI engine	Diesel, Biodiesel	➢ Effect of pilot fuel	➢ Higher BSEC and EGT while lower BTE under duel fuel mode ➢ Higher ID and CO emission while lower PCP under DF mode ➢ BTE increases while BSEC and CO emission decreases with load

Dhole *et al.* [63]	Four stroke, constant speed, vertical, water-cooled, direct injection, turbo charged CI engine	Diesel	➢ Effect of H_2 and PG mixture	➢ Optimum performance obtained with 60:40 mixture of PG and H_2 ➢ Slight decrease in BTE ➢ Higher CO and HC emission while lower NOx emission
Banapurmath *et al.* [174]	4-stroke single cylinder, direct injection water cooled CI engine	Honge, Neem , Rice bran oil and Diesel	➢ Effect of different pilot fuel	➢ Maximum BTE was obtained with Honge oil as pilot fuel ➢ 30% derating with DF mode ➢ Smoke and NO emission is lower while HC and CO emission is higher for DF operation.
Banapurmath *et al.* [56]		Diesel, Honge oil, Honge oil methyl ester (HOME)	➢ Effect of gas carburetor	➢ Carburetor improves results under DF operation ➢ BTE was reported to be improved with carburetor and was lower for HOME-PG operation ➢ Higher HC and NO emission obtained for Honge oil as pilot fuel ➢ Improvement of diesel fuel substitution and NO emission with carburetor
Ramadhas *et al.* [76]	Four-stroke direct injection naturally aspirated, single cylinder, C. I. engine	Diesel	➢ Effect of different PG quality	➢ Optimum performance of engine obtained at 70% load condition ➢ Higher BTE and diesel saving obtained using wood derived PG compared to coir-pith PG ➢ Higher CO and CO_2 emission while lower smoke density with DF mode
Yaliwal *et al.* [181]	Single-cylinder, four-stroke, direct injection diesel engine operated on a DF mode	Honge oil methyl ester	➢ Effect of biodiesel ➢ Effect of different PG	➢ BTE was found maximum for babul wood PG; EGT was maximum for Honge PG ➢ ID showed higher value with Honge PG at all loading condition ➢ Babul PG showed higher PCP ➢ HC emission and smoke opacity was maximum and NOx emission was minimum for Honge PG

Yaliwal *et al*. [180]	Single-cylinder, four-stroke, direct injection diesel engine	Honge oil methyl ester (HOME), Bioethanol	➢ Effect of different mixtures of HOME and bioethanol pilot fuels	➢ Optimum performance is obtained with 5% bioethanol and 95% HOME ➢ BTE decreases while EGT increases with increase in bioethanol percentage ➢ CO and HC emission increases while NOx emission decreases with higher percentage of bioethanol ➢ ID was lower with 5% bioethanol and 95% HOME
Hassan *et al.* [179]	Four-stroke single cylinder direct injection diesel engine	Diesel	➢ Effect of advanced IT	➢ BTE increases and BSEC decreases with advanced IT ➢ LFR increases with increasing ignition advance; maximum at lower engine speed ➢ Higher NOx and lower CO at ignition advance
Shrivastava *et al.* [52]	Single cylinder, four stroke air-cooled and naturally aspirated DI diesel engine	Diesel	➢ Effect of produce gas flow rate	➢ Optimum engine performance obtained at 4 lpm producer gas flow rate ➢ Lower BTE and BSEC while higher EGT with increase in gas flow rate ➢ Higher CO and HC emission while lower NO emission with increase in gas flow rate.
Lekpradit *et al*. [188]	4-strokes 4 cylinders 3.9 L were tested by constant of engine speed at the 1500 RPM	Diesel	➢ Effect of IT	➢ BTE increases while BSEC decreases with advance IT ➢ Lower CO_2 while higher NOx emission with advance IT
Deshmukh *et al.* [177]	Single cylinder, constant speed, water cooled, direct injection with rated output of 3.7 kW	Hingan oil methyl ester and diesel	➢ Effect of biodiesel and blend	➢ Lower BTE and higher BSFC with DF operation than single fuel mode ➢ CO emission was higher but negligible change for NOx and CO_2 emission

Malik *et al.* [199]	Single-cylinder, Four-stroke, Water-cooled Diesel Engine	Diesel	➢ Effect of cotton stalk derived PG	➢ BTE improved by 40% and diesel consumption reduced by 50% with DF mode ➢ Higher CO emission while, much lower NOx emission using DF mode
Roy *et al.*[53]	Four-stroke, single cylinder water cooled, direct injection diesel engine	Diesel	➢ Effect of H_2 percentage in PG	➢ Maximum ITE of 37-38% for high H_2 content PG within ER of 0.42-0.79 ➢ Higher engine power for high H_2 content PG ➢ Optimum ER obtained to be 0.42 ➢ HC and CO emissions with the high H_2-content PG were 10–25% lower but very high NOx emission
Deva kumar and Reddy [77]	Single cylinder, water cooled direct injection with rated output of 3.7 kW at constant speed of 1500 rpm	Fossil diesel	➢ Effect of different IP ➢ Effect of different PG	➢ Higher BTE with babul derived PG while lower EGT with mango derived PG ➢ CO and HC emission is lowest for mango derived PG and NOx emission is lowest for babul derived PG ➢ BTE increases with IP while maximum NOx and CO emission observed at 201 bar
Nataraja *et al.* [192]	Single cylinder four stroke water cooled direct injection TV1 CI engine	Rice bran methyl ester	➢ Effect of turbo charging ➢ Effect of optimized IT	➢ BTE under optimized and turbocharged condition increased by 4.24% with biodiesel as pilot fuel ➢ Lower CO and HC emission while higher NOx emission ➢ PCP and heat release rates were higher with turbocharging
Sombatwong *et al.* [78]	Four-stroke single cylinder, direct injection, naturally aspirated diesel engine	Diesel	➢ Effect of different quantity of pilot fuel	➢ Increase in pilot fuel quantity, BTE and BSEC improved ➢ Lower CO emission with higher quantity of pilot fuel ➢ Higher diesel saving with decrease in pilot fuel quantity

Hernandez *et al.* [189]	supercharged, common-rail injection, single-cylinder diesel engine	Diesel, Biodiesel	➢ Effect of biodiesel as pilot fuel ➢ Effect of EGR	➢ BTE decreases with replacement of diesel ➢ Higher EGR and biodiesel application improves BTE ➢ Heat release rates increases with pilot fuel replacement ➢ CO and HC emission increases while NOx emission decreases with pilot fuel replacement ➢ Lower HC and CO emission with biodiesel and lower NOx emission with diesel at higher EGR
Dassapa and Sridhar [200]	Naturally aspirated, six cylinders, inline, DI, Isuzu diesel engine	Diesel	➢ Effect of producer gas in DF engine	➢ Diesel saving of 79% over entire load range and lower SEC ➢ Overall efficiency is lower in DF mode compared to diesel mode ➢ Higher CO emission and lower NOx emission in DF mode
Raheman and Padee [98]	Single cylinder, four stroke direct injection diesel engine	Jatropha methyl ester, Diesel	➢ Effect of different blends of biodiesel with diesel	➢ Higher BTE while lower BSEC and EGT with increase in biodiesel blend ➢ ID and NHRR decreased with increase in biodiesel blend ➢ Lower CO, HC and NOx emission while higher CO_2 emission with increase in biodiesel blend
Nayak and Mishra [201]	Single cylinder, four stroke, vertical water cooled, diesel engine	Calophyllum Inophyllum biodiesel	➢ Effect of blending of biodiesel with PG	➢ Optimum results obtained at 20% biodiesel blend with PG at 8 kW loading condition ➢ BTE decreased while BSEC and EGT increased with increase in biodiesel blends ➢ Diesel saving of 80% obtained at 20% biodiesel blend at optimum load ➢ Higher CO and HC emission while lower NOx emission with increase in biodiesel blend

Nayak and Mishra [194]		Jojoba biodiesel	➢ Effect of blending of biodiesel and preheated jojoba oil	➢ Optimum results obtained at 20% biodiesel blend with PG at 8 kW loading condition ➢ Maximum pilot fuel saving was obtained for 30 % biodiesel blend and 20% preheated jojoba oil blend ➢ Lower NOx emission while higher CO, HC and CO_2 emission with increase in PG in both the cases
Nayak *et al.* [196]		Waste cooking oil	➢ Effect of waste cooking oil as pilot fuel	➢ NO and HC emission reduces while CO, CO_2 and smoke emission increases in DF mode compared to single fuel ➢ Increase in NO and CO_2 emission with load ➢ CO and HC emission decreases and then increases with increase in load
Nayak *et al.* [193]	Multi-cylinder, four-stroke, vertical water-cooled diesel engine with filter.	Quinine nut oil	➢ Effect of different pilot fuel blend	➢ Higher CO, HC and CO_2 emission while lower NO emission in DF mode ➢ Biodiesel blend of 30% shows lower HC, NO and CO_2 emission compared to other blends.
Sutheerasak *et al.* [202]	In-line, 4-stroke, turbocharged, low speed engine	Diesel	➢ Effect of PG flow rate	➢ Maximum diesel saving at 125 lpm and maximum BTE of at 116 lpm PG flow rate ➢ SEC decreased while EGT increased with increase in flow rate ➢ Higher CO ,HC and CO_2 emission at high PG flow rates
Yaliwal *et al.* [203]	Single cylinder four stroke water cooled direct injection TV1 CI engine with CR of 17:1	Diesel, Honge oil methyl ester (HOME)	➢ Effect of gas carburetor .	➢ Optimum performances were obtained for parallel flow gas entry carburetor ➢ Higher ER and BTE when operated with parallel flow carburetor ➢ HC and CO emissions were lower while NOx emission was comparatively higher for parallel flow carburetor ➢ Shorter ID and higher NHRR obtained for parallel flow carburetor

Shaw *et al.* [204]	Four stroke, CI, constant speed, vertical, water-cooled, direct injection, gen-set	Diesel	➢ Effect of different opening of PG	➢ BTE increases while BSEC decreases with increase in PG opening ➢ Maximum of 92% PG substitution obtained at 80% load and 100% PG opening ➢ Knock free engine operation obtained with the use of PG
Halewadimath *et al.* [4]	Single cylinder, 4-stroke, 5.2 kW, constant speed, direct-injection (DI), natural aspirated (NA), water-cooled diesel engine	Diesel and Neem oil methyl ester (NeOME)	➢ Hydrogen enriched producer gas	➢ At optimized IT and fuel injection pressure, Common rail direct injection system (CRDIS) showed better engine characteristics. ➢ At same condition, CRDIS with re-entrant combustion chamber (RCC) delivered 3.02% higher BTE than hemispherical combustion chamber (HCC).
Akkoli *et al.* [205]	Single cylinder, 4-stroke, 5.2 kW, constant speed, direct-injection (DI), natural aspirated (NA), water-cooled diesel engine	Diesel and Diesel-honge oil methyl ester (HOME)	➢ Effect of injector nozzle	➢ 4-hole injector nozzle resulted with better BTE for Diesel-PG, whereas HOME-PG showed increased BTE with 6-hole nozzle. ➢ At this condition, HC emission for diesel-PG is found to be 35 ppm, while for HOME-PG, 44 ppm. ➢ NOx emission for HOME-PG is 93 ppm and for Diesel-PG, 110 ppm.
Sharma and Kaushal [206]	4-stroke, single cylinder, water-cooled, DI, NA, 3.5 kW, constant speed diesel engine	Diesel	➢ Effect of compression ratio	➢ Maximum BTE for DF operation is found to be 23.81% ➢ Higher CR resulted in maximum reduction of diesel consumption, i.e. 46.66% for CR of 18. ➢ Similarly, DF operation with CR of 18 showed maximum CP of 53.66 bar. ➢ 12.06–37.27% reduction in NOx emission for DF mode compared to diesel.
Percy and Edwin [1]	Single cylinder, 3.75 kW, constant speed Multi fuel, VCR diesel engine	Diesel	➢ Effect of compression ratio	➢ Optimal BTE of 19.44% and diesel replacement of 48% is observed to be at CR of 17 and engine load of 1.87 kW. ➢ At this condition, HC and NOx emission is found to be 758.94 and 184.48 ppm, respectively

2.5 Government's initiatives in decentralization

Electricity generation in decentralized mode is termed as decentralized distribution generation (DDG) system which encompasses small, modular, decentralized off-grid energy systems combined with energy management and storage modules near the place where energy is to be used. These DDG systems can be applied for both conventional as well as non-conventional sources of energy which can be used for electricity generation in rural areas using locally available biomass. Government of India is promoting DDG through Rajiv Gandhi grameen vidyutikaran yojana (RGGVY). This scheme aims at electrifying about 1.15 lakh unelectrified villages and 2.34 lakh households below poverty line by providing Rs.900 crores capital subsidy under the 12th five-year plan [207]. Under this program, Central government provides 90% grant to construct rural electricity distribution backbone (REDB). This grant must provide with at least one 33/11 kV or 66/11 kV substation in each block, Village electrification infrastructure (VEI) with a minimum of one distribution transformer in each village/ hamlet/habitation and also DDG systems for those locations where grid supply is not at all feasible. In India, MNRE has been promoting various biomass-based gasifier and biogas plants for electricity production using local resources. Various biomass-based gasification plants have been installed in different states of India for the fulfilment of the energy needs. MNRE has also installed 130 biomass decentralized power generation projects which generate an aggregate of 999.0 MW and 1666.0 MW capacity power generation from 158 bagasse cogeneration projects in sugar mills. In addition to that another 350 MW capacity power generation from 30 biomass power projects in under various stages of execution. As per a report, the total installed decentralized biomass gasifier, and biogas energy system in India tallied to 1,55,495 no's and 46,69,054 no's, respectively [208].

Several RE agencies with the help of NGO's has taken various ambitious projects to meet up the electricity deficiency through decentralized mode of electricity generation and implemented successfully in many villages across the country. Through such initiations, NGO's can educate the local villagers about the benefits of non-conventional uses of energy resources [209]. Moreover, as the decentralized mode is to be run by local people without any involvement of the state electricity utilities, it also leads to direct and indirect employment opportunities to local youths [210]. Among the different companies and NGO's, one such company named Decentralized Energy Systems private limited (DESI) has done remarkable achievement in rural power generation using locally available biomass. Some of their most widely used technologies include biomass charcoal production, biomass combustion, biomass gasification, energy plantations and agro-forestry, methanation or biogas. The company

operates different biomass gasification plants with the help of local partners which may be an NGO, the panchayat, an industry or a cooperative body which actively participate in power production plants. The company's main motive is not only power production but also help in the economic development of the village by commercializing the electricity generated thereby promoting rural industries and employment opportunities [210].

2.6 Summary of the literature

Continuous research works have been reported by many researchers in the field of ICE focusing towards utilization of renewable resources for replacement of conventional fuels. The present study reviews the utilization of renewable fuels (biogas and producer gas) for rural electrification employing a CI engine. Some of the critical observation from the literature survey are summarized below:

i. Clean gaseous fuels (BG and PG) are composed of both combustible and non-combustible components. The energy value and energy density of biogas is higher compared to producer gas which resulted in higher de-rating of power for PG operated DF engine.
ii. Performance of BG operated DF engine is highly dependent on the CH_4/CO_2 ratio of biogas composition. CH_4 in BG enhances the fuel quality and improves the thermal efficiency. Higher % of CH_4 increase the octane rating and auto-ignition temperature of the fuel which improves the anti-knocking property. Moreover, presence of CH_4 suppresses the tendency of soot formation as it is the simplest member of paraffin series.
iii. Conversely, CO_2 present in BG reduces the thermal efficiency of the engine. This happens because CO_2 absorbs the heat released during the combustion process and lowers the local gas temperature, which lowers the burning speed of BG-air charge. Moreover, lower NOx and smoke emissions are achieved because of the presence of CO_2. Presence of lower sulphur content and absence of aromatics also lowers the emission of smoke.
iv. O_2 enrichment in air during DF resulted in better pre-oxidation reaction, better mixing temperature and higher propagation of diesel flame front which consequently increases the thermal efficiency. Moreover, enrichment of O_2 reduced ignition delay and increases cylinder pressure. Lower emission of CH_4 can also be observed with O_2 enriched air.
v. With high CR, combustion to occur at higher temperature which increases burning velocity of BG-air mixture leading to faster combustion and allows the exhaust to come out a lower temperature.
vi. Advancement of IT resulted in high heat release rate during premixed combustion, which enhances diffused combustion of BG at later stage. Moreover, full penetration, high

quantity of liquid fuel injection and early start of combustion resulted in maximum fuel burning and energy release.

vii. BTE decreases and SEC increases with increase in PG flow rate because of replacement of air in the chamber constitute to poor combustion. Moreover, high PG flow rate resulted in higher EGT. Increase in CR and advancement of IT lowers the EGT. Supercharged DF operation gives high EGT because of combustion of densified fuel.

viii. At higher CR, due to high temperature and pressure, gaseous fuel combustion enhances and replaces liquid fuel at low load. However, at high load, requirement of rich mixture of fuel increases the consumption of pilot fuel.

ix. H_2 present in the PG is reported to be the most influential component concerning the engine operation. Higher % of H_2 present in PG provides better Combustion behaviour and resulted with increase in PCP. However, higher % of inactive gases, i.e. CO_2 and N_2 present in PG suppresses the pre-flame reaction which causes knocking.

x. Incomplete combustion during DF operation resulted with higher emission of HC and CO compared to diesel mode. Application of biodiesel as pilot fuel improves the combustion process of both gaseous and liquid fuel by providing sufficient oxygen which resulted in a reduction of HC and CO. Furthermore, addition of H_2 in PG lowers the presence of carbon particle in the fuel and also raises the mean gas temperature, hence resulted in lower CO. On the other hand, regarding PG application, the presence of higher amount of H_2 produces higher NO_x emission.

2.7 Scope of the present work

Extensive research on alternative fuels is in progress across the globe. Use of clean fuels in internal combustion engines for sustainable power generation is also on the verge. Reviewing the literature, it has been observed that the performance of dual fuel engine operation is primarily dependent on engine load, compression ratio, injection timing, pilot fuel type, gaseous fuel composition and intake charge conditions. It is evident that both BG and PG have their own advantages and limitations to be used as a primary fuel for DF diesel operations. The literature survey indicates inferior combustion behaviour (i.e. prolonged ID, lower PCP and NHRR) in case of DF fuel mode with both biogas and producer gas compared to single fuel mode with diesel. However, these gases possess high anti-knocking properties and they have the potential to control the emission of NO_x. Further investigation is required to minimize the emission of HC and CO. Moreover, there are some other aspects which requires attention as far as decentralized power generation with biofuel is concerned. The study is essential as percentage of combustible gases present in PG (H_2 and CO) and BG (CH_4) is

varying with feedstock which influences the engine characteristics immensely. Moreover, no information on use of two or more gases as primary fuel simultaneously in CI engine on overall engine characteristics has been found in the open literature due to the complexity of unexplored combustion mechanism. Furthermore, no literature is available on the combined induction of BG and PG in dual fuel engine. Combining these two gases might subdue each other's limitations when introduced to the DF engines. Optimized combination of biogas and producer for maximizing engine performance and limiting the exhaust emission are the key challenges. The strategy for the current research is to provide a technology package for production clean power to the rural community.

Based on the current challenges and research gaps, the following objectives have been addressed in the present investigation:

- To analyse the performance, combustion and emission characteristics of a diesel engine using different tri-biodiesel-diesel blend to be applied as pilot fuel for dual fuel operations
- To investigate the performance, combustion and emission characteristics of a dual fuel diesel engine run by simulated biogas (SBG) and producer gas (SPG) using tri-biodiesel-diesel blend as pilot fuel.
- On-field investigation on improvement of diesel engine characteristics powered by biogas-producer gas mixture with biodiesel blend as pilot fuel.

2.8 Summary of the chapter

This chapter examines the potential impact of biogas and producer gas as the primary fuel in diesel engines operating under dual fuel mode, using diesel, biodiesel, and diesel/biodiesel as pilot fuels. The study investigates the effect of various engine operating parameters on the engine performance, combustion, and emissions characteristics. Although the introduction of gaseous fuels may result in a slight reduction in engine performance, it has been found to improve emission characteristics. The study also highlights the significant potential for using these gases as a primary source for generating electricity in rural areas. Based on the review, a critical summary has been formulated and scope of the study have been identified. The objectives of the thesis have been formulated based on this scopes and appropriate methodology has been devised to address them. The detailed description of the experimental setup, procedure and experimental matrix are presented in the next chapter (Chapter 3).

3

Experimental Setup and Procedure

Chapter Outline:

3.1 Introduction
3.2 The engine test setup
3.3 Instrumentations and measurements
3.4 Dual fuel modification
3.5 Experimental procedure
3.6 Summary of the chapter

CHAPTER 3: EXPERIMENTAL SETUP AND PROCEDURE

3.1 Introduction

The function of dual fuel engines is a crucial factor in facilitating decentralized power generation in rural areas. The present study aims to conduct a methodical experimental investigation on the utilization of gaseous fuels in dual fuel mode of operation. In order to achieve this objective, an experimental set up is developed for conducting the engine performance tests using two gaseous fuels viz., biogas and producer gas in a diesel engine. On-site biogas and producer gas generating units are installed to ensure a consistent supply of gaseous fuels, while combustible gas cylinders are also included to provide simulated gaseous fuels. The existing diesel engine setup is modified to operate under dual fuel mode. The essential equipments are designed, fabricated, and adapted accordingly. This chapter provides a detailed description of the engine, devices, and instruments utilized to carry out the experiments. Moreover, the gaseous and liquid fuel supply system is thoroughly explained. Furthermore, the modifications incorporated to convert the existing diesel configuration to operate under dual fuel mode are succinctly outlined. Finally, the experimental procedures employed for both single and dual fuel modes are comprehensively discussed.

3.2 The engine test setup

A 3.5 kW, 4-stroke, single-cylinder, direct injection (DI), water-cooled, naturally aspirated (NA), variable compression ratio (VCR) diesel engine is used for experiments shown in **Fig. 3.1**. The load is applied to the engine by an electromagnetic force generated using a water-cooled eddy current dynamometer. A regulator is attached to the panel box for controlling the engine load. The load signal in kg is sent to the digital display with the help of a load sensor fitted to the dynamometer. The setup is equipped with a tilting cylinder block arrangement for altering the CR at engine running condition without changing the geometry of the combustion chamber. The online variation of the IT of the pilot fuel is achieved by rotating a locknut of the screw which changes the gap between the camshaft and the plunger of the fuel pump. The continuous flow of water through the cooling jacket of the engine block, cylinder head, and the calorimeter is measured with the help of rotameters provided with the test setup. The air and pilot fuel flow rates are recorded using an air flow transmitter and a fuel flow transmitter, respectively. A data acquisition system (DAS) is connected to the computer through a USB port. A differential pressure transmitter is connected to the fuel line which transfers the signal of fuel flow rate to DAS. The signal of each degree rotation of the crank-

shaft is transferred to the computer through an optical encoder (crank angle sensor) for measuring the engine speed (rpm) and it is displayed in the indicator attached to the panel box. For the measurement of exhaust gas and water temperature, thermocouples are provided at the different locations of the setup. The experimental data recorded are transferred to the 'Enginesoft' software for performance analysis. The description of the engine setup and the specification of the instruments are presented in **Table 3.1** and **Table 3.2**.

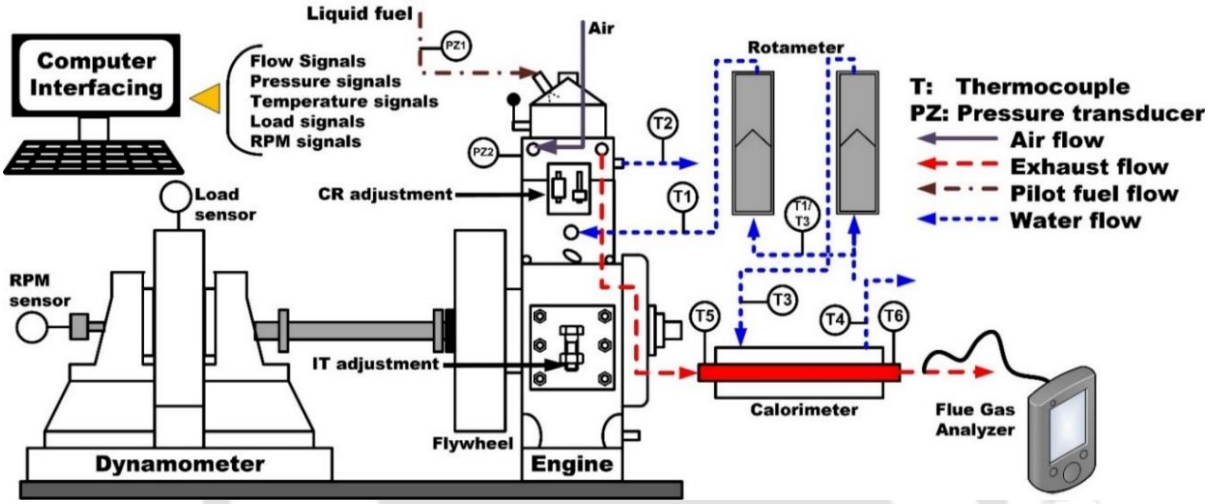

Fig. 3.1 Schematic of the diesel engine test setup

3.3 Instrumentations and measurements

The VCR diesel engine is equipped with a range of sensors, transmitters, and indicators, which are all interfaced with a computer and DAS to enable online measurement of both direct and indirect parameters. The following section provides a concise discussion of the critical parameters that are necessary to understand the performance quality of the engine.

3.3.1 Air and fuel flow measurement

Measurements of both air and fuel flow can be carried out either manually or online. The air flows to the engine manifold through an orifice meter which is interconnected between a U-tube manometer and the air box attached to the panel. An airflow transmitter fitted to the panel box delivers signal to the computer through DAS to measure air flow rate of the engine. The liquid fuel (pilot fuel) from the fuel tank reaches the fuel pump by gravitational force through a fuel measuring burette. A differential pressure transmitter is connected to the fuel line which transfers the signal of fuel flow rate to DAS. During dual fuel operation, the flow rates of the individual gases (CH_4, CO_2, H2 and CO), simulated biogas (SBG) and simulated producer gas (SPG) are recorded separately using pre-calibrated rotameters. The flow rates of biogas and producer gas generated on-field are noted individually using separate flow meters.

Table 3.1 Specification of variable compression ratio diesel engine

System specifications	
Parameter	**Specification**
Make and model	Kirloskar, Model TV1
Product	Research engine test setup, code 240
Type	Single cylinder, four stroke, DI, NA, VCR diesel engine
Power	3.5 kW (@1500 ± 50 rpm
Type of cooling	Water cooled
CR range	12:1 – 18:1
Injection variation	0 – 25° BTDC
Fuel injector	Three circular holes having 0.3 mm diameter spraying fuel with a spray angle of 120°
Fuel injection pressure	164 – 255 Bar
Combustion chamber	Hemispherical bowl in piston type
Dynamometer	Eddy current type, water cooled with loading unit
Air box	MS fabricated with orifice meter and manometer (100 – 0 – 100)
Type of air induction	Naturally aspirated
Fuel tank capacity	7 lit with measuring tube (0 – 450 ml)
Calorimeter	Pipe in pipe type
Rotameters	Engine cooling 40-400 lph, calorimeter 25-250 lph
Data acquisition software	Engine soft' engine performance analysis software
Transmitter, sensors and indicators	
Fuel flow transmitter	DP transmitter, range 0-500 mm WC
Air flow transmitter	Pressure transmitter (-) 250 mm WC
Pressure sensors	Piezo type, range 5000 psi, with low noise cable
Temperature sensors and Transmitter	PT100 (RTD) type, range 0-100° C, output 4-20 mA (4 nos), K type, range 0-1200° C, output 4-20 mA (2 nos)
Load sensor and indicator	Strain gauge type load cell with digital indicator, range 0-50 kg
Speed sensor and indicator	Resolution 1°, range (5500 rpm) with TDC pulse
Data acquisition software	'Enginesoft' engine performance analysis software
Setup constants	
Pulse per revolution	360°
No. of cycles	10
Fuel measuring interval	60 s
Speed scanning interval	2000 ms
Bore × Stroke	87.5 mm × 110 mm
Displacement volume	661 cc
Orifice diameter	20 mm
Dynamometer arm length	185 mm
Connecting rod length	234 mm
Theoretical constants	
Orifice coefficient of discharge	0.6
Specific heat of exhaust gas	1.00-1.25 kJ/kg-K
Specific heat of water	4.186 kJ/kg-K

Table 3.2 Specification of the instruments

Instrument	Make	Type	Accuracy	Resolution	Range
Fuel flow transmitter	Yokogawa Electrical	DP transmitter		0.1 cc	0-500 mm of water column
Air flow transmitter	WIKA instruments limited	Pressure transmitter	2%	1 mm	(-) 250 mm of water column
CH_4 flow meter	Five star	Mechanical	2%	-	0-5 kg/hr
CO_2 flow meter	Five star	Mechanical	2%	-	0-5 kg/hr
H_2 flow meter	Five star	Mechanical	2%	-	
CO flow meter	Five star	Mechanical	2%	-	
BG flow meter	Siya instruments	Mechanical	2%	0.001 m^3	10000 m^3/hr
PG flow meter	Scientific Devices	Mechanical	2%	-	0-200 Nm^3/hr
Pressure sensors	PCB Piezotronics	Piezo type with low noise cable	2%	0.1 psi	5000 psi
Temperature sensors	-	PT100 (RTD)	-	-	0 – 100°C
		K type	-	-	0 – 1200°C
Load sensor and indicator	Sensotronics	Strain gauge type load cell with digital indicator	-	-	0 – 50 kg
Speed sensor and indicator	Kubler	-	-	1°	5500 rpm
Data acquisition system	National instruments	NI USB-6210	-	-	16-bit, 250 kS/s

3.3.2 $P - \theta$ measurement

Two piezo type sensors are mounted on the cylinder head and fuel injector for combustion pressure and fuel line pressure measurement. The technical specification of these sensors are identical and capable of measuring pressure of compression, combustion, explosion, pulsation, blast etc. An optical crank-angle sensor is used to deliver a signal for each degree rotation of crank shaft with TDC pulse.

3.3.3 Temperature measurement

A total of six thermocouples are installed at various locations of the setup for measurement of water and exhaust gas temperature. Out of these, two PT100 temperature sensors are used to measures the inlet and outlet temperatures of the engine cooling water and other two

measures the inlet and outlet temperatures of calorimeter water. Two K type thermocouples are installed at the calorimeter to monitor the inlet and outlet temperature of exhaust gas.

3.3.4 Compression ratio variation control

The VCR diesel engine is facilitated to vary the compression ratio (CR) from 12 to 18 during the engine running condition. This can be done by tilting cylinder head with the help of locknut and adjuster arrangement. However, the engine must be started at the standard CR of 17.5 and the CR can be varied online later on. The appropriated value of CR should be entered manually in the software with every change of CR for data acquisition.

3.3.5 Injection timing and injection pressure variation control

The injection timing (IT) of the liquid fuel can be altered online by rotating the locknut of the screw, which changes the relative distance of camshaft and plunger of the fuel pump. The updated IT can be visualized from the fuel pressure data at a certain crank angle displayed in the software. There is a horizontal shift of the injection point on the plot to retard or advance the IT depending on the rotational way of the adjusting nut. Similarly, injection pressure (IP) can be varied manually by adjusting the fuel injector screw mounted on the top side of injector cap/bottom of the overflow connection. Standard IP is maintained at 243 bar and IP can be altered to a minimum and maximum value of 164 bar and 255 bar, respectively.

3.3.6 Performance measurement

Data for measuring the engine performance parameters are recorded after configuring the engine at a specific experimental condition. Depending on the requirements, the density and calorific value of the respective fuel are incorporated into the analysis. The analysis covers parameters such as air and fuel flow rates, air-fuel ratio, power, mean effective pressure, efficiencies, and heat balance. The basic correlation used for estimating the above parameters are present in Appendix-A.

3.3.7 Emission measurement

The emission analysis is carried out by using a Testo flue gas analyzer. The resolution, accuracy and range of these emission parameters are shown in **Table 3.3**. The analyzer uses ASTM-D6522 standard for emission measurement. The working principle of the gas analyzer is as follows. The analyzer sucks in pure air and rinses the passage leading to the sensors through condensation trap and filters. During steady engine operation, the flue gas is allowed to surge through a probe and dried out by a condensation trap. There- after, each of the CO, HC, NO_X and CO_2 emission concentrations in the flue gas is analyzed by individual sensors and readings are then displayed on the screen of the control unit.

Table 3.3 Specification of Testo 350 S/M/XL flue gas analyzer

Sl. No	Measured gas	Resolution	Accuracy	Range
1	O_2	0.1%	±0.8%	0-25%
2	CO	1 ppm	± 10 ppm <200 ppm	0 – 10000 ppm
3	CO_2	0.01% vol. <25%	± 0.3% vol. <25%	0 – 50%
		0.1% vol. >25%	± 0.5% vol. >25%	
4	NO	1 ppm	± 5 ppm <100 ppm	0 – 3000 ppm
5	NO_2	0.1 ppm	± 5 ppm < 100 ppm	0 – 500 ppm
6	HC	1 ppm	400 ppm < 4000 ppm	0 – 40000 ppm

3.4 Dual fuel modification

In dual fuel operation, induction of uniform air-gaseous fuel mixture through the suction line is essential for efficient combustion and enhanced engine performance. In order to supply a homogeneous air-gas mixture, a novel venturi type mixer [211] has been designed. The mixing device is connected between engine intake manifold and air suction box for controlled supply of air-gaseous fuel mixture to the engine. Along with that, a few additional components such as a gas cylinder arrangement, a mixer or surge tank, flow control valves, flow meters and pilot fuel control system are also incorporated into the existing diesel engine setup. The schematic diagram of the modified engine set up and gas cylinder arrangement is shown in **Fig. 3.2** and **Fig. 3.3**.

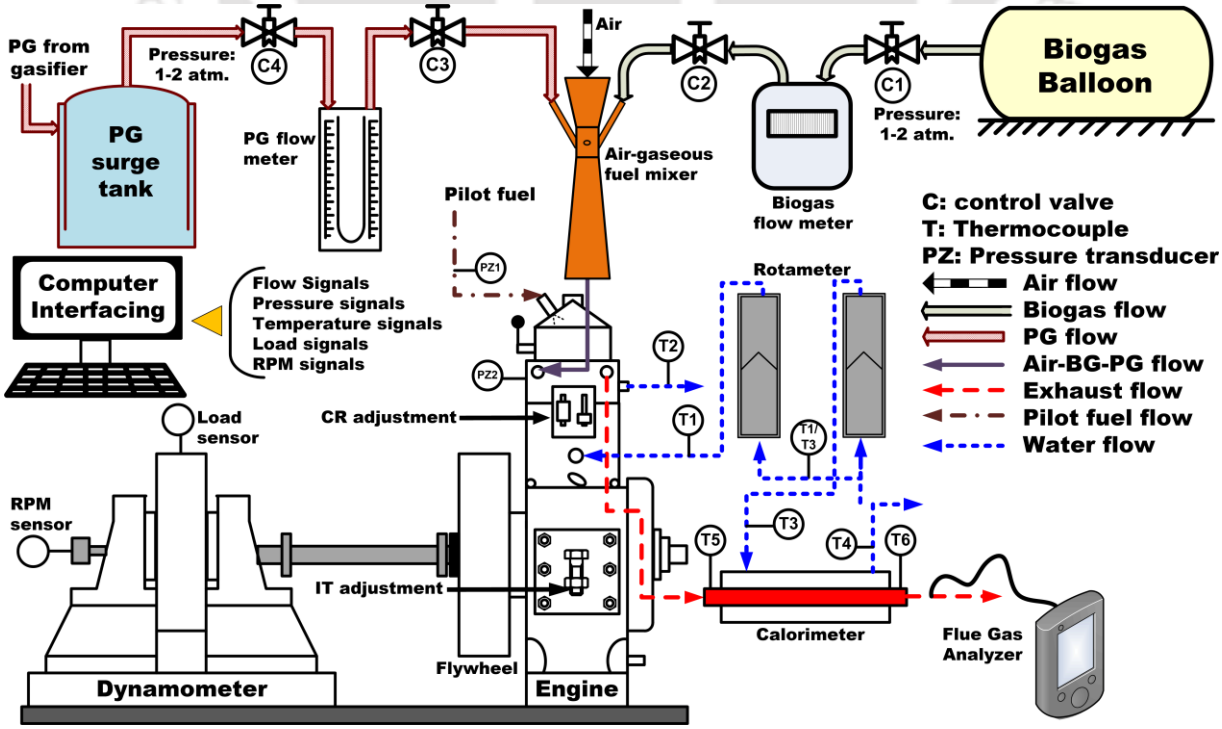

Fig. 3.2 Schematic of the modified diesel engine setup for DF operation

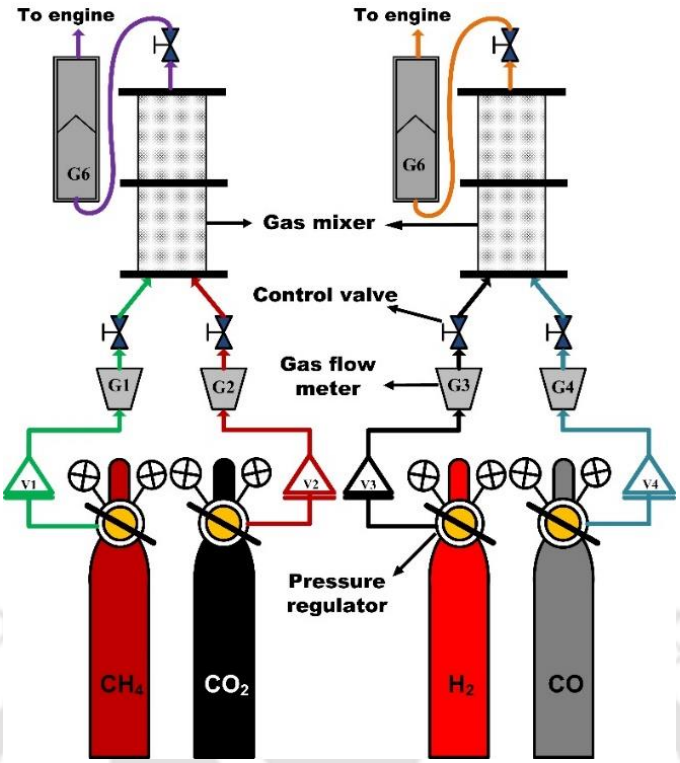

Fig. 3.3 Schematic of the simulated gas supply arrangement

3.4.1 Venturi type air-gas mixer

The gas mixture is designed with the concept of venturimeter having smooth convergent and divergent sections at either side of the throat. It has been claimed that gaseous fuel inlet in the throat sections provides a uniform mixing of gas with air and the presence of contraction and expansion section diminishes the chance of irreversible pressure loss [212,213]. In this work, the mixer has been redesigned with the motive of investigating the flow characteristic of two different gaseous fuels (i.e. biogas and producer gas) along with air. Hence, the mixer has two inlets for biogas and two inlets for producer gas, 90^{o} apart from each other and one outlet. The design of the venturi type air-gaseous fuel mixer is explained in Appendix-B.

3.4.2 Simulated gaseous fuel supply system

The present study involves the preparation of simulated biogas (SBG) and simulated producer gas (SPG) by combining pure gases, namely CH_4 and CO_2 for SBG, and H_2 and CO for SPG. These gases are stored in high-pressure cylinders prior to the mixing process. The pressure of these gases are controlled by the two-stage pressure regulators attached to the cylinders and the gases are supplied to the gas mixer through non-return valve. The individual gases (CH_4, CO_2, H_2 and CO) are fed to the mixer at an angle in order to generate turbulence for proper mixing. The desired flow rate required to maintain the different quality of SBGs and SPGs are determined based on the volumetric properties of the individual gases and monitored with

the help of gas flow meters. In order to simulate SBG and SPG, two 'gas mixers' or 'surge tanks' are designed and fabricated in such a way that the volume of the mixers can store at least ten times the requirement of engine swept volume. Wire mesh is provided inside the mixers to reduce the pressure of the simulated gases. Then SBG and SPG are supplied to the engine manifold through flow meters at atmospheric pressure using a single stage pressure regulator.

3.4.3 Liquid fuel control mechanism

The liquid fuel control mechanism (LFCM) helps to calculate the liquid or pilot fuel quantity replaced at any particular load with respect to engine speed. The mechanism is composed of a shaft, spindle, and a sleeve. The spindle is attached to one end of the shaft and the other end of the shaft is connected to the sleeve. The sleeve is again connected to the fuel shut off valve of the fuel pump to restrict the supply of pilot fuel. Once the spindle is rotated, the shaft linearly moves forward and pushes the sleeve which again pushes the control shut off valve connected with it. To determine liquid fuel replacement, first, the rpm and fuel consumption at a particular diesel load are recorded. When transitioning to dual fuel mode, biogas supply is gradually increased, resulting in increased engine rpm and energy output. The governor then reduces the rpm by limiting the liquid fuel supply until it matches the rpm of the diesel mode. This is accomplished using the fuel control shut valve connected to the fuel pump, which is marginally pushed by the control lever. **Fig. 3.4(a)-(e)** depicts the pictorial representation of the modifications incorporated for DF operations.

(a) VCR Diesel Engine

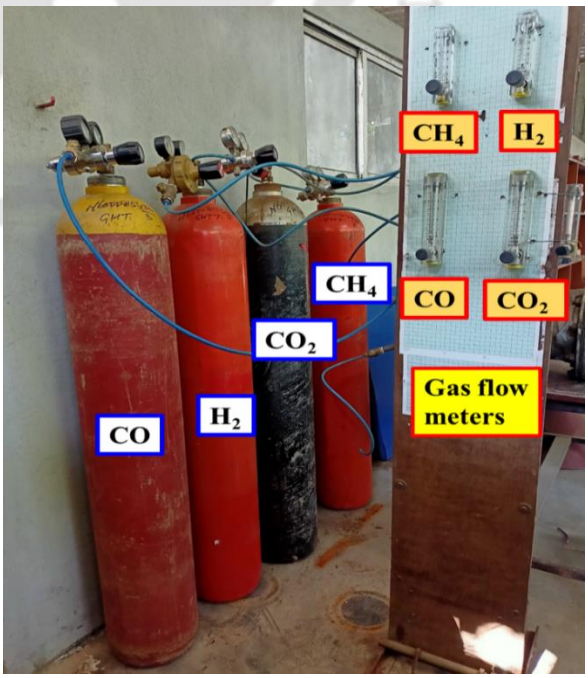

(b) Gas cylinder arrangements

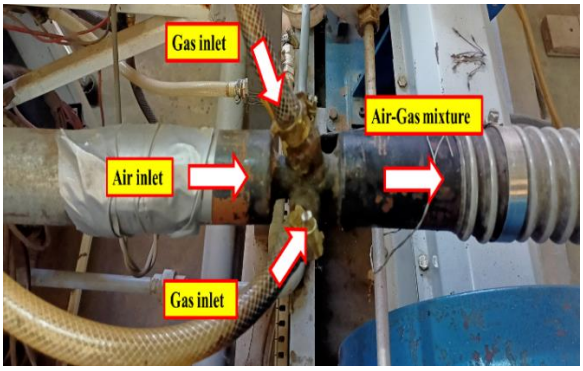

(c) Venturi type air-gas mixer

(d) SBG and SPG gas mixer

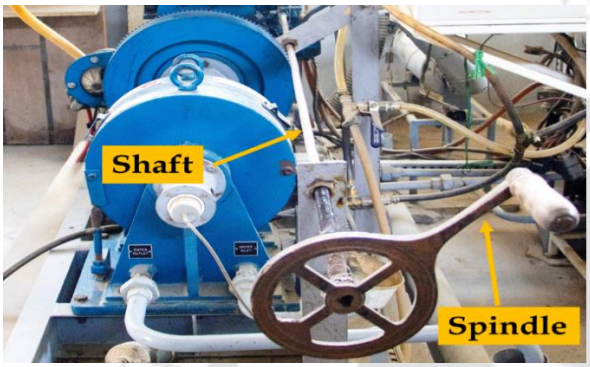

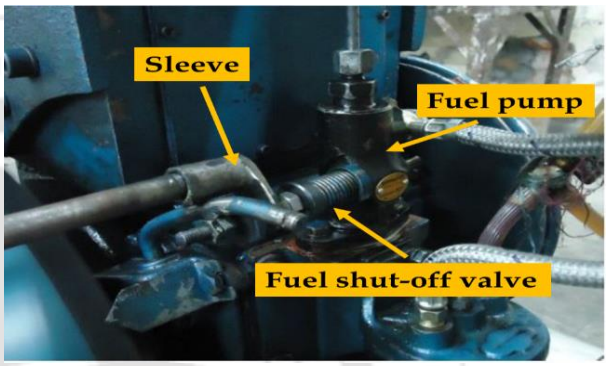

(e) Liquid fuel control mechanism

Fig. 3.4 Experimental facilities and key components for DF operation

3.5 Biogas and producer gas reactors

A Deenbandhu model of anaerobic digester of 3 m^3 capacity has been installed near the engine set up for the on-field generation of biogas. To maintain the temperature of the digester in mesophilic condition (33-37°C) for maximizing the biogas production rate, a helical type heat exchanger is installed at the bottom of the digester. A provision has also been made for sample collection at the top of digester. Experiments have been conducted considering cattle dung as feed stock mixed with equal quantity of water. The initial characterization of the cattle dung has been performed using proximate and ultimate analysis and results are tabulated in the **Table 3.4**. Biogas is collected in a 2 m^3 capacity balloon (Make: Siya Instruments) and the supply line is connected to the engine's intake manifold through a venturi air-gas mixer. The biogas flow rates is measured using a BG flow meter (Make: Siya Instruments). On the other hand, a downdraft biomass gasifier of 10 kW capacity is installed for on-field generation of producer gas. Locally available wood from Karas (Aquilaria malaccensis) tree is used as feedstock for the gasifier. Initial characterization of the biomass has been done using proximate and ultimate analysis as shown in **Table 3.5**. Combustion of wood inside the gasifier reactor is converted into producer gas and then went through the cooler. Gas containing various unwanted materials is removed by passing through gas filter. A

mechanical valve is applied at the filter vent to operate the gas flow rate. The flow rates is measured by a PG flow meter (Make: Scientific devices). The composition of both BG and PG utilized for the present study is measured through gas chromatography. The photograph of the anaerobic digester and downdraft gasifier are shown in the **Fig. 3. 5(a)-(b)**.

Fig. 3.5 Photograph of gaseous fuel generation units (a) anaerobic digester and (b) downdraft biomass gasifier

Table 3.4 Initial charaterization of cattle dung

Parameters	Value
Feedstock : Water ratio	1:1
Moisture (%)	90.82 ± 0.05
Total Solid (%)	9.0 ± 0.05
Volatile Solid (% TS)	83.1 ± 0.18
Carbon (% /TS)	36.69
Nitrogen (% /TS)	1.42
Hydrogen (%/TS)	3.51
Oxygen (%/TS)	58.39
C/N Ratio	25.82

Table 3.5 Proximate and ultimate analysis of wood

Parameters	Value
Moisture content	10.84 ± 0.15%
Volatile matter content	86.8 ± 0.28%
Ash content	3.67 ± 0.18%
Nitrogen	3.475 %
Carbon	42.529 %
Hydrogen	5.42

3.6 Experimental procedure

3.6.1 Single mode experiments

The engine is initially started with diesel fuel at standard engine specifications of CR of 17.5 and IT of 23°BTDC. To ensure optimal combustion of fuel, the engine is allowed to run at a no-load condition at 1500 ± 50 rpm for a certain period of time to reach an adequate warm-up temperature. The single mode experiments with fossil diesel (FD) and tri-biodiesel-diesel blends are conducted at five different load i.e. 20%, 40%, 60%, 80%, and 100%. The speed of the engine is noticed to be increased with the increase in load. For any specified load, the engine is ready for data acquisition only when it reaches the steady-state condition which is confirmed based on the exhaust gas and water outlet temperature. This signifies that the combustion process within the cylinder has stabilized and the engine is now prepared for data collection. Then the readings of temperatures, air and fuel flow rate, speed, cylinder and fuel pressure variation are automatically recorded by the DAS. After the completion of neat diesel experiments, the fuel tank is emptied and filled up with tri-biodiesel-diesel blends of Jatropha, Karanja and Mahua biodiesel. Then the engine is allowed to run for 10 minutes at no load condition to clear up the entire diesel present in the fuel line and to get steady. Necessary

modifications are made in DAS to insert the density and calorific value of the fuel for automatic calculation of the performance parameter. Once the engine has achieved a steady state condition, data recording begins. The testing procedure for the fuel blends is kept consistent with that of fossil diesel.

3.6.2 Dual fuel mode experiments

Before starting the experiments at DF mode with SBG and SPG, firstly, the liquid fuel tank filled with fossil diesel (FD) is emptied from the tank and filled with the pilot fuel. The engine is then run with the pilot fuel for a few minutes at a fix engine load and speed of the engine is monitored. Then the supply of simulated gases i.e. SBG and SPG is increased gradually by opening the valve till the engine shows any sign of misfire. Similar to the simulated gaseous fuel operations, the BG and PG valve is opened gradually by opening the control valve at desired angle according to the experimental condition. As the gaseous fuel enters into cylinder, the surplus energy from gaseous fuel takes part in the combustion process leading to the escalation of the engine speed. At this stage, the pilot fuel supply is regulated slowly with the help of fuel control mechanism to maintain the engine speed at 1500±20 rpm. Prior to taking the readings, engine is driven for a few minutes. The DAS automatically records the signals of air and pilot fuel flow rate, speed, load, fuel and cylinder pressure and temperature. The flow rates of SBG, SPG, BG and PG are noted individually using separate flow meters. Similar procedure is repeated to obtain readings at different load, CR and IT.

The uncertainty analysis of the entire experimental investigation is given in **Table 3.6** and **Table 3.7**. The detailed calculation for uncertainty analysis is given in Appendix-C.

Table 3.6 Relative error of independent variable

Sl. No.	Independent variable	Relative error
1.	Engine speed	0.5%
2.	Engine load	0.5%
3.	LHV of diesel	1%
4.	LHV of diesel/biodiesel blends	1%
5.	Air flow rate	0.5%
6.	Liquid fuel flow rate	1%
7.	LHV of gaseous fuel	1%
8.	BG flow rate	2%
9.	PG flow rate	2%
10.	Temperature	1.5%
11.	Cylinder pressure	0.1%
12.	Cylinder volume	0.1%

Table 3.7 Uncertainties of performance parameters

Sl. No.	Performance parameters	Single mode	Dual fuel mode	
			Simulated gas	Raw gas
1.	Brake thermal efficiency	1.5%	2.5%	3.35%
2.	Brake specific energy consumption	1.5%	2.5%	3.35%
3.	Liquid fuel substitution	-	1.41%	1.41%
4.	Net heat release rate	0.2%	0.2%	0.2%
5.	Ignition delay	0.1%	0.1%	0.1%
6.	Emission analysis	2.35%	2.80%	2.65%

3.7 Summary of the chapter

This chapter provides a concise overview of the necessary equipment and devices for conducting both single and dual fuel mode experiments, as well as a description of the engine setup. The modification executed in the existing setup are discussed and illustrated with schematic diagrams and photographs. Additionally, the experimental procedure for both diesel, tri-biodiesel-diesel blends and dual fuel modes are explained in detail. The results of the experiments generated based on the prescribed experimental procedure as followed in the subsequent chapters. The next chapter (Chapter 4) deals with the experimental investigation of tri-biodiesel-diesel blends for the selection of pilot fuel to be used for dual fuel experiments.

4

Experimental Analysis of Pilot Fuel

Chapter Outline:

CHAPTER 4: EXPERIMENTAL ANALYSIS OF PILOT FUEL

4.1 Introduction

In dual fuel mode, the gaseous fuel (known as primary fuel) is premixed with air and subsequently introduced to the engine. The mixture is then compressed similar to that of a conventional diesel engine. Next, a liquid fuel of higher Cetane number and lower auto-ignition temperature known as pilot fuel is then sprayed to initiate the combustion process. The pilot fuel spray forms ignition centers, which allow the flame to propagate through the homogeneous air-gas mixture. Once combustion is initiated, the gaseous fuel, becomes the main source of energy for the engine [214]. The type of pilot fuel employed in dual fuel diesel engines has a substantial effect on the combustion process, as it triggers the process itself. Compared to single fuel mode, the process of combustion in dual fuel engines which use both biogas and producer gas is more intricate. As the air-gaseous fuel mixture undergoes a relatively longer compression stroke, a pre-ignition chemical reaction takes place before the ignition of the pilot fuel. This reaction creates active radicals and partial combustion products, which are believed to impact the ignition of the injected pilot fuel [75]. Given the current fuel crisis, it is crucial to explore alternative pilot fuels for dual fuel diesel engines, as most previous studies [109,165,215,216] have primarily focused on the use of fossil diesel as pilot fuel. Examining alternative pilot fuels can provide valuable insights into improving the performance and efficiency of dual fuel engines. Biodiesels have the potential to serve as the ignition source for dual-fuel engines that run on biogas and producer gas. These renewable fuels, which are derived from vegetable oils, animal fats, or biomass are of interest for their ability to reduce life-cycle greenhouse gas emissions and potentially replace fossil fuels [217]. There has been a continuous research works on exploring new biodiesel preparations in order to identify the most efficient and environmental-friendly options for powering diesel engines under dual fuel mode. Various combinations are being tested [2,139,218,219] to identify the most effective solution to enhance engine efficiency and reduce harmful emissions. This dual fuel approach represents a promising solution for promoting sustainable energy production. The integration of renewable fuels into the DF compression ignition engine represents a significant step towards breaking the reliance on fossil energy sources. However, the optimization of performance, combustion, and emission characteristics in biodiesel-diesel blends is predominantly centered on a single type of biodiesel, where one variety is mixed with fossil diesel. There has been a lack of comprehensive investigations on the utilization of

blends comprising two or more biodiesels produced from varying feedstocks with fossil diesel for dual fuel engine applications.

4.2 Characterization of test fuels and experimental matrix

Three non-edible biodiesels namely Jatropha (*Jatropha Curcas*), Karanja (*Pongamia Pinnata*) and Mahua (*Madhuca Indica*) are considered for investigation was purchased from a local industrial company SVM Agro Processor, Nagpur, India. The biodiesels are mixed with the conventional diesel fuel to prepare ten different tri-biodiesel-diesel blends. Maximum biodiesel considered is 30% with diesel to form these blends. The physiochemical properties of diesel, raw biodiesel and diesel/biodiesel blends are measured in the laboratory following standard test guidelines prescribed by American Society for Testing and Materials (ASTM 6751) in order to use it in the engine. These properties of the tested fuels are presented in the **Table 4.1** and **Table 4.2**.

Table 4.1 physiochemical properties of diesel and biodiesels

Properties	Diesel	Jatropha biodiesel (KB)	Karanja biodiesel (KB)	Mahua biodiesel (MB)
Calorific value (kJ/kg)	42550	38825	37230	36520
Flash Point (^{0}C)	71	169	182	156
Cloud point (^{0}C)	-11	3	-1	-3
Viscosity at 40 ^{0}C (mm^2/s)	2.44	4.23	5.05	4.58
Density at 40 ^{0}C (kg/m^3)	829.67	875.33	890.00	899.67
Cetane no	50.12	58.06	57.45	55.97
Oxidation stability (hrs.)	23.7	3.27	2.35	8.92

Table 4.2 Physiochemical properties of tri-biodiesel-diesel blends

Blends	JB (%)	KB (%)	MB (%)	Calorific value (kJ/kg)	Flash Point (^{0}C)	Cloud point (^{0}C)	Viscosity at 40^{0}C (mm^2/s)	Density at 40^{0}C (kg/m^3)	Cetane no
Blend-1	20	5	5	41238	100.40	-7.30	3.04	845.32	53.874
Blend-2	15	10	5	41158	101.05	-7.50	3.08	846.05	53.613
Blend-3	10	15	5	41078	101.70	-7.70	3.12	846.78	53.732
Blend-4	5	20	5	40998	102.35	-7.90	3.16	847.52	53.907
Blend-5	5	5	20	40892	98.45	-8.20	3.09	848.97	54.093
Blend-6	5	10	15	40927	99.75	-8.10	3.11	848.48	53.553
Blend-7	5	15	10	40963	101.05	-8.00	3.14	848.00	53.830
Blend-8	10	5	15	41007	99.10	-7.90	3.07	847.75	53.579
Blend-9	15	5	10	41122	99.75	-7.60	3.05	846.53	53.129
Blend-10	10	10	10	41043	100.40	-7.80	3.09	847.27	53.245

The engine experiments for the tri-biodiesel-diesel blends are carried out at five different loads from 0 to 100% with an increment of 20% at standard diesel setting (i.e. Compression ratio =17.5 and Injection timing = 23° BTDC). The performance and combustion analysis are performed based on theoretical equations given in Appendix-A. The experimental matrix followed for the tri-biodiesel-diesel blends is depicted in the **Table 4.3**. The evaluation of the engine performance includes the analysis of brake thermal efficiency (BTE), brake specific fuel consumption (BSFC), volumetric efficiency (VE), and exhaust gas temperature (EGT). The analysis of combustion involves the assessment of cylinder pressure (CP) variation, rate of pressure rise, ignition delay (ID) and net heat release rate (NHRR). In addition, the analysis of emissions includes the measurement of carbon monoxide (CO), hydrocarbon (HC), carbon dioxide (CO_2) and oxides of nitrogen (NO_X).

Table 4.3 Experimental matrix

Mode	Fuel used	CR	IT	Loading conditions (%)
Single mode	Diesel / Tri-biodiesel-diesel blends (Blend 1- Blend 10)	17.5	23° BTDC	20, 40, 60, 80, 100

4.3 Performance characteristics of diesel engine

The brake thermal efficiency (BTE) is a measure of effective conversion of thermal energy available in the fuel into useful work by the engine and delivered to the crankshaft. It is calculated as the ratio of the power output of the engine to the heat energy contained in the fuel. The variation of BTE for all the diesel/biodiesel blends are analyzed and compared with diesel which is illustrated in **Figs. 4.1(a)-(b)**. It is evident from the figure that with the increase in load, BTE increases for all the cases with diesel and tri-biodiesel-diesel blends. This is due to reduced heat and friction losses and hence, enhanced combustion efficiency. It has been observed that the blending of biodiesel resulted in reduction of BTE. This can be attributed to the lower calorific value and higher density of tri-biodiesel-diesel blends compared to the fossil diesel [220]. The thermal efficiency also depends on the viscosity and volatility of the fuel. Poor atomization due to higher viscosity and poor volatility results in incomplete combustion in the fuel-rich regions [43]. The BTE for Blend-1 through blend-10 is found to vary in the range of 23.33-25.10%, these minimum and maximum values of BTE are found for the Blend-5 and Blend-1, respectively. The value of BTE for diesel fuel is found to be 27.57%. Among all the tri-biodiesel-diesel blends, calorific value of Blend-1 is found to be superior as the share of JB is maximum (as seen in **Table 4.2**) with high calorific value resulted in highest BTE for Blend-1. Blend-2, Blend-9 and Blend-10 showed closest BTE value to Blend-1.

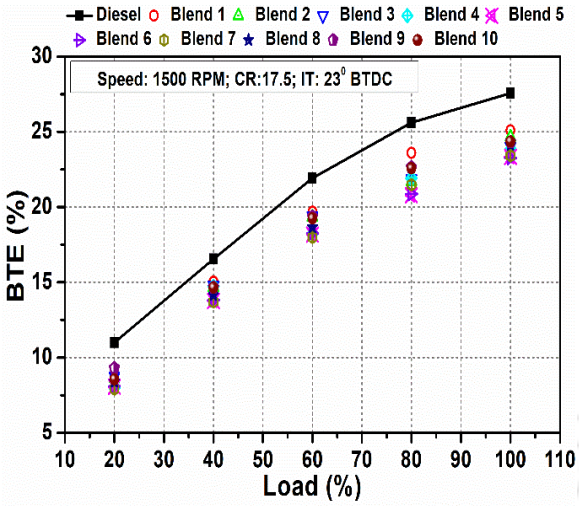

Fig. 4.1(a) Variation of BTE with engine load

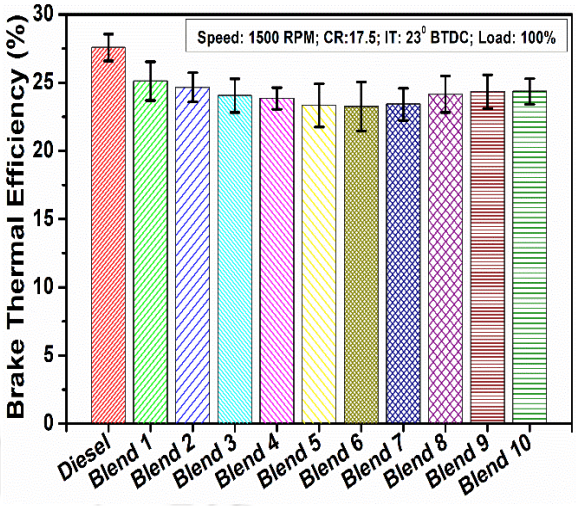

Fig. 4.1(b) Variation of BTE for different blends at full load

On the other hand, Brake specific fuel consumption (BSFC) showed a complete reverse trends in case of all the fuels tested. **Figs. 4.2(a)-(b)** showed the variation of BSFC for diesel and tri-biodiesel-diesel blends at different loading condition. BSFC refers to the ratio between the fuel mass flow rate and engine power and it decreases with increase in load. This can be attributed to the increase of the mechanical efficiency with the increase in load irrespective of the fuel type. Therefore, the BSFC has the lowering trend, as fuel consumption per unit of power reduces. It has been observed from the figures that minimum BSFC of 0.31 kg/kWh is found in case of diesel at full loading condition. Among the tri-biodiesel-diesel blends, Blend-1 and Blend-5 showed the minimum and maximum BSFC of 0.339 and 0.37 kg/kWh, respectively at full load. Moreover, considering the complete load range, the tri-biodiesel-diesel blends resulted in 14.18% average increment in BSFC compared to diesel. This study is performed under fixed engine speed and BP. Hence, to generate an equivalent amount of power, a greater volume of fuel must be introduced into the engine in case of blends compared to diesel, owing to its denser consistency and decreased energy content resulted in greater consumption of fuel [221,222].

The exhaust gas temperature (EGT) is a reliable indicator of the quality of combustion inside the combustion chamber. The variation of EGT for diesel and all the tri-biodiesel-diesel blends are presented in **Figs. 4.3(a)-(b)**. It has been evident from the **Fig. 4.3(a)** that with the increase in load, the EGT increases in case of all the fuel blends tested. The value of EGT is higher at higher loading condition because, as the engine load increases, a greater quantity of fuel is necessary to generate more power, which in turn resulted in more burning of fuel leading to higher temperature of the burnt gas [220,223]. It has been observed from the **Fig. 4.3(b)** that the blended fuel exhibit slightly higher EGT compared to diesel. At 100% load, diesel showed

a maximum EGT of 279.4°C whereas, out of all the biodiesel blends, maximum EGT of 297.2°C was recorded in case of Blend-7. The average rise in EGT for tri-biodiesel-diesel blends is 5.98% compared to diesel, attributable to the higher oxygen content present in the biodiesel. Higher exhaust gas temperature for biodiesel blended fuel compared to diesel was also reported in previous literatures [224,225]. This is because, presence of biodiesel in fuel blend results in shorter ignition delay, which leads to a longer premixed combustion phase and mixing controlled combustion phase. As a result, the maximum heat release rate occurs earlier, causing a greater increase in gas temperature inside the cylinder towards the end of the compression stroke. This in turn causes an additional increase in exhaust gas temperature due to the isentropic relationship between the exhaust gas temperature and the gas temperature inside the cylinder during the exhaust stroke.

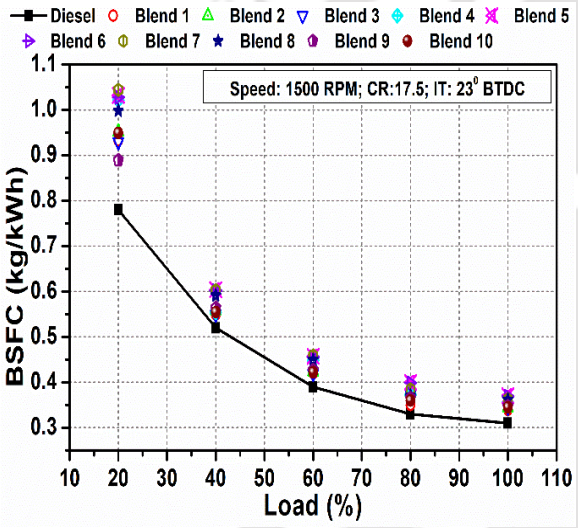

Fig. 4.2(a) Variation of BSFC with engine load

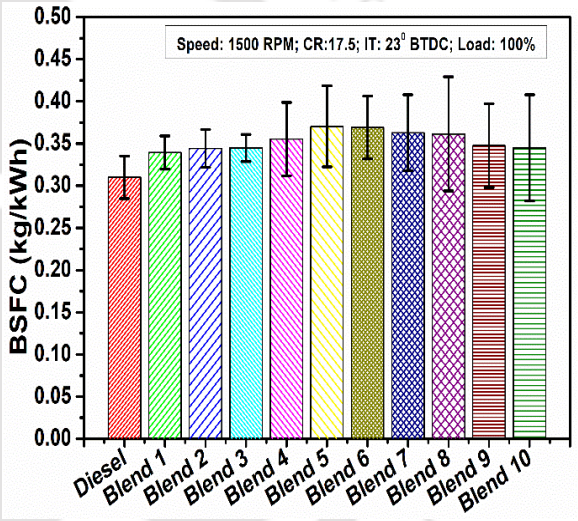

Fig. 4.2(b) Variation of BSFC for different blends at full load

The diagram presented in **Figs. 4.4(a)-(b)** displays the changes in volumetric efficiency (VE) for diesel and tri-biodiesel-diesel blends in relation to engine load. This is because, fuel consumption increases at high load but air consumption remain same at different loads due to constant engine speed which leads to increases in gas temperature. Consequently, volumetric efficiency also decreases. The results in the figure indicated that the VEs of the blended fuels are slightly lower to that of diesel. At full load, diesel showed a VE of 81.81% which is on an average 3.67% higher compared to the blended fuels. Among all the tri-biodiesel-diesel blends, the maximum average VE of 80.59% was found in case of Blend-2. The reason behind lower VE for biodiesel blends is the higher temperature of the residual gases from exhaust stroke. The higher cylinder temperature due to the presence of biodiesel in the blends causes the intake air temperature to increase, resulting in a reduction in the

amount of air drawn in and, consequently, a decrease in volumetric efficiency. A reduction in volumetric efficiency for biodiesel blends compared to diesel was also reported in the past studies [226,227].

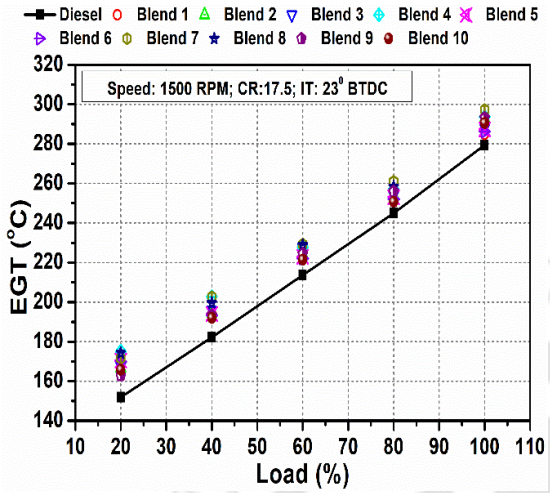

Fig. 4.3(a) Variation of EGT with engine load

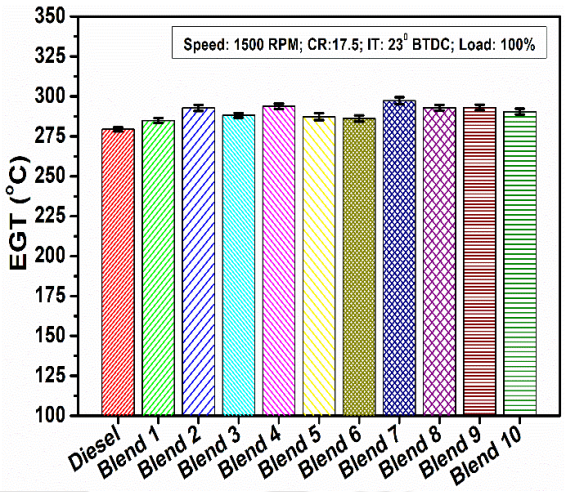

Fig. 4.3(b) Variation of EGT for different blends at full load

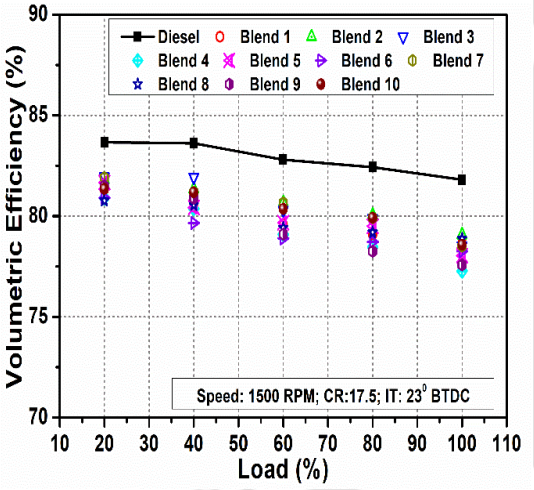

Fig. 4.4 (a) Variation of VE with engine load

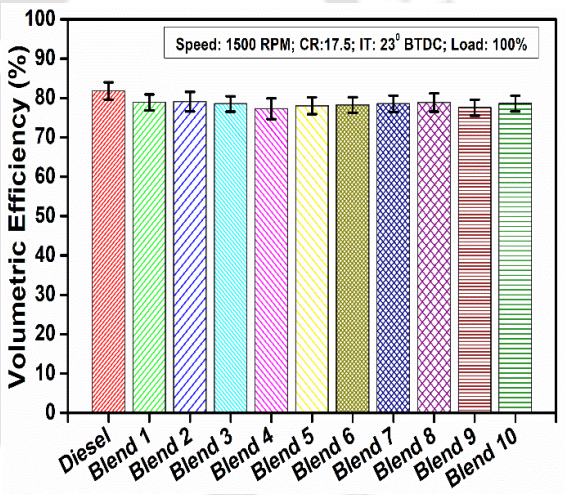

Fig. 4.4(b) Variation of VE for different blends at full load

4.4 Combustion characteristics of diesel engine

Cylinder pressure is one of the most important parameters to be evaluated to comprehend the combustion characteristics as it directly impacts the performance and exhaust emission of the engine [105]. The variations of rate of pressure rise and cylinder pressure at 100% load for the all test fuels i.e. diesel and tri-biodiesel-diesel blends are shown in **Fig. 4.5** and **Fig 4.6**. At full load, the diesel test shows a maximum rate of pressure rise of approximately 9.33 bar/°CA. However, when considering all the blended fuels, the maximum rate of pressure rise falls within the range of 7.23 to 9.02 bar/°CA, which is on an average of 11.18% lower than that of diesel. The rate of pressure rise was highest in case of Blend-2 (9.02 bar/°CA) and lowest for

Blend-4 (7.23 bar/°CA). This implies that presence of biodiesel in the fuel blends can result in a quieter and smoother operation than diesel. Blends exhibit an earlier onset of combustion due to their shorter ignition delay, resulting in a reduced quantity of premixed combustible fuel-air mixture available after the ignition delay. As a consequence, these blends produce a lower rate of pressure rise. Similar observation of lower rate of pressure rise for biodiesel blends is also experienced in past studies [228,229]. It has been estimated during the experiments that with increasing load, cylinder pressure (CP) increases irrespective of the fuels. It is also observable from **Fig. 4.6** that the tri-biodiesel-diesel blends showed more CP than diesel at full load condition. The reason behind higher CP for the blends is the fuel burns with far more intensity with the presence of biodiesel and elevates the pressure further at TDC. Compared to diesel with CP of 70.19 bar, tri-biodiesel-diesel blends showed an average of 6.42% higher value. The maximum CP at full load condition for Blend-1, Blend-2, Blend-3, Blend-4, Blend-5, Blend-6, Blend-7, Blend-8, Blend-9 and Blend-10 are found to be 74.55, 75.16, 74.53, 73.1, 75.21, 75.07, 75.75, 74.84, 75.01 and 73.79 bar, respectively. This observed variation in CP could be attributed to the disparity in ignition delay between diesel and biodiesel blends. With longer ignition delay of diesel causing combustion to initiate later in the expansion stroke, leading to a lower maximum CP value and further removed from TDC. The higher oxygen content due to presence of biodiesel in the blended fuels facilitates complete fuel combustion during the main combustion phase, while diesel fuel may continue to burn in the late combustion phase due to delayed combustion [230].

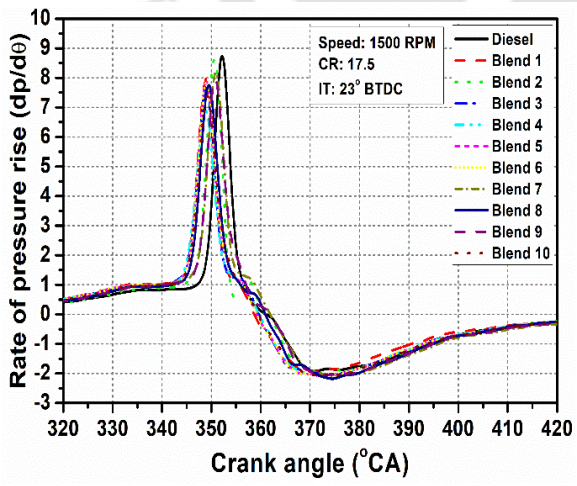

Fig. 4.5 Rate of pressure change for test fuels at full load

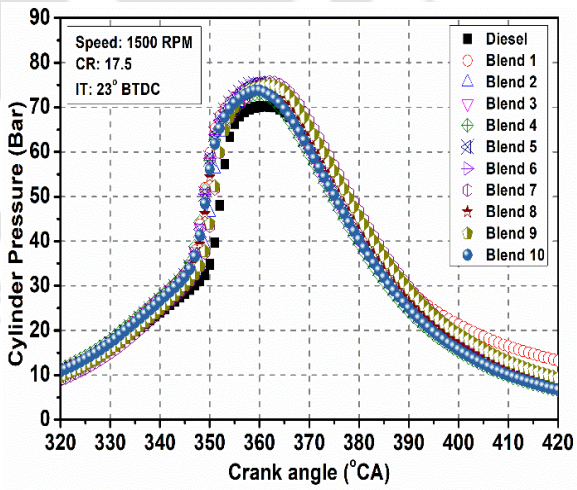

Fig. 4.6 Cylinder pressure for test fuels at full load

The shorter ignition delay (ID) for tri-biodiesel-diesel blends compared to diesel can be seen in the **Fig. 4.7**. Higher cetane number possessed by the blends due the presence of biodiesel tend to auto-ignite more readily and have shorter ID than diesel. Among all blends, for Blend-

1, Blend-4 and Blend-5, the cetane number was found maximum (as seen in **Table 4.2**), leading to minimum ID of 9 °CA at full load as compared to 14°CA for diesel. It can also be explained that biodiesel blends having high bulk modulus of compressibility than that of diesel [231] leads to faster liquid fuel pressure rise upon injection and quicker propagation of pressure waves towards the injectors. As a result, the ignition timing of the blends is advanced and minimizes the ID [232]. Irrespective of all the test fuels, minimum ID was found at higher load. Higher temperature generation during higher loads can cause biodiesel blends to undergo thermal cracking, resulting in the production of lighter compounds that can ignite earlier before TDC and lead to shorter ID [230]. The variation of NHRR with respect at full loading condition for all the fuels are shown in **Fig. 4.8**. A negative NHRR is experienced at the beginning due to the accumulation of fuel during ID. However, once the fuel ignites and combustion takes place, the heat release rate becomes positive. Blended fuels tend to exhibit earlier combustion initiation, and this effect is particularly noticeable with the addition of biodiesel to the blends. The higher calorific value of diesel than tri-biodiesel-diesel blends resulted in higher NHRR of 105.95 J/°CA for diesel. This also possibly because of a greater accumulation of fuel in the combustion chamber during the premixed combustion stage caused by longer ID, thereby leading to a higher NHRR. Another possible reason may be higher volatility and better mixing of diesel with air leads to higher heating rate in the premixed combustion phase [229]. It has been observed from the figure that the Blend-2 resulted in maximum NHRR of 108.23 J/°CA, while minimum NHRR of 77.83 J/°CA was found for Blend-4 at full engine load condition. Even though blended fuels exhibit lower NHRR, the peak NHRR of Blend-2 is observed to be comparable to that of diesel, indicating effective utilization of the oxygen content present in the fuel during the combustion process.

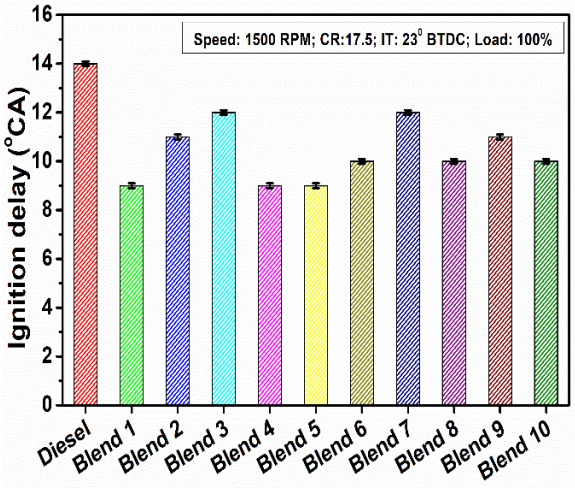

Fig. 4.7 Ignition delay for test fuels at full load

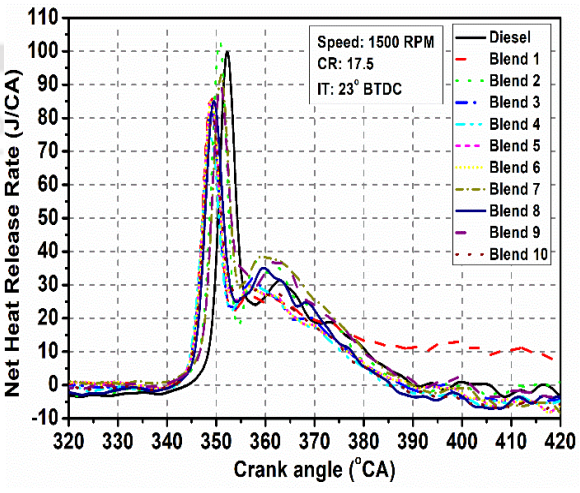

Fig. 4.8 Net heat release rate for test fuels at full load

4.5 Emission characteristics of diesel engine

Incomplete combustion of fuels can result in the release of harmful carbon monoxide (CO) in the exhaust gas. However, biodiesels are different from fossil fuels as they contain oxygen molecules in their composition. This oxygen helps to improve combustion and ultimately reduces the amount of CO emitted during the combustion process. Earlier studies have demonstrated that use of biodiesel containing abundant oxygen compared to diesel can effectively reduce the of CO emission [233]. The **Fig. 4.9** illustrates the level of CO emissions for both diesel and tri-biodiesel-diesel blends at different engine load. At 100% load, CO emission of 90.74 ppm was found in case of diesel, while Blend-2 showed the minimum emission of 46.24 ppm. On an average, the blended fuels resulted in 29.7% reduction in CO emission compared to diesel. Apart from the oxygen availability, higher cetane number, lower probability of fuel- rich zones formation and early start of combustion also may justify the CO reduction with the blends during engine running condition [230]. Emission of CO is found to be maximum at 20% (minimum) load for all the tested fuels. However, CO emission is found to be decreasing with increase in load up to 80% load and then it increases again. At low load (20%), low temperatures in the combustion chamber hinders the proper evaporation of the fuel and subsequent incomplete combustion, resulting in high CO emissions. At intermediate loads, improved vaporization of injected fuel and better fuel/air mixture preparation enhances the combustion process and reduce CO emissions approximately up to 80% engine load. But at full load, due to the large amount of injected fuel leads to the formation of rich air-fuel mixture, results in increase of CO emissions despite the relatively high temperature in the cylinder [234,235]. A study conducted by Dabi and Saha [236] observed similar trend of emission of CO. They reported that high-viscosity fuels restricts the effective atomization of fuel, creating a localized rich mixture under high engine load conditions. This, in turn, results in incomplete combustion and the generation of CO in the exhaust. The variation of unburned hydrocarbon (HC) for all tested fuels as a function of engine load depicted in **Fig. 4.10**. Hydrocarbon is released from the engine exhaust as a result of incomplete combustion and the figure showed a similar trend as CO emission. Several factors can reasonably contribute to HC emissions in diesel engines. These include fuel retention within the crevice volume of combustion, the quenching of oxidation reactions at low temperatures, the presence of locally over-lean or over-rich fuel mixtures, the formation of liquid wall filaments due to excessive spray impingement and incomplete fuel evaporation [225]. The factors that account for the differences in hydrocarbon emissions for diesel and tri-biodiesel-diesel blends can be considered identical to those previously described for CO emission. It happens because of the

presence of oxygenated compounds in biodiesel which provides better combustion. Analogous pattern of HC emission was also reported in a study conducted by Debnath *et al.* [237]. The author points out a clear connection between HC emissions and load variation. When the engine operates at lower loads, the temperature isn't high enough to combust all the supplied fuel effectively. Conversely, as the load increases, there's an insufficient quantity of air available to efficiently burn the greater amount of fuel supplied to meet the high load demands. Both of these scenarios lead to increased HC emissions in both low and high load conditions. Here, the average HC emission with diesel is found to be 41.09 ppm which was 37.61% higher compared to the average value of all blended fuels. Among all tri-biodiesel-diesel blends, Blend-2 resulted in minimum average HC emission of 24.25 ppm. Emission of carbon dioxide (CO_2) increases almost linearly with increase in engine load as shown in **Fig. 4.11**. In fact, increased loads result in a greater quantity of fuel injection, and the level of CO_2 emissions remains relatively consistent across all fuels. It was observed from the figure that, emission of CO_2 was higher at maximum engine loading condition, even though the highest emission of CO and HC was found to be a full load. Debnath *et al.* [238] also observed maximum emission of CO, HC and CO2 at full loading condition. It was reported in a study that the high viscosity of biodiesel hinders the efficient atomization and vaporization leading to improper air-fuel mixing process. When the engine operates under a higher loading condition, it results in the combustion of a richer fuel-air mixture, leading to increased emissions of CO and CO_2 [239]. At 100% load, CO_2 emission of 4.29% was found in case of diesel fuel. While, maximum and minimum CO_2 emissions for tri-biodiesel-diesel blends were achieved to be 6.89 and 4.62% for Blend-1 and Blend-7, respectively. On an average, tri-biodiesel-diesel blends resulted in 45.21% higher emission of CO_2 compared to diesel considering complete load range. A high level of CO_2 emissions from an engine in case of blended fuels may suggest that the fuel is being burned more efficiently. During the combustion inside the cylinder, the fixed amount of carbon present in the fuel is converted either into CO, HC, or CO_2, depending on degree of completeness of the combustion process. Previous literatures have also reported comparable results [240,241]. On the other hand, high temperature environment inside the cylinder, availability of excess intrinsic oxygen content in biodiesel, early fuel injection and the utilization of fuels with high cetane numbers enhances the formation of NO_X emission in engines [242,243]. It is evident from the **Fig. 4.12** that diesel contributes to lower emission of NO_X compared to all tri-biodiesel-diesel blends. With increase in load the emission of NO_X increases. This increasing tendency of NO_X emission with respect to load is dependent on the combustion temperature that is confirmed by the EGT

curves presented in **Fig. 4.3**. A study conducted by Dabi *et al.* [244] reported identical behaviour of NOx emission mentioning that increase in load allows a greater amount of fuel to enter the combustion chamber, resulting in higher gas temperatures. This, in turn, creates a favorable environment for increased NOx formation. On an average, the lowest and the highest NO_X emission of 82.94 ppm of 100.19 ppm have been observed for diesel and Blend-7, respectively. Among all the blends, the minimum average NO_X emission is found to be 91.04 ppm for Blend-1. For entire range of load, the blended fuel resulted in 15% higher emission of NO_X compared to that of diesel fuel.

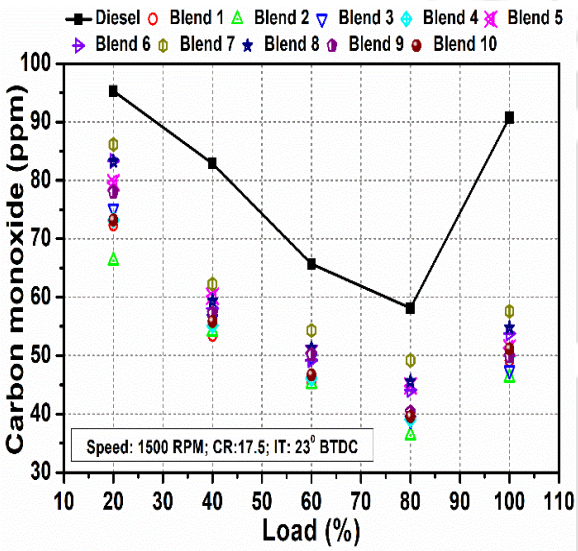

Fig. 4.9 Emission of CO with engine load

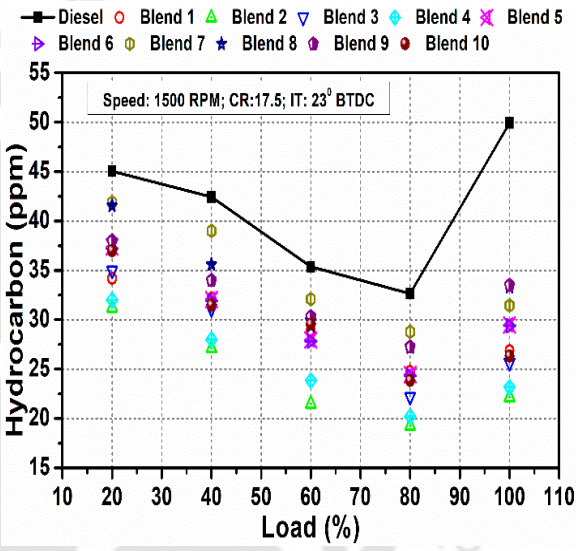

Fig. 4.10 Emission of HC with engine load

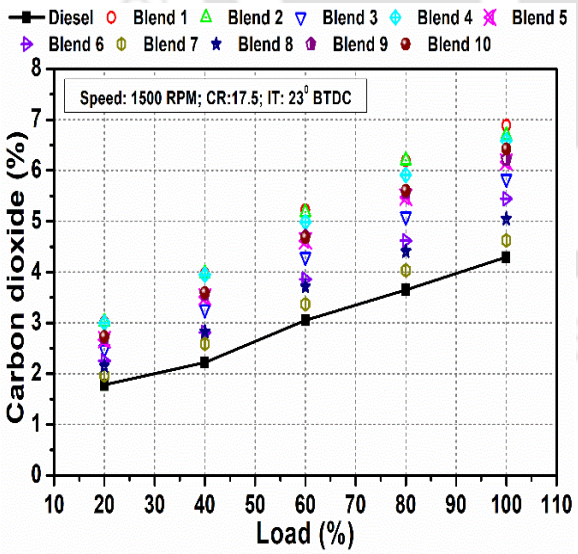

Fig. 4.11 Emission of CO_2 with engine load

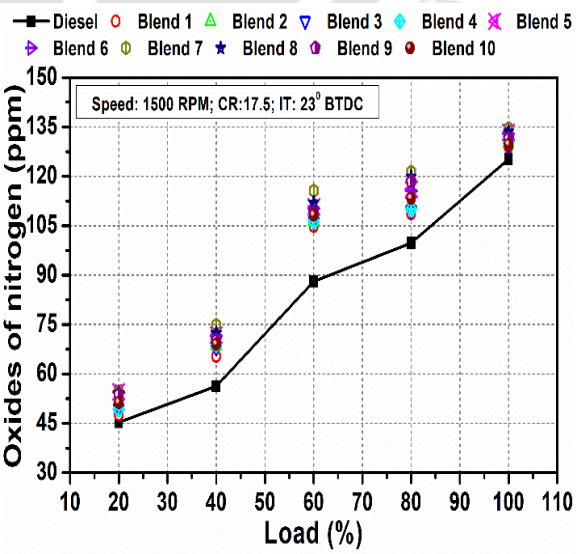

Fig. 4.12 Emission of NO_X with load

4.6 Summary of the chapter

Three non-edible biodiesels, namely Jatropha (JB), Karanja (KB), and Mahua (MB), were considered for experimental investigation. These biodiesels were mixed with conventional

diesel fuel in different proportions to form ten different tri-biodiesel-diesel blends (Blend-1-Blend-10), with a maximum of 30% biodiesel and 70% diesel. Experiments were conducted at a standard engine operating condition with a compression ratio of 17.5 and injection timing of 23° BTDC at different engine loads. The tri-biodiesel-diesel blends resulted in lower BTE and higher BSFC than that of diesel fuel under similar experimental conditions. However, in the case of blended fuels a lower value of CO and HC and higher NO_X were observed compared to diesel fuel under similar experimental conditions. Due to the higher cetane number of biodiesel and oxygenated compounds present in it, early combustion of the blended fuel resulted in shorter ignition delay and higher cylinder pressure, with a lower net heat release rate and rate of pressure rise compared to that of diesel fuel. In terms of performance, Blend-1 (20%JB+5%KB+5%MB) showed the maximum BTE of 25.1% compared to 27.57% BTE for diesel. However, engine emission especially CO and HC was found to be minimum in case of Blend-2 (15%JB+10%KB+5%MB). Moreover, among all the tri-biodiesel-diesel blends, NO_X emission was also found to be minimum for Blend-2. Additionally, the BTE with Blend-2 was determined to be 24.65%, which was only 1.85% lower than Blend-1. Therefore, based on the experimental results and global environmental concern, Blend-2 was selected as the pilot fuel and used in dual fuel experiments for investigation of engine performance and emission characteristics with simulated gaseous fuels and raw gas mixtures (BG and PG). These aspects are elaborated in the in the chapters 5 and 6.

5

Results and Discussion of Engine Characteristics with Simulated Gaseous Fuels

Chapter Outline:

CHAPTER 5: RESULTS AND DISCUSSION OF ENGINE CHARACTERISTICS WITH SIMULATED GASEOUS FUELS

5.1 Introduction

Dual fuel (DF) combustion is an intricate process compared to diesel mode. The existence of both combustible and non-combustible substances in biogas (BG) and producer gas (PG) further boosts the complexity of the combustion mechanism. Methane concentration in biogas determines the quality and energy value of the fuel [49]. Moreover, CH_4 with low carbon content also limits the engine exhaust pollutants, especially NO_X [115]. Conversely, CO_2 fraction in BG dilutes the intake charge, lowers the burning velocity, and also uplifts the self-ignition temperature due to which it behaves as a heat absorbing media during combustion, resulting in lower combustion temperature during biogas induction [94]. Apart from that, producer gas predominantly consists of two energy-rich molecules, hydrogen (H_2) and carbon monoxide (CO). Hydrogen is a promising environmental-friendly fuel for IC engines, as it only produces water vapours when burned, making it a clean option for reducing emissions. Additionally, IC engines are capable of effectively utilizing CO gas as fuel, as it is not contaminated and can be combusted efficiently. Considering the application of BG and PG in diesel engine, the most of the potential gases include CH_4, CO_2, H_2 and CO as main fuel compounds and it is crucial to comprehensively understand the impact of these gas components on the engine behaviour. Various researchers have tried to explore the application of these clean and low cost fuels in reciprocating engines for electricity generation. However, very less studies have been found on the application of two or more gases combinedly as primary fuel at a time to evaluate the overall engine characteristics. This present work aims to enhance the understanding of the individual and combined effects of these gas compounds on the performance, combustion and emission characteristics of a diesel engine. Thus, the results obtained from this study may contribute to the optimization of gaseous fuel production for engine usage by employing post-conditioning techniques to enhance the concentration of hydrogen (H_2) or methane (CH_4) in the gas composition.

5.2 Experimental design

This experimental work explores the parametric effect of gas composition, compression ratio (CR) and pilot fuel injection timing (IT) on the performance, combustion, and emission characteristics of diesel engine under dual fuel (DF) mode. The primary gaseous fuels utilized for the study are simulated biogas (SBG), simulated producer gas (SPG), and SPG-SBG

mixture. The compositions of the gaseous fuels are prepared based on the volumetric percentage of the individual gas components and are inducted into the engine cylinder using a novel venturi-type air-gas mixer (mentioned in Chapter 3 and Appendix-B). The best tri-biodiesel-diesel blends i.e. Blend-2 (discussed in Chapter 4) has been considered as pilot fuel for all the experiments conducted under DF mode. For the preparation of SBG, methane (CH_4) and carbon dioxide (CO_2) are mixed at four different ratio as depicted in **Table 5.1**. Similarly, hydrogen (H_2) and carbon monoxide (CO) are also mixed at four different ratios for the preparation of SPG. Again, in case of mixed mode experiments with SPG-SBG mixtures, 50% H_2 generation in a biomass gasifier is considered from the point of technical feasibility and the experimental matrix has been designed. Here, SPG-2 i.e. H_2 and CO at a 50:50 ratio are mixed with a four different SBGs (as mentioned in **Table 5.1**) to simulate the SPG-SBG mixture. The important properties of SBGs and SPGs used for the experiments are calculated and summarized in **Table 5.1**. DF engine experiments are conducted in three phases as per the experimental matrix illustrated in **Table 5.2**. In the first phase, four different combinations of SBGs, SPGs and SPG-SBG mixtures are tested at standard diesel engine operating condition, with at five different loads, viz. 20%, 40%, 60%, 80%, and 100%. Then in the second phase, engine parameters are investigated with best SBG, SPG and SPG-SBG mixture at varying CR (16, 17, 17.5 and 18) and fixed IT of 23° BTDC. In the final phase, experiments were conducted with varying IT of 23-32° BTDC with a step of 3° CA considering the best CR.

Table 5.1 Properties of simulated gaseous fuels used in the study

	Fuels	Chemical composition	Density (kg/m³)	Calorific value (MJ/kg)	Stoichiometric A/F ratio	Energy Density (MJ/Nm³)
Properties of simulated biogas (SBG)	**SBG-1**	55% CH_4 + 45% CO_2	1.275	15.431	5.304	19.69
	SBG-2	60% CH_4 + 40% CO_2	1.213	17.701	6.084	21.48
	SBG-3	65% CH_4 + 35% CO_2	1.151	20.216	6.948	23.27
	SBG-4	70% CH_4 + 30% CO_2	1.088	23.02	7.912	25.06
Properties of simulated producer gas (SPG)	**SPG-1**	40% H_2 + 60% CO	0.79	15.21	3.917	11.94
	SPG-2	50% H_2 + 50%CO	0.67	17.56	4.596	11.75
	SPG-3	60% H_2 + 40% CO	0.55	20.90	5.56	11.56
	SPG-4	70% H_2 + 30% CO	0.44	26.01	7.035	11.37

Table 5.2 Experimental matrix

Mode	Fuel used	Engine condition
DF-1	Primary fuel: SBG-1, SBG-2, SBG-3 and SBG-4 Primary fuel: SPG-1, SPG-2, SPG-3 and SPG-4 Primary fuel: SG-1 (SPG-2/SBG-1), SG-2 (SPG2/SBG-2), SG-3 (SPG-2/SBG-3) and SG-4 (SPG-2/SBG-4)	Load: 20, 40, 60, 80 and 100% CR: 17.5, and IT: 23° BTDC
DF-2	Primary fuel: Best of SBG, SPG and SPG-SBG mixture based on DF-1	Load: 20, 40, 60, 80 and 100% CR: 16, 17, 17.5 and 18 IT: 23° BTDC
DF-3	Primary fuel: Best of SBG, SPG and SPG-SBG mixture based on DF-1	Load: 20, 40, 60, 80 and 100% CR: Best CR based on DF-2 IT: 23°, 26°, 29° and 32° BTDC

5.3 Effect of gas composition on engine characteristics

The results are discussed focusing on three different sections namely performance, combustion and emission characteristics. The performance characteristics includes brake thermal efficiency (BTE), brake specific energy consumption (BSEC), exhaust gas temperature (EGT) and pilot fuel replacement (PFR). The combustion analyses include ignition delay (ID), peak cylinder pressure (PCP) and net heat release rate (NHRR). Finally, emission analysis is performed by measuring carbon dioxide (CO_2), carbon monoxide (CO), hydrocarbon (HC) and oxides of nitrogen (NO_X). The theoretical equations, based on which performance and combustion analysis are executed, are included in Appendix-A.

5.3.1 Performance characteristics

The brake thermal efficiency (BTE) of simulated biogas (SBG), simulated producer gas (SPG) and mixture of SPG-SBG operated under dual fuel (DF) mode are depicted in **Fig. 5.1(a)-(c)**. Maximum BTE is observed at higher load for all the DF operations because of the increased cylinder temperature. For all the DF operations, BTEs are observed to be lower than fossil diesel (FD) because of the lower calorific value of the gaseous fuels. Moreover, there are several factors like low combustion temperatures, combusted residual gas, gas residuals, reduced flame propagation speed, high compression work triggered by higher consumption of air-gas mixtures and heat rejection through combustion chamber that results in lower thermal efficiency in case of DF operations [75]. Increase in CH_4 volume fraction in SBG, BTE increases. At 100% load, 17.5 CR and 23° BTDC, BTE of 18.96% was found for SBG-4 as shown in **Table 5.3**, which was lower compared to 27.57% for FD. SBG-4 with high calorific value resulted in maximum BTE among the other biogas compositions. Similarly, increase in hydrogen fraction and augmenting the H_2/CO ratio in the fuel effectively enhanced the

thermal efficiency. For SPG-DF operations, maximum BTE of 19.05% was obtained in case of SPG-4 which is 24.19, 19.6 and 1.5% higher than SPG-1, SPG-2 and SPG-3, respectively (**Table 5.3**). Again, in case of SPG-SBG dual fuel operation, the SPG (SPG-2) composition was kept constant and the effect of addition of SBGs are analyzed. Again, with the addition of enriched biogas (i.e. SBG with higher CH_4 percentage) in the mixture resulted in the increment of BTE. At 100% load, SG-4, i.e. the combination of SPG-2/SBG-4 showed the maximum BTE of 20.04% which is 5.69 and 5.19% higher compared to SBG-4 and SPG-4, respectively (**Table 5.3**).

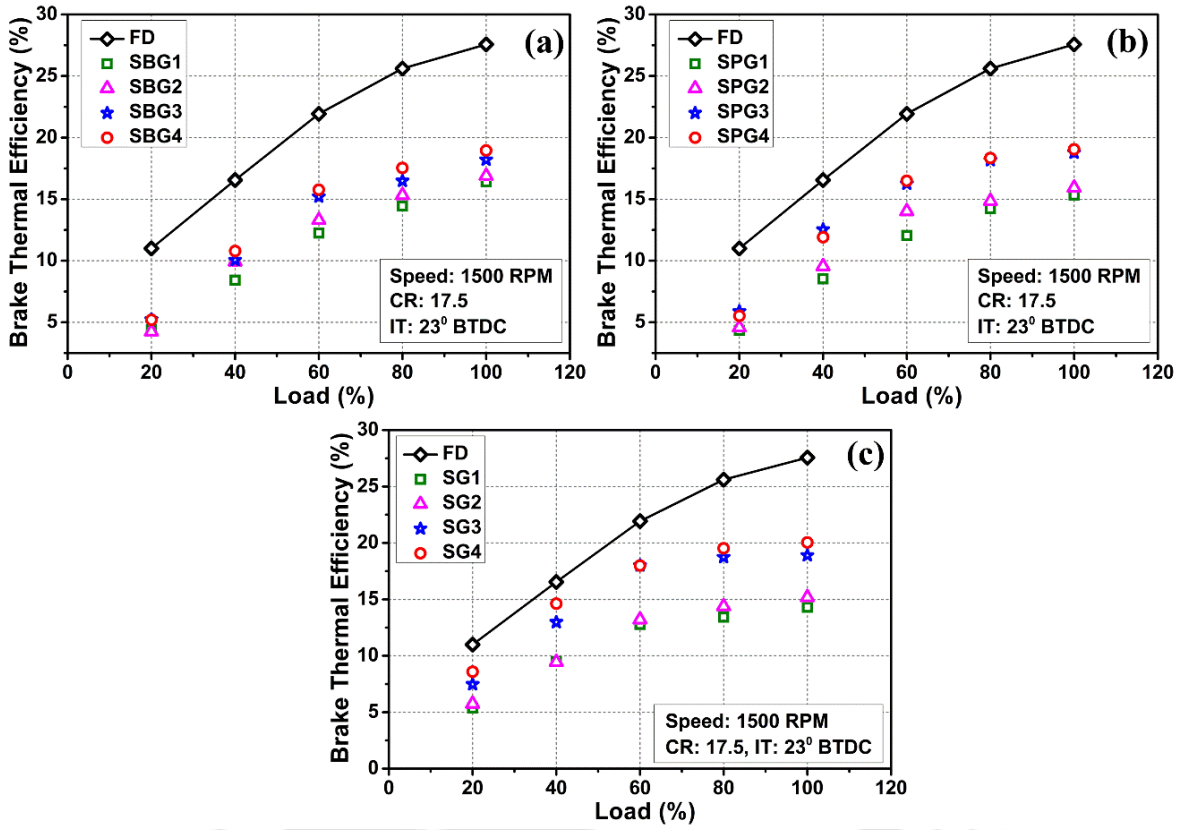

Fig. 5.1 Variation of BTE with load for (a) SBGs, (b) SPGs and (c) SPG-SBG mixtures

The change of brake specific energy consumption (BSEC) for different SBGs, SPGs and SPG-SBG mixtures at varying load is depicted in **Fig. 5.2(a)-(c)**. At low load of 20%, irrespective of the gas compositions, the differences in BSEC between FD and DF modes were higher. Gaseous fuels have lower flame velocity and undergo incomplete combustion, resulting in poorer performance compared to diesel fuel. However, as the load increases, the dual fuel modes exhibit an improvement in their BSEC, although it is still higher than that of the diesel mode. This is because, in order to produce the same power output as the diesel mode, gaseous fuels with low energy density require a larger amount of fuel. At full load and standard test condition, SBG-4 showed the minimum BSEC of 5.27 kJ/s of fuel/kW output which is higher compared to FD with BSEC of 3.65 kJ/s of fuel/kW output. This is ascribed to the lower calorific value, combustion temperature, stoichiometric air-fuel ratio of SBGs [245]. Moreover,

increase in the CH_4 concentration in SBGs from 55 to 70% resulted in 33.37% reduction in BSEC. Likewise for SPG-DF operation, lower BSEC of 5.24 kJ/s of fuel/kW output was found in case of SPG-4 which is 43.9% higher compared to FD. Among SPGs, the higher H_2 fuel (70%) produced a lower BSEC due to faster combustion rates of hydrogen. It can been observed from **Table 5.3** that, with the addition of SBGs with SPG-2, there was a reduction in BSEC for all the combination of SPG-SBG mixtures. Among SPG-SBG mixtures, SG-4 with higher thermal efficiency resulted in lower BSEC of 4.98 kJ/s of fuel/kW output at 100% load, which is 28.64, 24.21 and 6.49% lower than SG-1, SG-2 and SG-3, respectively. For the entire engine load range, SG-4 resulted with an average reduction of 26 and 21% BSEC compared to SBG-4 and SPG-4. Based on the analysis, it can be concluded that incorporating biogas with a high concentration of CH_4 is advantageous as it improves thermal efficiency and decreases energy consumption.

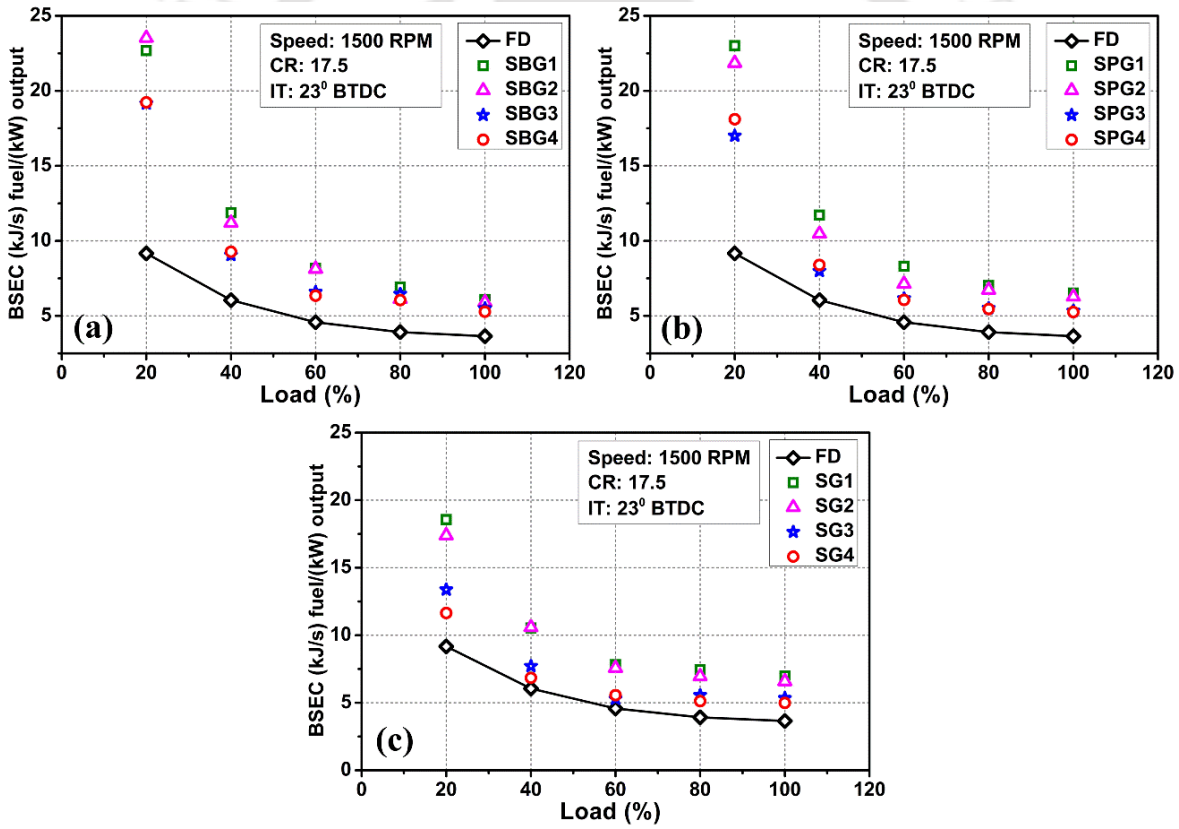

Fig. 5.2 Variation of BSEC with load for (a) SBGs, (b) SPGs and (c) SPG-SBG mixtures

The relationship between the exhaust gas temperature (EGT) and the load for SBGs, SPGs and SPG-SBG mixtures are illustrated in **Fig. 5.3(a)-(c)**. The figures reveled a linear incremental trend of EGT with the increase in load and this is because of the high energy input. SBG-DF operation showed greater EGT than FD mode due to high auto-ignition temperature and low burning velocity of SBGs, which delays the burning of air-SBG mixture and reduces the

combustion duration to extract engine power [215]. Additionally, CO_2 in SBG dilutes the intake mixture, absorbing more heat during combustion. This results in delayed combustion, causing the burned gases to exit at a higher temperature. Hence, SBG with higher CO_2 levels have higher EGT. At full engine load, SBG-4 with 70% CH_4 fraction, resulted in minimum EGT of 344.01°C (**Table 5.3**). Similar observations were made by Verma et al. [246] scrubbed biogas with higher CH_4 content. For SPG-DF mode, the EGT was found to be higher compared to SBG-DF operations, on an average 87.6% considering the entire range of engine load and gas compositions. This is because of the presence of H_2 in the fuel mixture of SPGs. Moreover, the highest EGT was observed for SPG-4 with 70%H_2 due to faster combustion and high cylinder temperature. At full engine load, minimum EGT of 642.4°C was observed for SPG-1 which is 3.14, 4.38 and 6.16% lower than that of SPG-2, SPG-3 and SPG-4, respectively. Analogous observation was also documented in past study [61]. Mixing of SBGs with SPG-2 resulted in reduction of EGT which can be seen in **Table 5.3**. On an average, compared to SPG-DF operation, SPG-SBG mixtures showed a reduction of 1.78% EGT considering entire range of engine load and gas compositions. Among all the SPG-SBG mixtures, minimum average EGT of 585.45°C was observed in case of SG-1 which is 2.25, 4.85 and 5.71% lower than SG-2, SG-3 and SG-4, respectively.

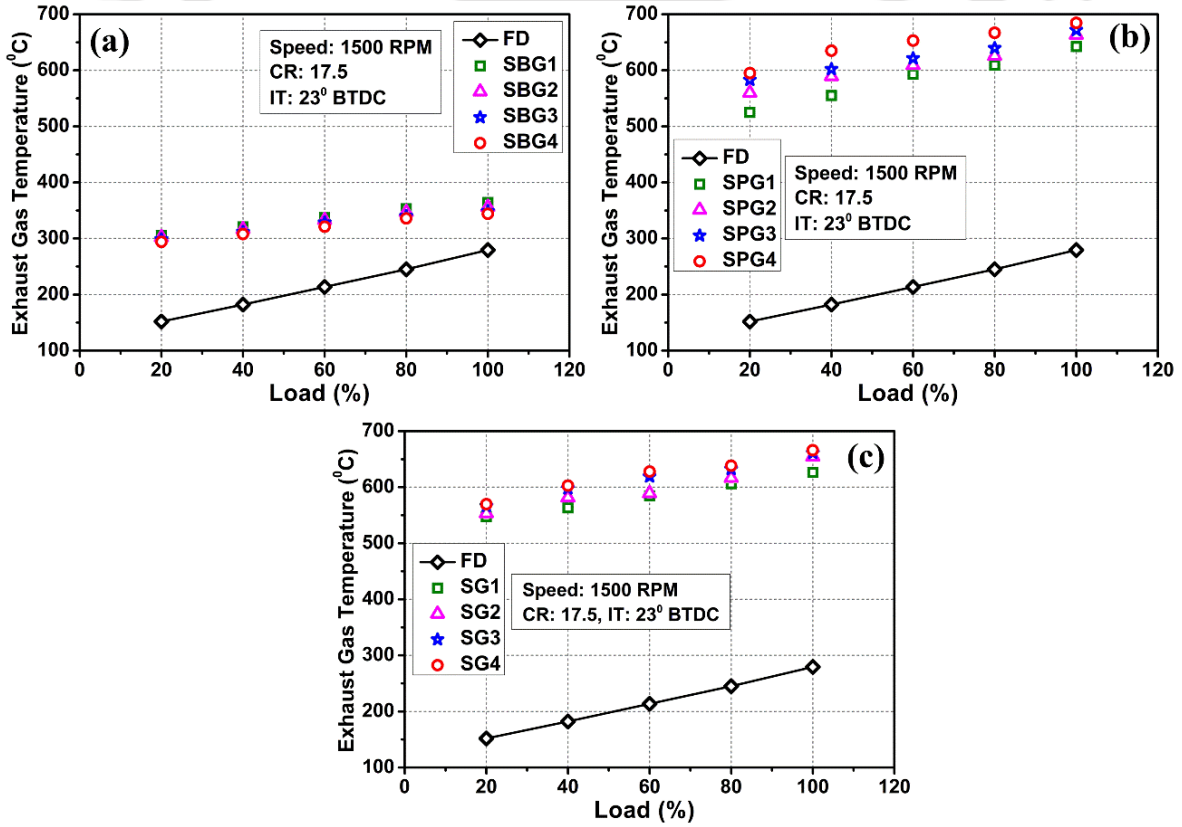

Fig. 5.3 Variation of EGT with load for (a) SBGs, (b) SPGs and (c) SPG-SBG mixtures

The pilot fuel replacement (PFR) found in case of DF experiments with SBGs, SPGs and SPG-SBG mixtures are depicted in **Fig. 5.4(a)-(c)**. Maximum replacement of pilot fuel was achieved at full engine load for all the gaseous fuel compositions. At higher loads, engine demand more energy, resulting in a significant increase in fuel consumption. This effect is more pronounced while using gaseous fuels with lower calorific values than pilot fuel, requiring higher gas flow rates to maintain fixed engine speed which result in the increase of PFR [247]. It can be observed from the figure that, SBG-4 having higher energy content with 70% CH_4 resulted in maximum PFR of 88% which is 22.2, 10 and 4.76% higher compared to SBG-1, SBG-2 and SBG-3, respectively (as shown in **Table 5.3**). Similarly, it can be seen from **Fig. 5.4(b)** that, for SPG-DF experiments, maximum PFR of 82.47% was observed for SPG-4 which is 9.39, 4.72 and 2.88% higher compared to SPG-1, SPG-2 and SPG-3, respectively. Lower PFR in case of SPG-DF experiments is due to the lower energy density of the SPG compared to SBG (as seen in **Table 5.1**). However, with the addition of SBGs with SPG-2, there was a noticeable increment in PFR. At full loading condition, SG-1, SG-2, SG-3 and SG-4 resulted in 0.13, 2.7, 5.3, 8.07% higher PFR compared to SPG-2. Therefore, it can be concluded that, combined introduction of SPG and SBG augments the combustion process and resulted in additional replacement of pilot fuel in dual fuel operations.

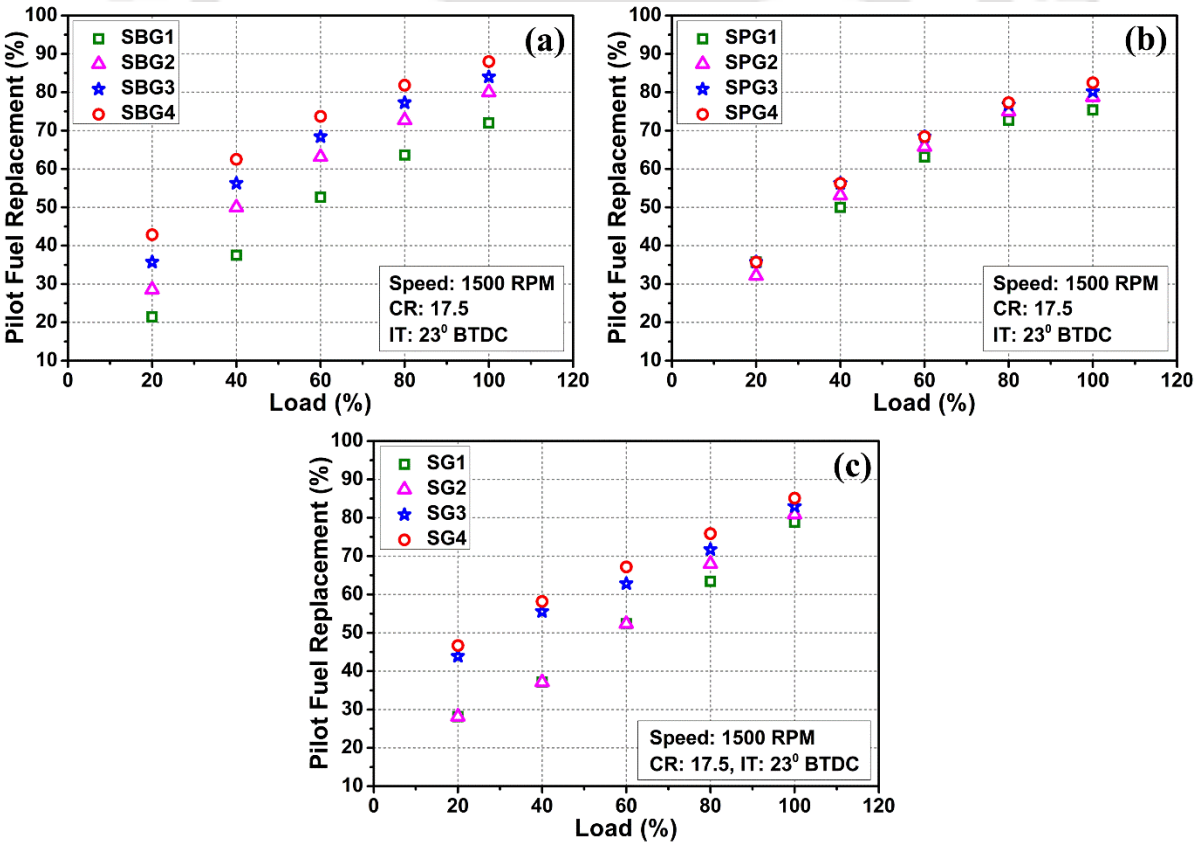

Fig. 5.4 Variation of PFR with load for (a) SBGs, (b) SPGs and (c) SPG-SBG mixtures

Table 5.3 Performance parameters of simulated gaseous fuels at full load condition

Simulated biogas (SBG)				
Performance Parameters	**SBG-1**	**SBG-2**	**SBG-3**	**SBG-4**
BTE (%)	16.42	16.90	18.20	18.96
BSEC (kJ/s fuel/kW output)	6.08	5.91	5.49	5.27
EGT	364.32	356.28	348.86	344.00
PFR (%)	72	80	84	88
Simulated producer gas (SPG)				
Performance Parameters	**SPG-1**	**SPG-2**	**SPG-3**	**SPG-4**
BTE (%)	15.34	15.92	18.77	19.05
BSEC (kJ/s fuel/kW output)	6.51	6.27	5.32	5.24
EGT	642.39	663.21	671.82	684.60
PFR (%)	75.38	78.74	80.15	82.47
SPG-SBG mixtures				
Performance Parameters	**SG-1**	**SG-2**	**SG-3**	**SG-4**
BTE (%)	14.30	15.19	18.90	20.05
BSEC (kJ/s fuel/kW output)	6.99	6.58	5.33	4.99
EGT	626.20	654.45	661.04	666.07
PFR (%)	78.86	80.88	82.93	85.11

5.3.2 Combustion characteristics

The ignition delay (ID) of pilot fuel with respect to engine load for SBGs, SPGs and SPG-SBG mixtures are shown in **Fig. 5.5(a)-(c)**. It is evident from the figures that ID progressively drops with increase in engine load for the single mode (with FD) and DF mode irrespective of the gas compositions. At lower loading condition, a higher ID is observed because of the low temperature inside the combustion chamber. For all loading condition, DF mode resulted in longer ID compared to FD mode. This is because, induction of gaseous fuel into the engine cylinder replaces certain amount of air, thereby diluting the oxygen concentration compared to single fuel mode, which leads to elongated ID. In case of SBG-DF operation, it is observed that ID was reduced when CH_4 concentration increased in the biogas composition as it is seen in **Table 5.4**. At full load with CR of 17.5 and IT of 23° BTDC, SBG-1, SBG-2, SBG-3 and SBG-4 showed ID of 22, 21, 20 and 19 °CA, respectively. This is mainly because of the presence of CO_2 in SBG which not only lowers the intake charge temperature but also augment the self-ignition temperature of the air-gas mixture [118,248]. Similarly, it can be also observed that with the increase of H_2 concentration in SPG, the ID decreased. At full load, SPG-4 showed minimum ID of 18 °CA compared to 22, 21 and 19 °CA for SPG-1, SPG-2 and SPG-3, respectively (**Table 5.4**). The ID in case of SPG-DF operation was found to be lower compared to SBG-DF operation. This is because of the higher participation of pilot fuel in SPG-DF mode which is evident from the PFR results. On the other hand, SPG-SBG mixture resulted in higher

ID compared to both SBG and SPG dual fuel operation because of the presence of both CO_2 and CO components in the gas mixture. It is also evident that SG-4 resulted in minimum ID of 21 °CA at full load, while SG-1, SG-2 and SG-3 showed ID of 25, 24 and 22 °CA, respectively.

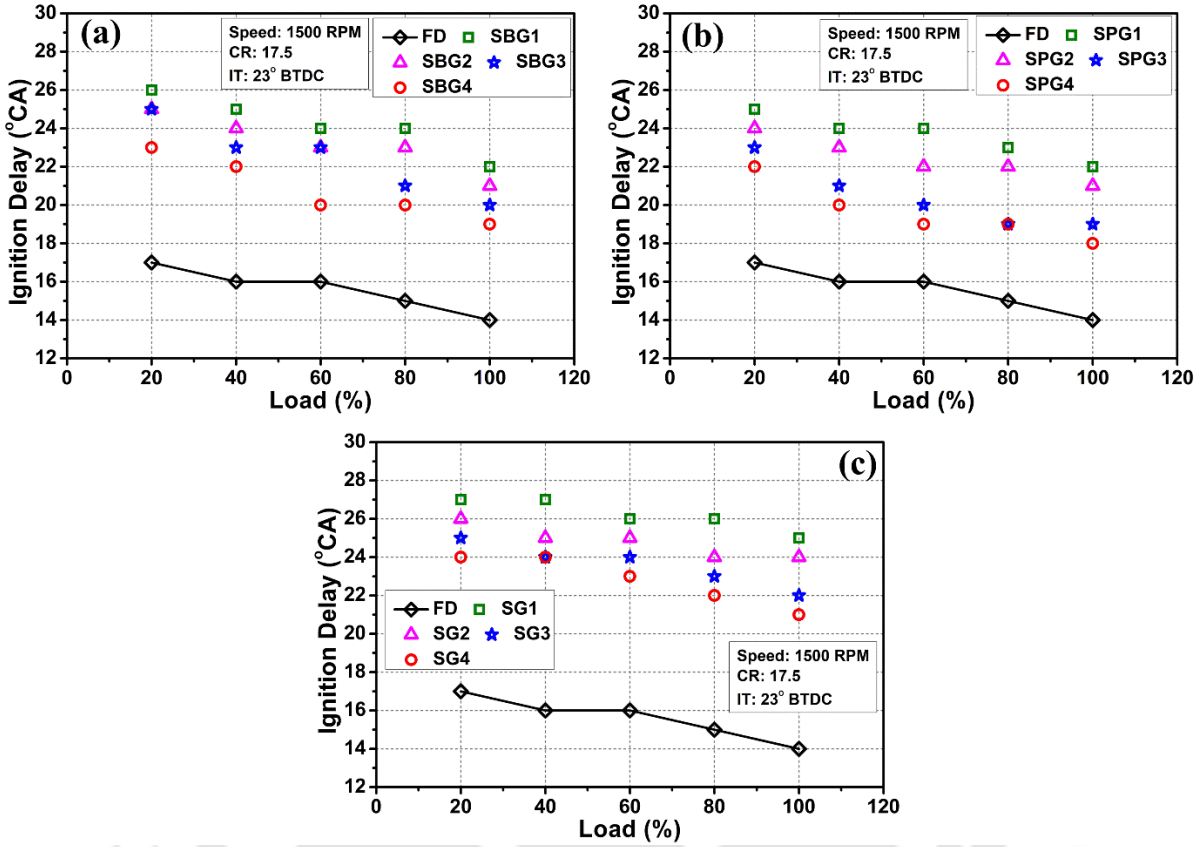

Fig. 5.5 Variation of ID with load for (a) SBGs, (b) SPGs and (c) SPG-SBG mixtures

As illustrated in **Fig. 5.6(a)-(c)**, the peak cylinder pressure (PCP) increases as the engine load increases, with the highest PCP being observed at 100% load in both fossil diesel and DF modes. For DF operations, shorter combustion duration and an increased ID shifted the overall combustion to expansion stroke, and hence, a reduction in PCP was noticed. As compared to FD mode with PCP of 70.19 bar, SBG-1, SBG-2, SBG-3 and SBG-4 resulted with 44.6, 41.5, 37.5 and 31.5% reduction in PCP at 100% load. This can be explained that the intake gas fuel mixture primarily influences the combustion rate which describes the PCP in the preliminary phase of combustion. Hence, low reactive SBG presence of CO_2 having high specific heat lowers the combustion rate leading to decrease in cylinder pressure [126,139]. Again, it was noticed during the experiments that with the increase of CH_4 in SBG, the gas flow rate decreases, that means lower amount of air is replaced in the intake charge and thereby more amount of oxygen is available in the fuel mixture to undergo better combustion. This may be the reason behind higher PCP of 48.04 bar for SBG-4 compared to 38.84, 41.01 and 43.87 bar for SBG-1, SBG-2 and SBG-3, respectively as reflected in the **Table 5.4**. On the other

hand, higher energy release rate of SPG, resulting from the presence of H_2 and greater proportion of pilot fuel with a higher calorific value, led to the rise of PCP for SPG-DF operation compared to SBG-DF mode, which can be observed from **Fig. 5.6(b)**. At 100% load, SPG-1, SPG-2, SPG-3 and SPG-4 resulted with PCP of 48.85, 58.06, 59.17 and 62.60 bar, respectively. Considering the entire load range, increase in the H_2 concentration from 40 to 70% in the SPG, on an average PCP was increased by 27.52%. This is also attributed to the poor combustion and low energy release rate of CO in the fuel mixture. Again, in case of SPG-SBG mixture, the average PCP was found to be slightly higher compared to SBG-DF. This is because of the combined effect of H_2 and CH_4 in the fuel mixture. As, the SPG composition was kept fixed (at 50% H_2 and 50% CO), the SBGs with increasing CH_4/CO_2 ratio showed a dominant effect on the cylinder pressure. It is observable from **Fig. 5.6 (c)** that at full load, maximum PCP of 57.51 bar was found for SG-4 having high CH_4/CO_2 ratio and lowest PCP was noted for SG-1 having low CH_4/CO_2 ratio. On an average, SPG-SBG mixtures exhibited 5% higher and 8.83% lower PCP in comparison with SBG-DF and SPG-DF operations, respectively.

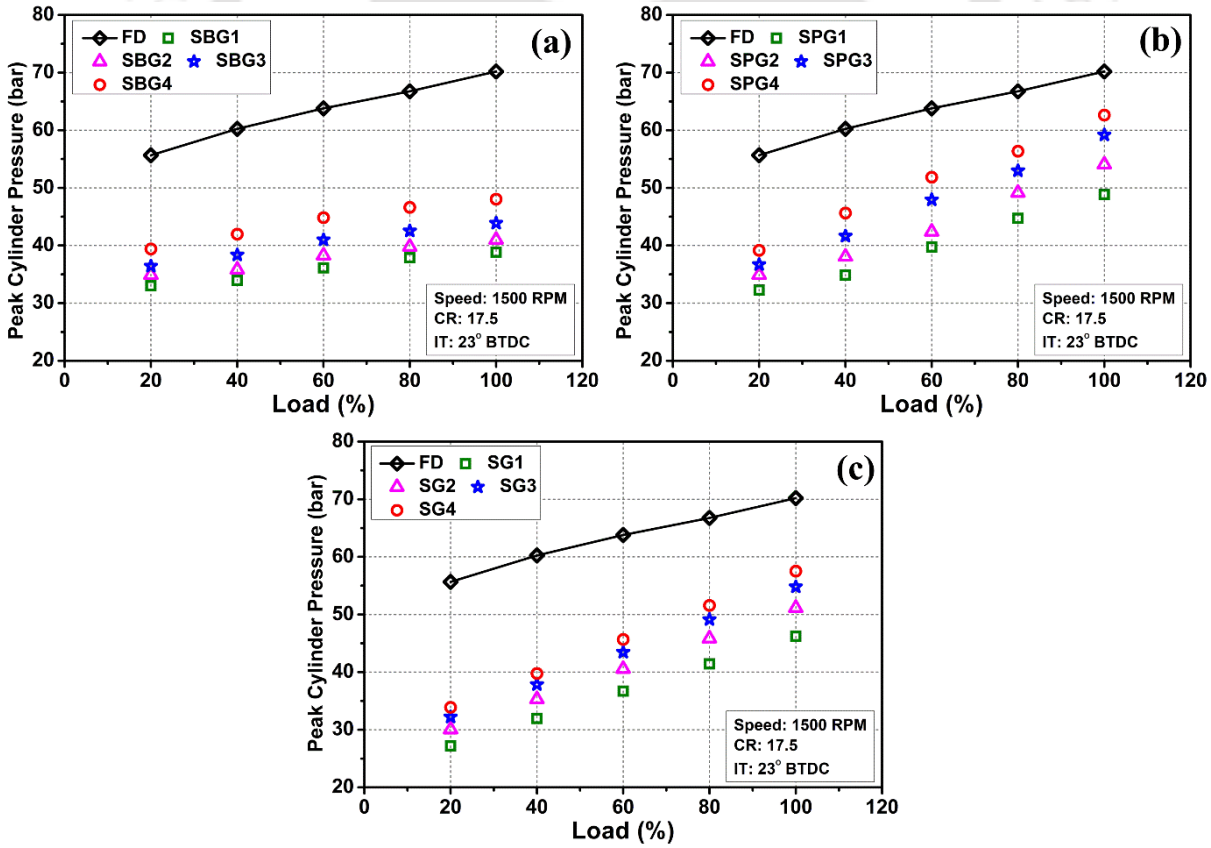

Fig. 5.6 Variation of PCP with load for (a) SBGs, (b) SPGs and (c) SPG-SBG mixtures

At maximum load, the fluctuation of cylinder pressure (CP) with crank angle for FD mode and DF mode with SBG, SPG and SPG-SBG mixture are illustrated as P-θ diagram in **Fig.**

5.7(a)-(c). **Fig. 5.7(a)** suggests that SBG-4 with higher CH_4 content, achieved a higher peak cylinder pressure (PCP) compared to other SBG compositions, and increasing the CH_4 content from 55% to 70% caused PCP to shift towards the TDC. At full load, the crank angle associated with PCP is noted to be 11°, 10°, 8° and 7° ATDC for SBG-1, SBG-2, SBG-3 and SBG-4, respectively compared to 1° ATDC for FD mode. Analogous observations were also reported in past studies [246]. In the SPG-DF mode, the presence of H_2 and CO in the fuel mixture resulted in slightly higher CP compared to SBG-DF mode. **Fig. 5.7(b)** shows that a higher percentage of H_2 in SPG-DF mode led to higher CP, but migration of the PCP towards the TDC is found to be lower in case of SPG-DF mode. This could be ascribed to the relatively slow energy release rate resulting from the lower energy density of the SPG fuel mixture. For SPG-1, SPG-2, SPG-3 and SPG-4, the maximum value of CP was achieved at crank angle of 14°, 14°, 13° and 12° ATDC, respectively. Again, in case of SPG-SBG mixture DF mode, the PCP value was observed to be shifted away from TDC as shown in **Fig. 5.7(c)**. At 100% load, SG-1, SG-2, SG-3, and SG-4 exhibited maximum CP at crank angles of 16°, 14°, 13°, and 11° ATDC, respectively.

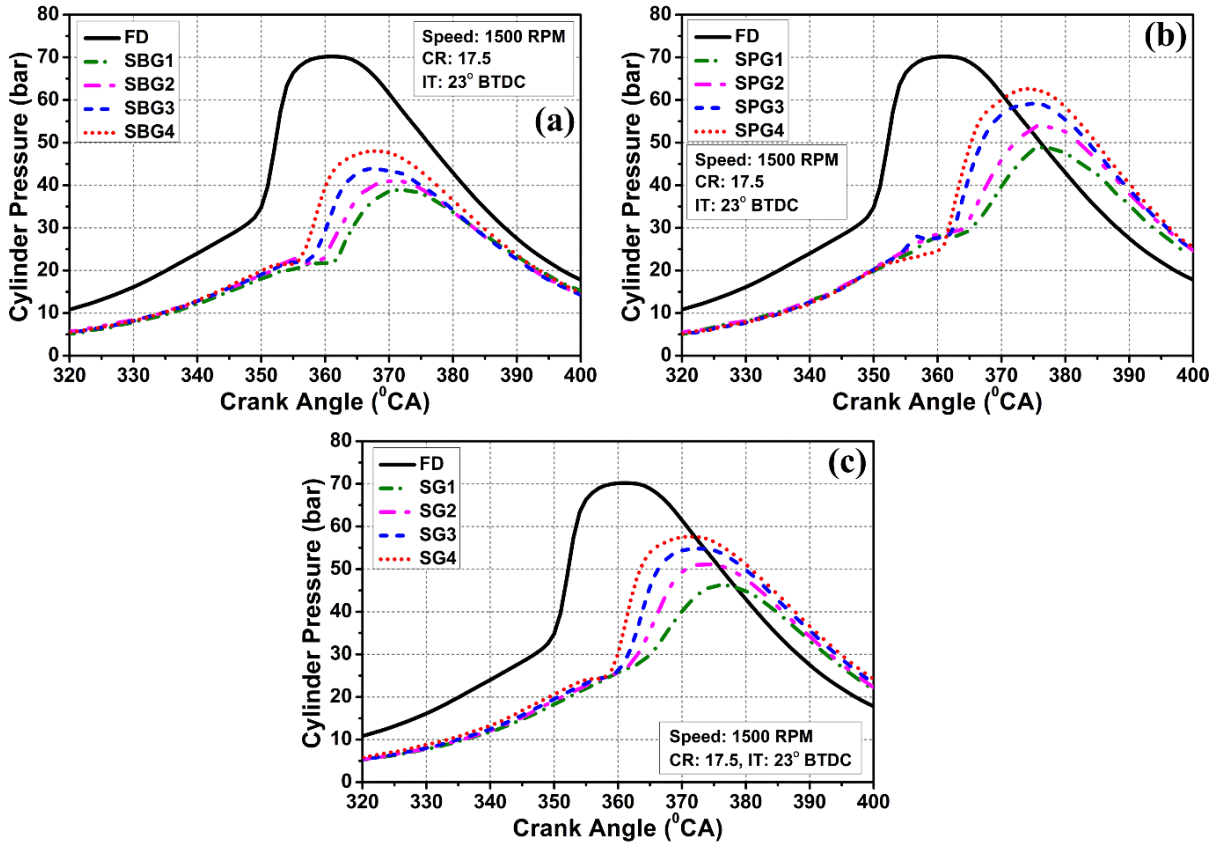

Fig. 5.7 Variation of CP at full load for (a) SBGs, (b) SPGs and (c) SPG-SBG mixtures

The corresponding net heat release rate (NHRR) diagrams of pressure crank-angle data for FD, SBG, SPG and SPG-SBG mixtures are indicated in **Fig. 5.8(a)-(c)**. The magnitude of heat

release rate increased for an increase in load due to the combustion of higher amount of gaseous fuel at higher loads. The higher calorific value of FD resulted in higher net heat release rate (NHRR) in contrast to DF mode considering all operating conditions. The quality of air-gas mixture aspirated inside the combustion chamber together with the pilot fuel and their energy densities highly defines the intensity of heat release [131]. It is revealed from **Fig. 5.8(a)** that the peak NHRR for SBG-1, SBG-2, SBG-3 and SBG-4 at 100% load and standard IT are 38.65, 40.012, 42.89 and 48.19 J/°CA which are 11°, 9°, 9° and 7° CA delayed correspondingly compared to FD with peak NHRR of 105.95 J/°CA. This is due to the existence of CO_2 and high specific heat of SBGs causing delay in the combustion process [165]. On the other hand, from **Fig. 5.8(b)** it can be seen that at 100% load, the peak NHRR were found to be 123.65, 115.76, 112.86 and 102 J/°CA for SPG-4, SPG-3 and SPG-4 having 70, 60, 50 and 40% H_2 content, respectively. The peak NHRR reaches high values for SPG-DF operations is due to the higher energy content of SPG. Similar trends were also exhibited with the P-θ variations. Similar to SBG-DF operation, peak NHRR values for SPG-DF mode were also delayed by 20°, 14°,13° and 12° CA with respect to FD mode. From the experiments of SPG-SBG mixtures, it was evident that SG-4 with combination of SPG-2/SBG-4 resulted in highest peak NHRR of 76.44 J/°CA at compared to NHRR of 26.61, 40.29, 60.4 and 76.44 J/°CA for SG-1, SG-2 and SG-3, respectively.

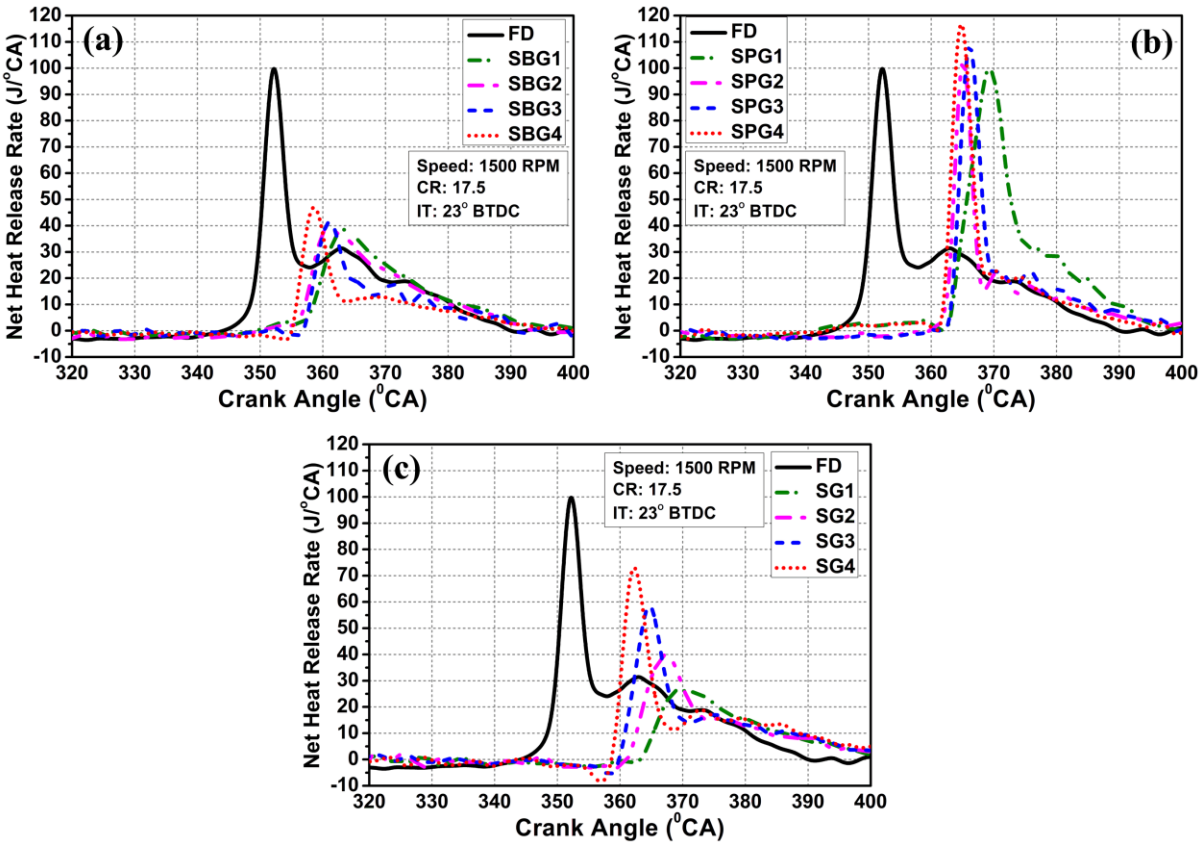

Fig. 5.8 Variation of NHRR at full load for (a) SBGs, (b) SPGs and (c) SPG-SBG mixtures

Table 5.4 Combustion parameters of simulated gaseous fuels at full load condition

Simulated biogas (SBG)				
Combustion Parameters	**SBG-1**	**SBG-2**	**SBG-3**	**SBG-4**
ID (°CA)	22	21	20	19
PCP (bar)	38.84	41.01	43.87	48.04
NHRR (J/°CA)	38.65	40.01	42.89	48.19
Simulated producer gas (SPG)				
Combustion Parameters	**SPG-1**	**SPG-2**	**SPG-3**	**SPG-4**
ID (°CA)	22	21	19	18
PCP (bar)	48.85	54.06	59.17	62.60
NHRR (J/°CA)	102.24	112.86	115.76	123.65
SPG-SBG mixtures				
Combustion Parameters	**SG-1**	**SG-2**	**SG-3**	**SG-4**
ID (°CA)	25	24	22	21
PCP (bar)	46.23	51.15	54.80	57.52
NHRR (J/°CA)	26.61	40.29	60.40	76.44

5.3.3 Emission characteristics

In this study, the emission of carbon dioxide (CO_2) is witnessed to be increased with the increase in engine load for every sets of experiments performed with SBGs, SPGs and SPG-SBG mixtures as portrayed in **Fig. 5.9(a)-(c)**. This is mainly because of the fact that more amount of fuel is consumed by the engine at higher loading condition in order to deliver the desired power. In case of SBG-DF mode, as the air-gaseous fuel intake charge comprises of CO_2, higher amount of CO_2 is released to the ambient as it does not participate in the combustion process. This is also the cause of higher emission of CO_2 for SBG-DF operations compared to FD mode as seen in **Fig. 5.9(a)**. It is clearly identifiable from the figure that for the entire loading range, with the increase of CO_2 fraction in the SBG resulted in higher component of CO_2 in the engine exhaust. At full load, CO_2 emission was increased by 101.63, 96.96, 80.41 and 68.99% for SBG-1, SBG-2, SBG-3 and SBG-4, respectively compared to FD (**Table 5.5**). On an average, maximum and minimum CO_2 emission of 7.8 and 6.6% was observed in case of SBG-1 and SBG-4, respectively. In case of SPG-DF operation, the emission of CO_2 is comparatively lower than that of SBGs. Again, it can be observed from **Fig. 5.9(b)** that with higher H_2 content in the SPG, resulted in higher emission of CO_2. This is because, higher H_2 in the SPG improved the combustion behaviour of the intake charge resulted in better oxidation of CO present in the fuel converted to CO_2 in the expansion stroke. The average CO_2 emission for SPG-1, SPG-2, SPG-3 and SPG-4 were found to be 5.95, 6.1, 6.32 and 6.6%, respectively **(Table 5.5)**. Furthermore, it is evident from the **Fig. 5.9(c)** that DF operation with SPG-SBG mixture resulted in average 3.54% higher and 11.03% lower emission of CO_2 compared to SBG-DF and SPG-DF operation. This can attributed to the presence of both CO

and CO_2 components in the fuel mixture. Moreover, at full loading condition, the emission of CO_2 for SG-1, SG-2, SG-3 and SG-4 were found to be 7.59, 7.11, 6.74 and 6.46%, respectively.

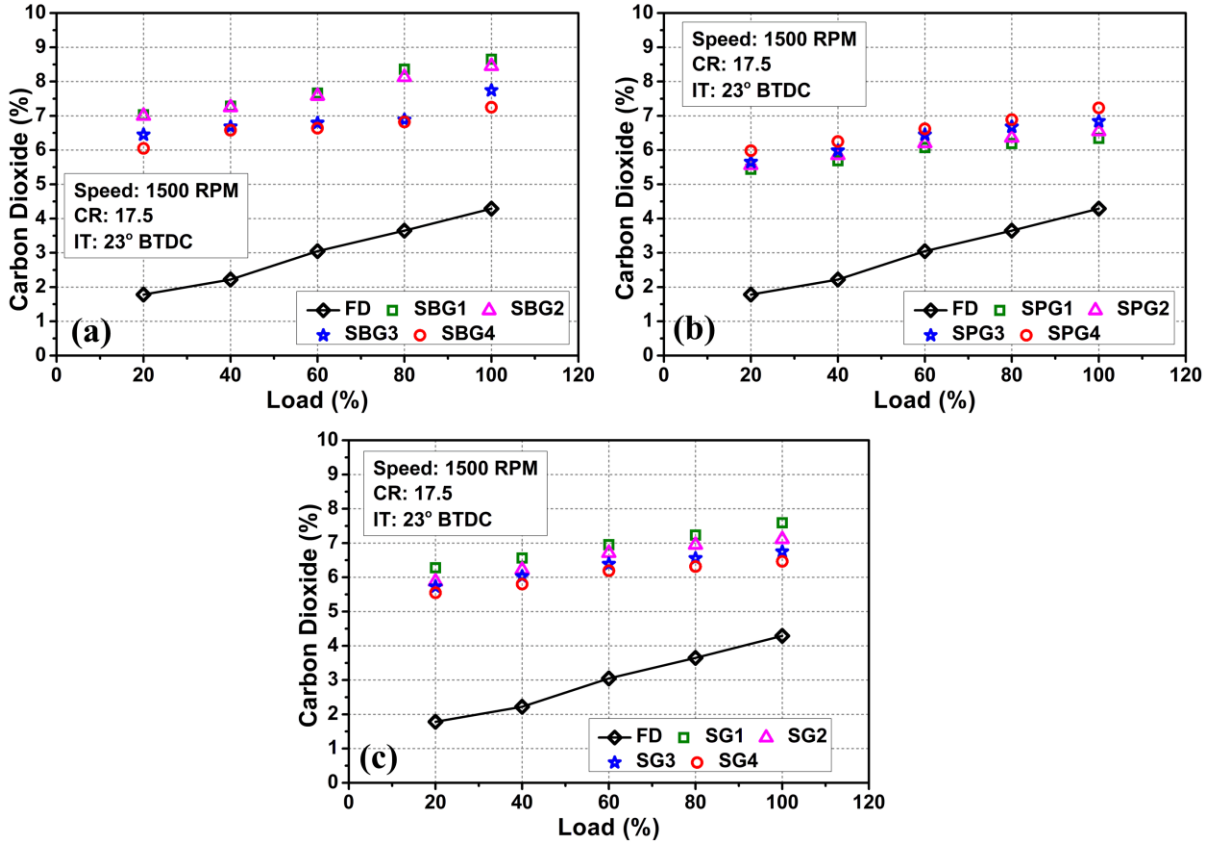

Fig. 5.9 Variation of CO_2 with load for (a) SBGs, (b) SPGs and (c) SPG-SBG mixtures

Table 5.5 Emission parameters of simulated gaseous fuels at full load condition

Simulated biogas (SBG)				
Emission Parameters	**SBG-1**	**SBG-2**	**SBG-3**	**SBG-4**
CO (ppm)	382.62	377	370	366
HC (ppm)	395.36	387.5	375	362
NO_X (ppm)	16	17	25	34.72
CO_2 (%)	8.65	8.45	7.74	7.25
Simulated producer gas (SPG)				
Emission Parameters	**SPG-1**	**SPG-2**	**SPG-3**	**SPG-4**
CO (ppm)	518	511	505	500
HC (ppm)	435	422	415	408
NO_X (ppm)	176	187	193	201
CO_2 (%)	6.34	6.55	6.84	7.23
SPG-SBG mixtures				
Emission Parameters	**SG-1**	**SG-2**	**SG-3**	**SG-4**
CO (ppm)	472.84	459.75	442.62	418.3
HC (ppm)	455.2	440.65	410.29	385.22
NO_X (ppm)	52.5	69.95	88.74	102.16
CO_2 (%)	7.5915	7.1136	6.7465	6.4668

The formation of NO_X is highly influenced by several factors such as the temperature produced inside the engine cylinder, oxygen availability for combustion, retention time and availability of nitrogen molecules [108,143]. NO_X emission for SBG, SPG and SPG-SBG mixture for varying load are illustrated in **Fig. 5.10(a)-(c)**. As the load increases, the NO_X emission escalates for both FD mode and DF mode due to higher equivalence ratio [165]. As illustrated in **Fig. 5.10(a)**, NO_X emission for SBG-DF operation was noted to be lower compared to FD mode. There are three main reasons behind this observations; firstly the high calorific value of diesel than SBGs, secondly, insufficient oxygen due to substitution of air by SBG and the presence of CO_2 in SBG. It is also evident that that increase in the fraction of CO_2 in SBG lowers the NO_X component in the engine exhaust. At full load, CR of 17.5 and 23° BTDC, NOx emission was recorded to be 16, 17, 25 and 35 ppm for SBG-1, SBG-2, SBG-3 and SBG-4, respectively compared to 125.23 ppm for FD. On the other hand, it can be noticed from the **Fig. 5.10(b)** that the high energy release and high temperature inside the combustion chamber due to the presence of both H_2 and CO, SPG-DF mode resulted in significant increase in emission of NO_X compared to SBG-DF operation. NO_X is primarily composed of nitrogen monoxide (NO) and nitrogen dioxide (NO_2). Out of these two, the predominant contribution arises from NO, which makes up over 90% of the NO_X emissions within the cylinder [17]. Shih *et al.* [249] conducted a study investigating the effect of composition on the NOx emissions when using syngas (H_2/CO, i.e. simulated producer gas) as a fuel. Their findings indicated that syngas flames with a higher hydrogen content produced increased NO_X emissions, primarily because of the elevated flame temperatures, in contrast to syngas flames with lower hydrogen content, which yielded lower NO_X levels. In the case of a H_2-rich syngas, there is a greater production of NO through the thermal route, specifically via the Zeldovich mechanism. This involves the reverse reactions R1 ($N_2 + O \rightarrow NO + N$) and R2 ($N + OH \rightarrow NO + H$), followed by R3 ($N + O_2 \rightarrow NO + O$). It is also stated that the contribution of the thermal route to NO production increases as pressure rises, aligning with the trend of higher maximum flame temperatures. Considering the entire load range, the average NO_X emission for SPG-1, SPG-2, SPG-3 and SPG-4 were recorded to be 97.4, 106.8, 111.4 and 117.6 ppm, respectively. From **Fig. 5.10(c)**, it is evident that the addition of SBG with SPG resulted in drastic reduction in the emission of NO_X. On an average, NO_X emission for SPG-SBG mixture was found to be 64.2% lower than that of SPG-DF operation because of the presence of CO_2 in the fuel mixture. NO production rates decrease with increasing dilution percentage, i.e. the percentage of CO_2. SPG-SBG mixture due to the presence of CO_2, produces more NO through N_2O-intermediate route. Initially, the reaction involves N_2 combining with an oxygen atom,

forming N_2O through the reversed reaction R4 (N2 + O (+M) → N_2O (+M)). Subsequently, N_2O undergoes conversion to NO through two chain-terminating reactions such as: R5 (N_2O + O → NO + NO) and the reverse of R6 (N_2O + H → NH + NO) [249]. At full load, NOx emission was recorded to be 52.5, 69.95, 88.74 and 102.16 ppm for SG-1, SG-2, SG-3 and SG-4, respectively. The maximum NO_X production for SG-4 is due to the presence of higher percentage of CH_4 in the fuel mixture. A study revealed that hydrogen-based species have the most significant impact on NO_X formation. They also reported that CH_4 is a highly sensitive species in the context of NO_X formation, underscoring its significant role in this process [250].

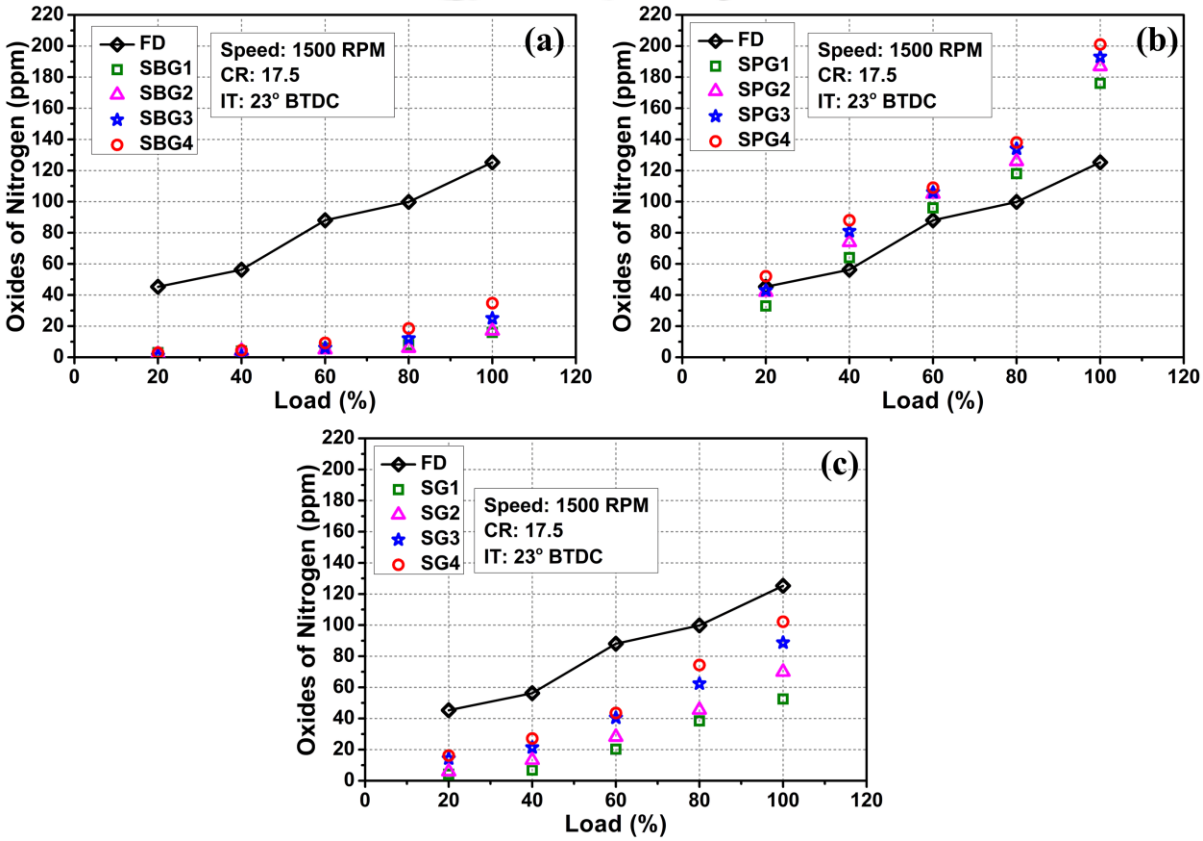

Fig. 5.10 Variation of NO_X with load for (a) SBGs, (b) SPGs and (c) SPG-SBG mixtures

The study investigated the release of carbon monoxide (CO) pollutants for both single and DF mode at different operating conditions. The release of CO components in the exhaust gas is mainly because of the incomplete combustion of fuel mixture. **Fig. 5.11(a)-(c)** demonstrates the variation of CO emission for both FD and SBG, SPG and SPG-SBG mixture under DF mode at varying engine load. Similar trend was found in case of both single mode and DF mode operations. It is clearly seen in the **Fig. 5.11(a)** that emission of CO initially drops as the load increases and after specified load, it again increases. Because at lower load, there is minimum temperature inside the cylinder causing improper burning of fuel. With increase in load, additional supply of fuel leads to the development of too rich air-fuel mixture to undergo

complete combustion and after a particular load, high CO is released. Moreover, the higher fraction of CH_4 in the SBGs promotes better combustion resulted in lower CO emission. At 23° BTDC and for entire load range, increasing the CH_4 content in SBGs from 55-70% leads to an average reduction of 6.5% in the emission of CO. On an average, SBG-1, SBG-2, SBG-3 and SBG-4 showed CO emission of 372.62, 363.2, 355.8 and 348.6 ppm, respectively. While, in case of SPG-DF operation, on an average the release of CO in the engine exhaust was found to be 31.7% higher compare to SBG-DF operation. This is because of the presence of CO component in SPGs. It can be clearly seen from **Fig. 5.11(b)** that, increase in CO fraction in SPG led to increase in release of CO pollutant in engine exhaust. Considering all load, SPG-1, SPG-2, SPG-3 and SPG-4 showed average CO emission of 482.4, 476.4, 471.1 and 467 ppm, respectively. Again, as depicted in **Fig. 5.11(c)**, DF experiments of SPG-SBG mixtures showed 2.84% average reduction in CO emission in contrast to SPG-DF mode with respect to entire load range. The combination of SPG-2/SBG-4 i.e. SG-4 showed the minimum average emission of 429.1 ppm compared to 491.96, 473.41 and 449.33 ppm for SG-1, SG-2 and SG-3, respectively.

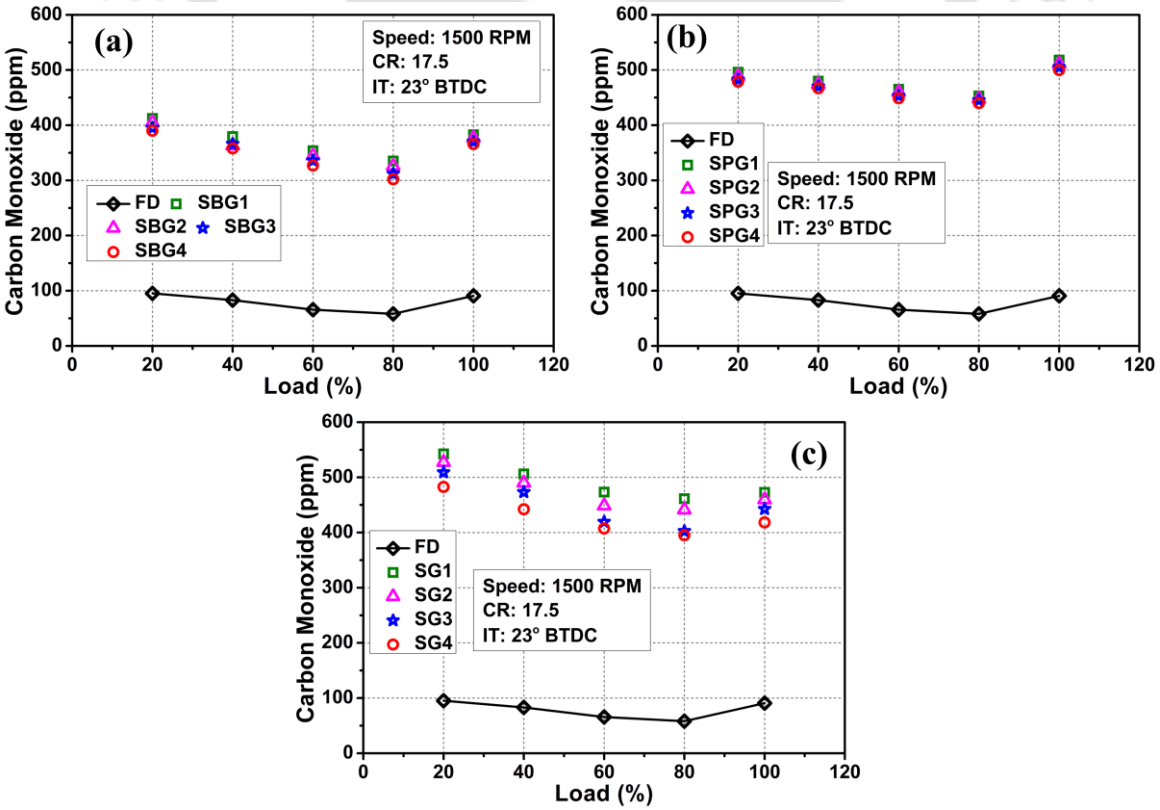

Fig. 5.11 Variation of CO with load for (a) SBGs, (b) SPGs and (c) SPG-SBG mixtures

The effect of SBG, SPG and SPG-SBG mixture compositions on hydrocarbon (HC) emission is depicted in **Fig. 5.12(a)-(c)**. Similar to the emission of CO, incomplete combustion upsurges the discharge of HC components in the exhaust gas. With increase in load, emission of HC

first increases, attains a minimum value and again increases for both the mode of operations corresponding to all load and operating conditions. The reason to this trend has already been discussed in the CO emission. From **Fig. 5.12(a)** it can be observed that the average HC emission for SBG-1, SBG-2, SBG-3 and SBG-4 were measured to be 362.48, 353.7, 331.4 and 320.6 ppm, respectively, which equals to 11.55% HC reduction when CH_4 fraction increased from 55 to 70% in SBG. In case of SPG-DF operation, as depicted in **Fig. 5.12(b)**, HC emission was observed to be higher compared to SBG-DF mode. This is mainly due to the lower energy density of the SPG fuels compared to SBG, results in reduction in combustion duration leading to higher release of combustion products at engine exhaust. The average emission HC was found to be 421.94, 413.2, 407.8 and 396.2 ppm for SPG-1, SPG-2, SPG-3 and SPG-4, respectively. It is also evident from the figure that increased H_2 fraction in SPG fuel mixture results in reduced HC emission. Because, addition of H_2 lowered the carbon content in the SPG fuel mixture. Again, **Fig. 5.12(c)** demonstrates the variation of HC emission for SPG-SBG mixtures. It can be seen from the figure that, the combined induction of SBGs, particularly SBG-3 and SBG-4 having higher CH_4 content mixed with SPG-2 resulted in reduction in HC emissions as compared to SPG-2. Minimum average HC emission of 385.25 ppm was found for the mixture of SPG-2/SBG-4 (SG-4) compared to SG-1, SG-2 and SG-3 with 473.23, 456.98 and 407.41 ppm, respectively. The addition of CH_4 beyond a certain limit signifies better combustion of the fuel mixture.

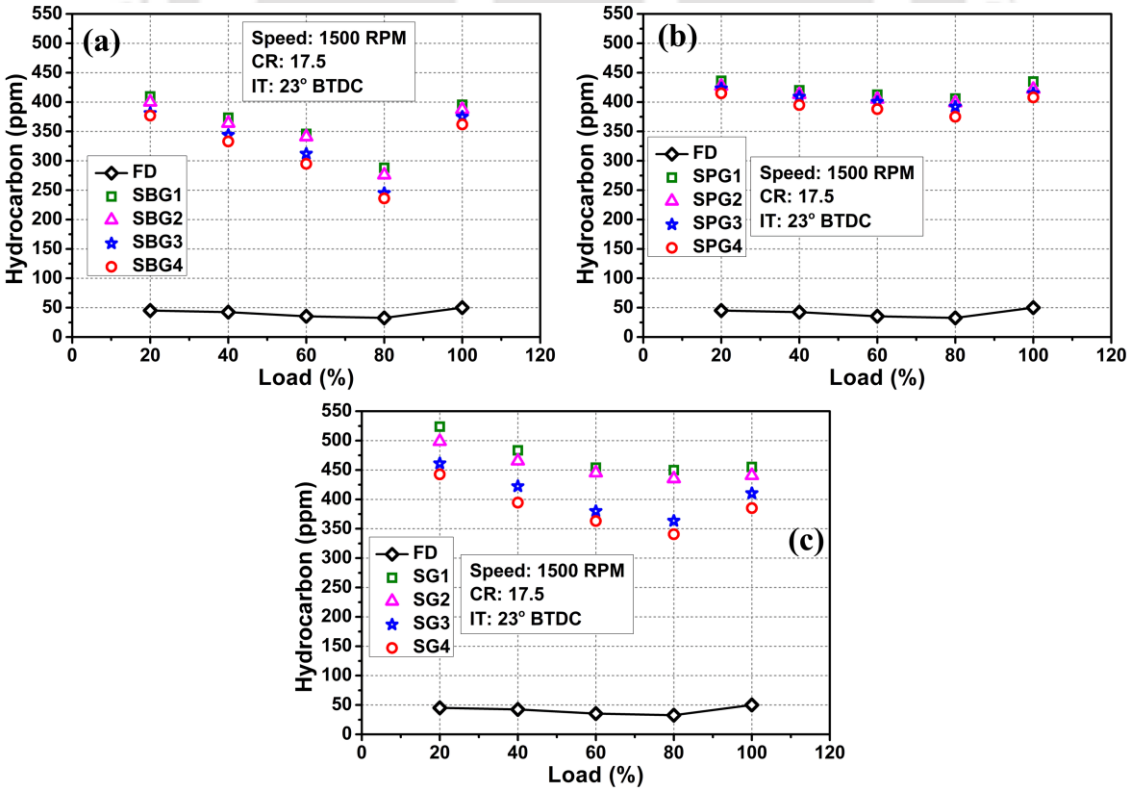

Fig. 5.12 Variation of HC with load for (a) SBGs, (b) SPGs and (c) SPG-SBG mixtures

5.4 Effect of compression ratio on engine characteristics

In this section, the dual fuel experiments were carried out to investigate the impact of compression ratio on the performance, combustion and emission characteristics of a diesel engine for SBG, SPG and SPG-SBG mixture. From the above analysis, it was found that, SBG-4, SPG-4 and SG-4 showed best results in terms of overall engine characteristics. Thus, these three compositions were chosen for further study. Varying compression ratios were applied while keeping the IT fixed at 23° BTDC and the engine load ranging from 20 to 100%. However, the plots depicting each parameter were displayed at 100% engine load as this condition showed best outcomes in the prior study.

5.4.1 Performance characteristics

The BTE under dual fuel mode for SBG-4, SPG-4 and SG-4 at 100% engine loading condition are depicted in **Fig. 5.13**. Significant enhancement in BTE was noted for high CR in case of all three gas compositions. For maximum load, the BTE of SBG-4 was found to be 20.67, 18.96, 16.12 and 15.17 for CRs of 18, 17.5, 17 and 16, respectively. On an average, BTE for SBG-4 was increased by 41.6% as CR is increased from 16 to 18. Similarly, in case of SPG-DF mode, the BTE for SPG-4 was found to be 16.08, 17.35, 19.05 and 20.94% with respect to CR of 16, 17, 17.5 and 18, respectively at 100% load with an average increase of 33.63%. Again, experiments with SPG-SBG mixture, addition SBG (70% CH4) i.e. SG-4 resulted in the increment of BTE. At full load, BTE of 17.12, 18.46, 20.05 and 22.11% was found at CR of 16, 17, 17.5 and 18, respectively with an average increase of 31.35%. This improvement in BTE is due to the fact that the average cycle temperature and pressure increase at high CR, which in turn increases the possibility of more amount of gaseous fuel to undergo complete combustion, better efficiency and thus high energy conversion capability [247].

On the other hand, the variation of BSEC for SBG-4, SPG-4 and SG-4 at 100% load is illustrated in **Fig. 5.14** and it was observed to be decreasing with the increase in CR. This is due to the better combustion of the air-gaseous fuel mixture at high CR, making it easier to convert gaseous fuel into useful work. At 100% load, the BSEC for SBG-4 was found to 6.11, 5.74, 5.27 and 5.01 kJ/s of fuel/kW output at CR of 16, 17, 18 and 17.5, respectively. At similar condition, SPG-4 showed BSEC of 6.03, 5.71, 5.25 and 4.86 kJ/s of fuel/kW output. Again, for SG-4, minimum BSEC of 4.62 kJ/s of fuel/kW output was observed at CR of 18. Considering the complete load range, the average reduction in BSEC was found to be 17.18, 16.65 and 13.98% in case of SBG-4, SPG-4 and SG-4, respectively, when the CR is increased from 16 to 18. Similar observations were also reported by [148]. The EGT was found to be decreased with the increase in CR for SBG-4, SPG-4 and SG-4 as depicted in **Fig. 5.15**. Because, at high CR, burning

velocity of gaseous fuel mixture increases which makes combustion process faster and decreases the time needed for complete combustion, thereby reducing the EGT [251]. At 100% load, the EGT of SBG-4 dual fuel operation was noted to be 361.21, 354.44, 344.01 and 328.18°C for CR of 16, 17, 17.5 and 18, respectively with an average reduction of 11.68%. While, in case of SPG-4, EGT was lowered on an average by 11.63% and at 100% load, EGT of 808.66, 774.74, 734.61 and 717.9°C was observed at CR of 16, 17, 17.5 and 18, respectively. Again for SG-4, the minimum EGT of 652.25°C was noted at CR of 18 compared to 666.07, 705.85 and 739.34°C at CR of 17.5, 17 and 16, respectively at 100% load. On an average, SPG-SBG mixture resulted in 12.78% reduction in EGT, as the CR was increased from 16 to 18. It was also observed that for DF modes, raise in CR resulted in increased percentage of PFR as shown in **Fig. 5.16**. On an average, SBG-4, SPG-4 and SG-4 resulted in 26.8, 19.06 and 8.03% rise in PFR, respectively, as CR was increased from 16 to 18.

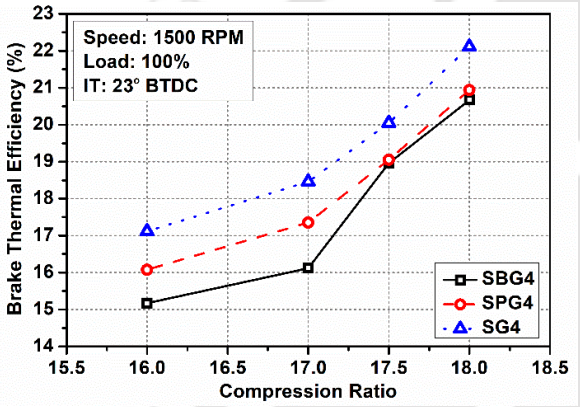

Fig. 5.13 Variation of BTE with CR for SBG, SPG and SPG-SBG mixture at full load

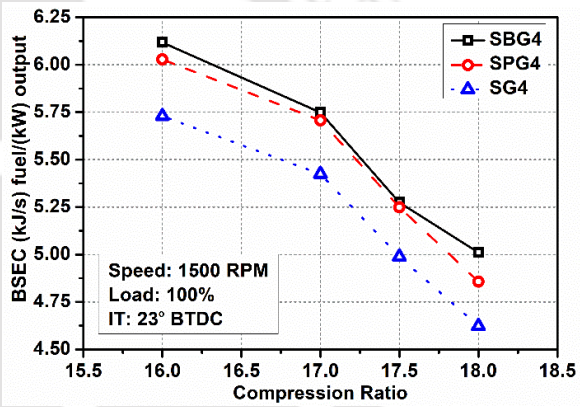

Fig. 5.14 Variation of BSEC with CR for SBG, SPG and SPG-SBG mixture at full load

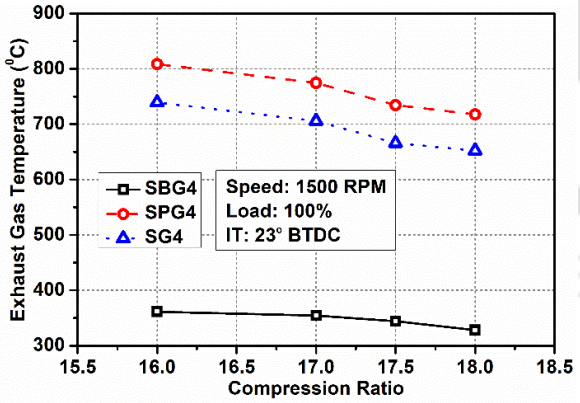

Fig. 5.15 Variation of EGT with CR for SBG, SPG and SPG-SBG mixture at full load

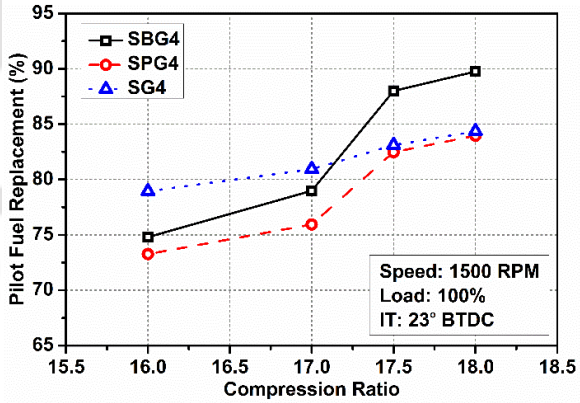

Fig. 5.16 Variation of PFR with CR for SBG, SPG and SPG-SBG mixture at full load

5.4.2 Combustion characteristics

The effect CR on ID for SBG-4, SPG-4 and SG-4 is illustrated **Fig. 5.17**. It is evident from that for all the gaseous fuel composition, ID found to be decreased with the increase in CR. Because, increasing the CR, elevates the temperature inside the cylinder and enables early

achievement of self-ignition temperature, which in succession reduces the ID. In case of SBG-DF, the ID at maximum load for SBG4 was witnessed to be 22, 21, 19 and 18 °CA at CR of 16, 17, 17.5 and 18, respectively. Again, at same load for SPG-DF operation, SPG-4 resulted with an ID of 21, 20, 18 and 17°CA at CR of 16, 17, 17.5 and 18, respectively. Furthermore, SG-4 also showed early ignition at CR of 18 with ID of 19°CA compared to 21, 22 and 24°CA at CR of 17.5, 17 and 16, respectively. On the other hand PCP was observed to be increased with the increase in CR and the variation of PCP with CR for SBG-4, SPG-4 and SG-4 is depicted in **Fig. 5.18**. There is a 34.8% rise in the PCP at full load and standard IT of 23° BTDC, as CR was increased from 16 to 18. For SBG-4, the average PCP at CR of 16, 17, 17.5 and 18 was found to be 35.29, 38.33, 44.16 and 47.35 bar, respectively. In case of SPG-4, rise in the PCP was found to be 29.5% at maximum load and considering the entire load range, average PCP of 42.74, 46.44, 51.11 and 53.82 bar at CR of 16, 17, 17.5 and 18, respectively. Moreover, average PCP increased by 22.26% in case of SG-4 when the CR was increased from 16 to 18. At full load, SG-4 resulted in PCP of 48.81, 53.34, 57.51 and 59.73 bar at CR of 16, 17, 17.5 and 18, respectively. Analogous trend of variation of ID and PCP was reported in past literature [35].

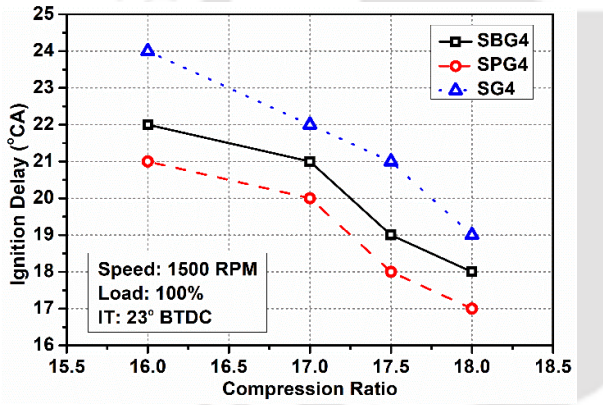

Fig. 5.17 Variation of ID with CR for SBG, SPG and SPG-SBG mixture at full load

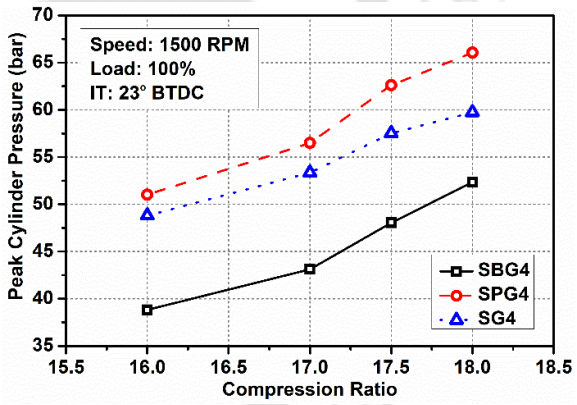

Fig. 5.18 Variation of PCP with CR for SBG, SPG and SPG-SBG mixture at full load

The P-θ diagram shown in **Figs. 5.19(a)-(c)**, illustrates the variation of CP with respect to crank angle for different CR. It can be seen from the figures that, increase in the CR resulted in shifting of the PCP value towards the TDC because of the minimization of self-ignition temperature of the gaseous fuel mixture. At 100% load and standard IT, SBG-4 showed the attainment of PCP at 10°, 8°, 7° and 6° CA after TDC for CR of 16, 17, 17.5 and 18, respectively. For SPG-4, the crank angle with respect to PCP was observed to be 14°, 13°, 12° and 11°CA after TDC at CR of 16, 17, 17.5 and 18, respectively. Furthermore the 4°CA shift of PCP value towards TDC was also notice in case of SG-4 at full engine load. The crank angle with respect to PCP was observed to be 14°, 13°, 12° and 10°CA after TDC at CR of 16, 17, 17.5 and 18, respectively. Analogous shifting of PCP was also discussed in the past literature [112]. The

experiments conducted with SBG-4, SPG-4 and SG-4 with higher CR resulted in higher NHRR at 100% loading condition as shown in **Figs. 5.20(a)-(c)**. For SBG-DF operation with SBG-4, as compared to CR of 17.5, CR of 18 showed 3.94% hike with peak NHRR of 50.09 J/°CA. While at CR of 16 and 17, peak NHRR is obtained to be 11.86 and 7.92% lower than CR of 17.5. On the other hand, at 100% load, the maximum NHRR value for SPG-4 was found to be 98.29, 105.53, 123.65 and 138.14 J/°CA at CR of 16, 17, 17.5 and 18, respectively. Again for SG-4, these values were observed to be 54.8, 71.36, 76.44 and 80.2 J/°CA at CR of 16, 17, 17.5 and 18, respectively with an increment 46.37%. Moreover, it was also witnessed that NHRR curve appears to be moving towards left with the increase of CR which signifies earlier start of combustion.

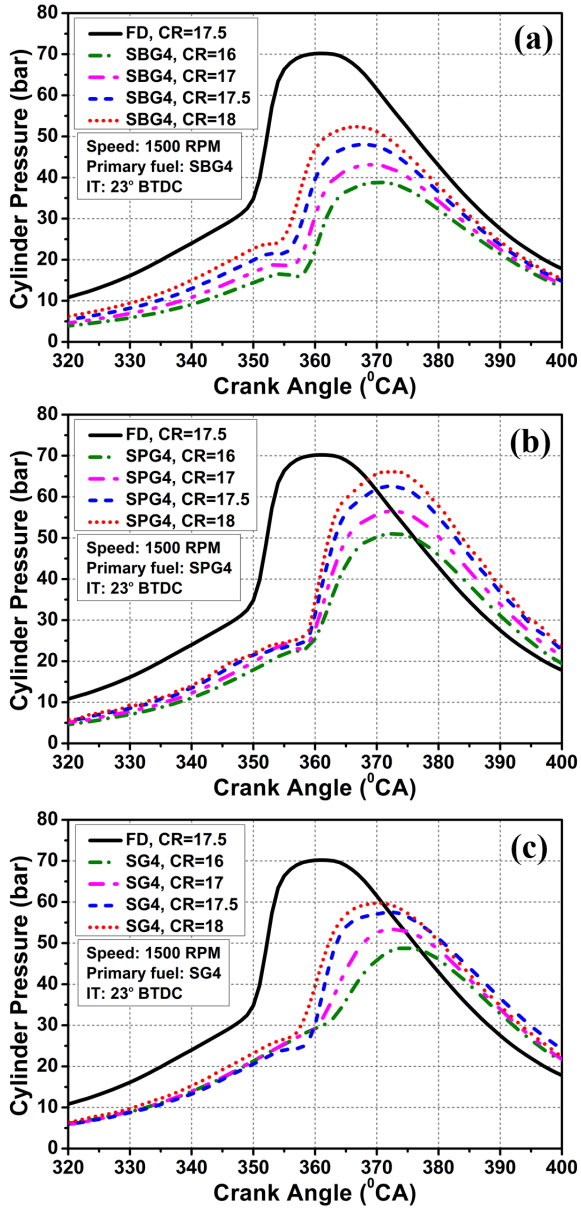

Fig. 5.19 Variation of CP with CR for (a) SBG, (b) SPG and (c) SPG-SBG mixture

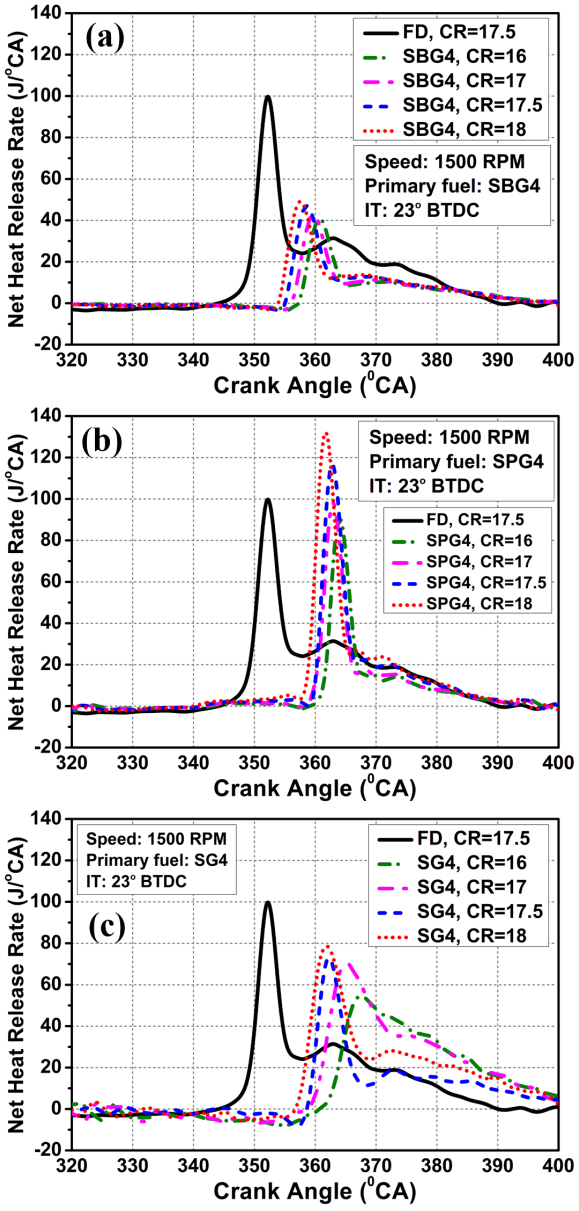

Fig. 5.20 Variation of NHRR with CR for (a) SBG, (b) SPG and (c) SPG-SBG mixture

5.4.3 Emission characteristics

The effect of CR on the emission of CO_2 for SBG-4, SPG-4 and SG-4 is illustrated in **Fig. 5.21**. It is noticeable from the figure that the increase in CR increased the release of CO_2 from the engine exhaust. This is because with high temperature and pressure inside the engine cylinder at high CR creates a favourable ambience for improved combustion reaction leading to further release of CO_2. Considering the entire range of load, on an average, SBG-4 showed a diminution of CO_2 pollutants by 16.2, 10.5 and 5.13% for CR of 16, 17 and 17.5 compared to CR of 18 at standard IT. Similarly for the complete load range, SPG-4 showed an average increase of CO_2 emission of 16.45% when the CR was increased from 16 to 18. At 100% load, CO_2 emission of 5.96, 6.29, 6.46 and 6.63% was found in case of SG-4 at CR of 16, 17, 17.5 and 18, respectively. On an average, 18.25% increment in CO_2 emission was noticed for SG-4. The study investigated the release of NO_X pollutants for SBG-4, SPG-4 and SG-4 as depicted in **Fig. 5.22**. It is clearly visible from the figure that high CR impels the formation of NO_X due to high combustion temperature inside the cylinder. Hence, CR of 18 resulted in maximum emission of NO_X over the entire loading range for SBG-4, SPG-4 and SG-4. On an average, 56.3, 36.11 and 44.53% hike in NO_X emission was monitored for SBG-4, SPG-4 and SG-4, respectively when the CR is increased from 16 to 18.

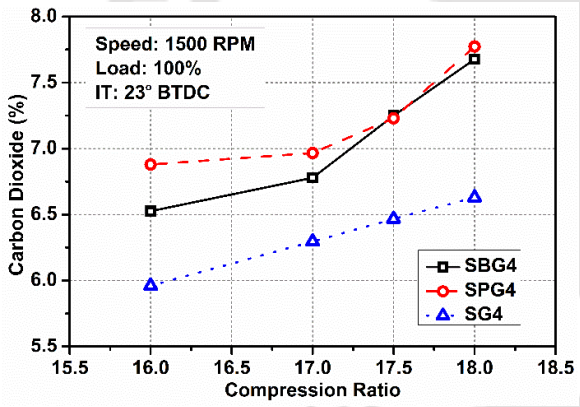

Fig. 5.21 Variation of CO_2 with CR for SBG, SPG and SPG-SBG mixture at full load

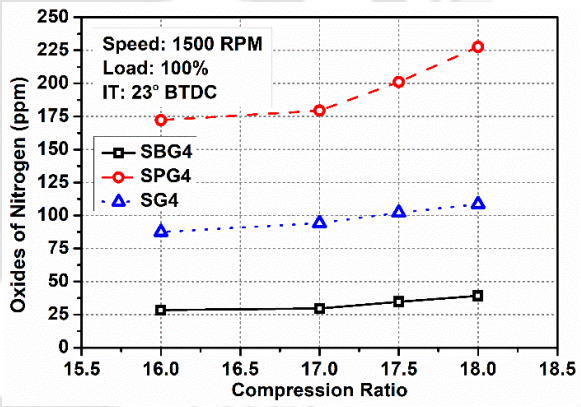

Fig. 5.22 Variation of NO_X with CR for SBG, SPG and SPG-SBG mixture at full load

The substantial reduction on CO emission for SBG-4, SPG-4 and SG-4 is noticeable in **Fig. 5.23** at higher CR. High CR develops a affirmative ambiance for the fuel to undergo oxidation reaction by rising the cylinder temperature and pressure and hence CO reduces [247]. At 100% load and standard IT, SBG-4 resulted with 400.3, 389.8, 366 and 351 ppm CO emission for CR of 16, 17, 17.5 and 18. For SPG-4, at maximum load, CO emission was found to be 481.5 ppm at CR of 18, which was minimum compared to 500, 532.5 and 570.82 ppm at CR of 17.5, 17 and 16, respectively. Again, in case of SPG-SBG mixture, SG-4 showed comparatively lower emission of CO than SPG-4. The CO emission was observed to be 403.24, 418.3, 448.42 and 478.04 ppm at

CR of 18, 17.5, 17 and 16, respectively at maximum load. On an average, the emission of CO was reduced by 10.5, 9.93 and 11.16% for SBG-4, SPG-4 and SG-4, respectively when CR was increased from 16 to 18. The variation of HC emission for SBG-4, SPG-4 and SG4 mixture under varying CR is demonstrated in **Fig. 5.24** and with the increase of CR, there was a reduction in HC. The explanation for these findings is similar to that of CO emission. The SBG-4 showed average HC emission of 361.94, 342.93, 320.6 and 303.51 ppm, respectively corresponding to the entire loading spectrum. Furthermore, the average release of HC pollutant in case of SPG-4 was 460.85, 450.13, 421.94 and 400.87 ppm at CR of 16, 17, 17.5 and 18, respectively. In addition to that for SG-4, the average HC emission was 443.86, 416.42, 385.25 and 354.75 ppm at CR of 16, 17, 17.5 and 18, respectively.

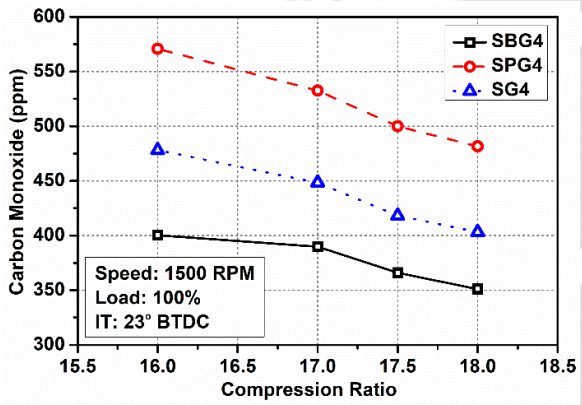

Fig. 5.23 Variation of CO with CR for SBG, SPG and SPG-SBG mixture at full load

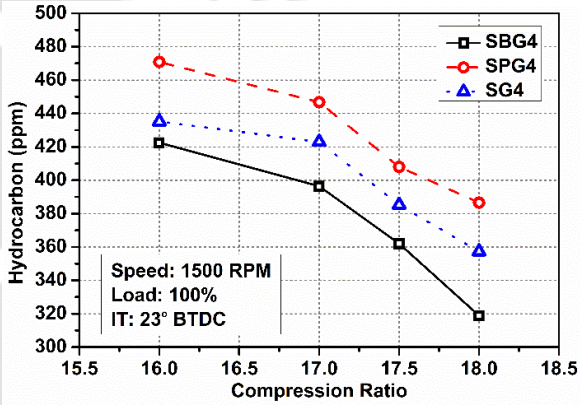

Fig. 5.24 Variation of HC with CR for SBG, SPG and SPG-SBG mixture at full load

5.5 Effect of injection timing on engine characteristics

In this section, the impact of pilot fuel injection timing (IT) on the performance, combustion and emission characteristics of a diesel engine were studied for SBG, SPG and SPG-SBG mixture. From the above experimental study, it was evident that CR of 18 resulted in best outcomes in terms of overall engine characteristics. Thus, keeping CR of 18 fixed, experiments were carried out at varying IT of 23, 26, 29 and 32° BTDC. Additionally, the engine load was varied between 20% and 100% during these experiments. However, the plots illustrating each parameter were presented based on data obtained at 100% load as this condition showed best results in the earlier studies.

5.5.1 Performance characteristics

The variation of BTE with IT for SBG-4, SPG-4 and SG4 at 100% load is depicted in **Fig. 5.25**. It is visible from this trend that BTE in case of all three fuel mixtures improved with the advancement pilot fuel IT up to 29° BTDC. Because, advanced IT allows early injection of pilot fuel into the engine cylinder than its standard IT, thereby providing excess time for the pilot

fuel to vaporize and mix homogeneously with the air-gaseous fuel charge [115]. This increases the probability of a better combustion of gaseous fuels. BTE for SBG-4 was noted to be 23.15, 25.10 and 24.84% at 26°, 29° and 32° BTDC, respectively at full load. Again, in case of SPG-4, the BTE was recorded to be 23.54, 25.58 and 25.05% at 26°, 29° and 32° BTDC, respectively. For same load and ITs, 22.3, 24.44 and 23.29% BTE was achieved in case of SG-4. Considering the complete load range, increase in IT from 23 to 29° BTDC resulted in 20.46, 14.8 and 5.96% average increment in BTE for SBG-4, SPG-4 and SG-4, respectively. On the other hand, reduction of BSEC for SBG-4, SPG-4 and SG-4 was noticed with the advancement of pilot fuel IT as shown in **Fig. 5.26**. BSEC was lowered by 8.16% with advancement of IT from 23° to 29° BTDC, at full load and CR of 18. Similarly, SPG-4 and SG-4 showed 4.57 and 6.53% reduction in BSEC. Similar trend in BTE and BSEC with the advancement of IT was observed in the past literature [148].

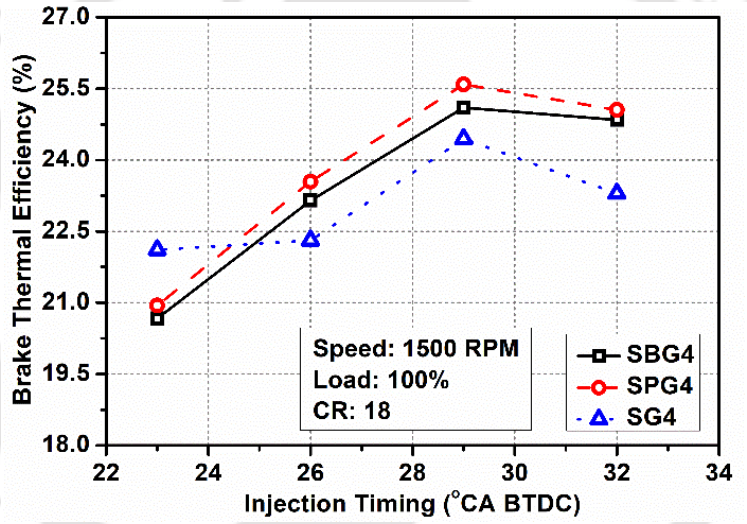

Fig. 5.25 Variation of BTE with IT for SBG, SPG and SPG-SBG mixture at full load

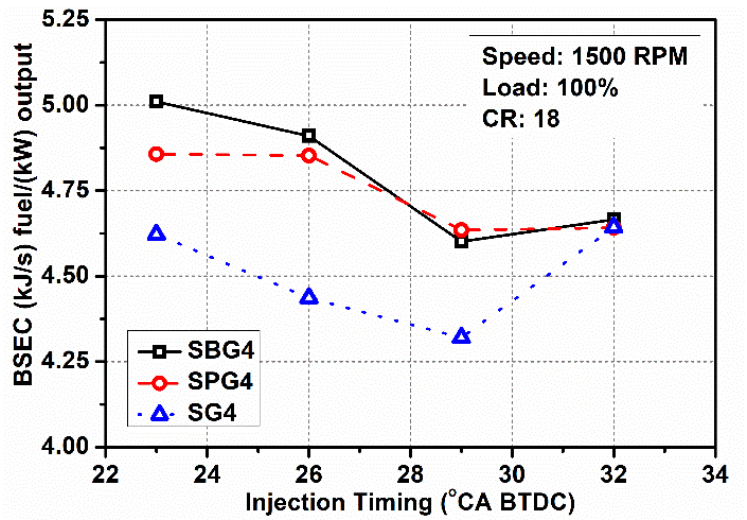

Fig. 5.26 Variation of BSEC with IT for SBG, SPG and SPG-SBG mixture at full load

Advancement of IT reduces the EGT for all the three gaseous fuel composition as illustrated in **Fig. 5.27**. At highest loading condition with CR of 18, SBG-4 showed EGT of 314.48, 313.47 and 312.37°C for 26°, 29° and 32° BTDC, respectively which is about 4.17, 4.48 and 4.81% reduction compared to 23° BTDC. Again for SPG-4, the reduction was found to be 5.45, 8.3 and 9.32% for 26°, 29° and 32° BTDC. In addition, compared to 23° BTDC, SG-4 resulted in 1.06, 2.24 and 2.53% reduction under same IT. **Fig. 5.28** demonstrated the effect of IT on PFR for SBG-4, SPG-4 and SG-4. Maximum PFR of 90.6, 87.7 and 86.41% was found for SBG-4, SPG-4 and SG-4, respectively at combination of CR of 18 and IT of 29° BTDC.

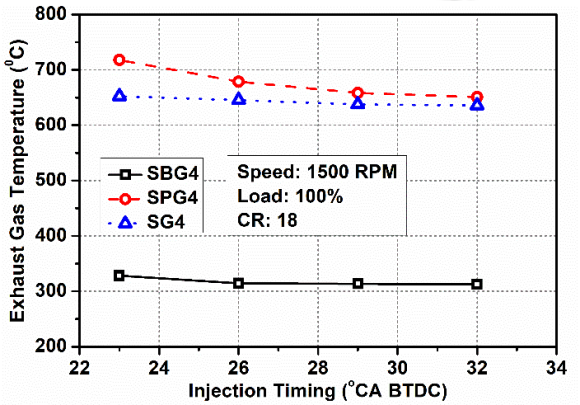

Fig. 5.27 Variation of EGT with IT for SBG, SPG and SPG-SBG mixture at full load

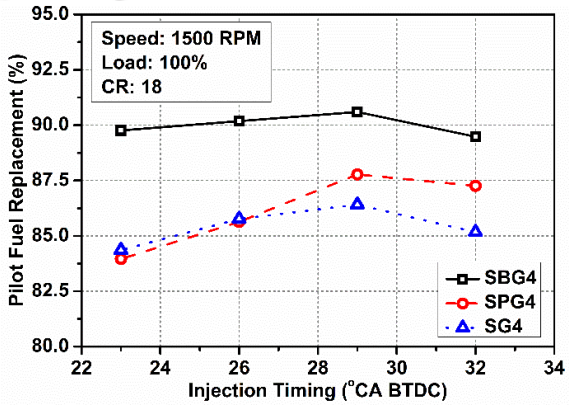

Fig. 5.28 Variation of PFR with IT for SBG, SPG and SPG-SBG mixture at full load

5.5.2 Combustion characteristics

The advancement of IT of pilot fuel from 23° to 32° BTDC resulted in elongation of ID for all three gas composition as shown in **Fig. 5.29**. As, IT is advanced, pilot fuel can be injected at low gas temperatures, which slows down the preignition reaction of the fuel mixture leading to prolonged ID. Similar observations was also reported by [105]. For SBG-4, at fixed CR of 18 and 100% load, the ID was delayed by 1°, 3° and 4° CA at 26°, 29° and 32° BTDC, respectively. While in case of SPG-4, advancement of IT by 3°, 6° and 9° causes an average rise of IDs by about 5.26, 11.57 and 13.68%, respectively. Similarly at same load and CR, SG-4 resulted in 2.8, 6.54 and 9.34% rise in ID when the IT is advanced by 3°, 6° and 9°, respectively. The PCP for SBG-4, SPG-4 and SG-4 was found to be increased with the increase IT of pilot fuel as depicted in **Fig. 5.30**. This can be attributed to the advanced pilot fuel injections forming a fuel rich mixture zone inside the combustion chamber [122]. The maximum PCP of 62.96 and 71.47 bar was found in case of SBG-4 and SPG-4, respectively at 100% load, CR of 18 and 32° BTDC. However, at same load and CR, SG-4 showed maximum PCP of 64.17 bar 32° BTDC. On an average, SBG-4, SPG-4 and SG-4 resulted in 18.47, 13.22 and 8.76% increment in PCP when the IT is advanced by 9°CA. Advanced IT of pilot fuel promoted additional shifting of PCP value towards the TDC for SBG-4, SPG-4 and SG-4 as portrayed in **Fig. 5.31(a)-(c)**. Because, as

the IT is advanced, the premixed stage of combustion shows quick burning of the fuel mixture due to start of combustion at early crank angle of the cycle which leads the occurrence of PCP nearer to the TDC [166]. At 100% engine load and CR of 18, PCP for SBG-4 was reached at 366°, 366°, 364° and 363° crank angle for 23°, 26°, 29° and 32° BTDC, respectively. Whereas, in case of SPG-4, crank angle corresponding to the PCP value was observed to be 373°, 372°, 371° and 371° CA at IT of 23°, 26°, 29° and 32° BTDC, respectively. Again, at similar operating condition, for SG-4, PCP were attained at 370°, 369°, 369° and 368° CA. Similar to P-θ curve, the NHRR curve appeared to be moving towards TDC with the advancement of IT for all three gaseous fuel composition as shown in **Fig. 5.32(a)-(c)**. Moreover, at maximum loading and CR of 18, the peak NHRR for SBG-4 is noted to be 54.65, 58.05 and 60.42 J/°CA at 26°, 29° and 32° BTDC, respectively. For SPG-4, peak NHRR was found to be increased by 5.15, 2.84 and 2.5% when the IT was advance to 26°, 29° and 32° BTDC, respectively. However, in case of SG-4, maximum NHRR of 94.14 J/°CA was observed at IT of 29° BTDC compared to 80.2, 87.89 and 90.92 J/°CA at IT of 23°, 26° and 32° BTDC, respectively. Thus, NHRR increased with the advancement of IT.

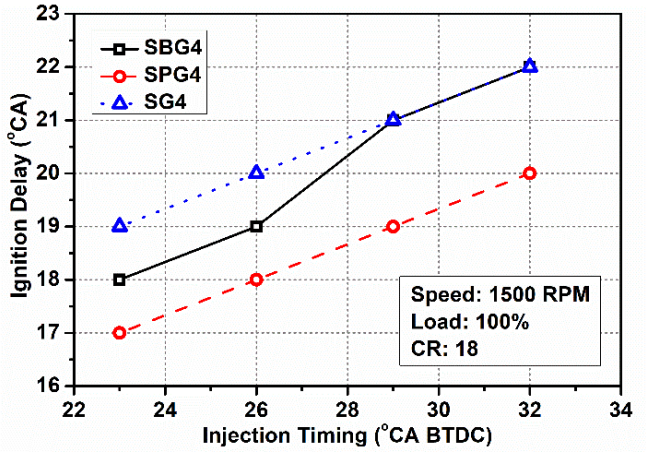

Fig. 5.29 Variation of ID with IT for SBG, SPG and SPG-SBG mixture at full load

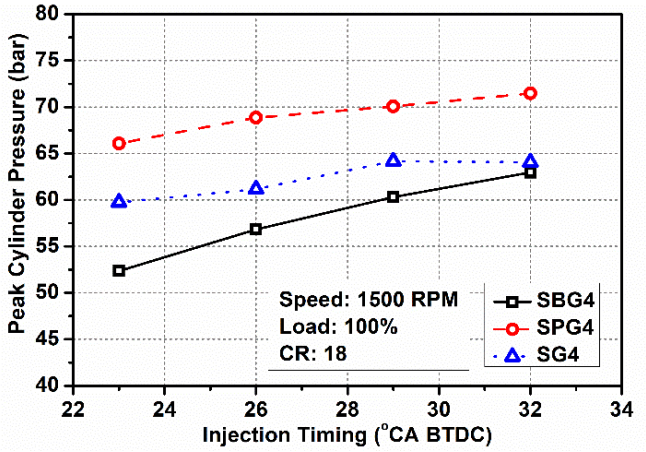

Fig. 5.30 Variation of PCP with IT for SBG, SPG and SPG-SBG mixture at full load

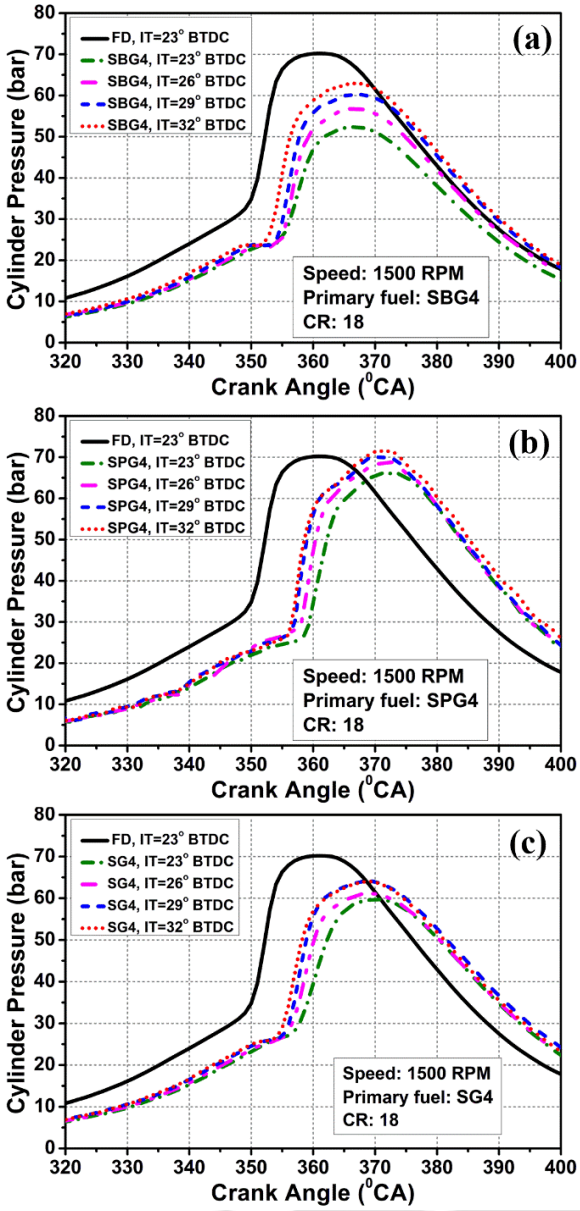

Fig. 5.31 Variation of CP with IT for (a) SBG, (b) SPG and (c) SPG-SBG mixture

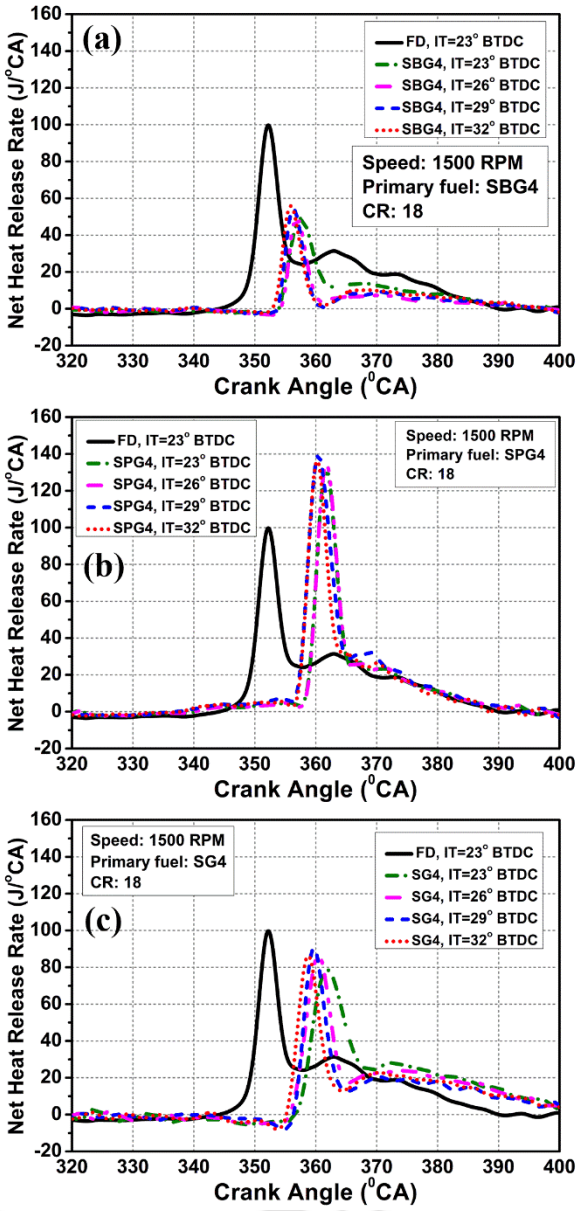

Fig. 5.32 Variation of NHRR with IT for (a) SBG, (b) SPG and (c) SPG-SBG mixture

5.5.3 Emission characteristics

Better combustion of gaseous fuel mixtures with advancement of pilot fuel IT resulted in increase of CO_2 component in the engine exhaust as depicted in **Fig. 5.33**. CO_2 emission of 7.67, 8.49, 9.86 and 11.23% was observed at 23°, 26°, 29° and 32° BTDC, respectively at full load condition. Thus for complete range of engine load, advancing the IT from 23° to 32° BTDC, an average hike of 34.27% CO_2 emission was observed for SBG-4 at CR of 18. In case of SPG-4, average emission of CO_2 was increased by 1, 10.61 and 11.58% when the IT was advanced by 3°, 6° and 9°CA, respectively. In addition to that, for SG-4, minimum value of average CO_2 emission of 6.3% was obtained at 23° BTDC compared to 6.6, 7.02 and 7.1% at 26°, 29° and 32° BTDC, respectively. Analogous observations was also discussed regarding the influence of

CR and IT on CO_2 emission [35,252]. From the **Fig. 5.34**, increase in the emission of NO_X for all the gaseous fuel composition was observed as the pilot fuel IT was advanced. At full load, experiments at 23°, 26°, 29° and 32° BTDC, SBG-4 showed NO_X emission of 39.18, 42.58, 43.97 and 51.51 ppm, respectively. At same load and CR, maximum and minimum NO_X of 188.92 and 135.3 ppm was observed at 23° and 32° BTDC, respectively for SPG-4. Furthermore, SG-4 resulted in 114.82, 119.5 and 123.41 ppm emission of NO_X when the IT was advanced to 26°, 29° and 32° BTDC, respectively at full loading condition. Considering complete load range, SBG-4, SPG-4 and SG-4 showed an average about 34, 39.63 and 13.85% rise in NO_X emission when the IT of pilot fuel is advanced from 23° to 32° BTDC at fixed CR of 18. This can attributed to better combustion of fuel mixture at advanced IT, which raises the combustion temperature and led to higher NO_X emission.

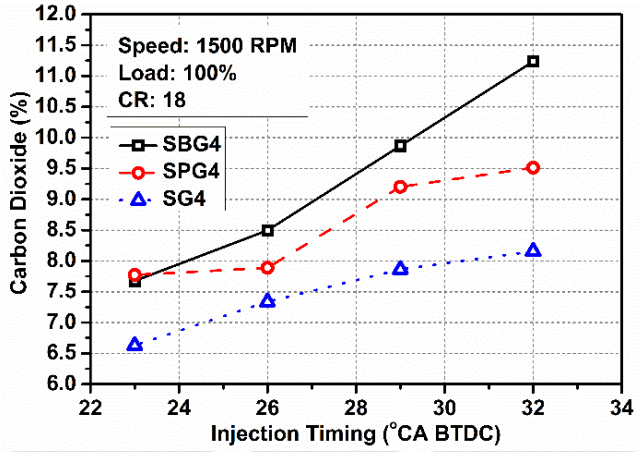

Fig. 5.33 Variation of CO_2 with IT for SBG, SPG and SPG-SBG mixture at full load

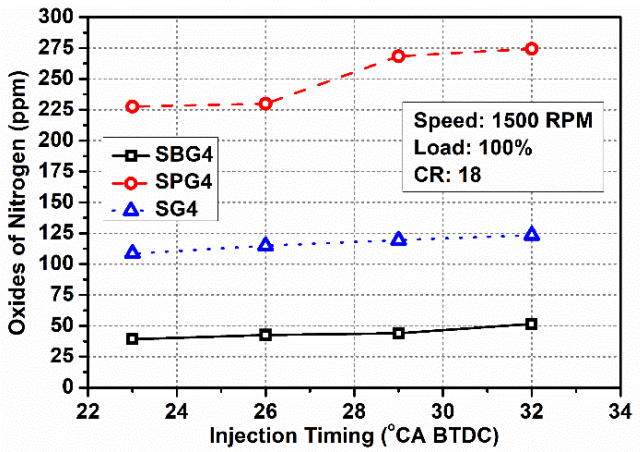

Fig. 5.34 Variation of NO_X with IT for SBG, SPG and SPG-SBG mixture at full load

On the other hand, the advancement of IT showed reduction of CO emission for all gas mixtures as depicted in **Fig. 5.35**. This is due to attainment of high temperature zone inside the cylinder as well as more time for conducting complete combustion. The average reduction of CO that was experienced for SBG-4 was 5.76, 9.73 and 11.3% when the IT was advanced by

3°, 6°, 9° CA, respectively. For SPG-4, same advancement of IT showed an average CO reduction of 5.33, 9.56 and 13.28%, respectively. Moreover, in case of SG-4, minimum average CO emission of 364.19 ppm was found at 29° BTDC, which was 11, 3.12 and 1.22% lower compared to CO emission at 23°, 26° and 32° BTDC, respectively. Analogous effect of CR and IT on reduction of CO was reported past studies [110,122]. Similar to the emission of CO, emission of HC decreases with the advancement of pilot fuel IT as shown in **Fig. 5.36**. At CR of 18, considering the entire load range, minimum average HC emission of 278.33 and 337.1 ppm was observed for SBG-4 and SPG-4, respectively when the IT was advanced by 9° CA. However, for SG-4, minimum average HC emission of 324.32 ppm was found which was 7.58, 2.66 and 1.07% lower than that of HC emission at 23°, 26° and 32° BTDC, respectively.

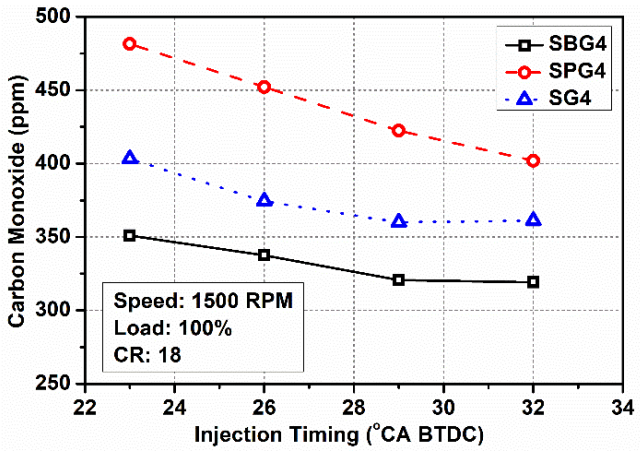

Fig. 5.35 Variation of CO with IT for SBG, SPG and SPG-SBG mixture at full load

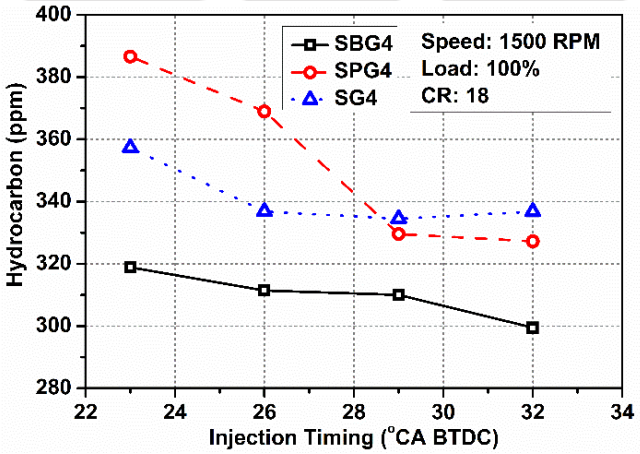

Fig. 5.36 Variation of HC with IT for SBG, SPG and SPG-SBG mixture at full load

5.6 Summary of the chapter

This chapter discusses the results of the experimental investigation of a dual fuel diesel engine operated with different composition of simulated biogas (SBG), simulated producer gas (SBG) and SPG-SBG mixture under varying engine load. Followed by a discussion of the results

obtained from the experimental study on varying compression ratio and pilot fuel injection timing. Compared to fossil diesel with a BTE of 27.57% at standard operating condition, SBG-4 (70% CH_4 and 30% CO_2), SPG-4 (70% H_2 and 30% CO) resulted with maximum BTE of 25.1 and 25.58% at full engine load, CR of 18 and IT of 29° BTDC. At similar operating condition, maximum PFR of 90.59 and 87.77% was achieved for SBG-4 and SPG-4, respectively. In case of SPG-SBG mixture, SG-4 (SPG-2/SPG-4) showed the maximum BTE and PFR of 24.44 and 86.41%, respectively. The combustion data indicated a decrement and increment in ID with an increase in CR and IT, respectively. However, the CP and NHRR was found to be increased with the increase in CR and IT. From the emission analysis it was evident that higher fraction of CH_4 in the SBGs and H_2 in SPGs resulted in better combustion of the fuel mixture leading to lower CO and HC emissions. Moreover, addition of SBG with SPG resulted in drastic reduction in the emission of NO_X. On an average, NO_X emission for SPG-SBG mixture was found to be 64.2% lower than that of SPG-DF operation. In addition to that increase in CR and advanced IT resulted in further reduction of CO and HC emission. Whereas, CO_2 and NO_X emission was found to be increased with the increase in CR and advancement of IT. Therefore, as a whole it can be concluded from the study that, utilization of biogas and producer gas with enriched CH_4 and H_2 concentration in diesel opened up a new vista to enhance thermal efficiency, reducing emissions and saving of pilot fuel. The study demonstrated that a dual fuel mode can be implemented in diesel engines using a combination of biogas and producer gas as the primary fuel. This finding suggests that both gases can be utilized together as a viable alternative fuel source for diesel engines. Moreover, advancement of IT and high CR is a very significant step for real application of biogas in diesel engine under dual fuel mode. Results of the dual fuel diesel engine experiments conducted using raw biogas (BG), producer gas (PG) and BG-PG mixtures generated on field are discussed in chapter 6.

6

Results and Discussion of Engine Characteristics with Biogas and Producer Gas

Chapter Outline:

CHAPTER 6: RESULTS AND DISCUSSION OF ENGINE CHARACTERISTICS WITH BIOGAS AND PRODUCER GAS

6.1 Introduction

Biogas (BG) and producer gas (PG) offer an attractive option for power generation in remote rural areas, as they can be generated from locally available biomass resources, providing decentralized energy production. The comprehensive review of existing literatures in Chapter 2 have demonstrated that BG and PG can be successfully utilized as primary fuels in diesel engines under dual fuel mode. Because of high auto-ignition temperature, these gases cannot be used directly in diesel engines but they are appropriate for dual fuel (DF) operation owing to their high anti-knocking characteristics [36–38]. Despite the potential decrease in thermal efficiency observed in DF modes, the significant replacement of fossil diesel and the reduced emissions can offset this drawbacks. In the recent past, there has been a great deal of research conducted on the combustion and application mechanisms of BG and PG in diesel engines and have reached an apparent horizon. Various literatures are available on performance of diesel engine, combustion characteristics and exhaust emission when using these gaseous fuels under DF mode. As reported in the literatures, biogas induction improves the degree of charge homogeneity and replaces pilot fuel with high carbon content results in low soot formation [96,139]. However, excess quantity of biogas inducted into the engine cylinder forms a rich air-gas mixture results in partial combustion of fuel [141,142]. Alternatively, induction of PG hinders the combustion process by compelling the engine to operate under reduced air-fuel ratio leading to lower thermal efficiency. Moreover, low energy density, low product-reactant mole fraction (0.87) compared to CH_4 (1.0) and low mixture energy density of PG contribute to de-rating of the engine [51,54,55]. Yet, H_2 in PG with low energy density enhances the laminar flame speed which minimizes the knocking intensity caused by preignition problems. Moreover, presence of inert gases like CO_2 and nitrogen (N_2) suppresses the pre-flame reaction and also controls engine knock [56–59]. PG with higher concentration of H_2 delivers high thermal efficiency and also lowers the emission of unburned CO and HC by substituting carbon particles in the fuel mixture. But, high combustion flame temperature due to H_2 raises the heat release rate and cylinder pressure which are responsible for higher NOx emission. In reverse, presence of carbon monoxide (CO) in PG lowers the adiabatic flame temperature and controls the release of NOx pollutant. Moreover, higher fraction of CO_2 in PG increases the specific heat capacity of the fuel mixture, which diminishes the in-cylinder combustion temperature leading to lower NOx emission [60–63]. It was evident that both BG and PG have their own advantages and limitations to be used as a primary fuel for DF diesel

operations. According to the reviews, DF operations individually with BG and PG exhibits inferior combustion characteristics compared to conventional diesel mode. However, these gases possess high anti-knocking properties and they have the potential to control the emission of NOx. Yet, researchers have not considered two or more gases as primary fuel at a time to evaluate the overall engine behaviour. Moreover, very limited literature is available on the combined induction of BG and PG. Combining these two gases might subdue each other's limitations when introduced to the DF engines. Hence, the novelty of the present work lies in introducing both BG and PG collectively as primary fuel in a diesel engine with an aim to analyze its combined impact on improvement of engine performance characteristics and exhaust emission.

6.2 Experimental design

This study investigates the impact of BG-PG mixtures, compression ratio (CR), and pilot fuel injection timing (IT) on the performance, combustion, and emission characteristics of a diesel engine operating in DF mode. The experimental work aims to provide an insights into the interplay between these parameters and their effects on the engine's overall performance, as well as its emissions profile. Biogas was generated from an anaerobic digester of 3 m^3 capacity loaded with cow dung. On the other hand, a downdraft biomass gasifier of 10 kW capacity was installed to generate PG. Locally available wood from Karas (Aquilaria malaccensis) tree was used as feedstock for the gasifier. The important properties of both the biogas and producer gas used for the experiments are summarized in **Table 6.1**. The best tri-biodiesel-diesel blends i.e. Blend2 (discussed in Chapter 4) has been considered as pilot fuel for all the experiments conducted under DF mode. Dual fuel experiments were performed in three different categories as per the experimental matrix illustrated in **Fig. 6.1**. Firstly, the experiments were carried out with raw BG, PG and four different BG-PG mixture namely DFM-1, DFM-2, DFM-3 and DFM-4 at standard engine condition under same load range viz. 20%, 40%, 60%, 80%, and 100%. The BG-PG mixture combinations were inducted to the engine based on controlled regulation of valve opening of BG and PG. Then in the second category, engine parameters were evaluated with best BG-PG mixture combination at varying CR (16, 17, 17.5 and 18) and standard IT of 23° BTDC. Finally, the effect of IT on engine characteristics were studied by varying the IT from 23-32° BTDC with a step of 3° CA considering the best combination of BG-PG mixture and CR.

Table 6.1 Properties of biogas and producer gas used in the study

	Fuels	Chemical composition	Density (kg/m³)	Calorific value (MJ/kg)	Stoichio-metric A/F ratio	Energy Density (MJ/Nm³)
Properties of raw biogas	**BG**	CH_4 (%) = 57.93±1.71 CO_2 (%) = 42.05±1.70	1.251±0.04	19.11±1.06	5.736	23.87±0.70
Properties of raw producer gas	**PG**	H_2 (%) = 14.55±0.51 CO (%) = 21.16±0.91 CH_4 (%) = 2.67±0.29 CO_2 (%) = 5.95±0.38 N_2 (%) = 55.68±1.35	1.11±0.01	5.225±0.21	1.27	5.79±0.21

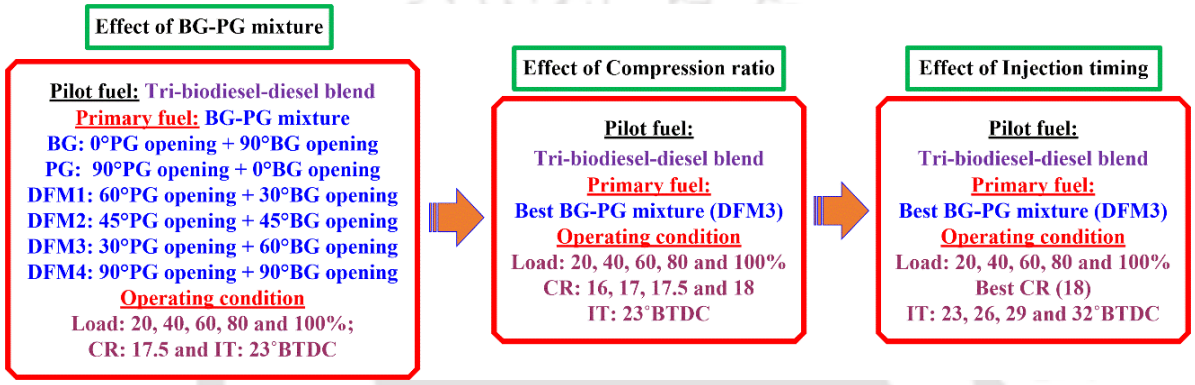

Fig. 6.1 Experimental matrix

6.3 Performance characteristics of diesel engine with biogas and producer gas

6.3.1 Brake thermal efficiency

The BTE of single mode operation with fossil diesel (FD) and DF mode operation with BG, PG, BG-PG mixtures, effect of CR and IT are depicted in **Fig. 6.2(a)-(c)**. It is evident from the figure that FD with higher calorific value resulted in higher BTE compared to BG-PG dual fuel operation in all engine conditions. Moreover, the inferior thermal efficiency for DF mode is due to several factors like low combustion temperatures, combusted residual gas, biogas residuals, reduced speed of flame propagation, amplified compression work instigated by higher consumption of air-biogas mixture and heat rejection through combustion chamber [114]. The maximum BTE has been observed at full load condition due to upsurge of cylinder temperature at high engine load. At 100% load, 17.5 CR and 23° BTDC, raw BG and PG showed BTE of 18.31 and 18.05%, respectively. At similar condition, different valve openings such as DFM-1, DFM-2, DFM-3 and DFM-4 showed BTE of 16.06, 17.18, 18.39 and 14.80%, respectively as compared to 27.57% for FD. In case of DFM-4, i.e. full valve opening (90°) of both BG and PG allows maximum induction of gases into the cylinder leads to an air deficit combustion process and results in minimum BTE. On the other hand, DFM-3 resulted in 0.41 and 1.9% higher BTE than BG and PG, respectively. Increase in the opening angle of BG flow valve (from 30° to 60°), allows higher amount of BG to participate in the combustion process,

enhancing the calorific value of gaseous fuel mixture. This can be the reason behind maximum BTE for DFM-3. Again, at the same operating condition, DFM-3 results in 23.62% increment in BTE, when CR has been raised from 16 to 18 as shown in **Fig. 6.2(b)**. The BTE for DFM-3 is found to be 16.04, 17.26, 18.39 and 19.83% at CR of 16, 17, 17.5 and 18, respectively. This is because, increased CR results in higher average cycle temperature caused by high CR, which assists in better combustion of gaseous fuel and high energy conversion capability [164,253]. Further increase in BTE is noted with the advanced IT of pilot fuel up to a certain limit and then decreases (**Fig. 6.2(c)**). At same loading condition and CR of 18, BTE for DFM-3 is found to be 21.87, 23.28 and 21.05% at 26°, 29° and 32° BTDC, respectively. The early injection of pilot fuel into the cylinder enables it to vaporize and homogeneously mix with the air-gaseous fuel charge, which results in this outcome [115,254].

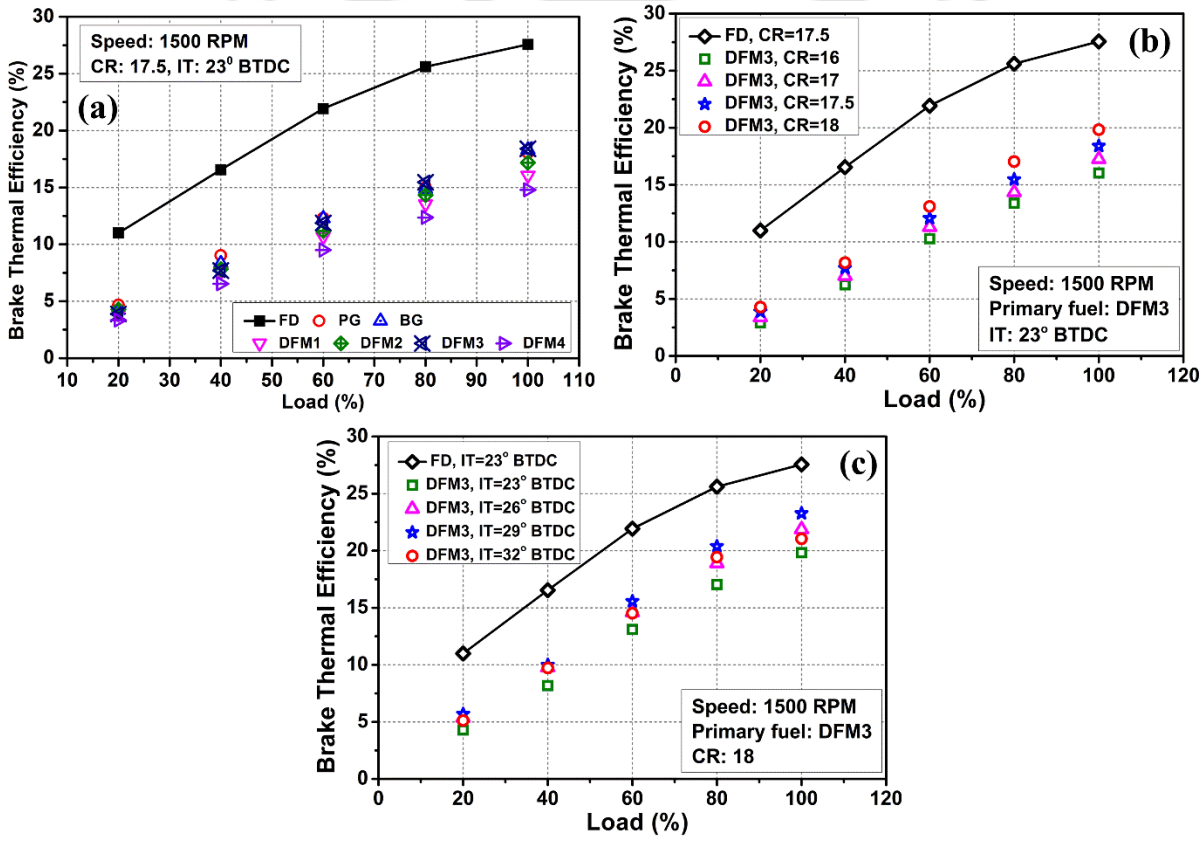

Fig. 6.2 Variation of BTE with load (a) for different BG-PG mixtures, (b) at different CRs and (c) at different ITs

6.3.2 Brake specific energy consumption

The changes of BSEC in response to load for different BG-PG dual fuel operation at varying CR and IT is portrayed in **Fig. 6.3(a)-(c)**. The figures revealed that BSEC for DF operations found to higher for all experimental condition due to the lower calorific values of BG and PG. However, there was a decrease in BSEC at higher load condition. At 100% load and standard CR and IT, the minimum BSEC of 5.44 kJ/s of fuel/kW output is obtained for DFM-3, whereas

DFM-4 resulted in maximum BSEC of 6.76 kJ/s of fuel/kW output compared to FD with BSEC of 3.65 kJ/s of fuel/kW output. Compared to BG and PG, DFM-3 showed 0.4 and 1.8% reduction in BSEC, respectively. Further decrease is BSEC is recorded with increasing of CR and advanced injection of pilot fuel considering the experiments with DFM-3. For the entire load range, an average reduction of 10.05% is observed with the increase of CR from 16 to 18. Again, for the same loading range and CR of 18, advancement of IT from 23° to 29° BTDC resulted in an average reduction of 4.02% BSEC. It has been observed that there is a significant rise in BSEC when the IT is advanced from 29 to 32° BTDC. This may be related to the lower BTE at 32° BTDC.

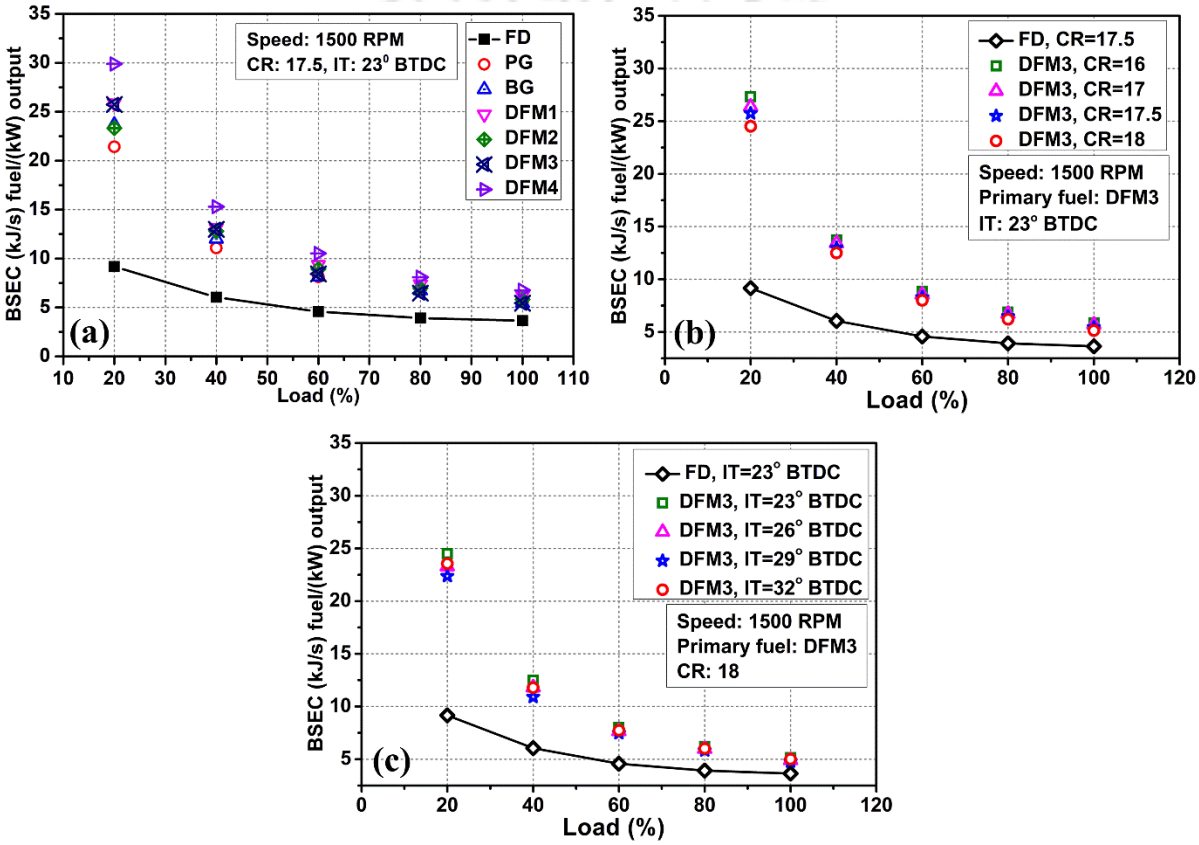

Fig. 6.3 Variation of BSEC with load (a) for different BG-PG mixtures, (b) at different CRs and (c) at different ITs

6.3.3 Gas flow rates and pilot fuel replacement

The variation of biogas flow rate (BGFR) and producer gas flow rate (PGFR) at different operating conditions is combinedly shown in **Fig. 6.4(a)-(d)**, whereas **Fig. 6.5(a)-(c)** represent the amount of pilot fuel replacement (PFR) for the complete DF operations. Both BG and PG flow rates increased with increase in engine load. In order to meet the higher energy demand of the engine, fuel consumption increased substantially at higher load. But, due to lower calorific value of gaseous fuels compared to pilot fuel resulted in higher flow rate of BG and PG than pilot fuel under identical engine operating condition [247]. This may be the reason

behind higher PFR at high load for all test conditions (**Fig. 6.5(a)**). Furthermore, it was observed that, for the entire loading condition, BGFR was recorded to be lesser in contrast to PGFR. The reason could be the higher calorific value associated with BG and opening angle of both the gases. At full load, DFM-3 resulted in minimum BGFR and PGFR of 2.4 and 2.72 kg/hr, respectively at standard CR and IT. At similar operating condition, raw BG and PG dual fuel mode showed BGFR of 3.27 and PGFR of 7.3 kg/hr, respectively. Hence, DF experiments with DFM-3 showed 26.6 and 62.7% reduction in BGFR and PGFR, respectively at full load. At this condition, raw BG and PG dual fuel mode resulted in PFR of 88 and 44%, respectively. In case of BG-PG mixtures, maximum PFR of 87.93% was also achieved in case of DFM-3 which is about 29.67, 10 and 15.91% higher than DFM-1, DFM-2 and DFM-4, respectively. As the CR increases, the combustion process enhances due high temperature and pressure inside the cylinder. This phenomenon reduces the gaseous fuel requirement in the combustion chamber. Hence, this results in lower gaseous fuel flow rates and higher replacement of pilot fuel. Considering the experiment of DFM-3 at standard IT, an average BGFR of 2.51, 2.49 and 2.34 kg/hr is noted, respectively for CR of 16, 17 and 18. While, for the same CR, PGFR is found to be 2.8, 2.78 and 2.64 kg/hr at CR of 16, 17 and 18, respectively. On the other hand, at the identical condition, PFR at CR of 16, 17 and 18 is recorded to be 84.2, 86.01 and 88.81%, respectively. Moreover, on advancing the IT of pilot fuel from 23° to 32° BTDC, DFM-3 resulted in an average drop of BGFR and PGFR by 3.15 and 1.38%, respectively at CR of 18 considering the entire range of load. Again, at full load and CR of 18, pilot fuel IT of 29° BTDC resulted in maximum PFR of 90.22% which is 1.58, 0.8 and 1.99% higher compared to 23°, 26°, and 32° BTDC, respectively. From this analysis, it can be concluded that increase in CR from 16 to 18 and advancement of IT from 23 to 29° BTDC lowers the gaseous fuel consumption and substitute maximum amount of pilot fuel.

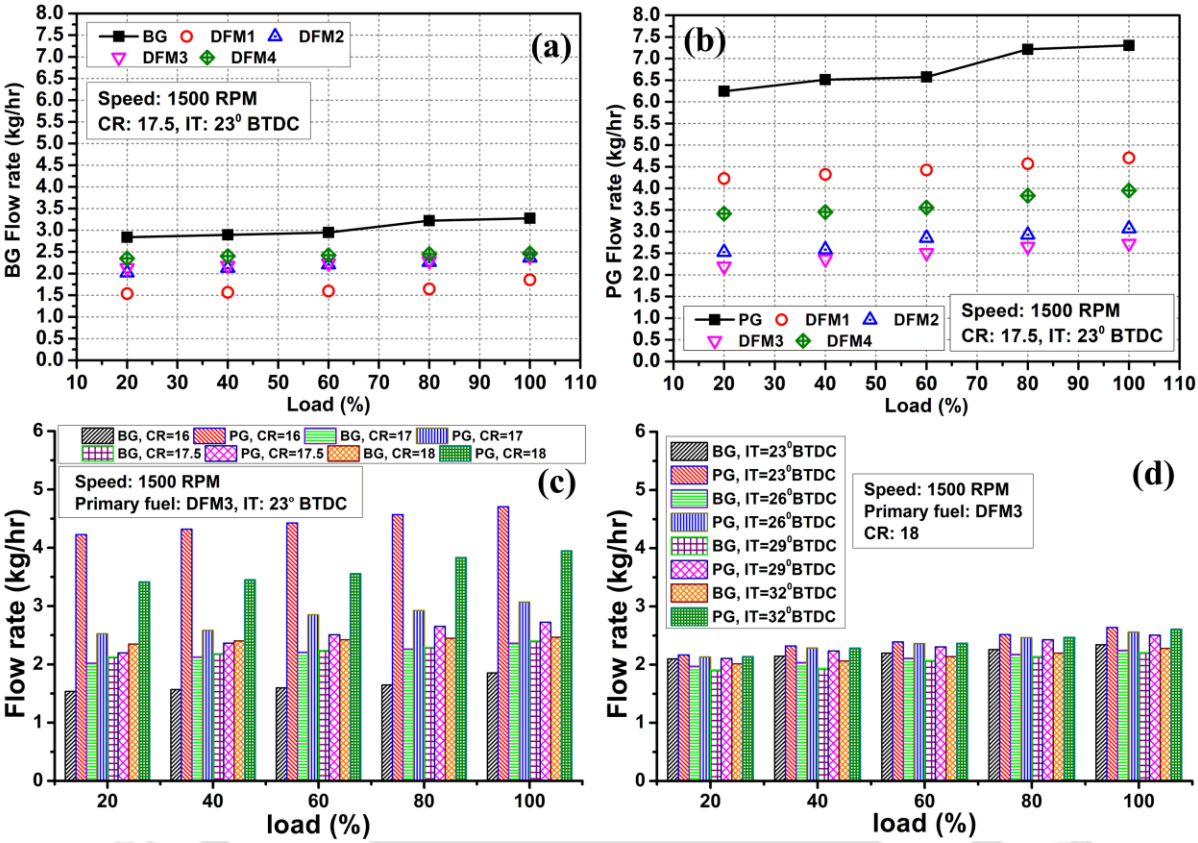

Fig. 6.4 Variation of gas flow rates with load for different BG-PG mixtures, at different CRs and different ITs

6.3.4 Exhaust gas temperature

The fluctuations of EGT with engine load for fossil diesel and DF operation at different BG-PG mixtures, CR and IT is shown in **Fig. 6.6(a)-(c)**. It was evident from the trend that, EGT for DF mode is higher compared to FD mode at all operating condition. The reason being, low burning velocity and high self-ignition temperature of BG and PG delays the burning and diminishes the combustion duration to extract engine power [215]. Furthermore, with the increase in load, the EGT increases for both FD and DF mode due to the supply of excess energy input. It was noticeable that, increase in the opening angle of PG flow valve (30 to 90°), the EGT increases. For the complete load range and standard CR and IT, the average value of EGT for BG, PG, DFM-1, DFM-2, DFM-3 and DFM-4 were found to be 461.58, 553.9, 536.28, 517.18, 506.64 and 551.12 °C, respectively as compared to 214.42 °C for diesel mode. This is because, significantly high amount of heat energy is retained in PG after gasification which is delivered to engine [206,253]. Moreover, the higher component of non-combustible gases (CO_2 and N_2) in BG-PG mixture dilutes the intake charge by absorbing additional heat during the combustion process. This delays the combustion of charge and compels the exhaust gases emerge at higher temperature. However, experiments with DFM-3 at higher CR showed significant improvement in lowering the exhaust gas temperature (**Fig. 6.6(b)**) because of the upsurge in burning velocity of the gaseous fuel mixture, thereby shortens the time required

for complete combustion [251]. For entire loading range and IT of 23° BTDC, the average EGT reduction was found to be 10.85% with increase in CR from 16 to 18. There is a further decrement in the EGT, when IT was advanced from 23° to 32° BTDC. At CR of 18, DFM-3 showed an average EGT of 471.26, 461.01 and 458.72 °C for 26°, 29° and 32° BTDC, respectively which is 3.29, 5.39 and 5.86% lower compared to 23° BTDC.

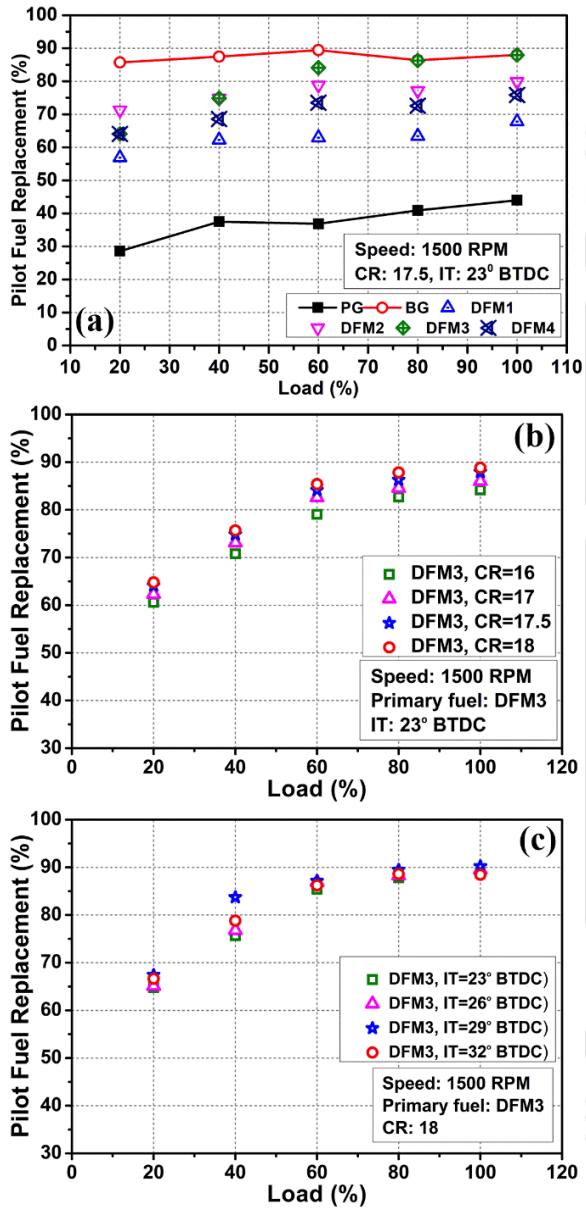

Fig. 6.5 Variation of PFR with load (a) for different BG-PG mixtures, (b) at different CRs and (c) at different ITs

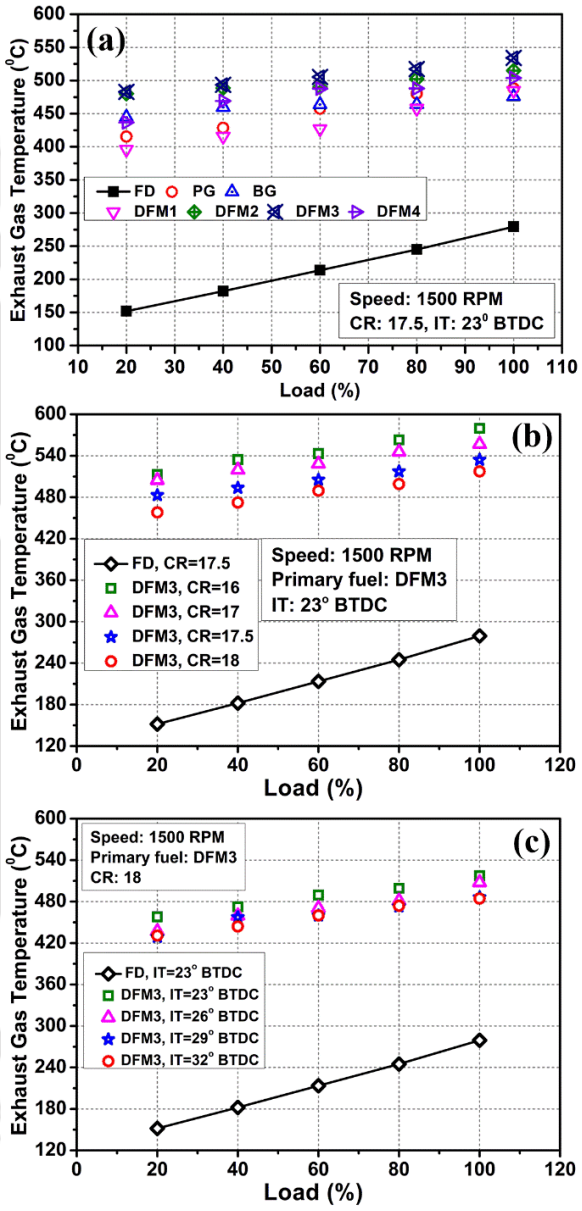

Fig. 6.6 Variation of EGT with load (a) for different BG-PG mixtures, (b) at different CRs and (c) at different ITs

6.4 Combustion characteristics of diesel engine with biogas and producer gas

6.4.1 Ignition delay

In this investigation, it has been observed that the ignition delay (ID) of pilot fuel gradually diminishes as engine load increases for both single and DF mode as illustrated in **Fig. 6.7(a)-**

(c). High temperature within the combustion chamber caused by higher loading condition results in reduction of ID. For all the experimental condition, DF operation with BG, PG and BG-PG mixtures showed greater ID compared to single mode with FD. This occurs because, as the gaseous fuel is inducted into the inlet manifold, it lowers the oxygen concentration in the air, which reduces the temperature of the incoming charge due to the presence of a significant amount of inert gases, collectively leading to elongation of ID [118,248,255]. At full load condition with CR of 17.5 and IT of 23° BTDC, minimum and maximum ID 20 and 28°CA was noted for BG and PG. However, intake charge of air-BG-PG with greater share of BG lowered the ID. This is because, greater share of BG could diminishes the auto-ignition temperature of the fuel mixture leading to lower ID. DFM-3 showed lower ID of 23°CA in contrast to 26, 25 and 27 °CA for DFM-1, DFM-2 and DFM-4, respectively (**Fig. 6.7(a)**). From the investigation, it has been witnessed that high CR lowers the ignition delay (**Fig. 6.7(b**)). Increase in the CR, upraises the temperature of the combustion chamber and empowers the intake charge to attain the auto-ignition temperature earlier and subsequently reduces the ID. Experiments with DFM-3 at standard IT, the ID is found to be 26, 25, 23 and 22° CA, respectively at CR of 16, 17, 17.5 and 18. On the other hand, advancement of pilot fuel IT from 23° to 32° BTDC elongates the ID as seen in **Fig. 6.7(c)**. For DFM-3, at fixed CR of 18 and 100% load, the ID is observed to be 22, 23 and 24° CA at pilot fuel IT of 26°, 29° and 32° BTDC, respectively. As, IT is advanced, it permits the introduction of pilot fuel in environments with lower gas temperatures, which slows down the preignition reaction of the fuel mixture leading to extended ID. Similar observations was also reported in the past literature [105].

6.4.2 Net heat release rate

Fig. 6.8(a)-(c) presents the fluctuation in net heat release rate (NHRR) per crank angle at maximum load for both single fuel mode and DF mode with different operating condition. The higher calorific value of FD resulted in higher net heat release rate (NHRR) than BG-PG mode irrespective of the operating conditions. Aspirated air-gaseous fuel mixtures and pilot fuel along with their energy densities have a considerable impact on heat release intensity [131]. From the **Fig. 6.8(a)**, it was revealed that the maximum NHRR for DFM-1, DFM-2, DFM-3 and DFM-4 at full load and standard IT and CR are 72.36, 69.76, 63.69 and 54.35 J/°CA which occurred at 10°, 8°, 4° and 10° CA ATDC correspondingly compared to FD with peak NHRR of 105.95 J/°CA occurred 8° BTDC. At similar operating condition, raw BG and PG resulted in NHRR of 48.5 and 79.36 J/°CA, respectively. This can be ascribed to the existence of inert gas and the high specific heat capacity of the BG-PG mixtures leading to delay in the combustion process. For DFM-1, pilot fuel has a greater share than gaseous mixture which could be the reason behind maximum NHRR. From the experiments with varying CR for

DFM-3, NHRR showed higher values at all loading conditions (**Fig. 6.8(b)**). At 100% load and IT of 23° BTDC, CR of 18 showed 7.76% hike in NHRR as compared to CR of 17.5, with a peak value of 68.64.09 J/°CA. While at CR of 16 and 17, peak NHRR is obtained to be 16.73 and 6.69% lower in contrast to CR of 17.5. Moreover, the NHRR curve is shifted 4° closer to TDC when CR is increased from 16 to 18. Analogous observations are also explained in the past studies [114,164,206,253]. Additionally, the NHRR is again increased with the advancement of pilot fuel IT. Experiments with DFM3 at CR of 18, the peak NHRR at 26°, 29° and 32° BTDC is noted to be 71.60, 75.18 and 73 J/°CA at 26°, 29° and 32° BTDC, respectively.

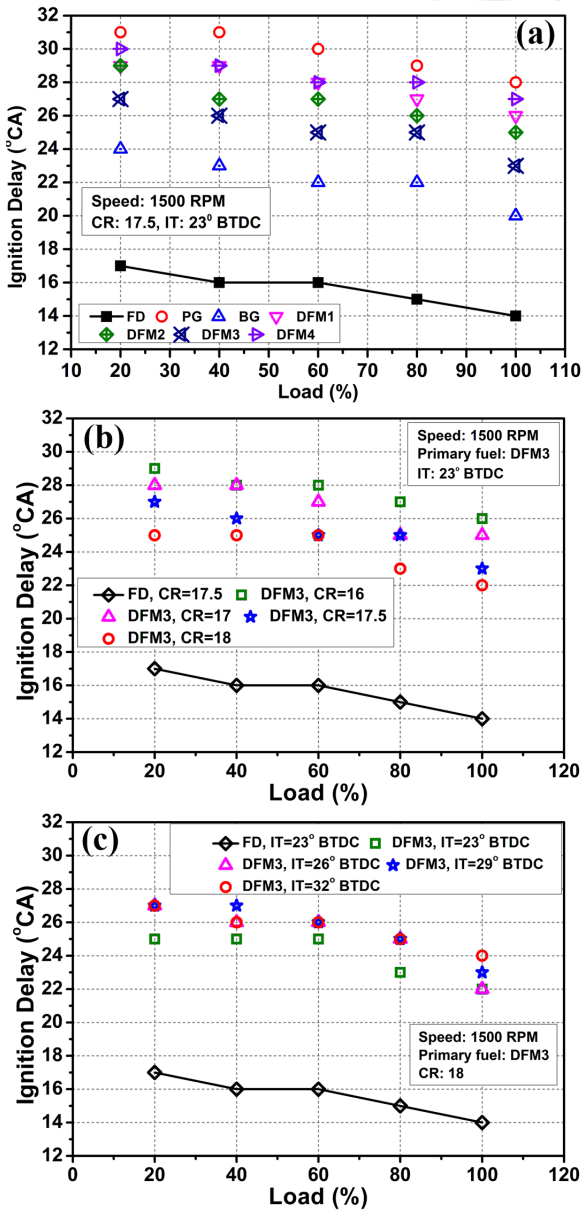

Fig. 6.7 Variation of ID with load (a) for different BG-PG mixtures, (b) at different CRs and (c) at different ITs

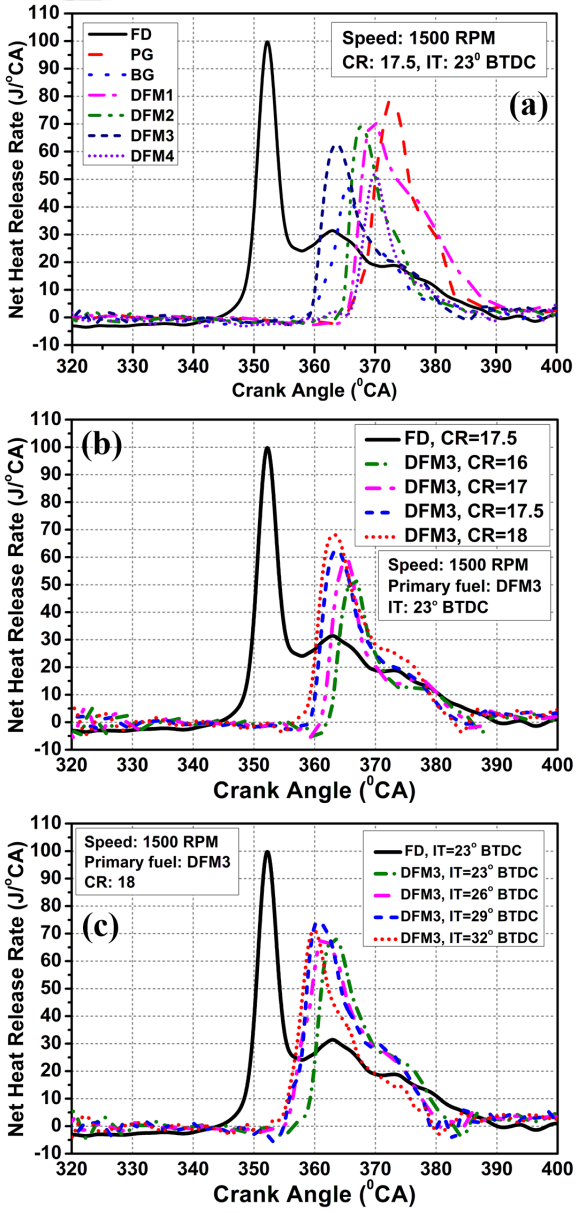

Fig. 6.8 Variation of NHRR at full load (a) for different BG-PG mixtures, (b) at different CRs and (c) at different ITs

6.4.3 Cylinder pressure and peak cylinder pressure

Fig. 6.9(a)-(c) illustrates the fluctuations of cylinder pressure (CP) per crank angle at maximum load for fossil diesel (FD) mode and DF mode with BG-PG mixtures under different CR and IT. Similar to NHRR, the peak cylinder pressure (PCP) value was found to be more in case of FD operation compared to DF mode for all operating condition. Maximum PCP of 64.15 bar was obtained in case PG operation, while BG operation showed PCP of 58.45 bar. With the increasing share of PG in the gas mixture, CP was found to be increased due to higher share of pilot fuel. In case of BG-PG mixture, maximum PCP of 60.59 bar was attained for DFM-1 compared to 57.40, 56.78 and 47.16 bar for DFM-2, DFM-3 and DFM-4, respectively. Moreover, CP curve was shifted towards the TDC with the increasing share of BG in the gaseous fuel mixture. At standard IT and CR, the crank angle with respect to PCP is recorded to be 15°, 12°, 11° and 14°CA ATDC for DFM-1, DFM-2, DFM-3 and DFM-4, respectively compared to 1°CA ATDC for FD mode. Whereas, for BG and PG, crank angle with respect to PCP value was found to be 9° and 16°CA ATDC. Rise in temperature and pressure due to increasing inside the combustion zone minimizes the auto-ignition temperature of the gaseous fuel mixture and shifts the PCP towards the TDC (**Fig. (6.9(b)**). Tests with DFM-3 confirms this behaviour by showing the attainment of PCP at 13°, 12°, 11° and 10° CA ATDC for CR of 16, 17, 17.5 and 18, respectively [112]. Advancing the injection angle from 23° to 32° BTDC witnessed an additional shift of 6° CA towards the TDC (**Fig. 6.9(c)**) for the experiments conducted with DFM-3 at CR of 18. The PCP value is attained at 370°, 368°, 366° and 364° CA for 23°, 26°, 29° and 32° BTDC, respectively. This is because, early start of combustion at advanced IT promotes quick burning of the fuel mixture in the premixed stage causing the PCP to occur nearer to the TDC [166]. As exemplified in **Fig. 6.10(a)-(c)**, higher engine load results in rise of PCP for all test conditions. It is also observed that, at full load, FD mode showed higher PCP of than DF mode 70.19 bar which was 9.42, 20.08, 15.84, 22.26, 23.61 and 48.80% higher in contrast to PG, BG, DFM-1, DFM-2, DFM-3 and DFM-4, respectively. This could be due to the low reactive BG-PG mixtures with high specific heat that lowers the combustion rate leading to decrease in CP [126,139]. Furthermore, with increase of CR form 16 to 18, the PCP of DFM-3 is elevated by 36.6% at full load and standard IT. In addition, DFM-3 at full load and CR of 18 showed maximum PCP of 61.70 bar at IT of 29° BTDC which is 6.21, 3.27 and 2.85% higher as compared to 23°, 26° and 32° BTDC, respectively. This may be due to the advancement of pilot fuel injection timing that creates a fuel rich mixture zone inside the combustion chamber [122].

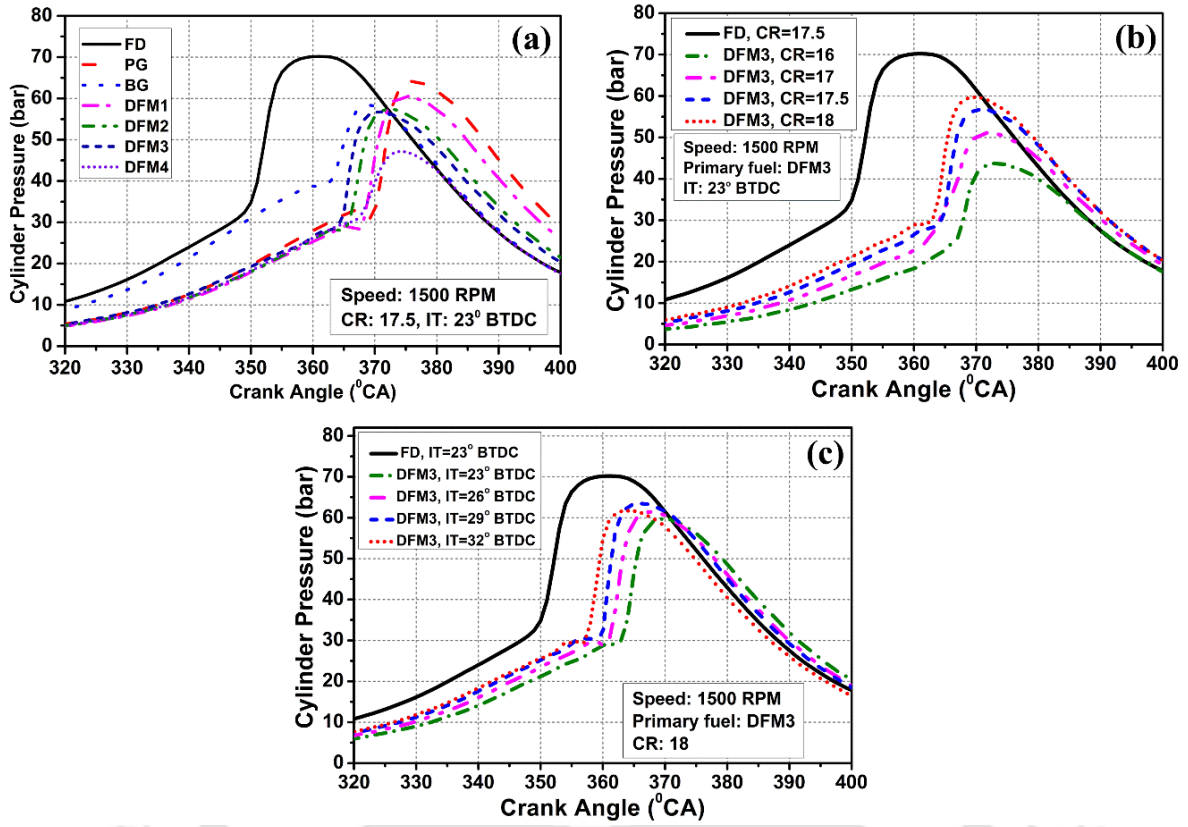

Fig. 6.9 Variation of CP at full load (a) for different BG-PG mixtures, (b) at different CRs and (c) at different ITs

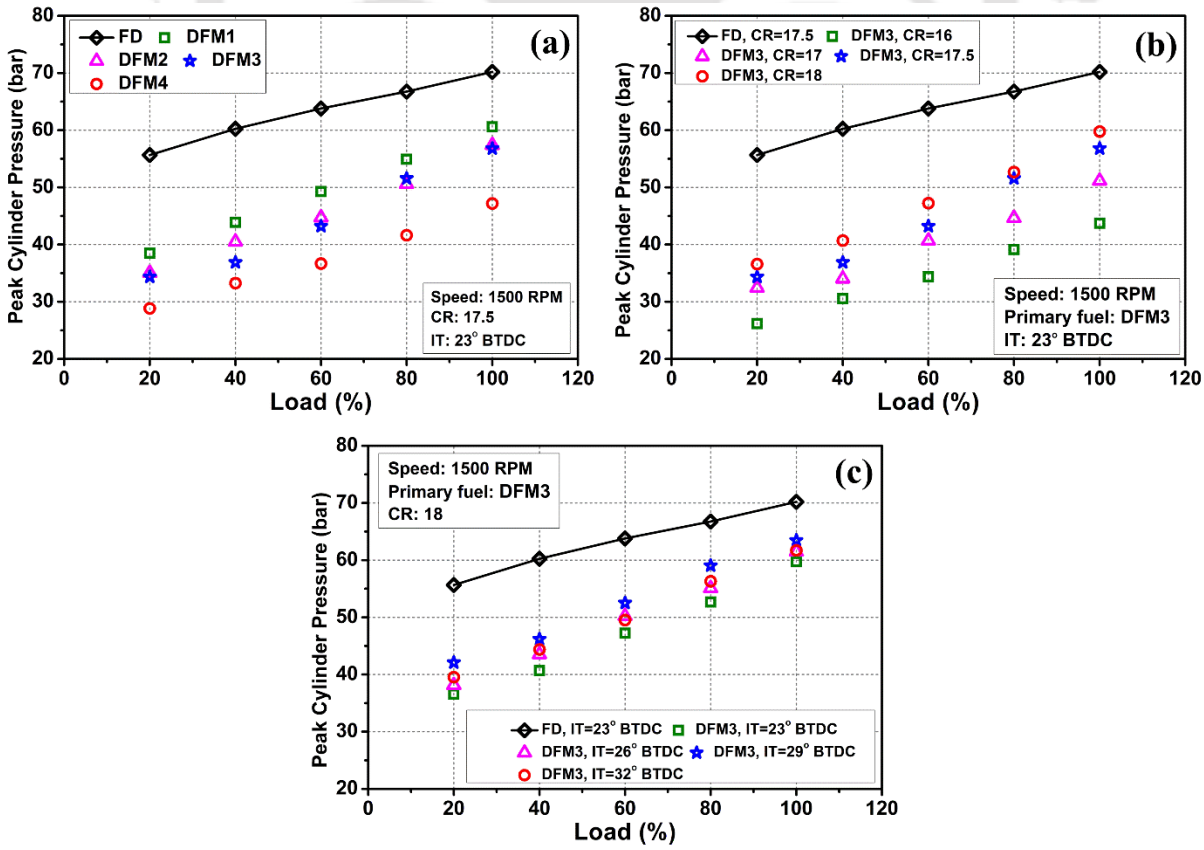

Fig. 6.10 Variation of PCP with load (a) for different BG-PG mixtures, (b) at different CRs and (c) at different ITs

6.5 Emission Characteristics of diesel engine with biogas and producer gas

6.5.1 Carbon dioxide emission

Fig. 6.11(a)-(c) portrays the variation of carbon dioxide (CO_2) for both single and DF mode with engine load at different operating conditions. From the figure, it was evident that, for entire range of load, DF operation resulted in higher fraction of CO_2 in the engine exhaust compared to FD mode. As the air-gaseous fuel intake charge comprises of CO_2, higher amount of CO_2 is released to the ambient without undergoing the combustion process. The primary reason behind such higher emission is the excessive presence of CO_2 in the air-gaseous fuel intake charge as both BG and PG composed of about 42 and 6% CO_2 (**Table 6.1**), respectively. Moreover, as the engine consumed more amount of fuel at higher loading condition to deliver desired power, emission of CO_2 increases at higher load. A study conducted by Perci and Edwin [256] reported that CO_2 emissions escalate as engine load increases. From the figure, it was also visible that increasing the opening angle of BG flow valve (30 to 90°), higher amount of CO_2 enters into the engine as air-gas mixture which resulted in higher component of CO_2 in the engine exhaust (**Fig. 6.11(a)**). Due to this, DFM-4 showed maximum CO_2 emission of 7.86% compared to 6.24, 6.09, 6.36, 6.39 and 6.38% in case of PG, BG, DFM-1, DFM-2 and DFM-3, respectively. This is because CO and CO_2 are constituents of PG gas, and their combustion leads to an amplified release of CO_2 emissions. Moreover, Better combustion phenomenon at high CR leads to higher release of CO_2 component in the exhaust (**Fig. 6.11(b)**). Considering the entire range of load experiments with DFM-3 at standard IT, the average CO_2 emission for CR of 16, 17 and 18 is obtained to be 6.21, 6.25 and 6.51%, respectively. For same IT, at 100% load, CR of 16, 17 and 17.5 showed 5.07, 4.17 and 4.77% reduction in CO_2 emission compared to CR of 18. A study conducted by Bora et al. [114] also reported similar observation. They stated that as the CR rises, the clearance volume diminishes, subsequently leading to increased temperature and pressure within the charge at the end of the compression stroke. This heightened temperature facilitates more efficient fuel combustion, ultimately resulting in an increase in CO_2 emissions. Furthermore, in this study, advancing the IT of pilot fuel from 23° to 32° BTDC, on an average 1.47% more release of CO_2 is observed because of the improvement of combustion process caused by better mixing of pilot fuel with the intake charge. Again, at full load and same CR, IT of 23°, 26°, 29° and 32° BTDC resulted in 6.70, 6.71, 6.73 and 6.78% release of CO_2, respectively. The findings of this investigation are consistent with existing studies [35,252].

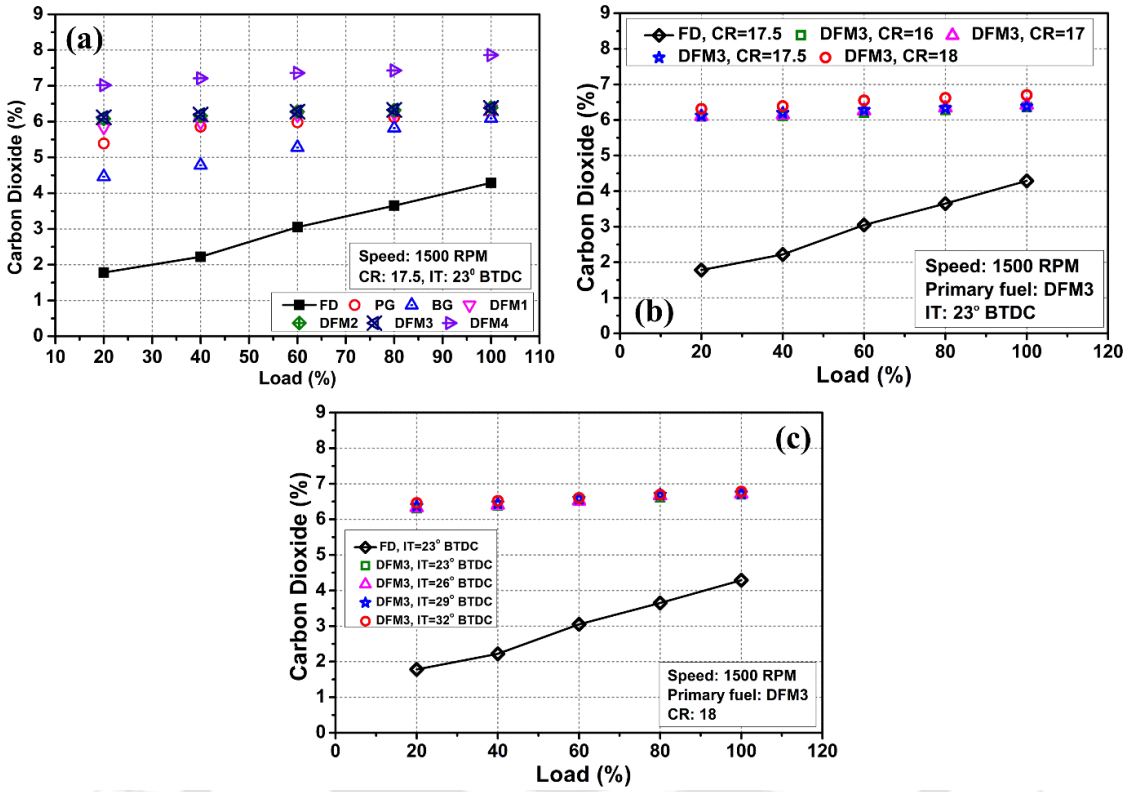

Fig. 6.11 Variation of CO_2 with load (a) for different BG-PG mixtures, (b) at different CRs and (c) at different ITs

6.5.2 Oxides of nitrogen emission

Oxides of nitrogen (NO_X) is one of the major pollutant that is released from engine exhaust. It is usually composed of higher level of NO and minor level of NO_2. The production of NO_X is largely dependent on the temperature generated within the combustion chamber, oxygen availability for combustion, retention time and availability of nitrogen molecules [108,143,257]. Fig 6.12(a)-(c) illustrated the emission of NO_X with load for both single and DF mode under varying operating condition. From the figure, it was observed that the emission of NO_X tended to rise as the engine load increases. Identical observation was also reported by Karagöz *et al.* [258]. The authors stated that as engine load rises, there is an increase in the quantity of fuel entering the cylinders and the post-combustion process tends to extend towards the latter part of the power stroke of the piston. They have also reported that combustion may continue during the exhaust phase, influenced by the increased quantity of gaseous fuel introduced into the cylinder. With load-dependent variations, the fuel quantity within the cylinder also increases, subsequently elevating exhaust gas temperatures. These higher temperatures at the end of combustion contribute to increased NO_X emissions. Likewise, it was also noticeable that the presence of greater fraction of N_2 in PG resulted in higher release of NO_X pollutant in the exhaust. Conversely, CO_2 components in BG controls the emission of NO_X by absorbing the combustion chamber's internal heat. In addition to that

H_2 and CO in PG elevates the combustion temperature which facilitates the formation of NO_X [259]. At standard IT and CR, considering complete load range, maximum and minimum average NO_X emission of 213.76 and 32.18 ppm was obtained for PG and BG, respectively as compared to 82.94 ppm for diesel mode. In addition, for BG-PG mixture, DFM-4 with full valve opening of both BG and PG results in maximum average NO_X formation of 98.07 ppm which is 14.25, 19.37 and 54.46% higher compared to DFM-1, DFM-2 and DFM-3, respectively. The maximum exhaust gas temperature in case of DFM-4 could be responsible for this observed results. High combustion temperature stimulates the formation of NO_X. Hence, CR of 18 resulted in maximum NO_X emission of 75.37 ppm throughout the entire loading spectrum for DFM-3. On an average, 45.20, 26.42 and 18.60% increase in the NO_X emission is obtained when the CR is increased to 18 from 16, 17 and 17.5, respectively. Likewise, DFM-3 shows a significantly higher release of NO_X, on an average 14.49%, when the IT is advanced from 23° to 32° BTDC at fixed CR of 18. At same CR and 100% load, experiments at 23°, 26°, 29° and 32° BTDC showed NO_X emission of 96.70, 100.06, 103.13 and 108.02 ppm, respectively.

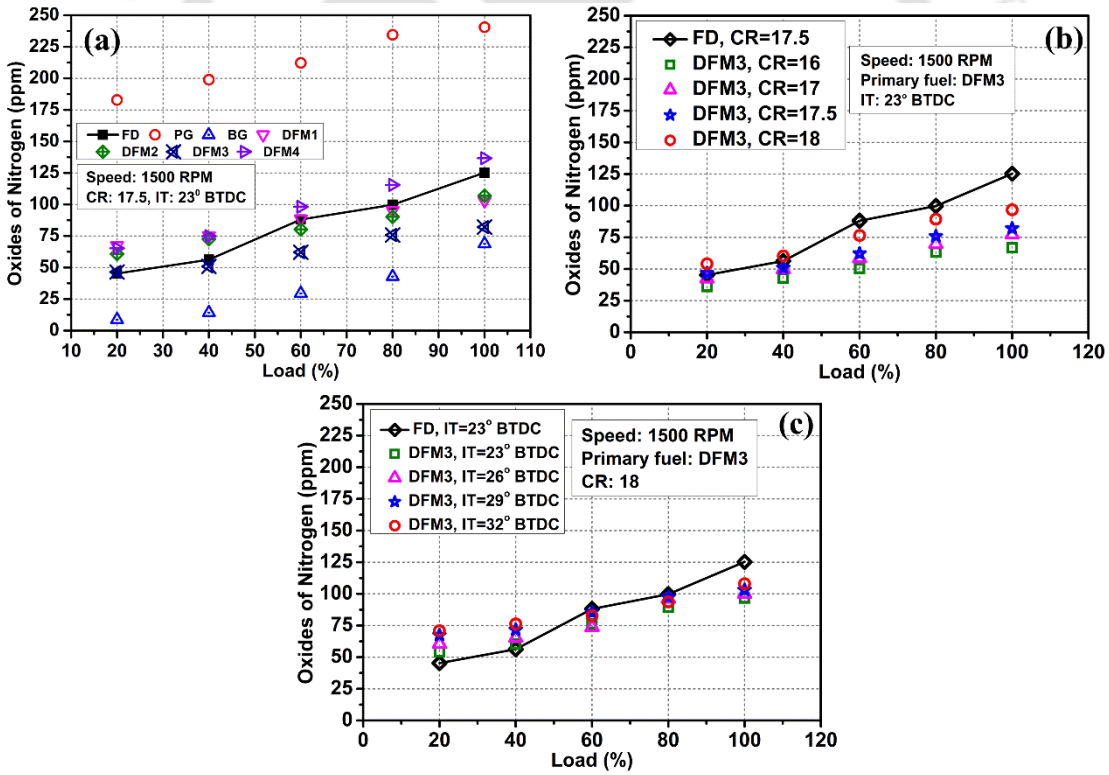

Fig. 6.12 Variation of NO_X with load (a) for different BG-PG mixtures, (b) at different CRs and (c) at different ITs

6.5.3 Carbon monoxide emission

It is widely accepted that, emission of CO_2 and CO follows a reverse trend. Both of these components in the engine exhaust defines the combustion behaviour of fuel mixture. Considering the emission of CO, lower its value, the more complete is the combustion [259]. **Fig. 6.13(a)-(c)** exemplified the changes in CO emissions in response to engine load for both

FD and DF mode at different operating condition. The figure clearly demonstrated an initial decrease in CO emission with the increasing load but after a specified load, it increases again. The reason for this behaviour is that lower cylinder temperature at low loads can lead to improper combustion of fuel. Increase in the load forms too rich fuel mixture to undergo complete combustion caused by additional fuel supply and hence after a particular load, high CO was released. Sharma and Kaushal [253] conducted DF experiments with PG and observed identical pattern of CO emission with respect to engine load. A study conducted by Barik and Murugan [115] also observed highest CO emission in low engine load and explained that low-load conditions, the fuel-air mixture at the periphery of the injection spray becomes excessively lean, making it unable to support flame propagation. Consequently, the local temperature decreases, leading to reduced CO oxidation and, as a result, higher emissions of CO. The authors also reported the inadequate mixing of gaseous and liquid fuels at higher engine loads could potentially be another factor contributing to increased CO emissions [117]. At full load, standard CR and IT, CO emission for PG, BG, DFM-1, DFM-2, DFM-3 and DFM-4 was observed to be 332.8, 266.24, 320.44, 280.84, 272.45 and 320.48 ppm, respectively in contrast to 90.74 ppm for FD. The highest CO emission in case of PG is because of greater components of CO in the fuel mixture, while in case of DFM-4, excessive gaseous fuel flow substitutes sufficient amount of oxygen which deteriorates the combustion of fuel mixture.

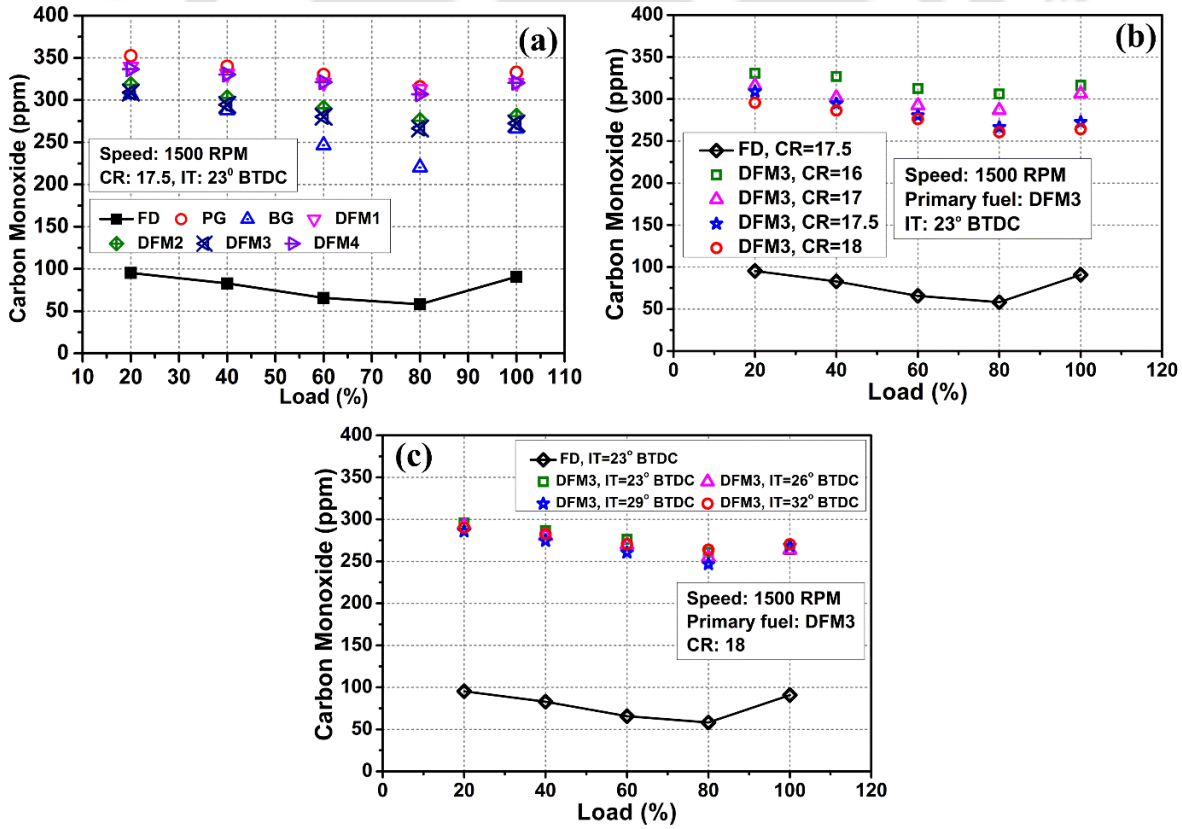

Fig. 6.13 Variation of CO with load (a) for different BG-PG mixtures, (b) at different CRs and (c) at different ITs

Substantial reduction in CO emission was observed at higher CR of 18 (**Fig. 6.13(b)**). Higher CR upsurge the cylinder temperature and developed an affirmative ambiance for carbonaceous component of the fuel to undergo oxidation reaction, hence CO reduced [247]. Considering the all loading condition and at standard IT, DFM-3 resulted in an average CO emission of 318.52, 300.71, 284.50 and 276.64 ppm for CR of 16, 17, 17.5 and 18. On an average, the CO emission reduction was observed to 13.14% when CR is increased from 16 to 18. Nonetheless, it is also evident that advanced IT further reduces the release of CO pollutant due to achievement of high temperature zone inside the cylinder as well as more time for conducting complete combustion. But, after a certain IT i.e. 29° BTDC, higher emission of CO is noted due to poor combustion caused by rich fuel mixture. Increase in the IT from 23° to 29° BTDC, an average CO reduction of 3.40% was experienced at CR of 18. Analogous effect of CR and IT on reduction of CO was reported by [110,122,255].

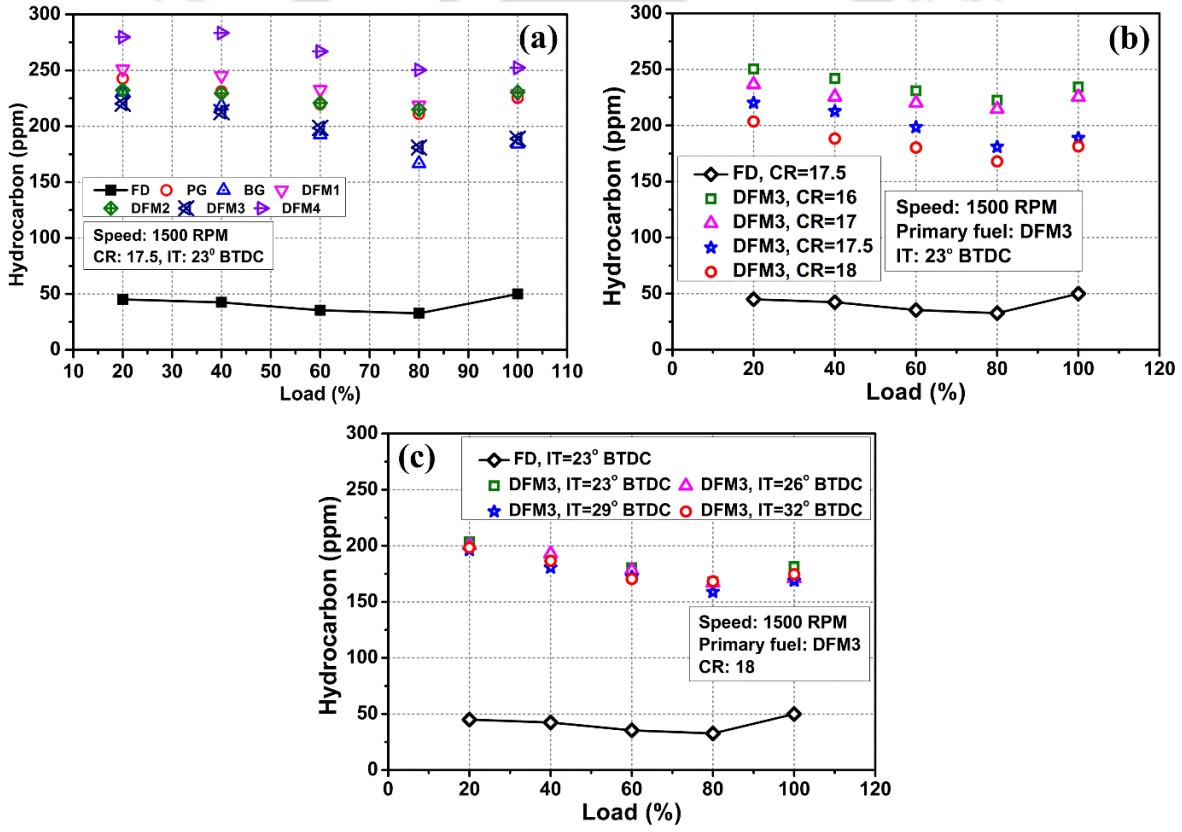

Fig. 6.14 Variation of HC with load (a) for different BG-PG mixtures, (b) at different CRs and (c) at different ITs

6.5.4 Hydrocarbon emission

Likewise, the emission of HC is also depends on the combustion of the fuel mixture. Poor combustion of fuel can result in greater discharge of HC pollutant in the engine exhaust. **Fig. 6.14(a)-(c)** represents the variation of emission of HC in response to engine load for both FD and DF mode at different experimental condition. Similar to the CO, release of HC pollutants initially increased with increase in load, achieved a lowest value and again increases after a

particular load for both the mode of operations. An identical trend in the emission of HC was also observed by Nayak and Sahoo [245]. The study reported higher emission of HC with BG as primary fuel compared to PG. The authors revealed that gaseous fuel mixture with higher amount of CO_2 lowers the combustion temperature due to higher heat capacity leading to improper combustion. At 100% load, CR of 17.5 and 23° BTDC, BG and PG dual fuel operation resulted in HC emission of 184.2 and 225.38 ppm, respectively. In case of BG-PG mixtures, DFM-1, DFM-2, DFM-3 and DFM-4 showed 229.05, 230.40, 188.79 and 252.29 ppm of HC emission, respectively compared to 49.93 ppm for FD. Improved combustion behaviour with higher fraction of BG in DFM-3 may be the underlying reason for minimum HC emission. Further decrement in the HC emission is recorded for DFM-3 when the engine CR is increased from 16 to 18. On an average, 21.91% reduction of HC emission is observed. Again, lowering of HC components in the engine exhaust is found with the advancement of IT. The reason for this could be an early initiation of combustion relative to TDC. As a result, the temperature of the cylinder charge elevates, and therefore less discharge of unburned HC into the atmosphere caused by proper burning of the intake [115,255]. Even though, as mentioned earlier, advancement of IT beyond 29° BTDC results in higher HC emission because of inadequate combustion of rich fuel mixture. At full load and CR of 18, HC emission is recorded to be 170.94, 168.80 and 174.60 ppm for 26°, 29° and 32° BTDC, respectively which is equal to 5.73, 6.91 and 3.71% lower than that of 23° BTDC.

6.6 Summary of the chapter

In the present investigation, dual fuel experiments with BG-PG mixtures under varying engine load, CR and pilot fuel IT with an aim to analyze the engine characteristics has been successfully conducted in DF engine. The experimental results are studied and compared with the standard diesel fuel based on the engine performance, combustion and emissions characteristics. A best combination of BG-PG mixture was found from the experimental results. At full load, standard CR and IT, DFM-3 (i.e. 60° opening of BG valve and 30° opening of PG valve) resulted in maximum BTE and PFR of 18.39 and 87.93%, respectively compared to rest of the BG-PG mixtures. Experimental results at full load, CR of 18 and IT of 29° BTDC showed the enhanced engine performance and reduction of engine emission for the BG-PG flow condition of DFM-3. At this operating condition DFM-3 showed highest BTE and PFR i.e. 23.28 and 90.22%, respectively. At similar condition, the BG and PG flow rate was found to be 2.21 and 2.51 kg/hr, respectively. It has been observed that with the increase of CR, ignition delay is reduced, while advancing the injection, ID found to be increased. On the other hand, the PCP and NHRR is noticed to be increased with the increment of CR and IT. The minimum emission of CO and HC is found for DFM-3 at CR of 18 and IT of 29° BTDC i.e. 267.21 and 175.31 ppm, respectively. However, DFM-3 showed an increment in the emission

of CO_2 and NO_X with the increase of CR and advancement of IT. Furthermore, there is a 17.64% reduction of NO_X emission of at full load, CR of 18 and 29° BTDC compared to FD mode. This investigation has clearly shown the advantage of higher share of BG in the BG-PG mixture for DF operations. Historically, at standard CR of 17.5 and IT of 23° BTDC under dual fuel operation results in inferior performance and emission behaviour. Higher CR and advancement of IT provides supplementary benefits in terms of augmenting the engine performance and minimizing the exhaust emission. Hence, by considering this novel protocol, it is possible to develop a technology package that could provide decentralized power remotely. A detailed summary of all the experimental findings are discussed in the next chapter.

7

Conclusions and Scopes for Future Work

Chapter Outline:

CHAPTER 7: CONCLUSIONS AND SCOPES FOR FUTURE WORK

7.1 Brief summary of the investigation

This study aims to conduct a comprehensive experimental analysis of a 3.5 kW single cylinder, variable compression ratio diesel engine powered by biogas and producer gas, using a blend of biodiesel and diesel as the pilot fuel. The ultimate goal of this research is to promote the use of biodiesel-biogas-producer gas as a clean energy source for rural electrification, thereby providing a viable alternative to traditional fossil fuels. At the very beginning, experiments were conducted with tri-biodiesel-diesel blends under single fuel mode under standard engine operating condition with a compression ratio of 17.5 and injection timing of 23° BTDC at different engine loads. Through this study, author could able to specify the best combination of blended fuels to be used as pilot fuel for dual fuel operation. For the purpose of this investigation, three types of non-edible biodiesels, namely Jatropha (Jatropha Curcas), Karanja (Pongamia Pinnata), and Mahua (Madhuca Indica), are being considered and mixed with diesel at 30:70 ratio to prepare ten different tri-biodiesel-diesel blends. Based on the experimental results a tri-biodiesel-diesel blend was found to be best and considered for the further study. The second phase of the study deals with the experimental investigation of the diesel engine under dual fuel mode utilizing simulated biogas (SBG), simulated producer gas (SPG) and SPG-SBG mixtures. For the preparation of SBG, four different ratios of CH_4 and CO_2 are mixed (SBG-1, SBG-2, SBG-3 and SBG-4). Similarly, H_2 and CO are also mixed at four different ratios for the preparation of SPG (SPG-1, SPG-2, SPG-3 and SPG-4). Additionally, H_2 and CO at a ratio of 50:50 is mixed with a four different SBGs to simulate the SPG-SBG mixtures (SG-1, SG-2, SG-3 and SG-4). A newly designed and fabricated gas venturi type air-gaseous fuel mixer was added to the inlet manifold of the base engine setup to work under dual fuel mode. Based on the experimental observation, SBG-4, SPG-4 and SG-4 has been found to give the best results in terms of efficiency and engine emissions. Considering these three gas compositions, the experiments are continued to analyze the impact of compression ratio (CR) and injection timing (IT) on engine performance, combustion and emission characteristics. Experiments at high CR and advancement of IT resulted in reduction of the carbon emission and increase of the engine performance. Final component of the study on-field investigation of dual fuel diesel engine run on mixture of producer gas (PG) and biogas (BG). For continuous supply of gaseous fuels, BG and PG are generated using a field-scale anaerobic digester and a biomass gasifier, respectively utilizing locally available bio resources. BG-PG mixtures are prepared based on flow conditions namely DFM-1, DFM-2, DFM-3 and

DFM-4. Based on the experiments, DFM-3 (i.e. 60° opening of BG) was found to be best compared to rest of the BG-PG mixtures. This was followed by the experiments with varying CR and IT considering DFM-3 and higher CR and advancement of IT provides supplementary benefits in terms of augmenting the engine performance and minimizing the exhaust emission. The important findings of the various components of the present study are presented in the subsequent subsections.

7.1.1 Summary of the experimental study of pilot fuel

The experimental investigation on performance, combustion and emission characteristics of a diesel engine with tri-biodiesel-diesel blends was performed at standard engine operating conditions. Tri-biodiesel-diesel blends, when compared to diesel fuel under similar experimental conditions, exhibited lower BTE and higher BSFC. The maximum BTE of 25.1% and minimum BSFC of 0.339 kg/kWh were obtained with Blend-1 at full engine load. On average, the tri-biodiesel-diesel blends showed a 14.53% lower BTE and a 14.18% higher BSFC compared to diesel. Throughout the entire load range, the blended fuel had an average EGT 5.9% higher and VE 3.67% lower than diesel, with Blend-2 achieving a maximum average VE of 80.59% compared to 82.86% for diesel. At full load, Blend-2 exhibited a maximum rate of pressure rise of 9.02 bar/°CA, slightly lower than the rate of 9.33 bar/°CA for diesel. On average, the rate of pressure rise for the blended fuels was 11.18% lower than that of diesel. The tri-biodiesel-diesel blends displayed an average of 6.42% higher CP compared to diesel, along with shorter ID. In terms of emissions, the blended fuels demonstrated a decrease of 29.7% in CO and 27.33% in HC compared to diesel. However, they resulted in 45.21% higher CO_2 and 15% higher NO_X emissions compared to diesel across the entire load range. In summary, tri-biodiesel-diesel blends exhibited lower BTE, higher BSFC, higher CP, shorter ID, reduced CO and HC emissions compared to diesel fuel.

7.1.2 Summary of DF experiments simulated gaseous fuels

This experimental work explores the parametric impact of gas compositions (SBG, SPG and SPG-SBG mixtures), compression ratio (CR) and pilot fuel injection timing (IT) on the performance, combustion, and emission characteristics of diesel engine under dual fuel (DF) mode. The dual fuel experiments are divided into three phases. The first phase of the experiments involved testing four different combinations of SBGs, SPGs, and SPG-SBG mixtures at five different loads under standard diesel engine operating conditions. Then second phase of the experiments were associated with investigation of the engine parameters using the most effective SBG, SPG, and SPG-SBG mixture, while varying the CR between 16,

17, 17.5, and 18. The last phase of study involved engine experiments with the best compression ratio, while varying the IT between 23-32° BTDC. The key findings are discussed below.

Dual fuel experiments with SBG:

Under full load conditions, the use of various SBGs resulted in lower BTE compared to fossil diesel (FD), with BTE values ranging from 16.42% to 18.96% compared to 27.57% for FD. Maximum BTE was found in case of SBG-4 compared to other SBGs. SBG-4 showed a 41.6% increase in BTE as CR increased from 16 to 18. Moreover, SBG-4 also achieved the maximum BTE of 25.10% and highest PFR of 90.6% at a CR of 18 and 29° BTDC. However, compared to FD, the use of SBGs resulted in increased emission of CO_2. In terms of NO_X emissions, minimum and maximum of 16 ppm to 35 ppm was found for SBG-1 and SBG-4, respectively compared to 125.23 ppm for FD at full load. Again, with the increase of CR and IT, significant rise in NO_X emission was noted for SBG-4. Furthermore, minimum average emission of CO and HC of 348.6 ppm and 320.6 ppm were observed, respectively for SBG-4 considering the complete load range. Again, increase in CR values of 16 to 18, SBG-4 showed an average reduction in CO and HC emissions of 10.51% and 16.13%, respectively. The emission of CO and HC for SBG-4 were further reduced by an average of 11.94% and 8.29% when IT was advanced by 9° CA.

Dual fuel experiments with SPG:

SPG-DF operation also resulted lower BTE than FD for all the operating conditions. At full load, SPG-4 achieved the maximum BTE of 19.05% among all the SPGs. At the same load, for SPG-4 BTE was increased to 20.94% at CR of 18. A maximum BTE and PFR of 25.58% and 87.7% were observed, respectively for SPG-4 at a CR of 18 and 29° BTDC. In case of SPG-DF operation, the emission of CO_2, NO_X, CO and HC was noted be higher compared to FD for complete load range. Increase of CR and advancement of IT, CO_2 and NO_X emission were further increased, however CO and HC emission showed significant reduction. Among all SPGs, minimum average CO emission of 467 ppm and HC emission of 496.2 ppm were observed for SPG-4 for the complete load range. Moreover, SPG-4 demonstrated a slight reduction in CO and HC emission, with a minimum average value of 451.45 ppm and 376.4 ppm at CR of 18. The emission of CO and HC were further reduced by 13.28% and 10.44% on average for SPG-4 when the IT was advanced from 23° to 32° BTDC.

Dual fuel experiments with SPG-SBG mixture:

Among all the SPG-SBG mixtures, the combination of SPG-2/SBG-4, referred to as SG-4 showed the maximum BTE of 20.05%, which increased to 22.11% at a CR of 18 at full load condition. For SG-4, the highest BTE and PFR of 24.44% and 86.41% were observed at CR of 18 and IT of 29° BTDC. In terms of emissions, SG-4 showed lower CO_2 and higher NO_X emissions with a minimum and maximum average of 6.06% and 52.65 ppm, respectively compared to the other SPG-SBG combinations. There was an average increment of 18.25% and 44.54% in CO_2 and NO_X emissions for SG-4 as CR was increased from 16 to 18. On the other hand, SG-4 showed a reduction in CO and HC emissions compared to other combinations. The average CO and HC emission were decreased by 11.16% and 20.07% as CR increased from 16 to 18. In addition to that a further average CO and HC emission reduction of 11.01% and 7.58% were achieved when the IT was advanced from 23° to 32° BTDC.

7.1.3 Summary of DF experiments with raw biogas and producer gas mixture

Among the various BG-PG mixtures tested, DFM-3 (70% BG opening and 30% PG opening) showed promising results in terms of efficiency, fuel consumption and engine exhaust emissions. At 100% load, CR of 17.5, and IT of 23° BTDC, DFM-3 achieved the highest BTE of 18.39%, greater than the other mixtures. Compared to raw BG and PG, DFM-3 demonstrated a 0.41% and 1.9% higher BTE, respectively, at the same operating conditions. A significant 23.62% increment in BTE for DFM-3 was observed with increasing the CR from 16 to 18. At full load, combination of CR of 18 and IT of 29° BTDC resulted in maximum BTE of 23.28%. DFM-3 also exhibited notable reductions of 26.6% and 62.7% in both BGFR and PGFR, respectively at full load condition compared to raw BG and PG DF operations. Additionally, DFM-3 showed reductions in BGFR and PGFR with the increase of CR and advancement of IT. The PFR for DFM-3 was also increased to 88.81% at CR of 18 and at 100% load. Again, at same load and CR, IT of 29° BTDC resulted in maximum PFR of 90.22% for DFM-3 was observed. In terms of emissions, DFM-3 showed the lowest CO_2 and NO_X emission of 7.86% and 63.49 ppm, respectively among the BG-PG mixtures. For the complete load range, minimum average CO and HC emission of 284.5 ppm and 200.2 ppm were obtained, respectively for DFM-3. The average CO and HC emission for DFM-3 were further reduced to 276.64 ppm and 184.28 ppm, respectively at CR of 18. In addition to that, at combination of CR of 18 and IT of 29° BTDC, DFM-3 resulted in minimum average CO and HC emission of 267.21 ppm and 175.31 ppm, respectively.

Based on the comprehensive investigation in this study, it can be concluded that the methodology and findings could be utilized sustainably for rural or remote power generation taking into account the availability of resources. The developed technology can be effectively applied to generate power at different scale according to the specific electricity demand.

Table 7.1 Summary of performance and emission characteristic of the dual fuel diesel engine run with different gaseous fuel

Primary fuel	IT (BTDC)	CR	BTE (%)	PFR (%)	Emission			
					CO_2 (%)	CO (ppm)	HC (ppm)	NO_X (ppm)
SBG-4	29°	18	25.1	90.59	9.86	320.65	310.01	43.97
SPG-4	29°	18	25.58	87.77	9.20	422.40	329.55	268.36
SG-4	29°	18	24.44	86.41	7.86	359.94	334.47	119.49
DFM-3	29°	18	23.27	90.21	6.73	268.34	168.8	103.13

7.2 Scope for future work

In the present study, a detailed experimental investigation has been conducted with clean gaseous fuels with an objective to enhance the performance and emission characteristics of a dual fuel diesel engine. The important finding of the current investigation have already been discussed in the section 7.1. However, it is possible to augment the performance, combustion and emission characteristics of a dual fuel diesel engine running on biogas and producer gas through further improvements. To address current challenges, it is imperative to conduct further research on novel technologies that promote sustainable and cost-effective utilization of these fuels. In this connection, some scope and suggestions for future studies are highlighted here.

- In the current study, experiments were conducted with raw biogas and producer gas. For biogas, the focus should be on purification process of biogas, which increases energy content and enables its efficient utilization in diesel engines. Research efforts should be directed towards investigating an economical and efficient production pathway for H_2-enrichment of biogas, which can contribute to the future hydrogen economy. Achieving the optimal biogas enrichment level may have potential benefits for the engine characteristics when operating in DF mode.
- Similarly for producer gas, a comprehensive experimentation of the impact of varying producer gas composition in DF diesel engine is a challenge which presents a significant research opportunity in this domain. Because, H_2% in PG profoundly affects the combustion phenomenon of producer gas run DF engine.

- In was evident from the experiments that at lower loads, DF operations exhibited a significant decrease in efficiency compared to the diesel mode. The reason for this is the inadequate combustion of gaseous fuel with a high self-ignition temperature in the low-temperature range. The increase in pilot fuel injection pressure (IP) is a viable approach to tackle the issues of poor combustion at medium and low loads. Effect of pilot fuel IP in DF diesel engine operation provides a huge scope of research.
- In the current study, all the DF experiments were conducted well in short-term tests. However, potential issues may arise when these engines operate on a commercial scale for extended periods. Furthermore, there is no particular literature available that specifically examines the long-term impacts of using biogas and producer gas in DF diesel engines, with a focus on corrosion of engine components, engine part wear, engine lubrication and carbon deposition. Thus, to establish the viability of utilizing biogas and producer gas in diesel engines in DF mode as an effective technology, it is crucial to conduct long-term dual fuel tests on these fuels.
- The present study involves the parametric investigation a DF diesel engine. However, to augment the engine performance characteristics and reduce the pollutant emission, optimization of engine operating parameters are of paramount important. In majority of the published literatures, overall engine performance were assessed by changing only one parameter at a time. Hence, assessment with multiple variables could be a useful approach to fully comprehend the features of the DF engine.
- Numerical models for simulating the combustion process of dual fuel engines running on biogas and producer gas is a challenge. The utilization of zero, two, or three-dimensional modeling can be employed to analyze the impact of DF combustion under different engine load conditions. Additionally, different software programs such as ANSYS, CHEMKIN PRO etc. can be utilized to predict the combustion parameters like ignition delay, combustion temperature, heat release rate, combustion duration etc. This approach would enable the optimization of extensive experimentation, resulting in significant savings in time, effort, and expenses.

REFERENCES

[1] Percy AJ, Edwin M. Studies on the performance and emission characteristics of a dual fuel VCR engine using producer gas as secondary fuel: An optimization approach using response surface methodology. Energy 2023;263:125685. doi:10.1016/j.energy.2022.125685.

[2] Khan D, Goga G. Evaluation of emission characteristics & performance of a biogas- biodiesel dual fuel engine using blends of butanol in different ratios. Mater Today Proc 2023. doi:10.1016/j.matpr.2022.11.452.

[3] Kumar Singh D, Raj R, Tirkey JV. Performance and emission analysis of triple fuelled CI engine utilizing producer gas, biodiesel and diesel: An optimization study using response surface methodology. Therm Sci Eng Prog 2022;36:101486. doi:10.1016/j.tsep.2022.101486.

[4] Halewadimath SS, Banapurmath NR, Yaliwal VS, Prasad MG, Jalihal SS, Soudagar MEM, et al. Effect of manifold injection of hydrogen gas in producer gas and neem biodiesel fueled CRDI dual fuel engine. Int J Hydrogen Energy 2022;47:25913–28. doi:10.1016/j.ijhydene.2022.02.135.

[5] Omer AM. Energy, environment and sustainable development. Renew Sustain Energy Rev 2008;12:2265–300. doi:10.1016/j.rser.2007.05.001.

[6] International Energy Agency. CO2 Emissions from Fuel Combustion 2019. Paris: 2019. doi:https://doi.org/10.1787/2a701673-en.

[7] International Energy Agency. CO2 Emissions in 2022. 2022.

[8] International Energy Agency. World Energy Outlook. 2018.

[9] Singh H, Mohapatra SK. Production of producer gas from sugarcane bagasse and carpentry waste and its sustainable use in a dual fuel CI engine: A performance, emission, and noise investigation. J Energy Inst 2016:1–12. doi:10.1016/j.joei.2016.11.002.

[10] Faria MMN de, Vargas Machuca Bueno JP, Ayad SMME, Belchior CRP. Thermodynamic simulation model for predicting the performance of spark ignition engines using biogas as fuel. Energy Convers Manag 2017;149:1096–108. doi:10.1016/j.enconman.2017.06.045.

[11] International Energy Agency (IEA). Renewable electricity 2022. https://www.iea.org/reports/renewable-electricity (accessed May 11, 2023).

[12] Alam M, Bhattacharyya S. Are the off-grid customers ready to pay for electricity from the decentralized renewable hybrid mini-grids? A study of willingness to pay in rural Bangladesh. Energy 2017;139:433–46. doi:10.1016/j.energy.2017.07.125.

[13] Bhattacharyya SC, Palit D. A critical review of literature on the nexus between central grid and off-grid solutions for expanding access to electricity in Sub-Saharan Africa and South Asia. Renew Sustain Energy Rev 2021;141:110792. doi:10.1016/j.rser.2021.110792.

[14] Palit D, Kumar A. Drivers and barriers to rural electrification in India – A multi- stakeholder analysis. Renew Sustain Energy Rev 2022;166:112663. doi:10.1016/j.rser.2022.112663.

[15] Palit D, Chaurey A. Off-grid rural electrification experiences from South Asia: Status and best practices. Energy Sustain Dev 2011;15:266–76. doi:10.1016/j.esd.2011.07.004.

[16] Okunlola A, Jacobs D, Nage L, Helgenberger S, Hakhu A, Kovac S. Secure and reliable electricity access with renewable energy mini-grids in rural India. Postdam, Germany: 2019. doi:DOI: 10.2312/iass.2019.020.

[17] Das S, Kashyap D, Kalita P, Kulkarni V, Itaya Y. Clean gaseous fuel application in diesel engine: A sustainable option for rural electrification in India. Renew Sustain Energy Rev 2020;117:109485. doi:10.1016/j.rser.2019.109485.

[18] Mohammed YS, Mustafa MW, Bashir N. Hybrid renewable energy systems for off-grid electric power: Review of substantial issues. Renew Sustain Energy Rev 2014;35:527–39.

doi:10.1016/j.rser.2014.04.022.

[19] Bazmi AA, Zahedi G, Hashim H. Progress and challenges in utilization of palm oil biomass as fuel for decentralized electricity generation. Renew Sustain Energy Rev 2011;15:574–83. doi:10.1016/j.rser.2010.09.031.

[20] Schäfer M, Kebir N, Neumann K. Research needs for meeting the challenge of decentralized energy supply in developing countries. Energy Sustain Dev 2011;15:324–9. doi:10.1016/j.esd.2011.07.001.

[21] Ruiz JA, Juárez MC, Morales MP, Muñoz P, Mendívil MA. Biomass gasification for electricity generation: Review of current technology barriers. Renew Sustain Energy Rev 2013;18:174–83. doi:10.1016/j.rser.2012.10.021.

[22] Veláquez SMSG, Moreira JR, Santos SA, Coelho ST. Electric power generation in isolated communities in the Amazon region: A perspective for sustainable development. 2011 Int. Conf. Electr. Control Eng. ICECE 2011 - Proc., 2011, p. 5254–7. doi:10.1109/ICECENG.2011.6058478.

[23] Smith A, Davies H. A review of the history of emission legislation, urban and national transport trends and their impact on transport emissions. Trans Built Environ 1996;23:1–3.

[24] Alalwan HA, Alminshid AH, Aljaafari HAS. Promising evolution of biofuel generations. Subject review. Renew Energy Focus 2019;28:127–39. doi:10.1016/j.ref.2018.12.006.

[25] Vijay V, Subbarao PMV, Chandra R. An evaluation on energy self–sufficiency model of a rural cluster through utilization of biomass residue resources: A case study in India. Energy Clim Chang 2021;2:100036. doi:10.1016/j.egycc.2021.100036.

[26] Bisht AS, Thakur NS. Small scale biomass gasification plants for electricity generation in India: Resources, installation, technical aspects, sustainability criteria & policy. Renew Energy Focus 2019;28:112–26. doi:10.1016/j.ref.2018.12.004.

[27] Karim GA. Dual-fuel diesel engine. 1st editio. London: CRC press; 2015.

[28] Pirker G, Wimmer A. Sustainable power generation with large gas engines. Energy Convers Manag 2017;149:1048–65. doi:10.1016/j.enconman.2017.06.023.

[29] Das S, Kashyap D, Bora BJ, Kalita P, Kulkarni V. Thermo-economic optimization of a biogas-diesel dual fuel engine as remote power generating unit using response surface methodology. Therm Sci Eng Prog 2021;24:100935. doi:10.1016/j.tsep.2021.100935.

[30] Kashyap D, Das S, Kalita P. Exploring the efficiency and pollutant emission of a dual fuel CI engine using biodiesel and producer gas : An optimization approach using response surface methodology. Sci Total Environ 2021;773:145633. doi:10.1016/j.scitotenv.2021.145633.

[31] Wei L, Geng P. A review on natural gas/diesel dual fuel combustion, emissions and performance. Fuel Process Technol 2016;142:264–78. doi:10.1016/j.fuproc.2015.09.018.

[32] Geng P, Cao E, Tan Q, Wei L. Effects of alternative fuels on the combustion characteristics and emission products from diesel engines: A review. Renew Sustain Energy Rev 2017;71:523–34. doi:10.1016/j.rser.2016.12.080.

[33] Bora BJ, Saha UK. Estimating the Theoretical Performance Limits of a Biogas Powered Dual Fuel Diesel Engine Using Emulsified Rice Bran Biodiesel as Pilot Fuel. ASME J Energy Resour Technol 2016;138:1–10. doi:10.1115/1.4031836.

[34] Yaliwal VS, Nataraja KM, Banapurmath NR, Tewari PG. Honge oil methyl ester and producer gas-fuelled dual-fuel engine operated with varying compression ratios. Int J Sustain Eng 2014;7:330–40. doi:10.1080/19397038.2013.837108.

[35] Bora BJ, Saha UK. Improving the Performance of a Biogas Powered Dual Fuel Diesel Engine Using Emulsified Rice Bran Biodiesel as Pilot Fuel Through Adjustment of Compression Ratio and Injection Timing. ASME J Eng Gas Turbines Power 2015;137:091505. doi:10.1115/1.4029708.

[36] Rosha P, Dhir A, Mohapatra SK. Influence of gaseous fuel induction on the various engine

characteristics of a dual fuel compression ignition engine: A review. Renew Sustain Energy Rev 2018;82:3333–49. doi:10.1016/j.rser.2017.10.055.

[37] Yilmaz IT, Gumus M. Investigation of the effect of biogas on combustion and emissions of TBC diesel engine. Fuel 2017;188:69–78. doi:10.1016/j.fuel.2016.10.034.

[38] Sahoo BB, Saha UK, Sahoo N. Theoretical performance limits of a syngas-diesel fueled compression ignition engine from second law analysis. Energy 2011;36:760–9. doi:10.1016/j.energy.2010.12.045.

[39] McKendry P. Energy production from biomass (part 2): conversion technologies. Bioresour Technol 2002;83:47–54. doi:Pii S0960-8524(01)00119-5\rDoi 10.1016/S0960-8524(01)00119-5.

[40] Yaliwal VS, Banapurmath NR, Gireesh NM, Tewari PG. Production and utilization of renewable and sustainable gaseous fuel for power generation applications: A review of literature. Renew Sustain Energy Rev 2014;34:608–27. doi:10.1016/j.rser.2014.03.043.

[41] Arena U, Di Gregorio F, Santonastasi M. A techno-economic comparison between two design configurations for a small scale, biomass-to-energy gasification based system. Chem Eng J 2010;162:580–90. doi:10.1016/j.cej.2010.05.067.

[42] Sakthivel R, Ramesh K, Purnachandran R, Mohamed Shameer P. A review on the properties, performance and emission aspects of the third generation biodiesels. Renew Sustain Energy Rev 2018;82:2970–92. doi:10.1016/j.rser.2017.10.037.

[43] P.Tamilselvan, N.Nallusamy, S.Rajkumarb. A comprehensive review on performance, combustion and emission characteristics of biodiesel fuelled diesel engines. Renew Sustain Energy Rev 2017;79:1134–59.

[44] Ramalingam S, Rajendran S, Ganesan P, Govindasamy M. Effect of operating parameters and antioxidant additives with biodiesels to improve the performance and reducing the emissions in a compression ignition engine – A review. Renew Sustain Energy Rev 2018;81:775–88. doi:10.1016/j.rser.2017.08.026.

[45] Sarin A, Arora R, Singh NP, Sarin R, Malhotra RK, Kundu K. Effect of blends of Palm-Jatropha-Pongamia biodiesels on cloud point and pour point. Energy 2009;34:2016–21. doi:10.1016/j.energy.2009.08.017.

[46] Aklouche FZ, Loubar K, Bentebbiche A, Awad S, Tazerout M. Experimental investigation of the equivalence ratio influence on combustion, performance and exhaust emissions of a dual fuel diesel engine operating on synthetic biogas fuel. Energy Convers Manag 2017;152:291–9. doi:10.1016/j.enconman.2017.09.050.

[47] Tippayawong N, Promwungkwa A, Rerkkriangkrai P. Long-term operation of a small biogas/diesel dual-fuel engine for on-farm electricity generation. Biosyst Eng 2007;98:26–32. doi:10.1016/j.biosystemseng.2007.06.013.

[48] Duc PM, Wattanavichien K. Study on biogas premixed charge diesel dual fuelled engine. Energy Convers Manag 2007;48:2286–308. doi:10.1016/j.enconman.2007.03.020.

[49] Makareviciene V, Sendzikiene E, Pukalskas SP, Rimkus A, Vegneris R. Performance and Emission Characteristics of Biogas used in Diesel Engine Operation. Energy Convers Manag 2013;75:224–33. doi:10.1016/j.enconman.2013.06.012.

[50] Burea of Indian Standards. IS 16087 (2013): Biogas (Biomethane) - Specification. New Delhi: 2013.

[51] Sridhar G, Sridhar H V., Dasappa S, Paul PJ, Rajan NKS, Mukunda HS. Development of producer gas engines. Proc Inst Mech Eng Part D J Automob Eng 2005;219:423–38. doi:10.1243/095440705X6596.

[52] Shrivastava V, Jha AK, Wamankar AK, Murugan S. Performance and emission studies of a CI engine coupled with gasifier running in dual fuel mode. Procedia Eng 2013;51:600–8. doi:10.1016/j.proeng.2013.01.085.

[53] Mohon Roy M, Tomita E, Kawahara N, Harada Y, Sakane A. Performance and emission comparison of a supercharged dual-fuel engine fueled by producer gases with varying hydrogen content. Int J Hydrogen Energy 2009;34:7811–22. doi:10.1016/j.ijhydene.2009.07.056.

[54] Sridhar G, Paul PJ, Mukunda HS. Biomass derived producer gas as a reciprocating engine fuel - An experimental analysis. Biomass and Bioenergy 2001;21:61–72. doi:10.1016/S0961-9534(01)00014-9.

[55] Martínez JD, Mahkamov K, Andrade R V., Silva Lora EE. Syngas production in downdraft biomass gasifiers and its application using internal combustion engines. Renew Energy 2012;38:1–9. doi:10.1016/j.renene.2011.07.035.

[56] Banapurmath NR, Tewari PG. Comparative performance studies of a 4-stroke CI engine operated on dual fuel mode with producer gas and Honge oil and its methyl ester (HOME) with and without carburetor. Renew Energy 2009;34:1009–15. doi:10.1016/j.renene.2008.08.005.

[57] Arunachalam A, Olsen DB. Experimental evaluation of knock characteristics of producer gas. Biomass and Bioenergy 2012;37:169–76. doi:10.1016/j.biombioe.2011.12.016.

[58] Cotana F, Vittori S, Marseglia G, Medaglia CM, Coccia V, Petrozzi A, et al. Pollutant emissions of a biomass gasifier inside a multifuel energy plant. Atmos Pollut Res 2019;10:2000–9. doi:10.1016/j.apr.2019.09.007.

[59] Marseglia G, Medaglia CM. Energy efficiency in gasoline direct injection engines. WIT Trans Built Environ 2019;182:85–91. doi:10.2495/UT180081.

[60] Azimov U, Tomita E, Kawahara N, Harada Y. Effect of syngas composition on combustion and exhaust emission characteristics in a pilot-ignited dual-fuel engine operated in PREMIER combustion mode. Int J Hydrogen Energy 2011;36:11985–96. doi:10.1016/j.ijhydene.2011.04.192.

[61] Sahoo BB, Saha UK, Sahoo N. Effect of load level on the performance of a dual fuel compression ignition engine operating on syngas fuels with varying H2/CO content. J Eng Gas Turbines Power 2011;133:1–12. doi:10.1115/1.4003956.

[62] Sahoo BB, Sahoo N, Saha UK. Effect of H2:CO ratio in syngas on the performance of a dual fuel diesel engine operation. Appl Therm Eng 2012;49:139–46. doi:10.1016/j.applthermaleng.2011.08.021.

[63] Dhole AE, Yarasu RB, Lata DB, Priyam A. Effect on performance and emissions of a dual fuel diesel engine using hydrogen and producer gas as secondary fuels. Int J Hydrogen Energy 2014;39:8087–97. doi:10.1016/j.ijhydene.2014.03.085.

[64] CPCB. Status of the Vehicular Pollution Control Programme in India. Delhi: 2010.

[65] CPCB. Vehicular Exhaust n.d. https://cpcb.nic.in/vehicular-exhaust/ (accessed March 11, 2023).

[66] Heywood JB. Internal Combustion Engine Fundamentals. New York, USA: McGraw-Hill Book; 1988.

[67] Pundir B. IC Engines Combustion and Emissions. New Delhi, India: Narosa Publishing House Private Limited; 2010.

[68] Stone R. Introduction to Internal Combustion Engines. Third. New York: Palgrave Macmillan; 1999.

[69] Pulkrabek WW. Engineering fundamentals of the internal combustion engine. Second. New Jersey: Pearson Education Limited; 2003.

[70] Sonntag RE, Wylen GJ van. Introduction to Thermodynamics. Third. New York: John Willey and Sons; 1991.

[71] Kassa M, Hall C. Dual-Fuel Combustion. In: Carlucci AP, editor. Futur. Intern. Combust. Engines, Intech Open; 2019, p. 1–17. doi:DOI: http://dx.doi.org/10.5772/intechopen.80570 Dual-fuel.

[72] Sahoo BB, Sahoo N, Saha UK. Effect of engine parameters and type of gaseous fuel on the

performance of dual-fuel gas diesel engines-A critical review. Renew Sustain Energy Rev 2009;13:1151–84. doi:10.1016/j.rser.2008.08.003.

[73] Sarkar A. Role of global fuel-air equivalence ratio and intake charge preheating in dual fuel diesel engines run on biogas and blended oxygenated pilot fuels. Indian Institute of Technology Guwahati, 2018.

[74] Barik D, Sivalingam M. Performance and Emission Characteristics of a Biogas Fueled DI Diesel Engine. SAE Int 2013. doi:10.4271/2013-01-2507.

[75] Yoon SH, Lee CS. Experimental investigation on the combustion and exhaust emission characteristics of biogas-biodiesel dual-fuel combustion in a CI engine. Fuel Process Technol 2011;92:992–1000. doi:10.1016/j.fuproc.2010.12.021.

[76] Ramadhas AS, Jayaraj S, Muraleedharan C. Power generation using coir-pith and wood derived producer gas in diesel engines. Fuel Process Technol 2006;87:849–53. doi:10.1016/j.fuproc.2005.06.003.

[77] Deva Kumar MLS, Reddy VK. Effect of fuel injection pressure on full load performance of diesel-producer gas. Indian J Sci Technol 2010;3:1056–61.

[78] Sombatwong P, Thaiyasuit P, Pianthong K. Effect of pilot fuel quantity on the performance and emission of a dual producer gas - Diesel engine. Energy Procedia 2013;34:218–27. doi:10.1016/j.egypro.2013.06.750.

[79] Masood M, Ishrat MM. Computer simulation of hydrogen-diesel dual fuel exhaust gas emissions with experimental verification. Fuel 2008;87:1372–8. doi:10.1016/j.fuel.2007.07.001.

[80] Yilmaz IT, Demir A, Gumus M. Effects of hydrogen enrichment on combustion characteristics of a CI engine. Int J Hydrogen Energy 2017;42:10536–46. doi:10.1016/j.ijhydene.2017.01.214.

[81] Sharma P, Dhar A. Compression ratio influence on combustion and emissions characteristic of hydrogen diesel dual fuel CI engine: Numerical Study. Fuel 2018;222:852–8. doi:10.1016/j.fuel.2018.02.108.

[82] Raihan MS, Guerry ES, Dwivedi U, Srinivasan KK, Krishnan SR. Experimental Analysis of Diesel-Ignited Methane Dual-Fuel Low-Temperature Combustion in a Single-Cylinder Diesel Engine. J Energy Eng 2015;141:1–13. doi:10.1061/(asce)ey.1943-7897.0000235.

[83] Guerry ES, Raihan MS, Srinivasan KK, Krishnan SR, Sohail A. Injection timing effects on partially premixed diesel-methane dual fuel low temperature combustion. Appl Energy 2016;162:99–113. doi:10.1016/j.apenergy.2015.10.085.

[84] Belgiorno G, Di Blasio G, Beatrice C. Parametric study and optimization of the main engine calibration parameters and compression ratio of a methane-diesel dual fuel engine. Fuel 2018;222:821–40. doi:10.1016/j.fuel.2018.02.038.

[85] Ahmad Z, Kaario O, Karimkashi S, Qiang C, Vuorinen V, Larmi M. Effects of ethane addition on diesel-methane dual-fuel combustion in a heavy-duty engine. Fuel 2021;289:119834. doi:10.1016/j.fuel.2020.119834.

[86] Wei L, Geng P. A review on natural gas/diesel dual fuel combustion, emissions and performance. Fuel Process Technol 2016;142:264–78. doi:10.1016/j.fuproc.2015.09.018.

[87] Kakaee AH, Rahnama P, Paykani A. Influence of fuel composition on combustion and emissions characteristics of natural gas/diesel RCCI engine. J Nat Gas Sci Eng 2015;25:58–65. doi:10.1016/j.jngse.2015.04.020.

[88] Esfahanian V, Salahi MM, Gharehghani A, Mirsalim M. Extending the lean operating range of a premixed charged compression ignition natural gas engine using a pre-chamber. Energy 2017;119:1181–94. doi:10.1016/j.energy.2016.11.071.

[89] Meng X, Tian H, Long W, Zhou Y, Bi M, Tian J, et al. Experimental study of using additive in the pilot fuel on the performance and emission trade-offs in the diesel/CNG (methane

emulated)dual-fuel combustion mode. Appl Therm Eng 2019;157:113718. doi:10.1016/j.applthermaleng.2019.113718.

[90] Liu J, Yang F, Wang H, Ouyang M, Hao S. Effects of pilot fuel quantity on the emissions characteristics of a CNG/diesel dual fuel engine with optimized pilot injection timing. Appl Energy 2013;110:201–6. doi:10.1016/j.apenergy.2013.03.024.

[91] Saleh HE. Effect of variation in LPG composition on emissions and performance in a dual fuel diesel engine. Fuel 2008;87:3031–9. doi:10.1016/j.fuel.2008.04.007.

[92] Kumaraswamy A, Prasad BD. Performance analysis of a dual fuel engine using LPG and diesel with EGR system. Procedia Eng 2012;38:2784–92. doi:10.1016/j.proeng.2012.06.326.

[93] Musthafa MM. A comparative study on coated and uncoated diesel engine performance and emissions running on dual fuel (LPG – biodiesel) with and without additive. Ind Crops Prod 2019;128:194–8. doi:10.1016/j.indcrop.2018.11.012.

[94] Pattanaik BP, Nayak C, Nanda BK. Investigation on utilization of biogas & Karanja oil biodiesel in dual fuel mode in a single cylinder DI diesel engine. Int J Energy Environ 2013;4:279–90.

[95] Luijten CCM, Kerkhof E. Jatropha oil and biogas in a dual fuel CI engine for rural electrification. Energy Convers Manag 2011;52:1426–38. doi:10.1016/j.enconman.2010.10.005.

[96] Ramesha DK, Bangari AS, Rathod CP, Samartha CR. Experimental Investigation Of Biogas-Biodiesel Dual Fuel Combustion In A Diesel Engine. J Middle Eur Constr Des Cars 2015;13:12–20. doi:10.1515/mecdc-2015-0003.

[97] Singh RN, SIngh SP, Pathak BS. Extent of replacement of methyl ester of rice bran oil by producer gas in CI engine. Int J Energy Res 2007;31:1545–55. doi:10.1002/er.1311.

[98] Raheman H, Padhee D. Combustion characteristics of diesel engine using producer gas and blends of Jatropha methyl ester with diesel in mixed fuel mode. Int J Renew Energy Dev 2014;3:228–35. doi:10.14710/ijred.3.3.228-235.

[99] Nayak SK, Mishra PC. Analysis of a diesel engine fuelled with jojoba blend and coir pith producer gas. Int J Automot Mech Eng 2017;14:4675–89. doi:10.15282/ijame.14.4.2017.7.0368.

[100] Ganesan V. Internal Combustion Engines. 4th editio. New Delhi: McGraw Hill Education (India) Private Limited; 2016.

[101] Qian Y, Sun S, Ju D, Shan X, Lu X. Review of the state-of-the-art of biogas combustion mechanisms and applications in internal combustion engines. Renew Sustain Energy Rev 2017;69:50–8. doi:10.1016/j.rser.2016.11.059.

[102] Lounici MS, Loubar K, Tazerout M, Balistrou M, Tarabet L. Experimental Investigation on the Performance and Exhaust Emission of Biogas-Diesel Dual-Fuel Combustion in a CI Engine. SAE Int 2014. doi:10.4271/2014-01-2689.

[103] Crookes RJ. Comparative bio-fuel performance in internal combustion engines. Biomass and Bioenergy 2006;30:461–8. doi:10.1016/j.biombioe.2005.11.022.

[104] Cheng-qiu J, Tian-wei L, Jian-li Z. A study on compressed biogas and its application to the compression ignition dual-fuel engine. Biomass 1989;20:53–9. doi:10.1016/0144-4565(89)90020-6.

[105] Barik D, Murugan S, Sivaram NM, Baburaj E, Sundaram PS. Experimental investigation on the behavior of a direct injection diesel engine fueled with Karanja methyl ester-biogas dual fuel at different injection timings. Energy 2017;118:127–38. doi:10.1016/j.energy.2016.12.025.

[106] Barik D, Murugan S. Experimental investigation on the behavior of a DI diesel engine fueled with raw biogas–diesel dual fuel at different injection timing. J Energy Inst 2016;89:373–88. doi:10.1016/j.joei.2015.03.002.

[107] Barik D, Murugan S. Investigation on combustion performance and emission characteristics of a DI (direct injection) diesel engine fueled with biogas-diesel in dual fuel mode. Energy 2014;72:760–71. doi:10.1016/j.energy.2014.05.106.

[108] Bedoya ID, Arrieta AA, Cadavid FJ. Effects of mixing system and pilot fuel quality on diesel-biogas dual fuel engine performance. Bioresour Technol 2009;100:6624–9. doi:10.1016/j.biortech.2009.07.052.

[109] Cacua K, Amell A, Cadavid F. Effects of oxygen enriched air on the operation and performance of a diesel-biogas dual fuel engine. Biomass and Bioenergy 2012;45:159–67. doi:10.1016/j.biombioe.2012.06.003.

[110] Barik D, Murugan S, Samal S, Sivaram NM. Combined effect of compression ratio and diethyl ether (DEE) port injection on performance and emission characteristics of a DI diesel engine fueled with upgraded biogas (UBG)-biodiesel dual fuel. Fuel 2017;209:339–49. doi:10.1016/j.fuel.2017.08.015.

[111] Ramesha DK, Bangari AS, Rathod CP, Samartha Chaitanya R. Combustion, performance and emissions characteristics of a biogas fuelled diesel engine with fish biodiesel as pilot fuel. Biofuels 2015;6:9–19. doi:10.1080/17597269.2015.1036960.

[112] Bora BJ, Saha UK. Experimental evaluation of a rice bran biodiesel - biogas run dual fuel diesel engine at varying compression ratios. Renew Energy 2016;87:782–90. doi:10.1016/j.renene.2015.11.002.

[113] Verma S, Das LM, Bhatti SS, Kaushik SC. A comparative exergetic performance and emission analysis of pilot diesel dual-fuel engine with biogas, CNG and hydrogen as main fuels. Energy Convers Manag 2017;151:764–77. doi:10.1016/j.enconman.2017.09.035.

[114] Bora BJ, Saha UK, Chatterjee S, Veer V. Effect of compression ratio on performance, combustion and emission characteristics of a dual fuel diesel engine run on raw biogas. Energy Convers Manag 2014;87:1000–9. doi:10.1016/j.enconman.2014.07.080.

[115] Barik D, Murugan S. Experimental investigation on the behavior of a DI diesel engine fueled with raw biogas - diesel dual fuel at different injection timing. J Energy Inst 2016;89:373–88. doi:10.1016/j.joei.2015.03.002.

[116] Sarkar A, Saha UK. Role of global fuel-air equivalence ratio and preheating on the behaviour of a biogas driven dual fuel diesel engine. Fuel 2018;232:743–54. doi:10.1016/j.fuel.2018.06.016.

[117] Barik D, Murugan S. Investigation on combustion performance and emission characteristics of a DI (direct injection) diesel engine fueled with biogas-diesel in dual fuel mode. Energy 2014;72:760–71. doi:10.1016/j.energy.2014.05.106.

[118] Bora BJ, Saha UK. Comparative assessment of a biogas run dual fuel diesel engine with rice bran oil methyl ester, pongamia oil methyl ester and palm oil methyl ester as pilot fuels. Renew Energy 2015;81:490–8. doi:10.1016/j.renene.2015.03.019.

[119] Barik D, Murugan S. Effects of diethyl ether (DEE) injection on combustion performance and emission characteristics of Karanja methyl ester (KME)-biogas fueled dual fuel diesel engine. Fuel 2016;164:286–96. doi:10.1016/j.fuel.2015.09.094.

[120] Verma VS, Bora BJ, Sarkar A, Saha UK. Experimental Investigation of a dual fuel diesel engine run on scrubbed biogas using the method of adsorption. 12th Bienn. Conf. Eng. Syst. Des. Anal., Copenhagen, Denmark: ASME; 2014, p. 1–9.

[121] Sarkar A, Saha UK. Impact of intake charge preheating on a biogas run dual fuel diesel engine using ternary blends of diesel-biodiesel-ethanol (Paper accepted). J Energy Eng 2018;144. doi:10.1061/(ASCE)EY.1943-7897.0000548.

[122] Agarwal AK, Srivastava DK, Dhar A, Maurya RK, Shukla PC, Singh AP. Effect of fuel injection timing and pressure on combustion, emissions and performance characteristics of a single cylinder diesel engine. Fuel 2013;111:374–83. doi:10.1016/j.fuel.2013.03.016.

[123] Barik D, Murugan S. Simultaneous reduction of NOxand smoke in a dual fuel di diesel engine. Energy Convers Manag 2014;84:217–26. doi:10.1016/j.enconman.2014.04.042.

[124] Murugan S, Ramaswamy MC, Nagarajan G. Assessment of pyrolysis oil as an energy source for

diesel engines. Fuel Process Technol 2009;90:67–74. doi:10.1016/j.fuproc.2008.07.017.

[125] Hansdah D, Murugan S. Bioethanol fumigation in a di diesel engine. Fuel 2014;130:324–33. doi:10.1016/j.fuel.2014.04.047.

[126] Barik D, Satapathy AK, Murugan S. Combustion analysis of the diesel–biogas dual fuel direct injection diesel engine–the gas diesel engine. Int J Ambient Energy 2017;38:259–66. doi:10.1080/01430750.2015.1086681.

[127] Anand K, Sharma RP, Mehta PS. Experimental investigations on combustion, performance and emissions characteristics of neat karanji biodiesel and its methanol blend in a diesel engine. Biomass and Bioenergy 2011;35:533–41. doi:10.1016/j.biombioe.2010.10.005.

[128] Ryu K. Effects of pilot injection timing on the combustion and emissions characteristics in a diesel engine using biodiesel – CNG dual fuel. Appl Energy 2013;111:721–30. doi:10.1016/j.apenergy.2013.05.046.

[129] Nwafor OMI. Effect of advanced injection timing on emission characteristics of a diesel engine running on biofuel. Int J Ambient Energy 2004;25:115–22. doi:10.1080/01430750.2004.9674950.

[130] Donateo T, Tornese F, Laforgia D. Computer-aided conversion of an engine from diesel to methane. Appl Energy 2013;108:8–23. doi:10.1016/j.apenergy.2013.03.002.

[131] Karim GA. Combustion in Gas Fueled Compression: Ignition Engines of the Dual Fuel Type. J Eng Gas Turbines Power 2003;125:827. doi:10.1115/1.1581894.

[132] Mustafi NN, Raine RR, Verhelst S. Combustion and emissions characteristics of a dual fuel engine operated on alternative gaseous fuels. Fuel 2013;109:669–78. doi:10.1016/j.fuel.2013.03.007.

[133] Kuo KK. Principal of Combustion. 2nd editio. New York: John Willey and Sons; 2005.

[134] Heywood JB. Internal Combustion Engines Fundamentals. New York: McGraw-Hill; 1988.

[135] Sun J, Caton JA, Jacobs TJ. Oxides of nitrogen emissions from biodiesel-fuelled diesel engines. Prog Energy Combust Sci 2010;36:677–95. doi:10.1016/j.pecs.2010.02.004.

[136] Fernando S, Hall C, Jha S. NO x Reduction from Biodiesel Fuels. Energy & Fuels 2006;20:376–82. doi:10.1021/ef050202m.

[137] Bowman CT. Destruction in Combustion. Prog Energy Combust Sci 1975;1:33–45.

[138] Inc. F. Prompt NOx formation n.d. http://jullio.pe.kr/fluent6.1/help/html/ug/node625.htm (accessed September 10, 2018).

[139] Kalsi SS, Subramanian KA. Effect of simulated biogas on performance, combustion and emissions characteristics of a bio-diesel fueled diesel engine. Renew Energy 2017;106:78–90. doi:10.1016/j.renene.2017.01.006.

[140] Karim GA. A Review of Combustion Processes in the Dual Fuel Engine - The Gas Diesel Engine. Prog Energy Combust Sci 1980;6:277–85. doi:10.1016/0360-1285(80)90019-2.

[141] Papagiannakis RG, Hountalas DT, Rakopoulos CD. Theoretical study of the effects of pilot fuel quantity and its injection timing on the performance and emissions of a dual fuel diesel engine. Energy Convers Manag 2007;48:2951–61. doi:10.1016/j.enconman.2007.07.003.

[142] Ryu K. Effects of pilot injection pressure on the combustion and emissions characteristics in a diesel engine using biodiesel – CNG dual fuel. Energy Convers Manag 2013;76:506–16. doi:10.1016/j.enconman.2013.07.085.

[143] Upatnieks A, Mueller CJ, Martin GC. The Influence of Charge-Gas Dilution and Temperature on DI Diesel Combustion Processes Using a Short-Ignition-Delay, Oxygenated Fuel. SAE Transections 2005;114:773–85.

[144] Karagöz Y, Sandalcı T, Koylu UO, Dalkılıç AS, Wongwises S. Effect of the use of natural gas–diesel fuel mixture on performance, emissions, and combustion characteristics of a compression ignition engine. Adv Mech Eng 2016;8:1–13. doi:10.1177/1687814016643228.

[145] Liu J, Yang F, Wang H, Ouyang M, Hao S. Effects of pilot fuel quantity on the emissions characteristics of a CNG/ diesel dual fuel engine with optimized pilot injection timing. Appl Energy 2013;110:201–6. doi:10.1016/j.apenergy.2013.03.024.

[146] Turns SR. An Introduction to Combustion: Concepts and Applications. Third edit. New York: McGraw Hill Education (India) Private Limited; 2016.

[147] Kovacs VB, Torok A. Investigation on Transport Related Biogas Utilization. Transport 2010;25:77–80. doi:DOI 10.3846/transport.2010.10.

[148] Bora BJ, Saha UK. Optimisation of injection timing and compression ratio of a raw biogas powered dual fuel diesel engine. Appl Therm Eng 2016;92:111–21. doi:10.1016/j.applthermaleng.2015.08.111.

[149] Bora BJ, Saha UK, Chatterjee S, Veer V. Effect of compression ratio on performance, combustion and emission characteristics of a dual fuel diesel engine run on raw biogas. Energy Convers Manag 2014;87:1000–9. doi:10.1016/j.enconman.2014.07.080.

[150] Barik D, Murugan S, Sivaram NM, Baburaj E, Shanmuga Sundaram P. Experimental investigation on the behavior of a direct injection diesel engine fueled with Karanja methyl ester-biogas dual fuel at different injection timings. Energy 2017;118:127–38. doi:10.1016/j.energy.2016.12.025.

[151] Ambarita H. Performance and emission characteristics of a small diesel engine run in dual-fuel (diesel-biogas) mode. Case Stud Therm Eng 2017;10:179–91. doi:10.1016/j.csite.2017.06.003.

[152] Mustafi NN, Raine RR, Verhelst S. Combustion and emissions characteristics of a dual fuel engine operated on alternative gaseous fuels. Fuel 2013;109:669–78. doi:10.1016/j.fuel.2013.03.007.

[153] Selim MYE, Radwan MS, Saleh HE. Improving the performance of dual fuel engines running on natural gas/LPG by using pilot fuel derived from jojoba seeds. Renew Energy 2008;33:1173–85. doi:10.1016/j.renene.2007.07.015.

[154] Gund MD, Tamboli SA, Mohite VR. Performance Evaluation of Single Cylinder Diesel Engine in Dual Fuel Mode with Biogas as Primary Fuel and Diesel and Biodiesel as Pilot Fuel. Int Res J Eng Technol 2017;04:1656–60.

[155] Mahla SK, Singla V, Sandhu SS, Dhir A. Studies on biogas-fuelled compression ignition engine under dual fuel mode. Environ Sci Pollut Res 2018;25:9722–9. doi:10.1007/s11356-018-1247-4.

[156] Swami Nathan S, Mallikarjuna JM, Ramesh A. An experimental study of the biogas-diesel HCCI mode of engine operation. Energy Convers Manag 2010;51:1347–53. doi:10.1016/j.enconman.2009.09.008.

[157] Mahla SK, Dhir A, Gupta N. Emission characteristics of diesel engine fuelled with biogas and n -propanol-biodiesel-diesel blend under dual fuel mode 2017;10:1–8.

[158] Cacua K, Olmos-Villalba L, Herrera B, Gallego A. Experimental evaluation of a diesel-biogas dual fuel engine operated on micro-trigeneration system for power, drying and cooling. Appl Therm Eng 2016;100:762–7. doi:10.1016/j.applthermaleng.2016.02.067.

[159] Barik D, Murugan S. Investigation on combustion performance and emission characteristics of a DI (direct injection) diesel engine fueled with biogas e diesel in dual fuel mode. Energy 2014;4:1–12. doi:10.1016/j.energy.2014.05.106.

[160] Sarkar A, Saha UK. Effect of Intake Charge Preheating and Equivalence Ratio in a Dual Fuel Diesel Engine Run on Biogas and Ethanol-Blended Diesel. ASME J Energy Resour Technol 2017;140:041802. doi:10.1115/1.4038624.

[161] Luijten CCM, Kerkhof E. Jatropha oil and biogas in a dual fuel CI engine for rural electrification. Energy Convers Manag 2011;52:1426–38. doi:10.1016/j.enconman.2010.10.005.

[162] Henham A, Makkar M. Combustion of simulated biogas in a dual-fuel diesel engine. Energy Convers Manag 1998;39:2001–9. doi:10.1016/S0196-8904(98)00071-5.

[163] Debnath BK, Bora BJ, Sahoo N, Saha UK. Influence of Emulsified Palm Biodiesel as Pilot Fuel in

a Biogas Run Dual Fuel Diesel Engine. J Energy Eng 2014;140:A4014005. doi:10.1061/(ASCE)EY.1943-7897.0000163.

[164] Verma S, Das LM, Kaushik SC, Bhatti SS. The effects of compression ratio and EGR on the performance and emission characteristics of diesel-biogas dual fuel engine. Appl Therm Eng 2019;150:1090–103. doi:10.1016/j.applthermaleng.2019.01.080.

[165] Chandrashekar J, Gumtapure V. Experimental investigation of methane-enriched biogas in a single cylinder diesel engine by the dual fuel mode. Energy Sources, Part A Recover Util Environ Eff 2022;44:1898–911. doi:10.1080/15567036.2019.1647314.

[166] Chandrashekar J, Gumtapure V. Experimental Study on the Effect of Injection Timing on a Dual Fuel Diesel Engine Operated With Biogas Derived From Food Waste. J Energy Resour Technol 2022;144. doi:10.1115/1.4054586.

[167] Sarkar A, Saha UK. Assessment of dual-fuel diesel engine performance by modulating biogas flow rate and intake charge preheating. Int J Ambient Energy 2020;0:1–7. doi:10.1080/01430750.2020.1726463.

[168] Banapurmath NR, Tewari PG, Hosmath RS. Experimental investigations of a four-stroke single cylinder direct injection diesel engine operated on dual fuel mode with producer gas as inducted fuel and Honge oil and its methyl ester (HOME) as injected fuels. Renew Energy 2008;33:2007–18. doi:10.1016/j.renene.2007.11.017.

[169] Dasappa S, Sridhar H V. Performance of a diesel engine in a dual fuel mode using producer gas for electricity power generation. Int J Sustain Energy 2013;32:153–68. doi:10.1080/14786451.2011.605945.

[170] Sheth PN, Babu B V. Experimental studies on producer gas generation from wood waste in a downdraft biomass gasifier. Bioresour Technol 2009;100:3127–33. doi:10.1016/j.biortech.2009.01.024.

[171] Das DK, Dash SP, Ghosal MK. Performance Study of a Diesel Engine by using producer gas from Selected Agricultural Residues on Dual-Fuel Mode of Diesel-cum-Producer gas. World Renew. Energy Congr. 2011, Sweden: Linköping University Electronic Press; Linköpings universitet; 2011, p. 3541–8. doi:10.3384/ecp110573541.

[172] McKendry P. Energy production from biomass (part 3): gasification technologies. Bioresour Technol 2002;83:55–63. doi:10.1016/S0960-8524(01)00120-1.

[173] Sridhar G, Paul PJ, Mukunda HS. Computational studies of the laminar burning velocity of a producer gas and air mixture under typical engine conditions. Proc Inst Mech Eng Part A J Power Energy 2005;219:195–201. doi:10.1243/095765005X6917.

[174] Banapurmath NR, Tewari PG, Yaliwal VS, Kambalimath S, Basavarajappa YH. Combustion characteristics of a 4-stroke CI engine operated on Honge oil, Neem and Rice Bran oils when directly injected and dual fuelled with producer gas induction. Renew Energy 2009;34:1877–84. doi:10.1016/j.renene.2008.12.031.

[175] Singh RN, Singh SP, Pathak BS. Investigations on operation of CI engine using producer gas and rice bran oil in mixed fuel mode. Renew Energy 2007;32:1565–80. doi:10.1016/j.renene.2006.06.013.

[176] Ramadhas AS, Jayaraj S, Muraleedharan C. Dual fuel mode operation in diesel engines using renewable fuels: Rubber seed oil and coir-pith producer gas. Renew Energy 2008;33:2077–83. doi:10.1016/j.renene.2007.11.013.

[177] Deshmukh SJ, Bhuyar LB, Thakre SB. Investigation on Performance and Emission Characteristics of CI Engine Fuelled with Producer Gas and Esters of Hingan (Balanites) Oil in Dual Fuel Mode. Int J Aerosp Mech Eng 2008;2:148–53.

[178] Banapurmath NR, Yaliwal VS, Kambalimath S, Hunashyal AM, Tewari PG. Effect of wood type and carburetor on the performance of producer gas-biodiesel operated dual fuel engines. Waste

and Biomass Valorization 2011;2:403–13. doi:10.1007/s12649-011-9083-5.

[179] Hassan S, Zainal ZA, Miskam MA. Effects of advanced injection timing on performance and emission of a supercharged dual-fuel diesel engine fueled by producer gas from downdraft gasifier. J Sci Ind Res (India) 2011;70:220–4.

[180] Yaliwal VS, Banapurmath NR, Tewari PG, Adaganti SY. Fuel efficiency improvement of a dual-fuel engine fuelled with Honge oil methyl ester (HOME)-bioethanol and producer gas. Int J Sustain Eng 2014;7:269–82. doi:10.1080/19397038.2013.843038.

[181] Yaliwal VS, Banapurmath NR, Tewari PG. Performance, combustion and emission characteristics of a single-cylinder, four-stroke, direct injection diesel engine operated on a dual-fuel mode using Honge oil methyl ester and producer gas derived from biomass feedstock of different origin. Int J Sustain Eng 2014;7:253–68. doi:10.1080/19397038.2013.834395.

[182] Lal S, Mohapatra SK. The effect of compression ratio on the performance and emission characteristics of a dual fuel diesel engine using biomass derived producer gas. Appl Therm Eng 2017;119:63–72. doi:10.1016/j.applthermaleng.2017.03.038.

[183] Bhattacharya SC, Shwe Hla S, Pham HL. A study on a multi-stage hybrid gasifier-engine system. Biomass and Bioenergy 2001;21:445–60. doi:10.1016/S0961-9534(01)00048-4.

[184] Uma R, Kandpal TC, Kishore VVN. Emission characteristics of an electricity generation system in diesel alone and dual fuel modes. Biomass and Bioenergy 2004;27:195–203. doi:10.1016/j.biombioe.2004.01.003.

[185] Pathak BS, Bining AS, Jain AK. Final Report of the Project, Energy in Agriculture and First Report of the School of Energy Studies for Agriculture. Ludhiana: 1985.

[186] Kashipura N, Banapurmath NR, Manavendra G, Nagaraj AM, Yaliwal VS, Kulkarni V, et al. Effect of Combustion Chamber Shapes on the Performance of Duel Fuel Engine Operated on Rice Bran Oil Methyl Ester and Producer Gas. J Pet Environ Biotechnol 2015;06:1–8. doi:10.4172/2157-7463.1000225.

[187] Balakrishnan N, Mayilsamy K, Nedunchezhian N. An investigation of the performance, combustion, and emission characteristics of a CI engine fueled with used vegetable oil methyl ester and producer gas. Int J Green Energy 2015;12:506–14. doi:10.1080/15435075.2013.849255.

[188] Lekpradit T, Tongorn S, Nipattummakul N, Kerdsuwan S. Study on Advanced Injection Timing on a Dual-Fuel Diesel Engine with Producer Gas from a Down-Draft Gasifier for Power Generation. J Met Mater Miner 2008;18:169–73.

[189] Hernández JJ, Lapuerta M, Barba J. Effect of partial replacement of diesel or biodiesel with gas from biomass gasification in a diesel engine. Energy 2015;89:148–57. doi:10.1016/j.energy.2015.07.050.

[190] Balakrishnan N, Mayilsamy K, Nedunchezhian N. An investigation of the performance, combustion, and emission characteristics of a CI engine fueled with used vegetable oil methyl ester and producer gas. Int J Green Energy 2015;12:506–14. doi:10.1080/15435075.2013.849255.

[191] Banapurmath NR NK. Effect of Turbo Charging on the Performance of Dual Fuel (DF) Engine Operated on Rice Bran Oil Methyl Ester (RBOME) and Coconut Shell Derived Producer Gas Induction. J Pet Environ Biotechnol 2015;06. doi:10.4172/2157-7463.1000216.

[192] Nataraja K, Banapurmath N, Yaiwal V, Manavendra G, Akshay P, Kulkarni C. Effect of Turbo Charging on the Performance of Dual Fuel (DF) Engine Operated on Rice Bran Oil Methyl Ester (RBOME) and Coconut Shell Derived Producer Gas Induction. J Pet Environ Biotechnol 2015;06:1–7. doi:10.4172/2157-7463.1000216.

[193] Nayak SK, Behera GR, Mishra PC. Exhaust from a dual-fuel engine using quinine nut oil and producer gas. Energy Sources, Part A Recover Util Environ Eff 2017;39:246–53. doi:10.1080/15567036.2015.1107863.

[194] Journal I, Issn ME, Publishing P. Analysis of a diesel engine fuelled with jojoba blend and coir

pith producer gas 2017;14:4675–89.

[195] Hadkar T, Amarnath HK. Performance and Emission Characteristics of Producer Gas derived from Coconut Shell (Biomass) and Honne Biodiesel with different Configuration of carburetor for dual fuel four stoke direct injection diesel engine. Int Res J Eng Technol 2015;2:1804–11.

[196] Nayak SK, Mishra PC, Behera GR. Experimental investigation on dual-fuel engine utilizing waste cooking oil and producer gas. Energy Sources, Part A Recover Util Environ Eff 2017;39:369–76. doi:10.1080/15567036.2015.1122684.

[197] Dawoud B, Amer E, Gross D. Experimental investigation of an adsorptive thermal energy storage. Int J Energy Res 2007;31:135–47. doi:10.1002/er.

[198] Hadkar T, Amarnath HK. Performance and Emission Characteristics of Producer Gas derived from Coconut Shell (Biomass) and Honne Biodiesel with different Configuration of carburetor for dual fuel four stoke direct injection diesel engine. Int Res J Eng Technol 2015;2:1804–11.

[199] Malik A, Mohapatra SK. Environmental Effects Power generation using cotton stalk-derived producer gas in diesel engines. Energy Sources, Part A Recover Util Environ Eff 2017;38:2816–22. doi:10.1080/15567036.2015.1111957.

[200] Dasappa S, Sridhar H V. Performance of a diesel engine in a dual fuel mode using producer gas for electricity power generation. Int J Sustain Energy 2013;32:153–68. doi:10.1080/14786451.2011.605945.

[201] Journal I, Issn ME, Publishing P. Emission from a dual fuel operated diesel engine fuelled with Calophyllum Inophyllum biodiesel and producer gas 2017;14:3954–69.

[202] Sutheerasak E, Pirompugd W, Sanitjai S. Performance and emissions characteristics of a direct injection diesel engine from compressing producer gas in a dual fuel mode. Eng Appl Sci Res 2018;45:47–55. doi:10.14456/easr.2018.7.

[203] Yaliwal VS. Effect of mixing chamber or carburetor type on the performance of diesel engine operated on biodiesel and producer gas induction. Int J Automot Eng Technol 2016;5:25–37. doi:10.18245/ijaet.02009.

[204] Shaw D, Akhtar SJ, Priyam A, Singh RK. Performance Study of Dual Fuel Engine Using Producer Gas as Secondary Fuel. Carbon-Science Technol 2016;8:63–71.

[205] Akkoli KM, Banapurmath NR, Shivashimpi MM, Soudagar MEM, Badruddin IA, Alazwari MA, et al. Effect of injection parameters and producer gas derived from redgram stalk on the performance and emission characteristics of a diesel engine. Alexandria Eng J 2021;60:3133–42. doi:10.1016/j.aej.2021.01.047.

[206] Sharma M, Kaushal R. Performance and exhaust emission analysis of a variable compression ratio (VCR) dual fuel CI engine fuelled with producer gas generated from pistachio shells. Fuel 2021;283:118924. doi:10.1016/j.fuel.2020.118924.

[207] Arunachalam K, Pedinti VS, Goel S. Decentralized distributed generation in India: A review. J Renew Sustain Energy 2016;8. doi:10.1063/1.4944966.

[208] Kumar A, Kumar N, Baredar P, Shukla A. A review on biomass energy resources, potential, conversion and policy in India. Renew Sustain Energy Rev 2015;45:530–9. doi:10.1016/j.rser.2015.02.007.

[209] India WI. Access to Clean Energy: A Glimpse of off grid projects in India. New Delhi: 2010.

[210] Sharma DC. Transforming rural lives through decentralized green power. Futures 2007;39:583–96. doi:10.1016/j.futures.2006.10.008.

[211] Das S, Kashyap D, Kalita P, Kulkarni V. Computational investigation of a venturi-type mixer for gaseous fuel application in a dual-fuel engine dual-fuel engine. Int J Ambient Energy 2022;43:7666–77. doi:10.1080/01430750.2022.2075932.

[212] Bora BJ, Debnath BK, Gupta N, Saha UK, Sahoo N. Investigation on the Flow Behaviour of a

Venturi Type Gas Mixer Designed for Dual Fuel Diesel Engines. Int J Emerg Technol Adv Eng 2013;3:202–9.

[213] Chandekar AC, Debnath BK. Computational investigation of air-biogas mixing device for different biogas substitutions and engine load variations. Renew Energy 2018;127:811–24. doi:10.1016/j.renene.2018.05.003.

[214] Debnath BK. Experimental and theoritical routes towards assessing the potential of emulsified palm biodiesel as an alternative to diesel fuel. Indian Institute of Technology Guwahati, 2013.

[215] Sahoo BB, Sahoo N, Saha UK. Performance and Environmental Studies of a Compression-Ignition Stationary Engine Under Biogas- Diesel Dual-Fuel Mode. J Inst Eng Ser C 2021;102:409–19. doi:10.1007/s40032-020-00651-x.

[216] Guo H, Neill WS, Liko B. The Combustion and Emissions Performance of a Syngas-Diesel Dual Fuel Compression Ignition Engine 2016. doi:10.1115/icef2016-9367.

[217] Dimitriou P, Tsujimura T, Suzuki Y. Adopting biodiesel as an indirect way to reduce the NOx emission of a hydrogen fumigated dual-fuel engine. Fuel 2019;244:324–34. doi:https://doi.org/10.1016/j.fuel.2019.02.010.

[218] Verma S, Kumar K, Das LM, Kaushik SC. Effect of Hydrogen Enrichment Strategy on Performance and Emission Features of Biodiesel-Biogas Dual Fuel Engine Using Simulation and Experimental Analyses. J Energy Resour Technol Trans ASME 2021;143:1–13. doi:10.1115/1.4049179.

[219] Kashipura N, Nagaraj AM BN. Effect of Combustion Chamber Shapes on the Performance of Duel Fuel Engine Operated on Rice Bran Oil Methyl Ester and Producer Gas. J Pet Environ Biotechnol 2015;06. doi:10.4172/2157-7463.1000225.

[220] Nalgundwar A, Paul B, Sharma SK. Comparison of performance and emissions characteristics of DI CI engine fueled with dual biodiesel blends of palm and jatropha. Fuel 2016;173:172–9. doi:10.1016/j.fuel.2016.01.022.

[221] Ahmed S, Hassan MH, Kalam MA, Ashrafur Rahman SM, Abedin MJ, Shahir A. An experimental investigation of biodiesel production, characterization, engine performance, emission and noise of Brassica juncea methyl ester and its blends. J Clean Prod 2014;79:74–81. doi:10.1016/j.jclepro.2014.05.019.

[222] Mofijur M, Masjuki HH, Kalam MA, Atabani AE. Evaluation of biodiesel blending, engine performance and emissions characteristics of Jatropha curcas methyl ester: Malaysian perspective. Energy 2013;55:879–87. doi:10.1016/j.energy.2013.02.059.

[223] Sayyed S, Kumar R, Kulkarni K. Experimental investigation for evaluating the performance and emission characteristics of DICI engine fueled with dual biodiesel- diesel blends of Jatropha , Karanja , Mahua , and Neem. Energy 2022;238:121787. doi:10.1016/j.energy.2021.121787.

[224] Sharma A, Murugan S. Investigation on the behaviour of a DI diesel engine fueled with Jatropha Methyl Ester (JME) and Tyre Pyrolysis Oil (TPO) blends. Fuel 2013;108:699–708. doi:10.1016/j.fuel.2012.12.042.

[225] Ruhul AM, Kalam MA, Masjuki HH, Shahir SA, Alabdulkarem A, Teoh YH, et al. Evaluating combustion, performance and emission characteristics of Millettia pinnata and Croton megalocarpus biodiesel blends in a diesel engine. Energy 2017;141:2362–76. doi:10.1016/j.energy.2017.11.096.

[226] Datta A, Palit S, Mandal BK. An experimental study on the performance and emission characteristics of a CI engine fuelled with Jatropha biodiesel and its blends with diesel. J Mech Sci Technol 2014;28:1961–6. doi:10.1007/s12206-014-0344-7.

[227] Gad MS, El-Shafay AS, Abu Hashish HM. Assessment of diesel engine performance, emissions and combustion characteristics burning biodiesel blends from jatropha seeds. Process Saf Environ Prot 2021;147:518–26. doi:10.1016/j.psep.2020.11.034.

[228] Agarwal AK, Dhar A. Experimental investigations of performance, emission and combustion characteristics of Karanja oil blends fuelled DICI engine. Renew Energy 2013;52:283–91. doi:10.1016/j.renene.2012.10.015.

[229] Gumus M. A comprehensive experimental investigation of combustion and heat release characteristics of a biodiesel (hazelnut kernel oil methyl ester) fueled direct injection compression ignition engine. Fuel 2010;89:2802–14. doi:10.1016/j.fuel.2010.01.035.

[230] Mohammed E-K, Nemit-allah MA. Experimental investigations of ignition delay period and performance of a diesel engine operated with Jatropha oil biodiesel. Alexandria Eng Journal 9-52:141;2013. doi:10.1016/j.aej.2012.12.006.

[231] Lapuerta M, Agudelo JR, Prorok M, Boehman AL. Bulk modulus of compressibility of diesel/biodiesel/HVO blends. Energy and Fuels 2012;26:1336–43. doi:10.1021/ef201608g.

[232] Canakci M. Combustion characteristics of a turbocharged DI compression ignition engine fueled with petroleum diesel fuels and biodiesel. Bioresour Technol 2007;98:1167–75. doi:10.1016/j.biortech.2006.05.024.

[233] Mahalingam A, Devarajan Y, Radhakrishnan S, Vellaiyan S, Nagappan B. Emissions analysis on mahua oil biodiesel and higher alcohol blends in diesel engine. Alexandria Eng J 2018;57:2627–31. doi:10.1016/j.aej.2017.07.009.

[234] Mosarof MH, Kalam MA, Masjuki HH, Alabdulkarem A, Ashraful AM, Arslan A, et al. Optimization of performance, emission, friction and wear characteristics of palm and Calophyllum inophyllum biodiesel blends. Energy Convers Manag 2016;118:985–95. doi:10.1016/j.enconman.2016.03.081.

[235] Daho T, Vaitilingom G, Ouiminga SK, Piriou B, Zongo AS, Ouoba,~S.~Koulidiati,~J. Influence of engine load and fuel droplet size on performance of a CI engine fueled with cottonseed oil and its blends with diesel fuel. Appl Energy 2013;111:1046–53.

[236] Dabi M, Saha UK. Implications of blended Mesua ferrea Linn oil on performance, combustion and emissions of compression ignition diesel engines. Therm Sci Eng Prog 2020;19:100579. doi:10.1016/j.tsep.2020.100579.

[237] Debnath BK, Saha UK, Sahoo N. An Experimental Way of Assessing the Application Potential of Emulsified Palm Biodiesel Toward Alternative to Diesel. J Eng Gas Turbines Power 2014;136:1–12. doi:10.1115/1.4025479.

[238] Debnath BK, Sahoo N, Saha UK. Adjusting the operating characteristics to improve the performance of an emulsified palm oil methyl ester run diesel engine. Energy Convers Manag 2013;69:191–8. doi:10.1016/j.enconman.2013.01.031.

[239] Srithar K, Arun Balasubramanian K, Pavendan V, Ashok Kumar B. Experimental investigations on mixing of two biodiesels blended with diesel as alternative fuel for diesel engines. J King Saud Univ - Eng Sci 2017;29:50–6. doi:10.1016/j.jksues.2014.04.008.

[240] Dubey P, Gupta R. Effects of dual bio-fuel (Jatropha biodiesel and turpentine oil) on a single cylinder naturally aspirated diesel engine without EGR. Appl Therm Eng 2017;115:1137–47. doi:10.1016/j.applthermaleng.2016.12.125.

[241] Dubey P, Gupta R. Influences of dual bio-fuel (Jatropha biodiesel and turpentine oil) on single cylinder variable compression ratio diesel engine. Renew Energy 2018;115:1294–302. doi:10.1016/j.renene.2017.09.055.

[242] Vijay Kumar M, Veeresh Babu A, Ravi Kumar P. Experimental investigation on the effects of diesel and mahua biodiesel blended fuel in direct injection diesel engine modified by nozzle orifice diameters. Renew Energy 2018;119:388–99. doi:10.1016/j.renene.2017.12.007.

[243] Prakash R, Singh RK, Murugan S. Experimental investigation on a diesel engine fueled with bio-oil derived from waste wood-biodiesel emulsions. Energy 2013;55:610–8. doi:10.1016/j.energy.2013.03.085.

[244] Dabi M, Sahoo BB, Saha UK. Increase of efficiency and reduction of CO and NOx emissions in a stationary compression ignition engine run on Mesua ferrea Linn oil-diesel and diethyl ether. Therm Sci Eng Prog 2021;25:100980. doi:10.1016/j.tsep.2021.100980.

[245] Nayak C, Sahoo BB. Comparative assessment of biogas and producer gas with diesel in a twin cylinder dual-fuel diesel engine. J Brazilian Soc Mech Sci Eng 2020;42:1–11. doi:10.1007/s40430-020-02615-9.

[246] Verma VS, Bora BJ, Sarkar A, Saha UK. Experimental Investigation of a Dual Fuel Diesel Engine Run on Scrubbed Biogas Using the Method of Adsorption. Proc. ASME 2012 12th Bienn. Conf. Eng. Syst. Des. Anal., 2014, p. 1–9.

[247] Verma S, Das LM, Kaushik SC, Bhatti SS. The effects of compression ratio and EGR on the performance and emission characteristics of diesel-biogas dual fuel engine. Appl Therm Eng 2019;150:1090–103. doi:10.1016/j.applthermaleng.2019.01.080.

[248] Jagadish C, Gumtapure V. Experimental studies on cyclic variations in a single cylinder diesel engine fuelled with raw biogas by dual mode of operation. Fuel 2020;266:117062. doi:10.1016/j.fuel.2020.117062.

[249] Shih HY, Hsu JR. Computed NO x emission characteristics of opposed-jet syngas diffusion flames. Combust Flame 2012;159:1851–63. doi:10.1016/j.combustflame.2011.12.025.

[250] Stylianidis N, Azimov U, Kawahara N, Tomita E. Chemical Kinetics and Computational Fluid-Dynamics Analysis of H2/CO/CO2/CH4 Syngas Combustion and NOx Formation in a Micro-Pilot-Ignited Supercharged Dual Fuel Engine. SAE Tech Pap 2017;2017-Septe. doi:10.4271/2017-24-0027.

[251] Bora BJ, Saha UK. Emission Reduction Operating Parameters for a Dual-Fuel Diesel Engine Run on Biogas and Rice-Bran Biodiesel. J Energy Eng 2017;143:1–12. doi:10.1061/(ASCE)EY.1943-7897.0000410.

[252] Bora BJ, Saha UK. On the Attainment of Optimum Injection Timing of Pilot Fuel in a Dual Fuel Diesel Engine Run on Biogas. Proc. ASME 2012 12th Bienn. Conf. Eng. Syst. Des. Anal., 2014, p. 1–10.

[253] Sharma M, Kaushal R. Performance and emission analysis of a dual fuel variable compression ratio (VCR) CI engine utilizing producer gas derived from walnut shells. Energy 2020;192:116725. doi:10.1016/j.energy.2019.116725.

[254] Halewadimath SS, Banapurmath NR, Jalihal SS, Akarsh BR, Rampur SB, Yaliwal V V., et al. Impact of injection timing (IT) on dual fuel engine fuelled with waste cooking oil methyl ester and producer gas. Mater Today Proc 2022;52:452–6. doi:10.1016/j.matpr.2021.09.108.

[255] Nayak SK, Hoang AT, Nižetić S, Nguyen XP, Le TH. Effects of advanced injection timing and inducted gaseous fuel on performance, combustion and emission characteristics of a diesel engine operated in dual-fuel mode. Fuel 2022;310:1–16. doi:10.1016/j.fuel.2021.122232.

[256] Percy AJ, Edwin M. Prediction on the Performance Parameters of a Variable Compression Ratio (VCR) Dual Fuel Diesel-Producer Gas CI Engine: An Experimental and Theoretical Approach. Arab J Sci Eng 2022. doi:10.1007/s13369-022-07514-w.

[257] Şanlı A, Yılmaz İT, Gümüş M. Investigation of combustion and emission characteristics in a TBC diesel engine fuelled with CH4–CO2–H2 mixtures. Int J Hydrogen Energy 2021;46:24395–409. doi:10.1016/j.ijhydene.2021.05.014.

[258] Karagöz M, Polat F, Sarıdemir S, Yeşilyurt MK, Ağbulut Ü. An experimental assessment on dual fuel engine behavior powered by waste tire-derived pyrolysis oil – biogas blends. Fuel Process Technol 2022;229. doi:10.1016/j.fuproc.2022.107177.

[259] Nadaleti WC, Przybyla G. Emissions and performance of a spark-ignition gas engine generator operating with hydrogen-rich syngas, methane and biogas blends for application in southern Brazilian rice industries. Energy 2018;154:38–51. doi:10.1016/j.energy.2018.04.046.

[260] Nouni MR, Mullick SC, Kandpal TC. Biomass gasifier projects for decentralized power supply in India: A financial evaluation. Energy Policy 2007;35:1373–85. doi:10.1016/j.enpol.2006.03.016.

[261] Jemni MA, Kantchev G, Abid MS. Influence of intake manifold design on in-cylinder flow and engine performances in a bus diesel engine converted to LPG gas fuelled, using CFD analyses and experimental investigations. Energy 2011;36:2701–15. doi:10.1016/j.energy.2011.02.011.

[262] Piemsinlapakunchon T, Paul MC. Effects of fuel compositions on the heat generation and emission of syngas/producer gas laminar diffusion flame. Int J Hydrogen Energy 2019;44:18505–16. doi:10.1016/j.ijhydene.2019.05.178.

[263] Umesh KS, Pravin VK, Rajagopal K, Veena PH. Development of a CFD 3D model to determine the effect of the mixing quality on the CNG-diesel engine performance. Int J Eng Res Technol 2012;1:1–12.

[264] Romańczyk M. Influence of gas inlet angle on the mixing process in a Venturi mixer. ITM Web Conf 2017;15:07005. doi:10.1051/itmconf/20171507005.

[265] Gorjibandpy M, Sangsereki MK. Computational investigation of air-gas venturi mixer for powered bi-fuel diesel engine. World Acad Sci Eng Technol 2010;4:1197–201.

[266] Romańczyk M, Elsner W. Effect of cylindrical turbulators on the mixing process in basic venturi gas mixer using openFOAM. MATEC Web Conf 2019;252:04004. doi:10.1051/matecconf/201925204004.

[267] Moffat RJ. Contributions to the theory of single-sample uncertainty analysis. J Fluids Eng Trans ASME 1982;104:250–8. doi:10.1115/1.3241818.

[268] Kline SJ, McClintock FA. Describing uncertainties in single-sample experiments. Mech Eng 1953;75:3–8.

APPENDIX-A

Equations used for Performance and Combustion Analysis

A1. Performance analysis

i. Brake power (BP):

$$BP = \frac{2 \times \pi \times N \times r \times W}{60 \times 1000}, kW \tag{A1}$$

where N, r and W are the speed of the engine (rpm), dynamometer arm radius (m) and engine load (kg-m/s^2), respectively.

ii. Brake thermal efficiency (BTE):

For single fuel mode, i.e. for FD,

$$BTE_{FD} = \frac{BP \times 3600 \times 100}{\dot{m}_{FD} \times LHV_{FD}}, \% \tag{A2}$$

For dual fuel mode,

$$BTE_{df} = \frac{\left(BP \times 3600 \times 100\right)}{\left(\dot{m}_{pf} \times LHV_{pf} + \dot{m}_{bg} \times LHV_{bg} + \dot{m}_{pg} \times LHV_{pg}\right)}, \% \tag{A3}$$

where $\dot{m}_{FD}$ (kg/s), $\dot{m}_{pf}$ (kg/s), $\dot{m}_{bg}$ (kg/s) and $\dot{m}_{pg}$ (kg/s) and mass flow rates of diesel, pilot fuel, biogas and producer gas, respectively. Similarly, LHV_{FD} (kJ/kg) LHV_{pf} (kJ/kg) LHV_{bg} (kJ/kg) and LHV_{pg} (kJ/kg) are the lower heating values of diesel, pilot fuel, biogas and producer gas, respectively.

iii. Brake specific fuel consumption (BSFC):

$$BSFC = \left[\frac{\sum\left(\dot{m}_f \times 3600\right)}{BP}\right] \frac{(kg/h)}{kW_{output}} \tag{A4}$$

iv. Brake specific energy consumption (BSEC):

$$BSEC = \left[\frac{\sum\left(\dot{m}_f \times LHV_f\right)}{BP}\right] \frac{(kJ/s)}{kW_{output}} \tag{A5}$$

where $\dot{m}_f$ (kg/s) and LHV_f (kJ/kg) are the fuel flow rate and lower heating value of fuel, respectively.

v. Air flow rate (AFR):

$$AFR, \dot{m}_{air} = C_d \times (\pi/4) \times d^2 \times 3600 \times A_{den} \times \sqrt{\frac{2gh \times W_{den}}{A_{den}}}, kg/h \quad \text{(A6)}$$

where C_d, d, h, A_{den} and W_{den} are coefficient of discharge, diameter of the orifice of air flow (m), manometer reading across orifice (m), density of ambient air (kg/m^3) and water density (kg/m^3), respectively.

vi. Volumetric efficiency (η_{vol})

$$\eta_{vol} = \frac{AFR}{(\pi/4) \times D^2 \times L \times (N/n) \times 60 \times K \times A_{den}} \times 100\% \quad \text{(A7)}$$

where D, L, n and K are engine cylinder diameter (m), engine stroke length (m), number of revolution per cycle (2 for four stroke engine) and number of cylinders, respectively.

vii. Pilot fuel replacement (Z):

$$Z = \frac{\dot{m}_{FD} - \dot{m}_{pf}}{\dot{m}_{FD}} \times 100, \% \quad \text{(A8)}$$

A2. Combustion analysis

i. Ignition delay (ID):

$$ID = \theta_{IN} - \theta_{CS} \quad \text{(A9)}$$

where θ_{IN} is the standard IT (i.e. 23° BTDC) adopted from the manufacturer guideline and θ_{CS} is the crank angle at which combustion begins and it is observed from the pressure gradient $\left(\frac{dP_n}{d\theta}\right)$ trend as it changes concavity.

ii. Pressure correction:

The raw cylinder pressure data per degree rotation of crank angle is recorded by the DAS and the following equation suggested by Masood and Ishrat [79] is considered for the after-treatment of instantaneous pressure data.

$$P_n = \frac{(P_{n-1} + 2P_n + P_{n+1})}{4} \quad \text{(A10)}$$

The pressure gradient $\left(\frac{dP}{d\theta}\right)$ is estimated through utilizing the following first order finite difference equation that exhibits fourth order accuracy [114].

$$\frac{dP_n}{d\theta} = \frac{P_{n-2} - 8(P_{n-1}) + 8(P_{n+1}) - P_{n+2}}{12(\Delta\theta)} \quad \text{(A11)}$$

iii. Net heat release rate (NHRR):

The Net heat release rate (NHRR) for both single fuel and DF mode of experiments are calculated utilizing the instantaneous pressure P_n and volume V_n data logged during tests. For the evaluation of NHRR, the specific heat ratio is taken as 1.35 [66,67]. The following equation is used for calculating the NHRR by applying the pressure and volume gradients based on the first law of thermodynamics [112,160].

$$\frac{dQ_n}{d\theta} = \left(\frac{\gamma}{\gamma - 1} \times P_n \times \frac{dV_n}{d\theta}\right) + \left(\frac{1}{\gamma - 1} \times V_n \times \frac{dP_n}{d\theta}\right) \quad \text{(A12)}$$

where $\frac{dQ_n}{d\theta}$, γ, P_n and V_n are NHRR (J/°CA), ratio of specific heats, instantaneous cylinder pressure (N/m^2) and cylinder volume (m^3), respectively. The change of instantaneous cylinder volume per change of unit crank angle $\left(\frac{dV_n}{d\theta}\right)$ are measured recorded during experiments.

APPENDIX-B

Development of a Venturi type air-gaseous fuel mixer

B1. Air-gas mixer design

In the present study, a mixer was designed with the goal of attaining maximum homogeneity of air and gaseous fuels. Connection of this mixer at the inlet manifold prior to the engine would accomplish the desired functional necessities and allows the combined utilization of BG and PG as primary fuel for DF operation.

The gas mixture is designed with the concept of venturimeter having smooth convergent and divergent sections at either side of the throat. The converging section results in reduction of static pressure and rise of fluid velocity which creates a pressure difference between the inlet and the throat. This pressure difference can be described from the Bernoulli's equation for a venturimeter where pressure drop and square of the area are inversely proportional keeping all other parameters constant as shown in equation B1. Thus, a minimum pressure and maximum velocity region allows more dragging of gas and enhances the turbulence mixing with air.

$$\Delta P = P_1 - P_2 = \frac{V_2^2 - V_1^2}{2}\rho \qquad \text{(B1)}$$

where ΔP is the total pressure drop at the throat, P is the pressure and V is the velocity. Suffix 1 and 2 are for inlet and throat, respectively.

The mixer has two inlets for BG and two inlets for PG, 90° apart from each other and one outlet. There are four major design parameters considered namely converging angle, diverging angle, nozzle angle and the ratio of the throat diameter to the inlet diameter (β) which are set to be 19°, 5°, 35°and 0.45, respectively [212,213]. The dimensions of the geometric parameters such as throat diameter and air inlet/mixture outlet diameter are set to be 16 mm and 34.3 mm, respectively. Based on the values of convergent angle, divergent angle and manifold diameter, the length of the conversion and diversion section are calculated to be 74.68 and 249.57 mm, respectively. The dimension and parts of the venturi mixer is shown in **Fig. B1**. Four fuel inlet manifolds are considered for incorporating two gases into the venturi gas mixer i.e. two nozzles each for producer gas and biogas inlets. The diameters of the fuel manifolds are determined based on calorific values of biogas and producer gas. Producer gas has a much lower calorific value (5.8 MJ/m^3) [260] compared to biogas (18.8 MJ/m^3) [149] and

so a larger volume of the producer gas is required to deliver equivalent amount energy as that of biogas. Considering the configuration of 3.5 kW rated power and 1500 rpm engine speed of a DF engine, the gas flow rate of the two gases are calculated for maximum diesel (pilot fuel) substitution of 80% [212]. Subsequently, with a constant velocity inflow of 20 m/s, the safe diameter of each inlet manifold of PG and BG are obtained as 10.46 mm and 5.8 mm, respectively. The design calculation of the inlet manifold of PG and BG is shown in **Table B1**.

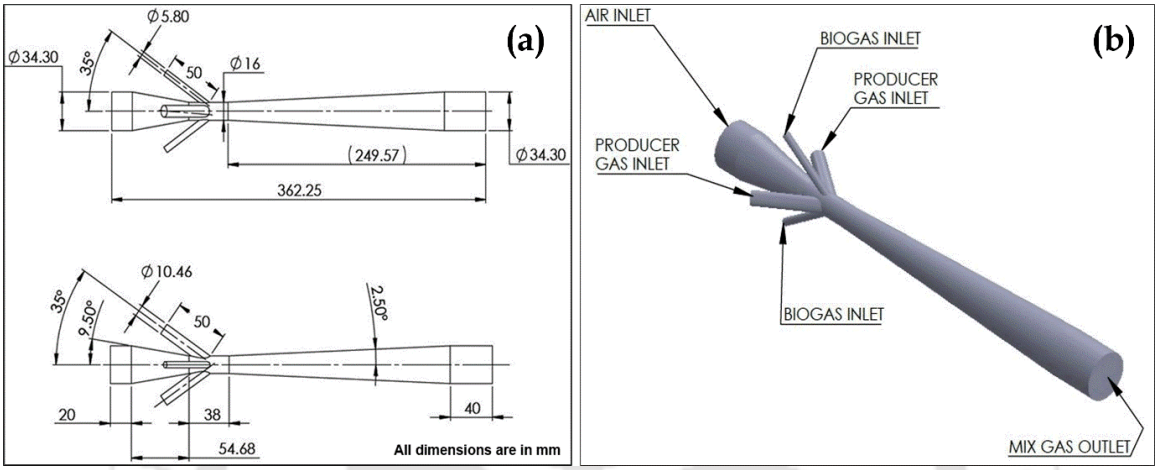

Fig. B.1 Design of the venturi mixer (a) Dimensions of parts (b) three dimensional (3D) model

Table B1 Design calculation of BG and PG inlet manifolds

Parameter	Biogas	Producer gas
Calorific value	20.67 MJ/kg	5 MJ/kg
Volumetric Air Intake	0.00744 m^3/s	0.00744 m^3/s
Density	0.91 kg/m^3	1.287 kg/m^3
Intake Velocity air	8.06 m/s	8.06 m/s
Mass Flow Rate of air	0.008928 kg/s	0.008928 kg/s
Mass Flow Rate of gas	0.000792 kg/s	0.003655 kg/s
Volumetric Intake of gas	0.00087 m^3/s	0.00284 m^3/s
Velocity of gas	20 m/s	20 m/s
Area of Each Nozzle Required	0.00002175 m^2	0.00007175 m^2
Diameter of Each Nozzle	5.28 mm	9.5 mm
Diameter of Each Nozzle (110% safety)	5.8 mm	10.46 mm
Area of Each Nozzle Required (Safe)	0.00002640 m^2	0.00008588 m^2

B2. Methodology

Computational fluid dynamics (CFD) is a most current day tool to study 3D flow behavior and heat transfer characteristics applying the elementary governing equations like continuity, momentum and energy equation. The fluent software available in ANSYS 15.0 is used to carry

out the CFD analysis of the venturi type air-gaseous fuel mixer. The mess pattern of the mixer is shown in **Fig. B2**. The computational investigation is conducted with five different flow combination of BG-PG i.e. 80-20%, 60-40%, 50-50%, 40-60% and 20-80%. The study focuses on the geometry of the venturi mixture to achieve better pressure drop, velocity, turbulence intensity and mixing quality of both these gaseous fuel with air.

B2.1 Modelling

Turbulence models are widely chosen for modelling of IC engine as it directly affects the mixing, homogeneity of mixture and combustion of an engine [261]. In the present work, standard $k-\varepsilon$ model is used to simulate the flow inside the venturi gas mixer where k and ε are the turbulence kinetic energy and eddy turbulent dissipation, respectively. The simulations are conducted with a pressure-based solver under steady state condition. The flow of fluid is continuous through the mixer and the gases are defined as being incompressible. A non-premixed combustion model is applied in the study to calculate the species mass fraction or mixture fraction. The elemental species of BG, PG and air are involved in the mixing phenomena. It is found from the literature that H_2 and CO are the most useful gases generated from the gasification process having higher heating values [262] and in case of dual fuel diesel engine operations, composition of H_2 and CO has been highly addressed [38,62]. Hence, in case of PG, H_2 and CO are taken as the major species. Likewise, CH_4 and CO_2 are considered to be the main species for BG whereas for air, oxygen (O_2) and nitrogen (N_2) is involved. The property parameters of these species are taken from the database present in FLUENT. Moreover, turbulence intensity is specified as 5% [261] while the global transport parameters are considered namely Prandtl number and Schmidt number with values 0.9 and 0.78, respectively. The convergence criteria for the residual has been set at 10^{-4}. The grid size or numbers significantly affect the simulation results. So, prior moving to the simulation, a grid independence test has been performed in order to evaluate the influence of grid size on the predicted results. An unstructured non-uniform tetrahedral mesh is generated throughout the computational domain using meshing module of ANSYS 15.0.

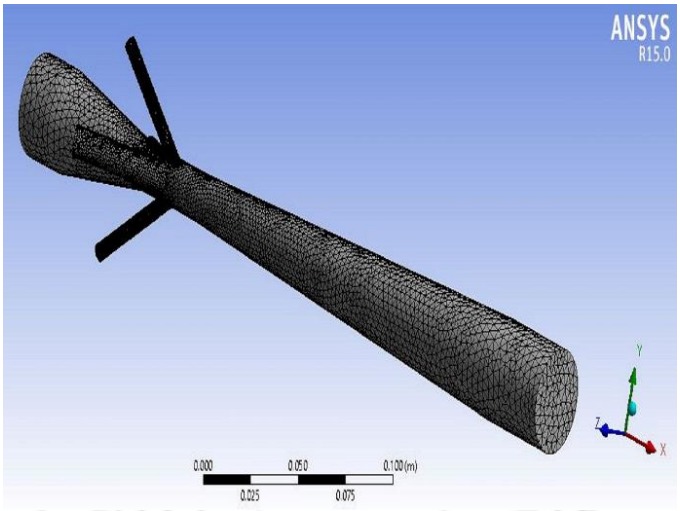

Fig. B2 Mesh pattern of the venturi mixer

B2.2 Governing equations

The flow of air and gas inside the venturi gas mixer is governed by the mass and momentum conservation equation. The variation of temperature inside the mixer is not an essential parameter for this work and therefore the energy equation is not considered. The equations are expressed in the conservative form of the Navier-Stokes equations and can be written as follows [212,213,261]:

$$\frac{\partial \rho}{\partial t} + \frac{\partial}{\partial x_i}(\rho u_i) = 0 \tag{B2}$$

$$\frac{\partial(\rho u_i)}{\partial t} + \frac{\partial(\rho u_i u_j)}{\partial x_i} = \left[-\frac{\partial P}{\partial x_i}\right] + \frac{\partial}{\partial x_i}\left[\mu \frac{\partial u_i}{\partial x_j}\right] + \frac{\partial}{\partial x_i}\left[(\lambda + \mu)\frac{\partial u_k}{\partial x_k}\right] + \rho b_i \tag{B3}$$

where, ρ, t, P, μ, λ and b are the density, time, pressure, dynamic viscosity, second coefficient of viscosity and body force, respectively.

In the present work, standard $k-\varepsilon$ model is employed for the flow analysis. The Reynold Stress tensor can be written as [212,261]:

$$\tau_{ij}^{R} = \mu_t\left(\frac{\partial u_i}{\partial x_j} + \frac{\partial u_j}{\partial x_i} - \frac{2}{3}\delta_{ij}\frac{\partial u_k}{\partial x_k}\right) - \frac{2}{3}\rho k \delta_{ij} \tag{B4}$$

when $i = j$, "δ_{ij}" = 1 or zero otherwise. In view of the $k-\varepsilon$ turbulence model, turbulence kinetic energy (k) and the eddy turbulent dissipation (ε) are the two basic turbulence

properties which define the turbulent eddy viscosity coefficient (μ_t) and can be written as [261]:

$$\mu_t = \frac{f_\mu C_\mu \rho K^2}{\varepsilon} \tag{B5}$$

where C_μ is constant and turbulence velocity factor, f_μ can be expressed as

$$f_\mu = \left(1 - e^{\left(-0.025\frac{\rho\sqrt{k}y}{\mu}\right)}\right)^2 \times \left(1 + \frac{20.5}{\frac{\rho k^2}{\mu\varepsilon}}\right) \tag{B6}$$

The function "y" is the distance from the wall which allows to take into account laminar-turbulent transition. There are two more transport equation which defines the turbulence kinetic energy and dissipation of turbulence eddy can be expressed as [213]:

$$\frac{\partial(\rho k)}{\partial t} + \frac{\partial(\rho k u_i)}{\partial x_i} = \frac{\partial}{\partial x_j}\left[\frac{\mu_t}{\sigma_k}\frac{\partial k}{\partial x_j}\right] + 2\mu_t E_{ij} E_{ij} - \rho\varepsilon \tag{B7}$$

$$\frac{\partial(\rho\varepsilon)}{\partial t} + \frac{\partial(\rho\varepsilon u_i)}{\partial x_i} = \frac{\partial}{\partial x_j}\left[\frac{\mu_t}{\sigma_\varepsilon}\frac{\partial \varepsilon}{\partial x_j}\right] + C_{1\varepsilon}\frac{\varepsilon}{k}2\mu_t E_{ij} E_{ij} - C_{2\varepsilon}\rho\frac{\varepsilon^2}{k} \tag{B8}$$

where u_i E_{ij} are the velocity component and component of rate of deformation in corresponding directions, respectively. $C_{\varepsilon 1}, C_{\varepsilon 2}, \sigma_k, \sigma_\varepsilon$ are the empirically defined constants.

B2.3 Initial and final boundary condition

The case set-up is performed for a non-deformable and stationary arbitrary control volume. At the beginning of simulation, the pressure and temperature applied on both air and gaseous fuels are 101325 Pa (1 atmospheric) and 300 K, respectively. Adiabatic condition is applied to the walls i.e. there is no heat interactions between the wall and the surroundings. For the analysis, the venturi mixer is comprised of different parts namely, venturi, fuel inlet manifolds, air inlet, BG inlet, PG inlet and mix gas out. It is assumed that no reaction occurs between air and gases. Inlet conditions for both air and gases are given as velocity inputs while the output is provided with fixed pressure outlet boundary condition. The velocity of

air, at the inlet is kept constant at 8.06 m/s for all the running condition. Conversely, BG and PG are employed with five different combinations of mass flow rate that simultaneously alters the velocity of BG and PG at each fuel inlet manifolds. This non-reacting system includes BG, PG and air as primary fuel stream, secondary fuel stream and oxidant stream, respectively with total species mass fraction of 1 at the individual inlets. The species mass fraction of primary stream is fixed with 0.353 for CH_4 and 0.647 for CO_2 whereas for secondary stream is taken as 0.067 of H_2, 0.93 of CO. Likewise, for oxidant stream, species mass fraction is considered as 0.23 and 0.77 for O_2 and N_2, respectively. The outlet boundary condition of venturi mixer is considered to have different simulated mixture fractions of air and fuel species. The boundary conditions of the present work are presented in the **Table B2**.

Table B2 Boundary conditions

Boundary		Type	Gas flow rate (m^3/s)	Velocity (m/s)	Turbulent intensity
Venturi	-	Stationary wall	-	-	-
Fuel inlet manifolds		Stationary walls	-	-	-
Air inlet		Inflow	-	8.06	0.05
Flow combination	**80BG20PG** (80% BG and 20% PG)	Inflow	BG= 0.000696 PG= 0.000568	BG= 26.35, PG= 6.61	0.05
	60BG40PG (60% BG and 40% PG)	Inflow	BG= 0.000522 PG= 0.001136	BG= 19.76 PG= 13.22	0.05
	50BG50PG (50% BG and 50% PG)	Inflow	BG= 0.000435 PG= 0.00142	BG=16.47 PG=16.53	0.05
	40BG60PG (40% BG and 60% PG)	Inflow	BG= 0.000348 PG= 0.001704	BG= 13.17 PG= 19.84	0.05
	20BG80PG= 20% BG and 80% PG	Inflow	BG= 0.000174 PG= 0.002272	BG= 6.59 PG= 26.43	0.05
Mix gas outlet	-	Outflow	-	-	-

B3. Results and discussion

B3.1 Pressure distribution

The distribution of pressure in a mixing device is one of the most qualitative parameters to be considered because change in pressure directly influences the flow velocity of gas components and subsequently the turbulence and mixing of the species are affected. In case of venturi type mixers, uniformity in the pressure drop at the throat section would confirm a proper mixing of air and fuel species in the downstream of the mixer. The pressure gradually decreases and

attains a minimum value at the throat section and start increasing. The total pressure drop obtained for combination of 80BG20PG, 60BG40PG, 50BG50PG, 40BG60PG and 20BG80PG are 1670 Pa, 1895.3 Pa, 1982.9 Pa, 2051.18 Pa and 2077.49 Pa, respectively. The increase in pressure drop in the venturi ensures attainment of higher velocity and also better suction of gases through the fuel inlet manifolds. Because of larger fuel inlet manifold of PG allows higher mass flow rate into the throat compared to BG which may have resulted in greater pressure drop. The pressure contour plot shown in **Fig. B3** illustrates the phenomena of pressure distribution inside the venturi. The contours plot clarifies the reduction of pressure at the throat section in case of all the flow combination and the pressure gradually increases as it reaches the mixer outlet. The variation of pressure along the venturi mixer is observed to be similar with the literatures [212,213,263].

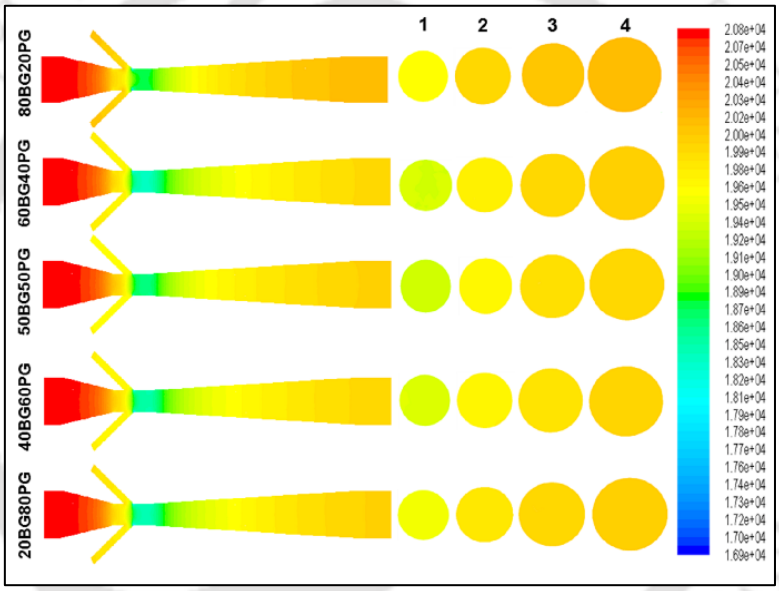

Fig. B3 Contours of pressure (Pa) along the length of the mixer with cross-sectional planes

B3.2 Velocity distribution

According to the concept of venturi, the fluid pressure drops as it passes through the contracted area (throat) which consequently increases the velocity in accordance with the principle of mass continuity. Further, such decrease in static pressure at throat converts the potential energy into kinetic energy, which resulted in increase in velocity of the fluid satisfying the law of energy conservation [264]. Moreover, formation of high velocity zone in case of venturi gas mixer reduces the probability of energy loss and formation of eddy, which in turn resulted in the enhancement of air-gaseous fuel mixing [212]. The velocity contour plot for all the cases shown **Fig. B4** also comply with the principal of continuity and energy conservation. At the throat, maximum velocity is attained which diminished gradually in the

diverging section. The maximum velocity observed was 54, 57, 59, 60 and 62 m/s for 80BG20PG, 60BG40PG, 50BG50PG, 40BG60PG and 20BG80PG, respectively. The maximum magnitude of velocity at the throat increases with the increase in PG velocity which may be attributed to the pressure drop at the throat section of the venturi. The difference in maximum velocity at the throat for all the analyzed cases with different BG/PG combinations are very less. The magnitude of average velocity distribution throughout the venturi is observed to be in the range of 34-36 m/s. The center of first two cross-sectional planes represents a high velocity zone and fades towards the exit with lower velocity for all the flow combinations. Furthermore, it is also evident from the contour that the periphery of the cross-sectional planes confirms lowest magnitude of velocity, which satisfy the no-slip boundary condition of the venturi mixture. The colour combination for the velocity contours obtained in the previous literatures [212,213,265] closely agreed with the present work.

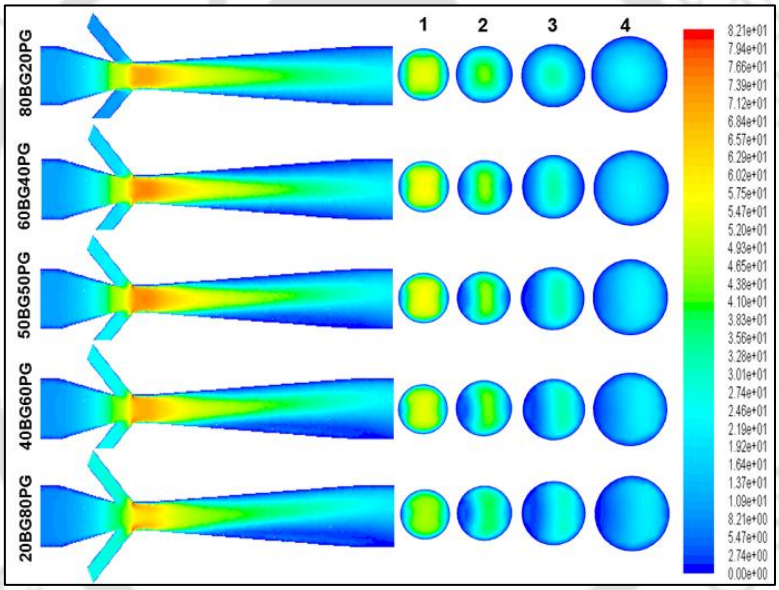

Fig. B4 Contours of velocity (m/s) along the length of the mixer with cross-sectional planes

B3.3 Turbulence kinetic energy

Turbulent kinetic energy (TKE), is the velocity fluctuations generated in a flow field. In general, it is defined as the mean kinetic energy per unit mass associated with eddies in a turbulent flow [266]. Analysis of TKE along the flow through venturi mixer is essential as it considerably influences the mixing behavior of species involved in the flow. TKE increases slightly at the throat section and then decreases drastically after passing through the venturi throat. Then it starts increasing, attains a maximum value at the diverging section of the venturi.

It is clearly visible from the contour of TKE illustrated in **Fig. B5** that in the second and third cross-sectional planes of the venturi for all the flow combination represents generation of uniform turbulence in the divergent segment. The severe rise in the turbulence in the downstream section of the venturi is may be because of the formation of steep gradients of high velocities. The TKE for the combination of 80BG20PG, 60BG40PG, 50BG50PG, 40BG60PG and 20BG80PG are 14, 19, 26, 34 and 42 m^2/s^2, respectively. With the increase of flow rate, turbulence increases [264]. Hence, the maximum value of TKE in case of 20% BG and 80% PG combination may be attributed to the higher PG flow rate at the inlet because of large pressure drop at the venturi throat. The maximum turbulence is visualized in case of 80% PG flow. Additionally, the high turbulence developed at the periphery just after the exit of the throat gradually disperses towards the center in the diverging section. This would result in formation of homogeneous air-gaseous fuel mixture and would further enhance the combustion efficiency.

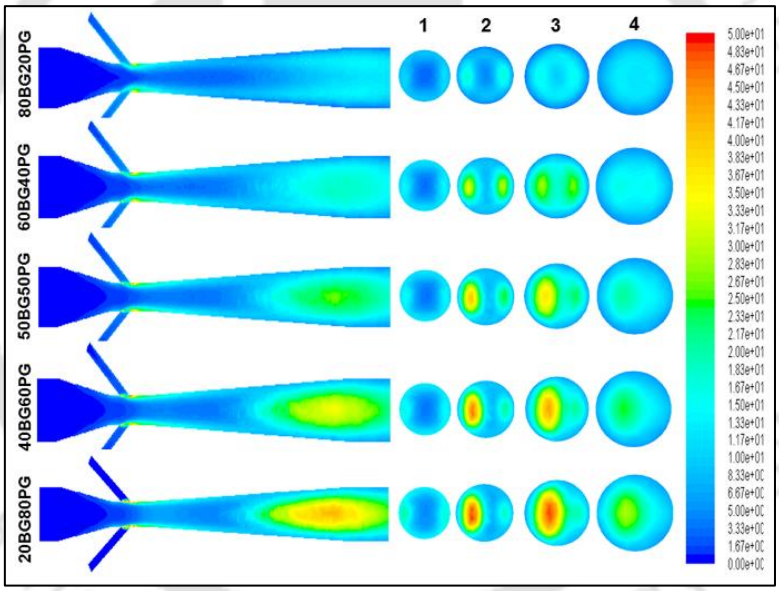

Fig. B5 Contours of TKE (m^2/s^2) along the length of the mixer with cross-sectional planes

B3.4 Mass fraction of air and gas components

The homogeneity of air-gaseous fuel mixture is the most decisive parameter for any gas mixing device. The energy content of BG and PG are majorly dependent on the concentration of CH_4, H_2 and CO, respectively. In case of a venturi mixer, reduction of pressure at the throat segment is primarily accountable for the inflow of gases through the fuel input pipes and simultaneously the distribution of the gases in air along the length of the mixer. The contours of CH_4, H_2, CO and O_2 for the flow combination of 50BG50PG are presented in **Fig. B6**. It is

realized from the figure that in the case of 50BG50PG, all the gaseous fuel elements disperses in air and similar diffusion of gases in air is also observed for all the other flow combination of BG and PG. The appearance in the first cross-sectional plane represents the higher concentration of gases and air (CH_4, H_2, CO and O_2) at the inlet. The study of CH_4 contour indicated two distinct stream of gases at the initial stage, which gradually blends with air at the downstream portion of the venturi mixture and is noticeable in the following cross-sectional planes. Such behavior is also visible in case of both H_2 and CO, which clarifies the uniform distribution of these gases at the exit of the mixer. Likewise, The analysis of mass fraction distribution for the present venturi closely matches with the previous literatures [212,213] and confirms a superior mixing quality.

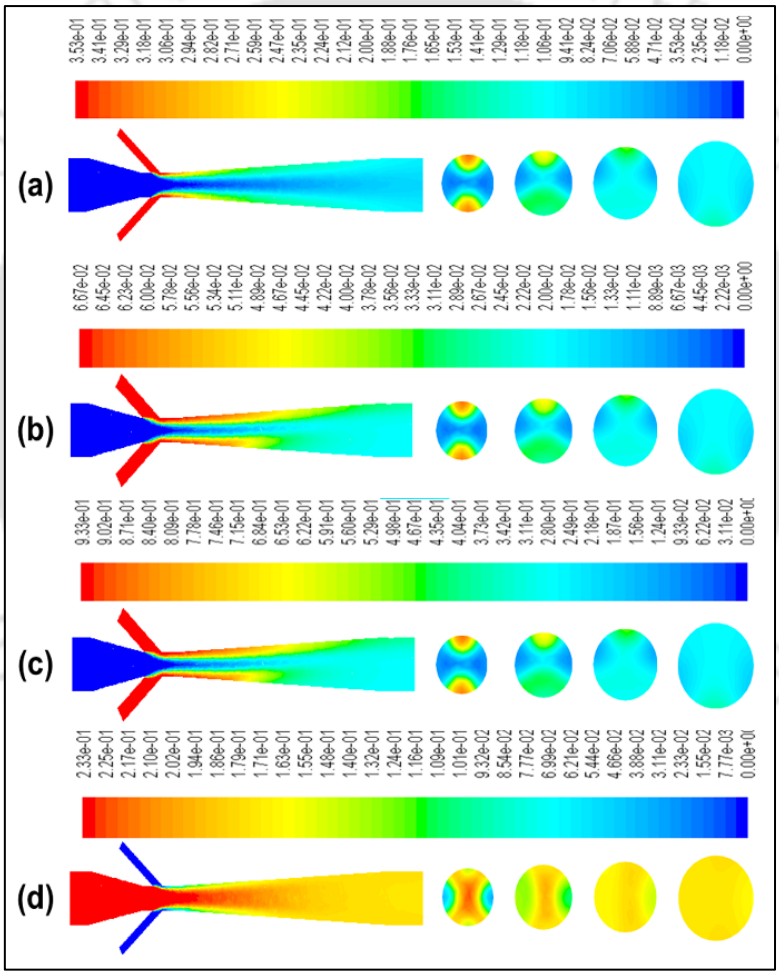

Fig. B6 Contours of mass fractions of gaseous fuel components for flow combination of 50BG50PG along the length of the mixer with cross-sectional planes (a) CH_4, (b) H_2, (c) CO and (d) O_2

APPENDIX-C

Measurement of Uncertainty Analysis

The presence of errors introduces a level of uncertainty in every experiment. The uncertainties of the parameters are calculated by using the sequential technique. A more precise method of estimating uncertainty in experimental results has been presented by Kline and McClintok (1953) and Moffat (1982) [267,268]. The method is described as follows.

If N is a dependent measuring parameter which is a function of independent variables $x_1, x_2, x_3, \ldots\ldots x_n$. Therefore,

$$N = N(x_1, x_2, x_3, \ldots\ldots x_n) \tag{C1}$$

If ΔN is the uncertainty created due to the individual uncertainties of the independent parameters termed as $\Delta N_1, \Delta N_2, \Delta N_3, \ldots\ldots \Delta N_n$. Then the uncertainty of the dependent variable can be written as

$$\Delta N = \left[\left(\frac{\partial N}{\partial x_1} \Delta N_1 \right)^2 + \left(\frac{\partial N}{\partial x_2} \Delta N_2 \right)^2 + \ldots\ldots + \left(\frac{\partial N}{\partial x_n} \Delta N_n \right)^2 \right]^{1/2} \tag{C2}$$

For understanding the concept, let us consider the example brake thermal efficiency (BTE). Before that, uncertainty of brake power (BP) has to be determined as it is directly linked with the BTE of an engine.

BP can be represented as,

$$BP = \frac{2 \times \pi \times N \times W \times r}{60 \times 1000}, kW \tag{C3}$$

Here, r is constant; N and W are independent variable. The uncertainties of N and W are 0.5% and 0.5%, respectively. Therefore, uncertainty associated with BP is calculated as

$$\Delta BP = \left(0.005^2 + 0.005^2\right)^{1/2}$$

$$= \pm 0.007$$

$$= \pm 0.7\%$$

Similarly, uncertainties of other dependent parameters are calculated.

LIST OF PUBLICATIONS

Journals

1. **Das, S**., Kashyap, D., Kalita, P., Kulkarni, V., "Computational investigation of a venturi type mixer for gaseous fuel application in dual fuel engine", ***International Journal of Ambient Energy***, 2022, 2075932.
2. **Das, S**., Kashyap, D., Bora, B. J., Kalita, P., Kulkarni, V., "Thermo-economic optimization of a biogas-diesel dual fuel engine as remote power generating unit using response surface methodology", ***Thermal Science and Engineering Progress***, **24**, 2021, 100935.
3. Basumatary, S., **Das, S.,** Kalita, P., Goswami, P., "Effect of feedstock/water ratio on anaerobic digestion of cattle dung and vegetable waste under mesophilic and thermophilic conditions", ***Bioresource Technology Report***, **14**, 2021, 100675.
4. Kashyap, D., **Das, S**., Kalita, P., "Exploring the efficiency and pollutant emission of a dual fuel CI engine using biodiesel and producer gas: An optimization approach using response surface methodology", ***Science of the Total Environment***, **773**, 2021, 145633.
5. **Das, S**., Kashyap, D., Kalita, P., Kulkarni, V., Itaya, Y. "Clean gaseous fuel application in diesel engine: A sustainable option for rural electrification in India", ***Renewable and Sustainable Energy Reviews***, **117**, 2020, 109485, 1-28.

Book chapters

1. Kashyap D., **Das S.**, Kalita P., (2021) Influence of Oxygenated Fuel and Additives in Biofuel Run Compression Ignition Engine. In: Agarwal A.K., Valera H. (eds) Potential and Challenges of Low Carbon Fuels for Sustainable Transport. Energy, Environment, and Sustainability. Springer, Singapore.
2. **Das, S.**, Basumatary, S., Kalita, P., Kulkarni, V., Goswami, P., Garg, A. and Peng, X. (2020). Bioelectricity Production from Lignocellulosic Biomass. In Lignocellulosic Biorefining Technologies (eds A.P. Ingle, A.K. Chandel and S.S. Silva).

Conferences

1. Das, S., and Kalita, P., "Exploring the effects of synthetic gaseous fuels on the performance, combustion, and emission characteristics of a dual fuel diesel engine", **Proceedings of the ASME 2023 Gas Turbine India Conference**, 2023, Bangalore, India. (Accepted)

2. Das, S., Basumatary, S., Kalita, P., "Experimental investigation of a diesel engine run on simulated gaseous fuels under varying compression ratio", **Proceedings of the 15th International Green Energy Conference**, 2023, Glasgow, Scotland
3. Kashyap D., **Das S.**, Kalita P., "Modelling and optimization of performance and emission characteristics of a dual fuel engine using honge oil methyl ester and producer gas", ***International conference on sustainable energy & environmental protection (SEEP)***, University of Sharjah, 18th November 2019.
4. Basumatary, S., **Das, S.,** Kalita, P., Goswami, P., "Effect of total solid concentration on biogas production rate from cattle dung and vegetable waste", Proceedings ***International conference on sustainable energy & environmental protection (SEEP)***, University of Sharjah, 18th November 2019.
5. **Das S.**, Kashyap D., Kalita P., "Response surface methodology based optimization of a biodiesel run variable compression ratio diesel engine"., ***International conference on future aspects of sustainable technologies***, CIT Kokrajhar, 11-12 November 2019.

Manuscripts to be communicated

1. **Das, S**., Kulkarni, V., Kalita, P., Exploring the effect of biogas composition, compression ratio and pilot fuel injection timing on performance, combustion and emission characteristics of a dual fuel diesel engine. (Submitted to International Journal of Hydrogen Energy, Elsevier).
2. **Das, S**., Basumatary, S., Kulkarni, V., Kalita, P., Field investigation on improvement of diesel engine performance and emission characteristics powered by biogas-producer gas mixture with biodiesel blend as pilot fuel (Submitted to Journal of Renewable Energy, Elsevier).
3. **Das, S**., Kulkarni, V., Kalita, P., Experimental evaluation of performance and emission characteristics of a diesel engine powered by simulated biogas-producer gas mixture under varying compression ratio and injection timing (To be communicated).
4. **Das, S**., Kulkarni, V., Kalita, P., Experimental investigation of a single cylinder diesel engine fueled with tri-biodiesel-diesel blends of Jatropha, Karanja and Mahua. (To be communicated).

Awards and achievements

[1]. Best poster award, International conference on future aspects of sustainable technologies (FAST-2019), CIT Kokrajhar, 11-12 November 2019.